National Library of Canada

Acquisitions and Bibliographic Services Branch

395 Wellington Street
Ottawa, Ontario
K1A 0N4

Bibliothèque nationale du Canada

Direction des acquisitions et des services bibliographiques

395, rue Wellington
Ottawa (Ontario)
K1A 0N4

Your file Votre référence

Our file Notre référence

NOTICE

The quality of this microform is heavily dependent upon the quality of the original thesis submitted for microfilming. Every effort has been made to ensure the highest quality of reproduction possible.

If pages are missing, contact the university which granted the degree.

Some pages may have indistinct print especially if the original pages were typed with a poor typewriter ribbon or if the university sent us an inferior photocopy.

AVIS

La qualité de cette microforme dépend grandement de la qualité de la thèse soumise au microfilmage. Nous avons tout fait pour assurer une qualité supérieure de reproduction.

S'il manque des pages, veuillez communiquer avec l'université qui a conféré le grade.

La qualité d'impression de certaines pages peut laisser à désirer, surtout si les pages originales ont été dactylographiées à l'aide d'un ruban usé ou si l'université nous a fait parvenir une photocopie de qualité inférieure.

Canada

Application and Comparison of Dynamic Routing Models For Unsteady Flow in Simple and Compound Channels

By

Jean George Chatila

A M.A.Sc. Thesis

submitted to the School of Graduate Studies and Research
in partial fulfilment of the requirements for the
Master of Civil Engineering Degree*

University of Ottawa
Ottawa, Ontario
Canada

*The Master of Civil Engineering Program is a joint program with Carleton University, administrated by the Ottawa-Carleton Institute for Civil Engineering

ISBN 0-315-85769-2

UNIVERSITÉ D'OTTAWA
UNIVERSITY OF OTTAWA

To my Parents,

Sisters,

and

Brother

ABSTRACT

The present research investigates the numerical modelling aspects of unsteady flow in compound channels, with special interest in the "flood plain conveyance" aspects. This is examined through applications of three unsteady flow dynamic routing models: DWOPER, EXTRAN, and ONE-D to both laboratory and field data sets.

In the context of applying DWOPER to the data sets three different approaches to define "off-channel" storage areas were considered. The first, which viewed the composite flow field as a single hydraulic unit without storage, produced significant differences between simulated and observed stage and discharge hydrographs. The second and third options separated the shallow and deep zones of the compound flow fields using different types of (imaginary) interface planes. The second option, which considered vertical interface planes, gave generally good results for the laboratory data but was less successful when applied to the field data. The third option used diagonal interface planes to define flood plain storage areas. The inclination of the diagonal plane to the horizontal (Θ) was adjusted to reflect changing hydraulic conditions. The form of the simulated hydrographs using this particular approach was found to be sensitive to variations in Θ. Statistical analyses were performed to determine optimum Θ-values for a wide range of hydraulic conditions. Finally, an equation was developed to define the flood plain hydraulic boundaries.

Applying EXTRAN to both data sets was not as successful as DWOPER. Discrepancies, due to rounding-off significant figures, arise in the laboratory-measured data in a step-wise manner. Unlike DWOPER and ONE-D, EXTRAN does not have the option of differentiating between the main channel and the flood plain flow fields. EXTRAN assumes the whole channel acting as a single hydraulic unit with irregular shape. Simulation results were satisfactory for the laboratory data set, but were less successful for the field data set.

With regard to ONE-D, two different options were used to define the off-channel storage areas. The first involved diagonal interface planes and made use of the flood plain hydraulic boundary equation developed for the DWOPER application. Significant differences were observed between simulated and observed stage and discharge hydrographs. The second option used vertical interface planes. Simulation results were deemed to be satisfactory, based on criteria established by Environment Canada and Water Survey of Canada.

Finally, a comparative study was performed on the simulation results of the three models. Different statistical methods were considered in selecting the best-fit hydrographs. The statistical methods selected for comparison purposes included: graphical method, sum of squares, Nash and Sutcliffe method, root mean square error, standard error of estimate, proportional error of estimate, reduced error of estimate, and total absolute relative error. The total absolute relative error resulted in a good evaluation of the simulated hydrographs.

ACKNOWLEDGEMENTS

Special appreciation is expressed to Dr. R. D. Townsend for his assistance, guidance, and supervision of this research.

Special thanks are extended to W.R.C. Myers from the University of Ulster in N. Ireland and A. Treske from Germany for providing the data used in this study.

The author also wishes to thank his parents, sisters, and brother for their understanding, patience, and ever-lasting encouragement and support.

CONTENTS

LIST OF TABLES

LIST OF FIGURES

NOTATIONS

A = cross-sectional area of flow,

A_o = off-channel cross-sectional area (wherein the velocity is negligible),

A_1--A_7 = tide coefficients,

A_2-A_1 = change in cross-sectional area during a period Δt,

A_j = sum of absolute areas of divergence from event j,

A_s = surface area of a node,

A_{st} = surface area of node at time t,

$A_{st+\Delta t}$ = surface area of node at time t+ Δt,

A_x^y = departure of bed from prismatic form,

B = top width,

B_T = wetted top width (active, and inactive or off-channel storage areas),

C = Courant number for the conduit,

Cz = Chezy's coefficient,

CP = Coefficient of Persistence,

d = flood plain depth,

D = total depth at the peak flow,

D_l = dynamic contribution of lateral discharge,

D_c = departure from the mean for the observed residual mass curve,

D_c = mean of departures from the mean for the observed mass curve,

D_e = departure from the mean of estimated or simulated mass curve,

DELT = Time step,

$dx_1(j)$ = influence on H(j) of unit H(1),

$dx_{11}(j)$ = influence on H(j) of unit H(N),

$dx_2(j)$ = influence on Q(j) of unit H(1),

$dx_{22}(j)$ = influence on Q(j) of unit H(N),

$dx_3(j)$ = influence on H(j) of unit Q(1),

$dx_{33}(j)$ = influence on H(j) of unit Q(N),

$dx_4(j)$ = influence on Q(j) of unit Q(1),

$dx_{44}(j)$ = influence on Q(j) of unit Q(N),

f = Darcy-Weisbach friction factor,

F = Froude number,

g = gravitational acceleration constant,

G = Wood's objective function,

h = depth above probe in mm,

H = z + y = hydraulic head,

H = water surface elevation referenced to a datum,

$H^o(j)$ = null solution for H(j),

H_j = junction depth at iteration j,

H_{j+1} = junction depth at iteration j+1,

HTIDE = elevation of outfall water surface,

I = inflow,

ISOL = solution technique parameter,

K = A C $\sqrt{R}$ = conveyance,

K_e = expansion-contraction coefficient,

L = conduit length,

m = number of events,

n = actual Manning's coefficient,

n_{eq} = equivalent Manning's roughness coefficient,

n_j = number of ordinates in event j,

O = outflow,

P = wetted perimeter,

Pr = probe reading in mV,

Q = discharge in a section,

Q_A = actual flow,

QDI = Initial discharge,

Q_{eq} = flow rate calculated by DWOPER,

Q_j = conduit flow at iteration j,

Q_{j+1} = conduit flow at iteration j+1,

$Q^o(j)$ = null solution for Q(j),

q = lateral inflow per unit width of channel,

q_o = the mean of observed flow rates,

$q_o(t)$ = observed flow rate at time t,

q_{po} = observed peak flow rate,

q_{ps} = simulated peak flow rate,

q_s = the mean of simulated flow rates,

$q_s(t)$ = simulated flow rate at time t,

$q_s(t)$ = simulated flow at time t, obtained from the regression line of $q_o(t)$ on $q_s(t)$,

R = hydraulic radius,

r^2 = correlation coefficient,

R^2 = the index of agreement,

R_{eq} = hydraulic radius calculated by DWOPER,

S^2 = sum of squared residuals,

S_o = bed slope,

S_f = resistance slope,

t = time coordinate,

T = top width of flow in a section,

u_1 = x-component of the inflow-velocity vector,

U_f = under-relaxation factor,

V = average velocity of flow,

V_x = lateral inflow velocity in the x-direction,

w = angular frequency,

W = channel top width,

W' = tidal period,

W_f = wind term,

x = distance along the longitudinal axis of the channel,

y = depth of flow normal to the bottom,

$\overline{y}$ = average depth,

YDI = initial water surface elevations,

z = invert elevation,

α = Weighting factor,

ΔQ = difference between inflow I and outflow O over a reach length,

ΔS = change in storage within the reach,

Δt = time increment, and

θ = angle that the diagonal interface planes make with the horizontal.

ABBREVIATIONS

CM = Method of Characteristics,
cms = Cubic meters per second,
DWOPER = Dynamic Wave Operational routing model,
EPA = U.S. Environmental Protection Agency,
EXTRAN = Extended Transport Block of the U.S. Environmental Protection Agency Storm Water Management Model (SWMM),
LMT = Lateral momentum transfer,
MD = mean deviation for one event,
MIT = Massachusetts Institute of Technology,
N & S = Nash and Sutcliffe criterion,
NWS = U.S. National Weather Service Hydrologic Research Laboratory,
ONE-D = One-Dimensional hydrodynamic model,
PEE = Proportional error of estimate,
REE = Reduced error of estimate,
RMCC = residual mass curve coefficient,
RMSE = Root mean square error,
SEE = Standard error of estimate,
SS = Sum of squares,
SWMM = Storm Water Management Model,
TARE = Total absolute relative error,
TSAA = total overall sum of absolute areas of divergence,
TSAR = total overall sum of absolute deviations,
TSSR = total overall sum of squared residuals, and
WSC = Water Survey of Canada.

CHAPTER 1

INTRODUCTION

1.1 FLOOD ROUTING

In a surface water system, runoff, floods, droughts, and stream water quality interact very closely. Excessive rainfall from extreme storms results in flooding along rivers whereas shortage of rainfall due to drought causes minimal stream flows, reduced water supply, restricted navigation and poor water quality. Water Resources Engineers strive to predict the inter-relationships between rainfall, runoff, floods, droughts, and stream quality.

Flood Routing is the process of tracing by calculation the course of a flood wave along a channel and/or through a reservoir. In large measure, it is the problem of applying the principles of unsteady flow to open channel systems. Flood Routing can also be defined as a mathematical method (model) for predicting the changing magnitude and celerity of a flood wave as it propagates along a river. The objective of any flood routing exercise is to trace the wave propagation by determining the following time and space variants:

1- Flow rate $Q = f(x,t)$,
2- Flow depth $y = g(x,t)$, and
3- Flow velocity $V = h(x,t)$.

Of special interest to the engineer involved in the flood routing exercise are the maximum water surface elevation and the rate of rise or fall of the water surface (structures across rivers and streams), peak discharge (spillways, bridges and channel sections), and total volume of water resulting from a design flood (storage facilities, flood control, irrigation and water supply). As a flood wave travels along a channel its peak is usually attenuated and its base extended. The channel flow is usually unsteady and non-uniform. The governing equations represent the conservation of mass and momentum and are known as the St. Venant equations.

Computational hydraulics is the reformulation of the hydraulics equations to suit the digital machine process and allow for algorithmic representation of natural phenomena. In general, computational hydraulics routing models incorporate differential equations with no direct mathematical solutions. In general, they are solved numerically by replacing the differential equations with equivalent (approximating) finite difference equations. However, other solution techniques are available, including finite element methods.

1.2 STUDY NEEDS

The growing intensity of land and water resources utilization has renewed efforts towards systematic research in the field of alluvial hydraulics. Drinking water distribution, storm drainage systems, irrigation networks, flood forecasting and pollution control are becoming increasingly important as water resources become scarcer. Many flow phenomena of great importance to the engineer are unsteady in character, variable with time, and can not be reduced to steady flow. Unsteadiness implies that the velocity may be increasing and the streamlines themselves may be shifting. However, in open channel flow only one complication arises, namely that of changing water-surface level. The equations of motion are not solvable in the most general case. Explicit solutions are possible in certain cases which are physically very simple but are real enough to be of engineering importance. For the less simple cases, approximations and numerical techniques can be developed which yield solutions of satisfactory accuracy.

The simplest example of routing is level-pool routing (storage) which is based on balancing inflow, outflow, and volume of water in the lake (continuity equation). Obviously storage routing is successful when applied to level pool. However, it is not successful when applied to a river reach. Clearly the continuity equation will still hold for a river reach, but the storage will no longer be uniquely determined by the outflow. It is expected that the inflow to a certain river reach is to be related to the upstream depth, and the outflow to the downstream depth.

The problem of flood flow through streams with storage areas can be divided into two categories: the first one is that in the storage area there is no significant longitudinal flow. The other is one in which a significant amount of longitudinal flow exists in the storage areas. The former represents cases such as flood plains having dikes perpendicular to the river, heavy vegetation, or both, or channels having a large number of boundary irregularities acting as a series of small reservoirs. Flood routing is important in compound channels, particularly when relatively shallow sections (flood plains) adjoin a deep (main) section. A major area of uncertainty in river channel analysis is that of accurately predicting the capacity of compound channels consisting of a central main channel and one or two side flood plains. If the compound section is treated as a single channel, discharge capacity is under-estimated, while if the more common method of dividing the section into main channel and flood plains is employed then the capacity is over-estimated. The cross-section is usually divided in such a way as to insure hydraulic homogeneity in flow computations.

An important feature in compound channel computations is the effect of momentum transfer between deep and shallow flows, which include reduction in main channel velocity and discharge capacity. Zheleznyakov (1965, 1971) was the first to investigate the momentum transfer which he called the "kinematic effect". De Long (1989) reports that the one-dimensional unsteady open channel flow equations can be extended to simulate floods in channels of compound section if it is assumed that lateral velocities are negligible, the water surface is level across the section, and the effects of turbulence and friction may be adequately described by resistance laws used for uniform flow.

During periods of extraordinary flood, the wetted perimeter increases rapidly as the flow spreads over the berm (flood plain). Previous literature (Liggett, 1968; and Baltzer and Lai, 1968, among others) considers that berms or over-bank portions of the flood plain

serve only to provide for the storage of flood waters. Tingsanchali and Ackermann (1976) report that if the velocity in the berms is relatively high, it is important to know the significance of the dynamic effect of the berm flow when modelling the river discharge and stage. During-the progression of flood waves the depth varies along the stream and mass exchanges across verticals at the boundary breaks will become more pronounced.

There has traditionally (and unfortunately) been a tendency to neglect the dynamics of fluid flow when dealing with the problem of hydrology; indeed the term "hydrologic" is often applied to the storage-routing techniques in which the dynamic equation is of secondary importance. Henderson and Wooding (1964) have contrasted the results of the dynamic approach with those of the Unit Hydrograph Theory. An important aspect that supports the application of hydrodynamic models rather than hydrologic models is the fact that hydrological flood routing methodologies can only be of limited accuracy as these methods are based on the continuity equation and a steady-state discharge relationship. The routing procedure by the method of characteristics, although more accurate because it makes use of the continuity and momentum equations for unsteady flows, is a one-dimensional approach that does not consider fluid exchange between channel subsections. Henderson (1966) points out that results of the foregoing dynamical argument differ from those predicted by standard hydrological methods. From the assumptions made in the Unit Hydrograph Theory it follows that for a given depth of rainfall excess h_o the runoff hydrograph becomes steadily longer and longer with increasing rainfall duration t_o, behaving in fact like an attenuating wave. The foregoing argument, on the other hand, shows that if $t_o < t_s$ (where t_s = time of equilibrium), then the peak runoff discharge is independent of t_o. However, when $t_o > t_s$ the situation is different, but this case is of lesser practical importance. Therefore, hydrodynamic models are best-suited for routing in compound channels.

While much work has been carried out in the past on unsteady flow in channels of simple cross-section, there has been a lack of research on the subject of routing floods through compound channels. The CSCE Task Committee on evaluation of river models (CSCE, 1990) recommended that future research efforts should include the application of routing models to non-prismatic channels and channels with flood plains (compound channels). Kouwen (1986) reports that dynamic models have the reputation of being "pesky". An important requirement, therefore, in applying dynamic models is the availability of appropriate and accurate field data. If only suspect data is available, then the

advantage of using the complete solution of the St. Venant equations would be lost. An important consideration in carrying out the present study was the availability of two highly reliable data sets. The first was laboratory data covering a wide range of model flood events in a compound channel that produced different depths over the channel's flood plains, (Treske, 1980). The second was a field data set recorded on the River Main in N. Ireland, (Myers, 1991). The River Main study reach was a non-prismatic reach with flood plains of high roughness compared to the main channel. Also, the data set for this system was for a relatively long-duration hydrograph. The availability of such accurate data sets was critically important in the present study of the numerical modelling aspects of flood plain conveyance.

Previous experience in the application of hydrodynamic models shows that mainly simulations were performed for single channels with no flood plains. A lack of research was noticed in the field of applying dynamic models to compound channels.

1.3 STUDY OBJECTIVE

This study of compound channel conveyance characteristics involves performing a comparative evaluation of a number of existing river models that are in the public domain. The model evaluation was carried out in two stages:

In stage one, the theoretical bases of three unsteady flow hydrodynamic routing models [DWOPER (Fread, 1978), EXTRAN (1973), and ONE-D (Harleman, 1974)] were examined. A comparison of the model capabilities and weaknesses was performed. The assumptions made in developing the theoretical and mathematical formulation of each model were investigated.

In stage two, evaluation involved testing the models using both laboratory and field data sets. Models of similar capabilities were tested against standard data sets, and the ability of the model to predict measured data was tested. Also, a comparison between the performance of the explicit finite difference techniques (EXTRAN) and the implicit finite difference techniques (DWOPER, and ONE-D) was presented.

Special consideration and attention was given to study the numerical modelling aspects of flood plain conveyance, in the context of unsteady flow in compound channels.

Traditional methods of splitting a compound channel into hydraulically homogeneous subdivisions were investigated, (Wormleaton, 1982) and a new approach to define the flood plain hydraulic boundaries was introduced. This new method uses outward-facing diagonal interface planes to define the flood plain storage areas. These diagonal planes make an angle Θ with the horizontal, and an equation relating Θ to the ratio of the flood plain depth to the total channel depth was developed.

1.4 THESIS DESCRIPTION

Chapter 2 deals with the major related research contributions of past years. The literature review is presented in a thematic rather than a chronological order.

Chapter 3 deals with the theoretical and mathematical formulation of the three dynamic routing models. For each model unsteady flow equations, assumptions, weaknesses, capabilities, and method of solution are discussed and evaluated.

Chapter 4 reviews possible statistical criteria for determining the best-fit simulated results as compared to observed data.

Chapter 5 deals with the application of DWOPER to both laboratory and field data sets. Model capabilities and data modifications are discussed. This chapter also addresses the question of flood plain conveyance.

Chapter 6 describes the application of EXTRAN to the two data sets. Model application, performance, calibration, and data modification are discussed.

Chapter 7 discusses the application of ONE-D to the data sets. The performance of the model is evaluated.

Chapter 8 compares the three model-simulated results to observed values. Also, a quantitative assessment of predictive errors of the three models is presented.

Finally, chapter 9 presents conclusions and recommendations for future research.

CHAPTER 2

LITERATURE REVIEW

2.1 INTRODUCTION

The literature dealing with flood routing is vast. However, there are a number of review papers and reports which sum up much of the existing knowledge and give a clear indication of the practical methods implemented to provide good results.

One of the most important phenomena in river hydraulics is the movement of flood waves in natural channels. A flood is the result of an excessive volume of run-off entering a channel over a restricted period of time, resulting in a translation of the wave which moves downstream. Flood routing is defined as a mathematical method (model) for predicting the changing magnitude and celerity of a flood wave which propagates through

a river, reservoir, or estuary. Flood waves are corresponding changes in water surface profile due to fluctuation in discharge rate. Flood waves travel downstream at a velocity greater than the water velocity. The wave becomes longer (dispersion) or lower (attenuation) as it moves downstream. Therefore, in the simulation exercise, predicting wave deformation or subsidence is one of the most important practical problems related to wave propagation along a channel.

The literature shows that engineers and mathematicians have been concerned with the behaviour of flood waves in channels for at least a century. In general, they used models to calculate hydrographs at a downstream station resulting from known hydrographs at an upstream station. Fletcher and Hamilton (1967) reported that routing equations can be written in terms of total flow rate or average velocity. Therefore, details of the velocity distribution are of no interest.

2.2 PERSPECTIVE ON FLOOD ROUTING

From a hydraulics viewpoint the propagation of flood waves in river channels is a gradually-varied unsteady flow problem. The theoretical basis for this problem was developed as early as the 17th century by eminent scientists, such as Newton (1687), Laplace (1776), Poisson (1816), and Boussinesq (1871), among others. In 1871, A. J. C. Barre' de Saint-Venant (1871) developed the one-dimensional differential equations for gradually-varied unsteady channel flow. The St. Venant equations consist of a conservation of mass equation:

$$A \frac{\partial V}{\partial x} + V T \frac{\partial y}{\partial x} + T \frac{\partial y}{\partial t} + V A_x^y + q = 0 \qquad (2\text{-}1)$$

where:

A = cross-sectional area of flow,

x = distance along the longitudinal axis of the channel,

y = depth of flow normal to the bottom,

t = time,

V = average velocity of flow,

Q = discharge in a section,

T = top width of flow in a section,

A_x^y = departure of bed from prismatic form, and

q = lateral inflow per unit width of channel.

and a conservation of momentum equation:

$$\frac{1}{g}\frac{\partial V}{\partial t} + \frac{V}{g}\frac{\partial V}{\partial x} + \frac{\partial y}{\partial x} = S_o - S_f + D_1 \qquad (2\text{-}2)$$

where:

S_o = bed slope, and

S_f = resistance slope, which is expressed as:

$$S_f = \frac{V|V|}{R\,C^2} = \frac{Q|Q|}{K^2} \qquad (2\text{-}3)$$

where:

C = the Chezy Coefficient,

R = hydraulic radius,

$K = A\,C\,\sqrt{R}$ = conveyance, and

D_1 = dynamic contribution of lateral discharge, expressed as:

$$D_1 = 0 \ , \quad \textit{for bulk lateral outflow} \qquad (2\text{-}4)$$

$$D_1 = \frac{V\,q}{2\,A\,g} \ , \quad \textit{for seepage outflow} \ , \qquad (2\text{-}5)$$

$$D_1 = \frac{V - u_1}{A\,g}\,q \ , \quad \textit{for lateral inflow} \qquad (2\text{-}6)$$

where:

u_l = x-component of the inflow-velocity vector, and
g = gravitational acceleration.

The St. Venant equations are based on the following assumptions:

- Flow in the channel is of substantially homogeneous density,
- Velocity is uniform over any cross-section,
- channel is sufficiently straight,
- Reach geometry is sufficiently simple,
- Channel slope is sufficiently mild and uniform throughout the reach to permit mathematical representation by one-dimensional model,
- Friction-resistance coefficient is the same as that for steady flow; hence, Manning's or Chezy's formulae are applicable.

Several research investigations have been done to thoroughly explore and understand the hydrodynamics of transient flows in rivers and estuaries, and then develop accurate, reliable, and economically practical techniques to devise a systematic approach for determining or predicting such flows.

The theoretical development and formulation of the St. Venant equations is mathematically complex. Hence, simplifications are necessary to attain a feasible solution of the salient properties of the wave. Studies were developed before the end of the 19th century, where simplifications included ignoring the inertial terms. These studies concluded that the speed of propagation of the kinematic wave is defined as the ratio of the increment of discharge to the increment of wetted area of the channel. Kleitz (1877) performed the

theoretical development of the aforementioned studies; whereas, Seddon (1900) performed experimental observations on the Mississippi-Missouri Rivers to validate the results obtained. Simplified methods can be categorized as: purely empirical; linearization of the Saint Venant equations; hydrologic, (based on the conservation of mass and an approximate relation between flow and storage); and hydraulic, (based on the conservation of mass equation and a simplified form of the conservation of momentum equation).

Analytical solution of the complete St. Venant equations is not mathematically feasible although Strelkoff (1970) states that analytical solutions can be obtained for very simplified and restricted cases. However, Massau (1889) established the first method of graphical integration of the Saint Venant equations based on the concept of characteristic lines. This graphical technique served the purpose of giving some solutions until the advent of large-scale electronic digital computers provided impetus to the development of rapid, routine, numerical solution techniques.

Contemporary numerical solutions appear to fall into one of the following categories:

- Development of a network of characteristics (Lai, 1965-a; Amein, 1966; Fletcher and Hamilton, 1967; and Baltzer and Lai, 1968).

- Explicit finite-differencing of characteristic equations on a rectangular network in the x-t plane (Stoker, 1957; Amorocho and Strelkoff, 1965; and Strelkoff and Amorocho, 1965).

- Direct, explicit finite-differencing of the equations of continuity and momentum in a rectangular net (Isaacson, Stoker and Troesch, 1965).

- Direct, implicit finite-differencing of the equations of continuity and momentum in a rectangular net (Lai, 1965-b; and Vasilev et al., 1965).

- Finite element techniques.

Liggett and Woolhiser (1967) presented a comprehensive study dealing with finite difference solutions of the shallow water equations. They concluded that experience with each of the above solution categories will show the best-suited for a specific application. In addition, the advent of high-speed computers have made it possible to obtain solutions of the complete St. Venant equations.

2.3 ROUTING MODELS

Many different simplified routing models have been developed throughout the last 50 years. Miller and Yevjevich (1975) presented an excellent summary dealing with various simplified approximations of flood wave propagation. In recent years, flood routing models based on the complete St. Venant equations have become economically feasible as a result of advances of computing equipment and improved numerical solution techniques.

2.3.1 EMPIRICAL MODELS

Empirical models are limited to applications with sufficient observations of inflows and outflows to calibrate the essential coefficients. They provide best results when applied to slowly fluctuating rivers with negligible lateral inflows and backwater effects. They are extremely economical in computational requirements; however, considerable effort may be required to derive the empirical coefficients.

2.3.1.1 Lag Models

Lag is defined as the time difference between inflow and outflow within a routing reach. Flood routing lag models are based on intuition and observations of past flood wave motion. Tatum (1940) developed a successive average-lag method based on the assumption that there is some point downstream where the flow (I_2) at time (t_2) is equal to an average

flow ($[I_1+I_2]/2$). Dividing the wave time of travel by the reach length, Tatum found the number of successive averages occurring within a reach. Also, outflow at the end of each reach is computed by:

$$O_{n+1} = C_1 I_1 + C_2 I_2 + \ldots + C_{n+1} I_{n+1} \qquad (2\text{-}7)$$

where n = number of sub-reaches (successive averages) within the routing reach. The routing C-coefficients can be computed by trial and error, or by Tatum's approach. In addition, Linsely et al. (1949) proposed that these coefficients can be computed using the least-squares correlation of inflow and outflow hydrographs.

Harris (1970) discussed a similar lag model known as the Progressive Average-Lag model which was developed by the U.S. Army Corps of Engineers (1935).

2.3.1.2 Gage Relations

Gage relations relate the flow at a downstream point to that at an upstream station. These relations may be based on flows, stages, or a combination of each, in which the effect of lateral inflow is automatically contained in the empirical relation; (Linsely et al, 1949).

2.3.2 LINEARIZED MODELS

Because of the complexity of the St. Venant equations simplifications are introduced to obtain solutions. Simplifications include totally ignoring the least important non-linear terms and/or linearizing the remaining terms of the equations. Common simplifying assumptions include:

- Ignore the $V\partial V/\partial x$ in the momentum equation, (eq. 2-2),

- Assume constant cross-sectional area, usually rectangular,

- Assume constant channel bottom slope, often set to zero,

- Friction slope term is linearized with respect to velocity and depth,

- No lateral inflow, and

- The routed flood wave has a simple shape that is amenable to an analytical expression.

2.3.2.1 Classical Wave Models

The classical wave models are developed by neglecting any lateral inflow terms, frictional resistance, and non-linear terms, such as $V\partial A/\partial x$ and $V\partial v/\partial x$. Abbott (1966) proposed the following analytical solution:

$$V = C_1 \ (x - \sqrt{g\,\bar{y}}\ t) + C_2 \ (x + \sqrt{g\,\bar{y}}\ t) \qquad (2\text{-}8)$$

where:

$\bar{y}$ = average depth, and

C_1 and C_2 = functions determined by initial flow and boundary conditions.

Dronkers (1964) studied extensively the case in which the channel cross-section is assumed rectangular with zero bottom slope, linearized resistance, and neglecting the $V\partial V/\partial x$ term.

2.3.2.2 Simple Impulse Response Model

Dooge (1973) used linear systems theory, which states that any linear system is completely and uniquely characterized by its unit impulse response, to develop routing techniques. In this approach, the routing model is assumed to be composed of linear reservoirs connected by linear channels. Maddaus (1969) and Sauer (1973) proposed a unit-

response approach for routing through a single linear reservoir. This approach is analogous to the unit hydrograph used by hydrologists to compute precipitation run-off. Also, it can be closely related to the lag-models.

2.3.2.3 Complete Linearized Models

Lighthill and Whitham (1955) and Harley (1967) developed linearized models of the complete St. Venant equations. The equations are written in terms of unit discharge (q) and depth (y) and then combined and linearized about a reference flow velocity ($V_o = q_o/y_o$). Bravo et al. (1970) report that the accuracy of the linearized model depends on the reference flow.

2.3.2.4 Multiple Linearized Models

Keefer and McQuivey (1974) introduced the concept of multiple linearization. They applied this concept to the Complete Linearized model of Harley (1967) and the Diffusion Analogy model of Hayami (Chow, 1959). However, they concluded that the latter was more practical.

Therefore, applicability of linearized models is limited by the assumptions adopted in their derivation. The Complete Linearized model and the Diffusion Analogy model of Hayami are the least restrictive.

2.3.3 HYDROLOGIC MODELS

In the early 1900's, significant river improvement projects led to the development of hydrologic models. Hydrologic models, alternatively known as simplified flood routing methods, are those where parameters are primarily obtained from hydrologic data such as measured hydrographs. They are based on the conservation of mass equation written as:

$$I - O = \frac{\Delta S}{\Delta t} \qquad (2\text{-}9)$$

where:

ΔS = change in storage within the reach,

Δt = time increment,

I = inflow,

O = outflow, and

$$S = K\,[\,X\,I + (1-X)\,O] \qquad (2\text{-}10)$$

X = weighting factor.

2.3.3.1 Reservoir Routing Models

These hydrologic routing models are developed based on assuming X = 0 in eq. 2-10. In other words, storage is assumed independent of inflow and is only dependent on outflow. Then eq. 2-9 is expressed in centred finite difference and solved step-by-step, based on known conditions of outflow and storage at the upstream end, to obtain a relation between S and O at the other end of the reach (S_2 and O_2). Another relation between S_2 and O_2 is obtained using observed inflow-outflow hydrographs. Consequently, the outflow (O_2) is determined.

2.3.3.2 Muskingum Model

The Muskingum model was developed by McCarthy (1938). Chow (1959) summarizes the Muskingum method for flood routing as follows:

$$\frac{S_2 - S_1}{\Delta t} = I - O \qquad (2\text{-}11)$$

where S_1 and S_2 are initial and final storage in a reach of length Δx. In addition, the flow and storage in any reach can be written as power functions of depth:

$$
\begin{aligned}
I &= a\, y_I^n \\
O &= a\, y_o^n \\
S_I &= b\, y_I^m \\
S_o &= b\, y_o^m
\end{aligned}
\tag{2-12}
$$

where a, n, b, and m are the fitted parameters. Combining eqs. 2-11 and 2-12 gives:

$$
\begin{aligned}
S_I &= b \left[\frac{I}{a} \right]^{\frac{m}{n}} \\
S_o &= b \left[\frac{O}{a} \right]^{\frac{m}{n}}
\end{aligned}
\tag{2-13}
$$

A weighting factor is introduced to represent the relative dependence of storage on its inflow and outflow. This is represented as:

$$S = X\, S_I + (1 - X)\, S_o \tag{2-14}$$

substituting eqs. 2-12 and 2-13 in eq. 2-14 gives eq. 2-10 where K = b/a and m/n = 1. Also, substituting eq. 2-13 in eq. 2-11 gives:

$$O_2 = C_1\, I_1 + C_2\, I_2 + C_3\, O_1 \tag{2-15}$$

where:

$$
\begin{aligned}
C_1 &= \frac{K X + \frac{\Delta t}{2}}{K (1 - X) + \frac{\Delta t}{2}} \; ; \\
C_2 &= \frac{-K X + \frac{\Delta t}{2}}{K (1 - X) + \frac{\Delta t}{2}} \; ; \; and \\
C_3 &= \frac{K (1 - X) - \frac{\Delta t}{2}}{K (1 - X) + \frac{\Delta t}{2}}
\end{aligned}
\tag{2-16}
$$

Time increments are chosen in such a manner to give positive coefficients. The coefficients are all positive satisfying the following condition:

$$C_1 + C_2 + C_3 = 1 \qquad (2\text{-}17)$$

Singh and McCann (1980) used several methods to determine the parameters K and X from observed inflow-outflow hydrographs. These techniques include:

- Least Squares or its equivalent graphical method,
- Method of moments,
- Method of cumulants, and
- Direct optimization method.

However, Singh and McCann conclude that there is no advantage of one technique over the other.

The Muskingum method has enjoyed notable success and preference over other hydrologic models due to its flexibility in calibration. Another advantage is that it does not require a knowledge of the river bed geometry. It has only two parameters which can be closely linked to the speed and subsidence of the wave crest. Kouwen (1984) states:" The application of the Muskingum method requires measured hydrographs at the upstream and downstream sections of a reach before the parameters can be determined. However, no knowledge of the channel dimensions is needed ".

2.3.3.3 The Convex Method

The convex method is based on the following principle: when a natural flood passes through a stream channel having negligible local inflows or transmission losses there is a reach length L and a time interval Δt such that O_2 is not more than the larger nor less than the smaller of the two flows I_1 and O_1. Δt is considered as both the travel time of the flood

wave through the reach measured at the beginning of the rising portion of the hydrograph at both ends of the reach; and the required routing time interval.

In other words, this principle can be expressed as:

$$If \quad I_1 \geq O_1 \ , \quad then \ I_1 \geq O_2 \geq O_1 \tag{2-18}$$

$$If \quad I_1 \leq O_1 \ , \quad then \ I_1 \leq O_2 \leq O_1 \tag{2-19}$$

and

$$O_2 = (1 - C)\ O_1 + C\ I_1 \tag{2-20}$$

where C is a parameter between zero and one. From similarity of triangles in (figure 2.1), the following relation can be written:

$$\frac{O_2 - O_1}{\Delta t} = \frac{I_1 - O_1}{K} \tag{2-21}$$

where K is the reach travel time for a selected steady flow, measured in seconds. Manipulating eqs. 2-20 and 2-21 leads to:

$$\frac{\Delta t}{K} = C \tag{2-22}$$

2.3.3.4 Muskingum-Cunge Method

Cunge (1969) developed an important variation of the Muskingum model based on the Kinematic Wave theory. The basic assumption is that there exists a unique single-value stage-discharge relationship along with the use of a four-point implicit finite difference approximation technique. Cunge (1969) states: "When strictly applied, the assumption leads to a differential equation whose analytical solution does not allow for wave damping". In addition to the Muskingum equations, Cunge introduced the following expressions:

$$K = \frac{\Delta x}{C}$$

$$C = \frac{dQ}{dA} \qquad (2\text{-}23)$$

$$X = 1 - \theta_x = \frac{1}{2} - \frac{Q_o}{2\, B_o\, C\, S_o\, \Delta x}$$

where:

C = kinematic wave speed corresponding to a reference discharge Q_o,

B_o = channel width corresponding to the reference discharge Q_o, and

S_o = channel bottom slope.

Cunge explains that the numerical solution of the differential equations results in attenuation. He suggests that it is pointless to explain this attenuation in terms of "Wedge or Prism" storage. However, Cunge concludes that damping effects are due to the use of coefficients in the Muskingum formula which, according to him, is an approximation of the exact differential equation. Among his many conclusions, he showed that the wave speed w, as obtained from the "approximate" equation, is different from C. Also, he derived the weighting coefficient X based on an error correction term.

Price (1975) elaborated on this topic and introduced an attenuation parameter related to the total reach length, flooded area in sub-reach, length of sub-reach, and bottom slope of sub-reach. This parameter can be applied when the attenuation along the reach is not more than 10 % of the peak inflow. After that range (10 %), the higher order derivatives should not be neglected in the basic formulation.

2.3.3.5 Kalinin-Miljukov Model

Miller and Cunge (1975) reported the Kalinin-Miljukov method as a variation of the Muskingum method. It was developed in the 1950's in the U.S.S.R. with K = Δx/C and X = 0. Also Miller and Cunge (1975) showed that the SSARR Routing Model (Rockwood,

1958) is another modification of the Muskingum model in which X = 0.

2.3.3.6 Lag and Route Model

This is a storage routing model (Linsely et al.,1958) based on a combination of storage routing principles and empiricism introduced through the lag factor. Yet another lag and route model was reported by Quick and Pipes (1975).

2.3.4 HYDRAULIC MODELS

Hydraulic routing models are those whose parameters are obtained from channel cross-sections and other physical river data. Several hydraulic methods have been introduced based on the complete St. Venant equations or simplifications of the momentum equation.

2.3.4.1 Simplified Hydraulic Models

2.3.4.1.a "Storage" or "Simple" Routing Models

Simplifications include neglecting the last 3 terms of the momentum equation (eq. 2-2) which basically reduces to the Chezy formula for uniform flow. In this method, a reach is subdivided into suitable length increments and the continuity and simplified momentum equations are solved recursively. Writing the continuity equation in finite difference form gives:

$$\frac{I - O}{\Delta x} + \frac{A_2 - A_1}{\Delta t} = q \qquad (2\text{-}24)$$

where:

$\partial Q = \Delta Q =$ difference between inflow I and outflow O over a reach length,

A_2-A_1 = change in cross-sectional area during a period Δt.

Multiply eq. 2-24 by $\Delta x\ \Delta t$ and rearrange to give:

$$S_2 = [S_1 + I_1 - O_1 - O_2]\ \frac{\Delta t}{2} \qquad (2\text{-}25)$$

where:

$$S = A\ \Delta x = storage\ in\ a\ reach \qquad (2\text{-}26)$$

O_1 and S_1 represent the initial conditions. The simplified form of the momentum equation can be used to relate S_2 and O_2 to lead to the solution of S_2.

Viessmann et al.(1977) states that this method is recommended for watershed and reservoir routing. However, the exclusion of the extra slope terms of the momentum equation reduces its usefulness.

2.3.4.1.b Storage-Indication Routing Models

These models are also referred to as the Modified Puls Method. They are very similar to Simple Routing Models in formulation and are applicable to reservoir routing.

2.3.4.1.c Kinematic Wave Routing Model (K-W)

Lighthill and Whitman (1955) sparked interest in this model. It is based on the following simplification of the momentum equation:

$$S_f - S_o = 0 \qquad (2\text{-}27)$$

which basically states that the momentum of unsteady flow is assumed equal to that of steady flow. It can be represented using Chezy's or Manning's equation or any other similar expression. Using the cross-sectional data of the river, a single-value stage-

discharge relationship is obtained having the following form:

$$A = \alpha Q^{\beta} \tag{2-28}$$

where:

$$\alpha = \left[\frac{B}{C^2 S_o} \right]^{\frac{1}{3}} ,$$

$$\beta = \frac{2}{3} \quad , \quad and \tag{2-29}$$

$$C = Chezy's\ coefficient .$$

Li et al.(1975, 1976) derived the non-linear kinematic wave model by combining eq. 2-28 with the continuity equation of the following form:

$$\frac{\partial Q}{\partial x} + \alpha \beta Q^{\beta-1} \frac{\partial Q}{\partial t} = 0 \tag{2-30}$$

The resulting equation can be solved using explicit or implicit finite difference techniques.

Henderson (1966) states that routing is a pure translation of the flood wave. He supports his conclusion by saying that if an observer is moving with a velocity equal to the speed of the wave crest in a prismatic rectangular channel, the depth and flow will appear to be constant. This means that the shape of the wave is not changed , and no attenuation of the peak occurs.

Wooding (1965); Liggett and Woolhiser (1967); and Gburek and Overton (1973) successfully applied the K-W model to overland flow routing of precipitation run-off. On the other hand, Harley et al.(1970) used the K-W model in the M.I.T. Catchment Model for stream flow applications.

The Kinematic Wave Model is limited to applications where single-value stage-

discharge ratings exist, and where backwater effects are insignificant because flow disturbances can only propagate in the downstream direction in a K-W model. Also K-W models require river flow properties to be properly described by simple differentiable functions [A = fn (Q)]. This is difficult to meet for complex natural cross-sections. Also, the lack of attenuation essentially precludes their use for practical applications.

2.3.4.1.d Diffusion Model

Diffusion models involve another simplification of the momentum equation, which allows for upstream directed flows, where:

$$S_f - \frac{\partial h}{\partial x} = 0 \qquad (2\text{-}31)$$

This equation can be expressed in terms of the channel conveyance K in a single-value stage-discharge relationship as:

$$Q = \frac{-K\left(\frac{\partial h}{\partial x}\right)^{\frac{1}{2}} \frac{\partial h}{\partial x}}{\left|\frac{\partial h}{\partial x}\right|} \qquad (2\text{-}32)$$

Brakensiek (1965) solved eqs. 2-31 and 2-32 using a four-point centred finite difference solution technique whereas Harder and Armacost (1966) used an explicit finite difference technique.

Since the simplified momentum equation includes the water surface elevation term then the diffusion model allows to describe attenuation of the flood wave. This is a basic improvement over the K-W models. However, the diffusion model does not account for inertial terms in the simplified momentum equation. Consequently, its application is limited to slow to moderately rising flood waves in almost uniform-geometry channels.

2.3.4.2 COMPLETE (DYNAMIC) HYDRAULIC MODELS

In general, diffusion models have wider applicability than K-W models. For example, they can accommodate milder bottom slopes. However, there are some applications where simplified modelling is not suitable and a complete solution of the St. Venant equations should be performed. As early as the 1950's, several attempts were made to solve the complete dynamic St. Venant equations for flood routing on the Ohio River; (Stoker, 1953; and Isaacson et al, 1954). Later efforts saw the development of several dynamic flow models with different solution schemes.

2.3.4.2.a Characteristic Models (CM)

These models were developed as early as the 1960's. Liggett and Woolhiser (1967); Streeter and Wylie (1967); and Baltzer and Lai (1968) used explicit characteristic schemes in developing their models. On the other hand, Amein (1966) and Wylie (1970) used implicit characteristic schemes. The CM is based on four total differential equations which are solved using curvilinear or rectangular grids. Curvilinear grids are not practical for applications in natural waterways of irregular geometry. Also, rectangular grids in the x-t domain require interpolation formulae meshed within the finite difference solution procedure. Therefore, based on these restrictions, the CM is not suitable for flood routing.

Sivaloganathan (1978) developed a new technique called the Characteristic Method of specified distances. Also, he compared a rectangular grid characteristic method using Langrangian interpolation and a special algorithm for the downstream boundary that enables the method to be used for all types of downstream boundary conditions. He concluded that his method takes appreciably less computing time than the rectangular grid characteristic method. However, the latter requires less storage and is easier to program.

Liggett and Woolhiser (1967) state that the CM method is most accurate for the same initial point spacing. It is fast where it covers a given part of the x-t plane in the least

time. However, they conclude that it is difficult to obtain acceptable data at intermediate points, and this constitutes the chief disadvantage of the CM method.

2.3.4.2.b Power Series Method

Baltzer and Lai (1968) used the Power Series method to solve the St. Venant equations for unsteady flows in waterways. The Power Series method uses a Maclaurin series expansion of the governing partial differential equations. The expansion is made for a given moment at a point (X_1), along the waterway in terms of water stage (Z_1), in order that the associated stage (Z) at a nearby point X may be determined. Then a unique finite difference solution for the transient flows at subsequent times is obtained using the known boundary conditions. Dronkers and Schönfeld (1955) used a somewhat similar iterative procedure.

2.3.4.2.c Explicit Methods

Explicit methods, as the term indicates, solve directly the following two algebraic linear equations for the unknowns:

$$A \frac{\partial V}{\partial x} + V \frac{\partial A}{\partial x} + B_T \frac{\partial y}{\partial t} - q = 0 \ , \quad and \tag{2-33}$$

$$\frac{\partial V}{\partial t} + V \frac{\partial V}{\partial x} + g \left[\frac{\partial y}{\partial x} - S_o + S_f \right] + \frac{(V - v_x)\, q}{A} = 0 \tag{2-34}$$

where: B_T = wetted top width (active, and inactive or off-channel storage areas).

Explicit methods advance the solution, point by point from one time line to the next in the x-t domain until all the unknowns associated with the time line are evaluated. Explicit methods were applied as early as the 1950's by Stoker (1953) and Isaacson et al. (1954, 1958) to route floods in the Ohio River. Dronkers (1969) and Thatcher and

Harleman (1972), among others, used explicit methods to analyze tidal movements in estuaries. On the other hand Johnson (1974) and Garrison et al.(1969) applied this method for flood routing in reservoirs.

Many variations of the explicit schemes were introduced. Richtmyer and Morton (1957) reported the Lax-Wendroff two-step scheme to successfully obtain solutions of the gas dynamics equations. However, disappointing results were obtained when Liggett and Woolhiser (1967) applied this scheme to shallow water equations with particular boundary conditions. A second popular scheme is the Leap-Frog which led to the same result as the Lax-Wendroff schemes when applied to shallow water equations. A third one is the Diffusion Scheme, which proved empirically stable for all cases except the rising part of the hydrograph under certain conditions.

Although simple in formulation, the explicit method has a restriction on the size of the computational time step due to numerical stability considerations. The Courant Condition:

$$\Delta t \leq \frac{\Delta x}{V + \sqrt{g \frac{A}{B}}} \qquad (2\text{-}35)$$

is necessary for numerical stability. However, satisfying the Courant condition does not guarantee that the method is stable. Investigating the Courant criterion indicates that the time step is substantially reduced as the hydraulic depth (A/B) increases. The stability requirement imposes that the time step size should be in the order of seconds or few minutes as a maximum. Correspondingly, the explicit method is inefficient in the use of computer time.

Strelkoff and Amarocho (1965) found that even if the method is empirically stable, the equation of continuity may not be satisfied. In other words, over a long period of time, inflow may be greater or less than outflow plus accumulation of storage. Liggett and Woolhiser (1967) state: "In general, this method (explicit) is completely unsatisfactory for

even rough and approximate calculations".

2.3.4.2.d Implicit Method

Implicit finite difference schemes advance the solution of the St. Venant equations from one time line to the next simultaneously for all points along the time line. Implicit methods are ideally applied to solutions of problems requiring computations over a long time period. Ponce et al (1978) report that implicit numerical schemes are generally preferred over explicit schemes because they allow larger time steps and consequently reduce the computational effort. Amein and Fang (1970) state that implicit methods give the same results as those obtained using any other numerical scheme; however, they provide the results much faster.

Cunge and Wegner (1964), Amein and Fang (1970), and Fread (1974), among others, used the Four-Point implicit finite difference scheme to solve the unsteady flow equations. This scheme, also referred to as Preissmann's scheme, has received wide attention. A weighting factor is introduced to approximate the spatial derivatives by a finite difference quotient positioned between two adjacent lines. Baltzer and Lai (1968) and Amein and Chu (1975) used a weighting factor of 1.0, which resulted in the formation of a fully implicit scheme. Amein and Fang (1970) used a weighting factor of 0.5, which led to a "box" scheme. Fread (1974) examined the influence of the weighting factor on stability and convergence properties. He concluded that accuracy decreases as the weighting factor departs from 0.5 and approaches 1.0, and that this effect becomes more pronounced as the time step size increases. A value of 0.55 is often used to minimize loss of accuracy while avoiding weak or pseudo-instability, as reported by Baltzer and Lai (1968) when a weighting factor of 0.5 was used.

Cunge (1966), Abbott and Ionescu (1967), Gunaratnam and Perkins (1970), Fread (1974), and Ponce (1978), among others, analyzed the numerical stability of the various implicit techniques. Chaudry and Contractor (1973) and Fread (1974) showed that

instability can occur if the time step is too large. In addition, the time step is chosen in such a way as to satisfy accuracy requirements.

In an implicit scheme, a system of 2N algebraic equations is generated from the St. Venant equations applied simultaneously to the N cross-sections along the x-axis. This system could be linear or non-linear depending on the type of implicit scheme adopted. Linear implicit schemes require only one solution of the system of equations at each time step; (Chen et al., 1957). The time step should be small enough to satisfy accuracy requirements for rapidly changing transient flows using linear methods. On the other hand, non-linear implicit schemes require an iterative solution where the system of equations is solved once or more at each time step. The Newton-Raphson method is efficient for solving non-linear systems which are effective when applied to waterways with non-prismatic geometry.

Abbott and Ionescu (1967) and Vasilev et al (1965) proposed a six-point implicit scheme; however, this scheme requires the use of regular Δx intervals whereas the four-point schemes allow variable Δx spacing. Amein and Fang (1970) state two factors that work in favour of implicit methods:

- The method is stable for large time steps with no loss of accuracy.

- Although the system of equations is large, each equation by itself contains at most only four unknowns.

In addition, they state: "The implicit method can also handle varying channel geometry even where the changes from section to section and in the bottom slope are quite significant".

2.3.5 FINITE ELEMENT MODELS

Cooley and Moin (1976) applied the finite element method to solve the complete St. Venant equations. For one dimensional flow, the finite element method is not advantageous over the four-point implicit scheme because its mathematical basis is not easily understood and applied. However, it is advantageous when applied to two-dimensional unsteady flow problems.

2.3.6 TWO-DIMENSIONAL MODELS (2-D)

Hinwood and Wallis (1975, a, b) and Abbott (1976), among others, applied two-dimensional models in their complete form, whereas Cunge (1975) and Vicens et al.(1975) used the simplified forms. The 2-D models are more complex than the 1-D models, and their use is limited to applications where a large amount of flow information is desired in complex unsteady flow problems.

2.4 STABILITY OF NUMERICAL TECHNIQUES

Stability refers to the ability of the numerical scheme to march in time without generating unbounded error growth; (Ponce et al., 1978). Stability is governed by round-off errors and is impaired if the discretization is made finer. In the past few decades, research has mainly aimed at thoroughly exploring and understanding the hydrodynamics of transient flows in rivers and estuaries, and then, to develop accurate, reliable, and economically practical techniques to devise a systematic approach for determining or predicting such flows.

A finite-difference procedure for calculating time-dependent phenomena is considered stable when small numerical errors of truncation and round-off inevitably introduced at time t_0, are not amplified during successive applications of the procedure, and at subsequent time t have not grown so large as to obscure the valid part of the solution;

(Strelkoff, 1970). In practical computation experience, instability of a process for calculating unsteady open-channel flows shows wide oscillation in both stages and discharges with respect to both distance and time (x and t).

Historically, the stability of numerical schemes was based on the representation of the corresponding function in terms of a Fourier Series. Richtmyer (1962), among others, attributes the stability method to John Von Neuman who in turn credits Courant with the original idea. Von Neuman considers his work as a "slightly simplified version". He applied his analysis to a system of two parabolic equations describing two-phase flow in an oil-bearing porous stratum. Based on the report for the Standard Oil Company (1963), the stability of numerical methods for solving hyperbolic equations in open channel flow had been developed at the SOOGREAH Laboratories (France) and the Steklov Institute Of Mathematics (Moscow) and at the Hydrodynamics Institute (Akademgorodok, Novosibirsk).

2.4.1 Von Neuman Technique

There is no criterion to determine the stability of the non-linear hyperbolic differential equations. However, stability can be investigated for a simpler system, related to the complex original system assuming constant coefficients and linearizing the system. Stability analyses are carried out, not so much to ensure that a given scheme will be stable, but to permit the researcher to discard those schemes which can be shown unstable from the start.

The basic procedure involves assuming error functions between computed and observed stages and discharges. The growth or decay of these errors after repeated applications is investigated for the linearized system with constant coefficients. The assumption of constant coefficients is valid because if the scheme is unstable, then the error function will vary far more rapidly than the coefficients. These error functions are assumed to be composed of the Fourier Series. The amplitude of each component of the series is examined to see if it increases after repeated applications. If the amplitude remains

bounded, then the scheme is judged stable.

2.5 CONVERGENCE OF NUMERICAL SCHEMES

Convergence refers to the ability of the scheme to reproduce the terms of the differential equation with sufficient accuracy. Convergence is governed by discretization errors. It is not impaired if the discretization is made finer. Convergence is the focal issue because if the model is shown to be stable, it becomes necessary to assess the convergence properties.

Ponce et al. (1978) analyzed the convergence of the Four-Point implicit numerical model. Ponce tested the convergence by establishing the ratio of attenuation and translation given by numerical and analytical techniques. He concludes that convergence is a function of the complex interaction of five parameters:

- The Froude number (F),
- Dimensionless wave number ($2\pi d/S_o L$),
- Spatial resolution ($\pi\Delta x/L$),
- Courant number C ($c\Delta t/\Delta x$), and
- Weighting factor of the implicit scheme (θ).

2.6 CONVEYANCE CHARACTERISTICS

In analyzing flow through open channels of regular cross-sectional shape and hydraulic roughness, it is sufficient, in general, to use the overall hydraulic radius as the parameter which best characterizes the properties of the cross-section. However, if the

cross-sectional shape is irregular, this approach can introduce considerable error. An example of this is a compound channel consisting of a relatively deep main channel flanked by shallow flood plains. The velocity difference between the main channel and the flood plain flows results in lateral transfer of momentum from the relatively fast main channel flow to the much slower flood plain flows. The high longitudinal shear stresses arising in the interface zones (and consequent energy losses) tend to reduce the discharge capacity of the compound section; (Wormleaton, 1982).

The most commonly used and expedient methods for calculating discharges in compound channels are based on the concept of splitting the cross-section into hydraulically homogeneous subdivisions. The discharges for each subdivision are calculated individually and then summed to give the overall section discharge. Different methods based on this concept were introduced by various investigators. However, they only differ in the assumptions made regarding the location and nature of the imaginary interface planes separating the main channel and flood plain zones. Wright and Carstens (1970) proposed that such interfaces should be included in the wetted perimeter calculation for the main channel subdivision only. Wormleaton (1982) examined the relative effectiveness of the different types of imaginary interface planes commonly used; namely, horizontal, vertical, and diagonal planes. He noted that the most commonly used method in calculating discharge in rectangular compound channels adopts a vertical interface plane. He also stated that using horizontal or (inward) diagonal interface planes, in general, gave better results than vertical planes for low flood plain depths.

Yen and Overton (1973) found an empirical relationship between the angle of inclination of (inward) diagonal interface planes and the depth of flow on the flood plain. The angle of inclination to the horizontal increased with flood plain depth. Moreover, they suggested that the interfaces could be reasonably closely approximated by lines drawn from the main channel/flood plain junction to a point on the water surface at the main channel centre-line. These interfaces were referred to as diagonal interfaces.

2.7 CONCLUSIONS

In the literature a wide spectrum of usable and reasonably accurate mathematical models are available for flood routing. The variability can be attributed to the fact that the phenomenon is very important from the physical point of view.

Among the models reviewed, those based on the complete form of the St. Venant equations are undoubtedly the most descriptive. Calibration (estimation of the roughness parameter) is notably simple in these models due to the presence of one parameter. However, their use may be numerically complex especially for applications where the river bed has significant length and abruptly varying section.

Other models, which are only based on the continuity equation, are certainly the oldest and even today earn wide acceptance for their intrinsic simplicity. In these simpler models the dynamic phenomena of the flood wave propagation are implicitly resolved during the calibration. Simple characteristics of the flood wave such as the speed and the flattening rate of the crest are required and the results obtained are reasonably acceptable.

To sum up, combining the theoretical investigations with the concrete applications, it can be accepted that the general principles of flood wave propagation in open channels are now well understood.

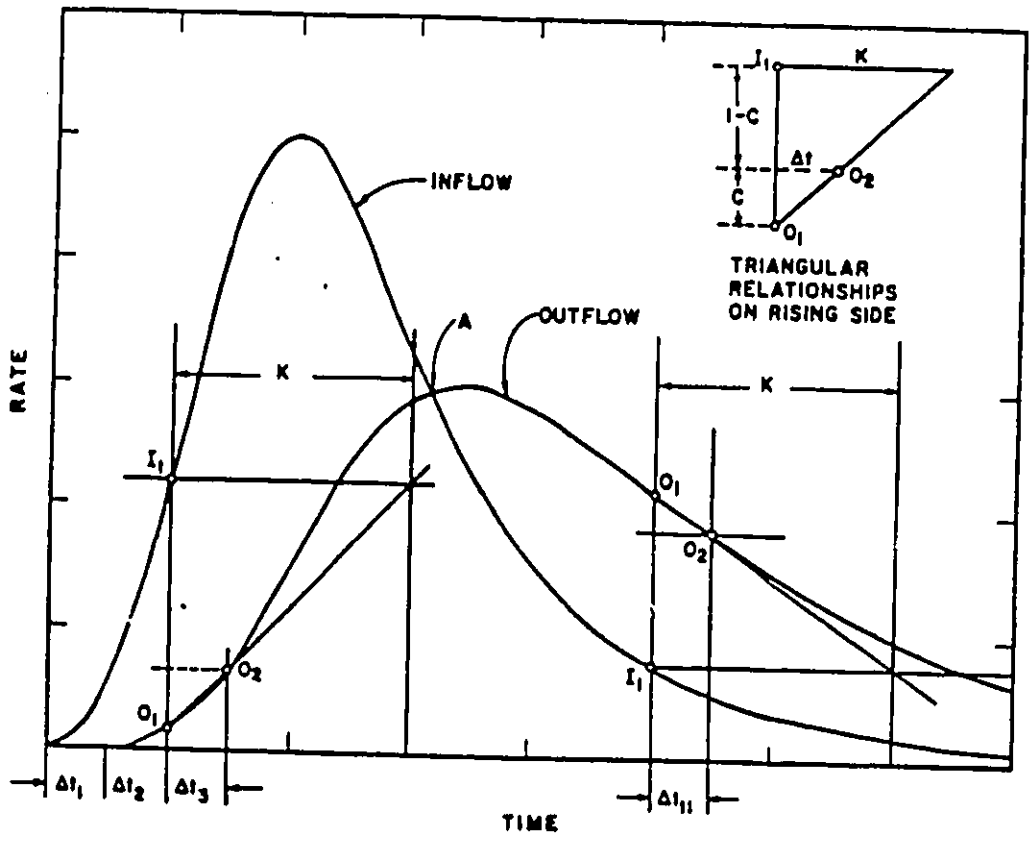

Figure 2.1 RELATIONSHIP FOR CONVEX METHOD OF CHANNEL ROUTING.

CHAPTER 3

THEORETICAL BACKGROUND

3.1 FLOOD ROUTING

3.1.1 Definition and Objective

Flood routing is defined as a mathematical method (model) for predicting the changing magnitude and celerity of a flood wave which propagates through a river or estuaries The objective of any flood routing method is to trace the wave propagation along a channel (or conduit). Flood routing aims at determining the following time and space variants:

1- Flow rate $Q = f(x,t)$,
2- Flow depth $y = g(x,t)$, and
3- Flow velocity $v = h(x,t)$.

3.1.2 Governing Equations

As a flood wave travels through a channel (or conduit) its peak is usually attenuated and its base extended. The channel flow is usually unsteady and non-uniform. The governing equations which represent conservation of mass and momentum are known as the St. Venant equations.

The conservation of mass equation is referred to as the continuity equation. It has the following form:

$$\frac{\partial Q}{\partial x} + \frac{\partial A}{\partial t} = q \qquad (3\text{-}1)$$

Expressed in terms of velocity, the continuity equation takes the following form:

$$A \frac{\partial V}{\partial x} + V B \frac{\partial y}{\partial x} + B \frac{\partial y}{\partial t} = q \qquad (3\text{-}2)$$

where:

Q = flow rate,

V = flow velocity,

A = cross-sectional area,

x = space coordinate,

t = time coordinate,

y = flow depth,

B = top width, and

q = lateral inflow per unit length of channel.

The terms on the left hand side of the eq. 3-2 represent prism storage, wedge storage, and a rate of rise respectively; (figure 3.1).

The other equation in flood routing exercise is the conservation of momentum

equation which takes the following form:

$$\frac{1}{A}\frac{\partial (Q/A)^2}{\partial x} + \frac{1}{A}\frac{\partial Q}{\partial t} + \frac{q}{B}\frac{\partial A}{\partial x} - g\,(S_o - S_f) = -\frac{V\,q}{A} \qquad (3\text{-}3)$$

where:

S_o = channel bed slope, and

S_f = friction slope.

In terms of velocity it is written as:

$$V\frac{\partial V}{\partial x} + \frac{\partial V}{\partial t} + g\frac{\partial y}{\partial x} - g\,(S_o - S_f) = -\frac{V\,q}{A} \qquad (3\text{-}4)$$

The terms on the left hand side of the momentum equation (eq. 3-3) represent convective acceleration, local acceleration, pressure force, gravity force, and friction force respectively.

Flow resistance can be approximated by applying expressions developed for uniform steady flow. Thus, the friction slope S can be expressed in terms of Manning's n, Chezy's C, or the Darcy-Weisbach friction factor f. When the channel geometry is known, the only parameter involved in the solution of the St. Venant equations is the roughness coefficient.

3.1.3 Hydraulic Routing Models

Hydrauiic routing methods can be divided into:

i- Complete dynamic models, which are based on solutions of the full St. Venant equations, and

ii- Approximate hydraulic routing models which are based on conservation of mass and simplified forms of the momentum equation.

Simplifications of the momentum equation are usually obtained by omitting or linearizing

some of the terms involved. In the "Kinematic Wave" Approximation, the momentum equation is simplified to:

$$S_o = S_f \qquad (3\text{-}5)$$

On the other hand, in the "Diffusive Wave" Approximation, the momentum equation is written as:

$$\frac{\partial y}{\partial x} = S_o - S_f \qquad (3\text{-}6)$$

Therefore, hydraulic routing models incorporate differential equations with no direct mathematical solutions. They can only be solved numerically by replacing the differential equations with equivalent (approximating) finite difference equations.

3.2 DWOPER MODEL

3.2.1 Introduction

DWOPER, or Dynamic Wave Operational Model, is a hydrodynamic wave routing model based on an implicit finite difference solution of the complete one-dimensional St. Venant equations of unsteady flow. It was developed by the U.S. National Weather Service (NWS) Hydrologic Research Laboratory in 1978, (Fread, 1987). Being based on an implicit scheme, DWOPER features the ability to use large time steps for slowly varying floods, and to use cross-sections of varying physical features. The model has a highly efficient automatic calibration feature for determining the optimum roughness coefficients for a single channel or a system of channels.

3.2.2 Mathematical Basis

DWOPER is based on a finite difference solution of the conservation form of the one-dimensional equations of unsteady flow. These equations confirm the conservation of

mass and momentum. The conservation of mass equation, alternatively called the continuity equation, has the following form:

$$\frac{\partial Q}{\partial x} + \frac{\partial (A - A_o)}{\partial t} - q = 0 \qquad (3\text{-}7)$$

The conservation of momentum equation takes the following form:

$$\frac{\partial Q}{\partial t} + \frac{\partial (Q^2/A)}{\partial x} + g A \left[\frac{\partial y}{\partial x} + S_f + S_e\right] - q V_x + W_f B = 0 \qquad (3\text{-}8)$$

where:

A_o = off-channel cross-sectional area (wherein the velocity is negligible),

g = gravitational acceleration constant,

V_x = lateral inflow velocity in the x-direction,

W_f = wind term,

S_f = friction slope, and is defined as:

$$S_f = \frac{n^2 Q |Q|}{2.2 A^2 R^{4/3}} \qquad (3\text{-}9)$$

where:

n = Manning's roughness coefficient, and

R = hydraulic radius.

The term S_e is defined as follows:

$$S_e = \frac{K_e}{2g} \frac{\partial (Q/A)^2}{\partial x} \qquad (3\text{-}10)$$

where K_e = expansion-contraction coefficient.

3.2.3 Solution Techniques

Equations (3-7) and (3-8) are non-linear differential equations which can be solved, without any further mathematical simplifications, by finite difference (explicit or implicit)

techniques. Explicit methods are restricted by stability requirements to very small computational time steps. Time steps in the order of seconds or few minutes on the maximum are usually used. The Courant criteria is used to check the stability of the explicit scheme. Therefore, explicit techniques are not efficient in the use of the computer time.

Implicit methods on the other hand are more suitable when modelling long-term unsteady flow phenomena, such as flood waves. The implicit formulation allows the time step size to be selected according to accuracy requirements rather than numerical stability requirements, (Fread, 1987). This feature makes efficient use of the computer time. Price (1974) states that "implicit schemes are preferred over explicit schemes because they allow larger time steps and thus reduce the computational effort". Among the implicit schemes, the "weighted four-point" method received wide attention. This method was first used by Preissmann (1961), and later by Quinn and Wylie (1972), Chaudry and Contractor (1973), Fread (1973, 1974), and Ponce et al.(1978). Ponce (1978) states that "the stability and convergence properties of this technique are as yet not fully understood". Ponce (1978) concluded that the convergence is a function of the complex interaction of five parameters:

1- Froude number of the equilibrium flow,
2- Dimensionless wave number,
3- Spatial resolution,
4- Courant number, and
5- Weighting factor of the implicit scheme.

3.2.4 Solution Method

The weighted four-point implicit scheme is considered superior to other implicit schemes proposed. It can be used with unequal distance steps and its stability-convergence properties can be controlled. Using this method, the x-t region, where solutions of Q and h are sought, is represented by a rectangular net of discrete points of equal or unequal

intervals of distance and time steps along the x and t axes, respectively. Each point in the domain is identified by a subscript (i) designating the x-position, and a superscript (j) representing the t-position.

The time derivative of any variable, represented by K, can be approximated using the following equation:

$$\frac{\partial K}{\partial t} \approx \frac{K_i^{j+1} + K_{i+1}^{j+1} - K_i^j - K_{i+1}^j}{2\,\Delta t} \qquad (3\text{-}11)$$

Furthermore, the spatial derivatives are approximated by a finite difference quotient positioned between two adjacent time lines. These derivatives are weighted by factors of α and $(1\text{-}\alpha)$, and take the following form:

$$\frac{\partial K}{\partial x} \approx \alpha \frac{K_{i+1}^{j+1} - K_i^{j+1}}{\Delta x} + (1-\alpha) \frac{K_{i+1}^j - K_i^j}{\Delta x} \qquad (3\text{-}12)$$

In the same manner variables, other than derivatives, can be approximated. In general, an approximation of K-variable can be weighted thus:

$$K \approx \alpha \frac{K_i^{j+1} + K_{i+1}^{j+1}}{2} + (1-\alpha) \frac{K_i^j + K_{i+1}^j}{2} \qquad (3\text{-}13)$$

The weighting factor α was introduced to approximate the spatial derivatives by a finite difference quotient positioned between two adjacent time lines. Amein and Chu (1975) and Baltzer and Lai (1968) used a weighting factor of 1.0, which resulted in the formation of a fully implicit scheme. Amein and Fang (1970) used a weighting factor of 0.5, which led to a "box" scheme. Fread (1974) examined the influence of the weighting factor on the stability and convergence properties. He concluded that accuracy decreases as the weighting factor departs from 0.5 and approaches 1.0, and that this effect becomes more pronounced as the time step size increases. A value of 0.55 is often used to minimize loss of accuracy while avoiding weak or pseudo-instability, as reported by Baltzer and Lai (1968) when a weighting factor of 0.5 was used.

Substitution of the finite difference equations 3-11, 3-12, and 3-13 into equations 3-7 and 3-8 results in two algebraic equations having the following form:

$$\begin{aligned} &\frac{1}{2\,\Delta t}\left[(y_{i+1}^{j+1}+y_i^{j+1})-(y_{i+1}^{j}+y_i^{j})\right] \\ &+\frac{1}{2\,\Delta x}\left[v_{i+\frac{1}{2}}^{j+\frac{1}{2}}\right]\left[(y_{i+1}^{j+1}+y_{i+1}^{j})-(y_i^{j+1}+y_i^{j})\right] \\ &+\frac{1}{2\,\Delta x}\left(\frac{A}{B}\right)_{i+\frac{1}{2}}^{j+\frac{1}{2}}\left[(v_{i+1}^{j}+v_{i+1}^{j+1})-(v_i^{j}+v_i^{j+1})\right] \\ &-\left(\frac{q}{B}\right)_{i+\frac{1}{2}}^{j+\frac{1}{2}}=0\ ,\quad \textit{and} \end{aligned} \tag{3-14}$$

$$\begin{aligned} &\frac{g}{2\,\Delta x}\left[(y_{i+1}^{j+1}+y_{i+1}^{j})-(y_i^{j+1}+y_i^{j})\right] \\ &+\frac{1}{2\,\Delta t}\left[(v_{i+1}^{j+1}+v_i^{j+1})-(v_{i+1}^{j}+v_i^{j})\right] \\ &+\frac{1}{2\,\Delta x}\,v_{i+\frac{1}{2}}^{j+\frac{1}{2}}\left[(v_{i+1}^{j+1}+v_{i+1}^{j})-(v_i^{j}+v_i^{j+1})\right] \\ &+\frac{g}{4}\left(S_{f_i}^{j}+S_{f_{i+1}}^{j}+S_{f_i}^{j+1}+S_{f_{i+1}}^{j+1}\right)-\left(\frac{g}{\Delta}x\right)\left(z_i^{j}-z_{i+1}^{j}\right) \\ &+q\left(\frac{v}{A}\right)_{i+\frac{1}{2}}^{j+\frac{1}{2}}=0 \end{aligned} \tag{3-15}$$

These equations are non-linear with respect to the unknowns y and Q at the net points on the j+1 time line. Initial conditions or previous computations are involved to determine all the terms associated with the j^{th} time line. Initial conditions are either estimated or obtained from a previous unsteady flow solution. Small errors of estimate in the initial conditions dampen out within the first few time steps. The resulting two equations have four unknowns, y and Q at point i and i+1 on the j+1 time line.

Therefore, a system of two non-linear equations in four unknowns is available. However, they are not sufficient to evaluate the unknowns at the points (i, j+1) and (i+1, j+1). Nevertheless, two unknowns are common to any two contiguous rectangular grids. As there are N-points on the row j+1, there are (N-1) rectangular grids providing 2(N-1) equations for the evaluations of 2N unknowns. Two additional equations for determining all the unknowns are supplied by boundary conditions, and consequently making the system of equations determinate. If a known stage hydrograph is the upstream boundary condition,

then the following is available as one supplementary equation:

$$y_1^{j+1} - f_1(t^{j+1}) = 0 \qquad (3\text{-}16)$$

On the other hand, if a known discharge hydrograph is the upstream boundary, then

$$v_1^{j+1} A_1^{j+1} - Q_1^{j+1} = 0 \qquad (3\text{-}17)$$

becomes available as one supplementary equation. Furthermore, if a discharge relationship is known from the property of the control section or from a rating curve at the downstream boundary, then

$$y_N^{j+1} - f_N(v_N^{j+1}) = 0 \qquad (3\text{-}18)$$

becomes available as the second supplementary equation.

In this system of equations the values of the variables at the time step t^j are known, and may be treated as constants. The unknowns consist of all the variables with superscripts (j+1). Equations 3-16, 3-17, and 3-18 respectively can be rewritten as:

$$G_o(y_1) = y_1 - \lambda = 0 \qquad (3\text{-}19)$$

$$G_o'(y_1, v_1) = v_1 A_1 - Q_1 = 0, \text{ and} \qquad (3\text{-}20)$$

$$F_N(y_N, v_N) = y_N - f_N(v_N) = 0 \qquad (3\text{-}21)$$

Thus, the resulting system of 2N non-linear equations with 2N unknowns is solved by a functional iterative procedure, the Newton-Raphson method. Amein and Fang (1970) stated that the application of the Newton-Raphson method is made by assigning trial values to the unknowns. In this iterative procedure trial values are obtained through linear or parabolic extrapolation from solutions of y and Q at previous time steps. These values are assigned for the 2N unknowns, which when substituted in the system of non-linear equations, would yield a set of 2N residuals. Solutions are obtained by adjusting the values until each

residual vanishes or is reduced to a tolerable quantity. The computations may be organized in a series of iteration steps where convergence may occur during the first or second iteration.

As reported by Chen and Simon (1975), if the Newton-Raphson method is applied only once each time step, the solution procedure degenerates to the equivalent of a quasi-linear finite difference approximation. A linear difference solution requires smaller time steps than the non-linear formulation for the same degree of accuracy. In some instances insignificant loss of accuracy using linear formulation is incurred compared to the inaccuracy resulting from data un-availability or data involving very gradually varied flows.

3.2.5 Solution of the Linear System

Any of the standard methods, such as the "Gaussian elimination" or the "matrix inversion" can be used for the solution of each iteration cycle. The values of the variables found in the terminal iteration cycle (satisfying tolerable limits) will be taken as the values of the variables for the time step (j+1). The computations with then advance to the next time step (j+2). A significant feature of the coefficient matrix is that it has a maximum of only four non-zero elements in any row, because each equation involves at most four of the 2N unknowns. The non-zero elements are banded around the main diagonal. This property of the linear system can be used to great advantage in devising fast solution methods. Therefore, the system of non-linear equations is reduced to the successive solutions of systems of linear equations in the generalized Newton-Raphson iteration method.

3.3 EXTRAN MODEL

3.3.1 Introduction

EXTRAN, or Extended Transport Block of the U.S. Environmental Protection

Agency Storm Water Management Model (SWMM), is a dynamic flow routing model that routes inflow hydrographs through an open channel and/or a closed conduit system in which the flow is unsteady, (EXTRAN, 1973). EXTRAN was primarily developed to be used in urban drainage systems including combined and separate systems. Also, it can be used for stream channels through the use of arbitrary cross-sections or if the cross-section can be adequately represented as a trapezoidal channel.

3.3.2 Governing equations

The governing equations are those used for gradually varied one-dimensional, unsteady flow for open channels. These equations are known as the St. Venant equations or shallow water equations. Yen (1986) and Lai (1986) derived the continuity equation without accounting for lateral inflows. This equation has the following form:

$$\frac{\partial A}{\partial t} + \frac{\partial Q}{\partial x} = 0 \qquad (3\text{-}22)$$

The form of the momentum equation depends on the choice of the dependent variables. Lai (1986) selected flow Q and head H as the dependent variables, which resulted in the following form:

$$\frac{\partial Q}{\partial t} + \frac{\partial (Q^2/A)}{\partial x} + g A \frac{\partial H}{\partial x} + g A S_f = 0 \qquad (3\text{-}23)$$

where:

H = z + y = hydraulic head,

z = invert elevation, and

y = water depth.,

The bottom slope of the channel is incorporated in the gradient of H.

The continuity equation can be written in a non-differential form as:

$$Q = A V \qquad (3\text{-}24)$$

Furthermore, eq. 3-24 can be written as:

$$\frac{Q^2}{A} = V^2 A \qquad (3\text{-}25)$$

Differentiating eq. 3-24 with respect to x gives:

$$\frac{\partial Q}{\partial x} = A \frac{\partial V}{\partial x} + V \frac{\partial A}{\partial x} \qquad (3\text{-}26)$$

Substituting eq. 3-26 in the continuity equation (eq. 3-22) leads to:

$$\frac{\partial A}{\partial t} + A \frac{\partial V}{\partial x} + V \frac{\partial A}{\partial x} = 0 \qquad (3\text{-}27)$$

Rearrange terms in eq. 3-27 and multiply by V:

$$A V \frac{\partial V}{\partial x} = - V \frac{\partial A}{\partial t} - V^2 \frac{\partial A}{\partial x} \qquad (3\text{-}28)$$

Differentiating the term (AV^2) with respect to x leads to:

$$\frac{\partial (A V^2)}{\partial x} = 2 A V \frac{\partial V}{\partial x} + V^2 \frac{\partial A}{\partial x} \qquad (3\text{-}29)$$

Substituting eqs. 3-25 and 3-29 into the momentum equation (eq. 3-23) and simplifying gives:

$$\frac{\partial Q}{\partial t} + 2 A V \frac{\partial V}{\partial x} + V^2 \frac{\partial A}{\partial x} + g A \frac{\partial H}{\partial x} + g A S_f = 0 \qquad (3\text{-}30)$$

EXTRAN uses the momentum equation in the links and a special lumped continuity equation for the nodes. Thus, momentum is conserved in the links and mass in the nodes.

Combining eq. 3-28 and eq. 3-30 gives:

$$\frac{\partial Q}{\partial t} - 2 V \frac{\partial A}{\partial t} - V^2 \frac{\partial A}{\partial x} + g A \frac{\partial H}{\partial x} + g A S_f = 0 \qquad (3\text{-}31)$$

This equation is to be solved along each link at each time step.

Based on Manning's equation, the friction factor is defined as:

$$S_f = \frac{K}{g A R^{\frac{4}{3}}} Q | V | \qquad (3\text{-}32)$$

where:

K = $g(n/1.49)^2$ for U.S. customary units and = gn^2 for metric units, and

R = hydraulic radius.

The absolute value sign is used for the velocity to make S_f a directional quantity. This ensures that the frictional force always opposes the flow.

Substituting eq. 3-32 in the momentum equation and expressing in finite difference form gives:

$$Q_{t+\Delta t} = \frac{1}{1 + \frac{K \Delta t | V |}{R^{\frac{4}{3}}}} \{ Q_t + 2 \overline{V} \left(\frac{\Delta A}{\Delta t}\right) \Delta t + \overline{V^2} \left[\frac{(A_2 - A_1)}{L} \right] \Delta t - g \overline{A} \left[\frac{(H_2 - H_1)}{L} \right] \Delta t \} \qquad (3\text{-}33)$$

The values $\overline{V}$, $\overline{R}$, and $\overline{A}$ are weighted averages of the conduit end-values at time t, and $(\Delta A/\Delta t)_t$ is the average area time derivative from the previous time step. Eq. 3-33 has two basic unknowns; Q and H. Another equation relating Q and H should be supplied to obtain a solution. This relation is provided writing the continuity equation at a node as follows:

$$\frac{\partial H}{\partial t}\Big|_t = \sum \frac{Q_t}{A_s}\Big|_t \qquad (3\text{-}34)$$

where A_s = surface area of a node. Writing eq. 3-32 in finite difference form gives:

$$H_{t+\Delta t} = H_t + \sum Q_t \frac{\Delta t}{A_s} \Big|_t \qquad (3\text{-}35)$$

Numerical integration of eqs. 3-34 and 3-35 is accomplished by the "Improved Polygon" or "Modified Euler" method. This method gives fairly stable results when some constraints are met. Eqs. 3-33 and 3-35 are solved sequentially to determine discharge in each link and head in each node over a time step Δt. The following procedure is adopted to determine the slope (figure 3.2) at the half-step value of discharge:

1- Compute $(\partial Q/\partial t)_t$ from the properties of the system at time t,

2- Project $Q_{(t+\Delta t)}$ where:

$$Q\ (t+\Delta t)\ =\ Q\ (t)\ +\ \left(\frac{\partial Q}{\partial t}\right)_t\ \frac{\Delta t}{2} \qquad \textbf{(3-36)}$$

3- Compute system properties at (t+Δt/2), and consequently form $[\partial Q/\partial t]_{t+\Delta t/2}$,

4- Project Q(t+ Δt) where:

$$Q\ (t+\Delta t)\ =\ Q\ (t)\ +\ \left(\frac{\partial Q}{\partial t}\right)_{t+\frac{\Delta t}{2}}\ \Delta t \qquad \textbf{(3-37)}$$

This method is referred to as the modified Euler solution for discharge based on half-step, and full-step projection. Furthermore, the corresponding half-step calculations of head, written in finite difference form, are as follows:

Half-step at node j, time t+ Δt/2

$$H_j\left(t+\frac{\Delta t}{2}\right)\ =\ H_j(t)\ +\ \left(\frac{\Delta t}{2}\right)$$

$$\left\{\frac{\left(\frac{1}{2}\right)\ \sum\ [\ Q\ (t)\ +\ Q\ (t+\frac{\Delta t}{2})\ ]\ +\ \sum\ [\ Q\ (t+\frac{\Delta t}{2})\ ]}{A_{sj}(t)}\right\} \qquad \textbf{(3-38)}$$

Full-step at node j, time t+ Δt

$$H_j(t+\Delta t) = H_j(t) + \left(\frac{\Delta t}{2}\right) \left\{ \frac{\left(\frac{1}{2}\right) \sum \left[Q(t) + Q(t+\frac{\Delta t}{2}) \right] + \sum \left[Q(t+\frac{\Delta t}{2}) \right]}{A_{s_j}(t)} \right\} \quad (3\text{-}39)$$

It should be noted that the half-step computation of discharge is used in the half-step computation of head. The same applies to full-step computations.

3.3.3 Solution Options

EXTRAN has three solution options called by the card B0 (ISOL). The first solution option uses ISOL = 0 and is referred to as the explicit method. Eq. 3-31 is the basis for solving ISOL = 0. The second solution option ISOL = 1, is referred to as the enhanced explicit solution, and the third option, ISOL = 2, is an iterative solution procedure. The momentum equation for ISOL = 1 and ISOL = 2 is derived as follows: first expand the term $\partial(Q^2/A)/\partial x$ as a product of Q and Q/A instead of V^2/A. This is mathematically represented as:

$$\frac{\partial(Q^2/A)}{\partial x} = Q^2 \frac{\partial(1/A)}{\partial x} + 2\,(Q/A) \frac{\partial Q}{\partial x} \quad (3\text{-}40)$$

or

$$\frac{\partial(Q^2/A)}{\partial x} = Q^2 \frac{\partial(1/A)}{\partial x} + 2\,V \frac{\partial Q}{\partial x} \quad (3\text{-}41)$$

Substitute the continuity equation (eq. 3-22) in eq. 3-41 and rearrange to get:

$$\frac{\partial(Q^2/A)}{\partial x} = Q^2 \frac{\partial(1/A)}{\partial x} - 2\,V \frac{\partial A}{\partial t} \quad (3\text{-}42)$$

Also substitute eq. 3-42 in the momentum equation (eq. 3-23) and rearrange to get:

$$\frac{\partial Q}{\partial t} + g A S_f - 2 V \frac{\partial A}{\partial t} + Q^2 \frac{\partial (1/A)}{\partial x} + g A \frac{\partial H}{\partial x} = 0 \qquad (3\text{-}43)$$

3.3.4 Solution by the Enhanced Explicit Method

The friction factor is expressed using Manning's formula as eq. 3-32. Substitute eq. 3-32 in eq. 3-43 and write the resulting equation in finite difference form to get:

$$Q_{t+\Delta t} = Q_t - \frac{K \Delta t}{R^{\frac{4}{3}}} |V_t| Q_{t+\Delta t} + 2 V \left(\frac{\Delta A}{\Delta t}\right) \Delta t - Q_{t+\Delta t} Q_t \left[\frac{1/A_2 - 1/A_1}{L}\right] \Delta t - g A \left[\frac{H_2 - H_1}{L}\right] \Delta t \qquad (3\text{-}44)$$

where L = conduit length.

Rearranging and simplifying terms in eq. 3-44 gives the final form of the finite difference equation for the enhanced explicit dynamic flow method as follows:

$$Q_{t+\Delta t} = \frac{Q_t + 2 \overline{V} \left(\frac{\Delta A}{\Delta t}\right)_t - g \overline{A} \left[(H_2 - H_1)/L\right] \Delta t}{1 + \frac{K \Delta t}{R^{\frac{4}{3}}} |V| + \left[Q_t \left(1/A_2 - 1/A_1\right)_t / L\right] \Delta t} \qquad (3\text{-}45)$$

where $\overline{V}$, $\overline{R}$, and $\overline{A}$ are weighted averages of the conduit upstream, middle and downstream values at time t and $(\Delta A/\Delta t)_t$ is the average area time derivative from the previous half time step. The enhanced explicit method (ISOL = 1) differs from the explicit method (ISOL = 0) by the following two significant factors:

1- The $\partial(Q^2/A)/\partial x$ term in the momentum equation has a different derivation, and

2- An additional $Q_{t+\Delta t}$ is factored out of equation 3-37.

The effect of these differences is prominent during the rising and falling portions of the hydrographs.

The enhanced explicit solution allows substantially longer time steps than the

explicit solution, especially as the flow is increasing or decreasing. Eq. 3-35 still holds to define another relation between H and Q. In addition, the solution procedure that was adopted for the explicit method can still be used for the enhanced explicit method. Therefore, both the explicit and enhanced explicit solutions use the same numerical techniques, but differ in the representation of the momentum equation.

3.3.5 Solution by the Iterative Method

Eq. 3-44 was derived as the basis for the enhanced explicit solution, called by ISOL = 1. The same equation is the basis for the iterative method solution. However, appropriate weighting coefficients (or factors) are introduced. Thus, the resulting finite difference iterative dynamic equation takes the form:

$$
\begin{aligned}
Q_{t+\Delta t} = \{\, & Q_t + (1-w)\left[-g\bar{A}\,\frac{H_2 - H_1}{L}\,\Delta t\right. \\
& \left. + \frac{K\,\Delta t}{R^{\frac{4}{3}}}\,|V| + \frac{Q/A_2 - Q/A_1}{L}\,\Delta t\right]_t \\
& + w\left[-g\bar{A}\,\frac{H_2 - H_1}{L}\,\Delta t\right]_{t+\Delta t} + V\,\frac{\Delta A}{\Delta t}\,\} \,/ \\
& w\left[\frac{K\Delta t}{R^{\frac{4}{3}}}\,|V| + \frac{Q/A_2 - Q/A_1}{L}\,\Delta t\right]_{t+\Delta t}
\end{aligned}
\qquad \text{(3-46)}
$$

where $\overline{V}$, $\overline{R}$, and $\overline{A}$ are weighted averages of the conduit upstream, middle and downstream values at time t and/or t+ Δt. The values at time t+Δt are the values for the current iteration; whereas they are equated to the previous time step's values for the first iteration. V is the average conduit velocity, and $\Delta A/\Delta t$ is the conduit average area time derivative. These averages are based on the average or difference of the previous time step and the current iteration. The time weighting factor (w) is set equal to 0.55.

Once again, the continuity equation provides another relation between Q and H. It is applied at a node and takes the following form:

$$\left(\frac{\partial H}{\partial t}\right)_t = \sum \frac{[Q_t + Q_{t+\Delta t}]/2}{[A_{s_t} + A_{s_{t+\Delta t}}]/2} \qquad (3\text{-}47)$$

where:

A_{st} = surface area of node at time t, and

$A_{st+\Delta t}$ = surface area of node at time t+ Δt.

Therefore, the momentum equation (eq. 3-46) and the continuity equation (eq. 3-47) are solved iteratively to determine discharge in each link and head at each node for each time step t.

An under-relaxation iterative matrix solution is employed to numerically integrate these dynamic flow equations. This is accomplished by introducing an under-relaxation factor U_f. At any iteration $Q_{t+\Delta t}$ is defined as:

$$Q_{t+\Delta t} = (1 - U_f)\ Q_j + U_f\ Q_{j+1} \qquad (3\text{-}48)$$

where:

U_f = 0.75 for the first iteration,

U_f = 0.50 for any subsequent iteration,

Q_j = conduit flow at iteration j, and

Q_{j+1} = conduit flow at iteration j+1.

In a similar fashion, the under-relaxation factor is applied to junction depth for any iteration:

$$H_{t+\Delta t} = (1 - U_f)\ H_j + U_f\ H_{j+1} \qquad (3\text{-}49)$$

where:

H_j = junction depth at iteration j, and

H_{j+1} = junction depth at iteration j+1.

The iterative method uses a variable time step with a maximum allowable value specified

by the model user. This maximum value satisfies the Courant number criterion:

$$C = \frac{L}{V + \left[\frac{g A}{T}\right]^{\frac{1}{2}}} \qquad (3\text{-}50)$$

where:

C = Courant number for the conduit,

L = Channel (conduit) length,

T = Channel (conduit) width, and

V = Average velocity of flow.

3.4 ONE-D MODEL

3.4.1 Introduction

ONE-D applies an implicit finite-difference scheme to integrate the St. Venant equations over a wide range of transient flows and conditions. It uses the Galerkan techniques of weighted residuals in solving the linearized St. Venant equations. The model, which was developed at the Massachussetts Institute of Technology, (Harleman, 1974), is used by the Water Planning Management Branch, Inland Water Directorate, Environment Canada. ONE-D can be applied to simulate steady state flow as well as transient flow.

3.4.2 Governing Equations and Assumptions

The conservation of mass and momentum equations (St. Venant equations) are used to represent the propagation of waves in open channel flows. Deriving the St. Venant equations is based on the following assumptions:

- The flow is assumed to be one-dimensional. The free surface is taken to be a horizontal line across the cross-section, and velocity distribution is approximated

by a uniform velocity over the cross-section. In this instance, any centrifugal or Coriolis effects due to channel curvature are neglected.

- Pressure distribution is assumed hydrostatic where the vertical acceleration is neglected, and the density of the fluid is assumed homogeneous.

- Empirical equations, such as Manning's or Darcy-Weisbach, are used to account for the boundary friction and turbulence in the channel.

Two different methods are used to formulate these conservation equations; namely the "material" method and the "control volume" method. In the material method the flow characteristics are obtained by following the motion of a given mass of the fluid through a small increment of time in the vicinity of the fixed section. In the control volume method the equations are derived by considering the fluxes of mass and momentum through a fixed control volume; (figure 3.3). Harleman (1967) used the material method to derive the St. Venant equations, and based the derivation on the average velocity V and the water surface elevation H. In this exercise the continuity equation takes the following form:

$$B \frac{\partial z}{\partial t} + B V \frac{\partial z}{\partial x} + A \frac{\partial V}{\partial x} + V \frac{\partial A}{\partial x}\Big|_{z\text{-constant}} = q_l \qquad (3\text{-}51)$$

where the respective terms in the continuity equation represent:

- Storage variations due to water surface elevation changes with time,

- Prism storage term due to variation in velocity with space; (figure 3.1),

- Wedge storage term due to areal variations in velocity with space,

- Wedge storage term due to variation of area with space, and

- q_l = lateral inflow term which gives the net mass change spatially and temporally

beyond the storage terms.

In addition, the momentum equation takes the following form (Harleman 1967):

$$\frac{\partial V}{\partial t} + V \frac{\partial V}{\partial x} + V \frac{q_l}{A} = g \left(S_o - \frac{V|V|}{C_z^2 R}\right) - g \frac{\partial y}{\partial x} \qquad (3\text{-}52)$$

The terms in eq. 3-21 represent the acceleration due to time variation in flow, acceleration due to spatial variation in velocity, acceleration effects due to lateral inflow, body force due to bed slope with frictional force effects, and a pressure force term respectively.

For a wide rectangular channel the top width B can be assumed approximately equal to the wetted perimeter. Thus, the hydraulic radius R will be approximately equal to the depth of flow y:

$$R = y \,, \quad and \quad A = B\, y \qquad (3\text{-}53)$$

Substitute eq. 3-53 in eqs. 3-51 and 3-52 to get the continuity and momentum equations for a wide rectangular channel. In this instance the continuity equation takes the following form:

$$\frac{\partial y}{\partial t} + V \frac{\partial y}{\partial x} + y \frac{\partial V}{\partial x} = \frac{q_l}{B} \qquad (3\text{-}54)$$

and the momentum equation becomes:

$$\frac{\partial V}{\partial t} + V \frac{\partial V}{\partial x} + V \frac{q_l}{B\, y} = g \left(S_o - \frac{V|V|}{C_z^2 y}\right) - g \frac{\partial y}{\partial x} \qquad (3\text{-}55)$$

In general, the boundary conditions are specified in terms of discharge Q or water surface elevation H, rather than depth y. Thus, the corresponding St. Venant equations take the form:

$$B \frac{\partial z}{\partial t} + \frac{\partial Q}{\partial x} = q_l \,, \quad and \qquad (3\text{-}56)$$

$$\left(\frac{\partial Q}{\partial t} + 2V \frac{\partial Q}{\partial x} \right) \frac{1}{A g} = -\left(1 - F^2 \right) \frac{\partial H}{\partial x} - F^2 \left(\frac{1}{B} \frac{\partial A^H}{\partial x} \right) - \frac{Q|Q|}{K^2} \quad (3\text{-}57)$$

where:

F = Froude number,

K = A $C_z \sqrt{R}$, and

$\partial A^H/\partial x$ = non-prismatic channel effects which is alternatively written as:

$$\frac{\partial A^H}{\partial x} = B \left(S_o + \frac{1}{B} \frac{\partial A^Y}{\partial x} \right) - \left. \frac{\partial A}{\partial x} \right|_{H\text{-constant}} \quad (3\text{-}58)$$

3.4.3 Vertical Acceleration Terms

Vertical acceleration terms may be significant and should not be neglected in the derivation of the St. Venant equations. Keulegan and Patterson (1943) proposed a form for the vertical acceleration terms; however, the form was restricted to the following simplified cases:

1- wide rectangular channels,

2- variation with H of the x-component of local velocity, V is negligible; in other words, V = V(x,t), and

3- Lateral inflow and lateral velocity are neglected.

Due to these simplifications, it is possible to focus attention solely on the effects of vertical acceleration associated with rapid changes in water surface elevation. Keulegan and Patterson (1943) presented a derivation of the governing St. Venant equations based on his assumptions as follows:

$$\frac{\partial y}{\partial t} + V \frac{\partial y}{\partial x} + y \frac{\partial V}{\partial x} = 0 \quad , \quad and \tag{3-59}$$

$$\frac{\partial V}{\partial t} + V \frac{\partial V}{\partial x} + \frac{y V^2}{3} + \left(\frac{\partial^3 y}{\partial x^3} + \frac{2}{V} \frac{\partial^3 y}{\partial x^2 \partial t} + \frac{1}{V^2} \frac{\partial^3 y}{\partial x \partial t^2} \right) = g \left(S_o - \frac{V|V|}{C_z^2 y} \right) - g \frac{\partial h}{\partial x} \tag{3-60}$$

Comparison of eqs. 3-59 and 3-60 with the continuity and momentum equations (eqs. 3-54 and 3-55), derived for the case of wide rectangular channels with no lateral inflows, leads to the conclusion that accounting for the vertical acceleration terms did not affect the derivation of the continuity equation. On the other hand, vertical acceleration terms appear in the momentum equation in the following form:

$$\frac{y V^2}{3} + \frac{\partial^3 y}{\partial x^3} + \frac{2}{V} \frac{\partial^3 y}{\partial x^2 \partial t} + \frac{1}{V^2} \frac{\partial^3 y}{\partial x \partial t^2} \tag{3-61}$$

These terms are only significant when the water surface curvatures are large. Keulegan and Patterson (1943) reported that these acceleration terms are second order ones for normal transient flows in which y/L is much less than 1, where y is the flow depth and L is the characteristic wave length of the transient. Schonfield (1951) and Peregine (1967) showed that the effect of these acceleration terms, under strong water surface curvatures of a steep front due to a rapid transient, is to disperse the front.

Correspondingly, for an engineering application the effect of vertical acceleration terms need not be represented in detail because they damp out rapidly. Therefore, their effect is neglected in the ONE-D solution of the St. Venant equations.

3.4.4 Computational Method (Principle of Superposition)

Gunaratnam and Perkins (1970) proposed the method of superposition, used in

structural analysis, for channel computations based on influence functions. At each time step the solution for water surface elevations and discharges is based on sets of simultaneous linear equations. Linearity makes the principle of superposition valid. The solution proceeds as follows:

1- Assume zero solution values at the boundary mesh points.

2- Solve a set of equations for the interior mesh points to get the null solution.

3- Compute, using the same set of equations, the influence factors due to unit solution values at the boundary mesh points at the interior mesh points.

4- Using boundary conditions, solve the set of linear equations to get boundary mesh points solution values.

5- Multiply the influence factors (step 3) by the boundary solution values (step 4).

6- Obtain the interior solution values by adding the products of step 5 to the null solution (step 2).

3.4.5 Solution Procedure

The solution procedure for the interior mesh points is based on the work of Gunaratnam and Perkins (1970). Whereas the solution for the boundary mesh points is based on the research of Wood et al. (1972).

3.4.5.1 Interior Mesh Points

The solution values for the water surface elevation z(j) and the discharge Q(j) take the following form:

$$H(j) = H^{\circ}(j) + dx_1(j)\ H(1) + dx_3(j)\ Q(1) + dx_{11}(j)\ H(N) + dx_{33}(j)\ Q(N) \quad \textbf{(3-62)}$$

$$Q(j) = Q^{\circ}(j) + dx_2(j)\ H(1) + dx_4(j)\ Q(1) + dx_{22}(j)\ H(N) + dx_{44}\ Q(N) \quad \textbf{(3-63)}$$

where:

$H^{\circ}(j)$ = null solution for H(j),

$dx_1(j)$ = influence on H(j) of unit H(1),

$dx_3(j)$ = influence on H(j) of unit Q(1),

$dx_{11}(j)$ = influence on H(j) of unit H(N),

$dx_{33}(j)$ = influence on H(j) of unit Q(N),

$Q^{\circ}(j)$ = null solution for Q(j),

$dx_2(j)$ = influence on Q(j) of unit H(1),

$dx_4(j)$ = influence on Q(j) of unit Q(1),

$dx_{22}(j)$ = influence on Q(j) of unit H(N), and

$dx_{44}(j)$ = influence on Q(j) of unit Q(N).

The set of simultaneous linear equations resulting from the finite difference scheme can be written in a matrix form. The null solution and the influence coefficients may be obtained in a single operation by solving the following matrix equation:

$$[\ A\ ]\ .\ [\ X\ ] = [\ d\ ] \quad \textbf{(3-64)}$$

where [A] = (2N-4) by (2N-4) bitridiagonal submatrix. The first column in the matrix [d] supplies the null solution when the water surface elevation and discharge are set to zero at the upstream and downstream boundaries.

Gunaratnam and Perkins (1970) proposed a bitridiagonal coefficient mat ix where a double sweep algorithm is used to solve a set of simultaneous linear equations. The solution is essentially the Gauss reduction.

3.4.5.2 Boundary Mesh Points

Boundary values are obtained by solving the following set of equations:

$$\alpha_1 H(1) + \alpha_2 Q(1) + \alpha_3 H(N) + \alpha_4 Q(N) = D_2^1 \qquad (3\text{-}65)$$

$$\beta_1 H(1) + \beta_2 Q(1) + \beta_3 H(N) + \beta_4 Q(N) = D_1^N \qquad (3\text{-}66)$$

where α and β terms are related to coefficients in the matrix [A] by some mathematical relationships. The above equations along with the two upstream and downstream boundary conditions are sufficient to solve for the water surface elevations and discharges at the boundary mesh points.

3.5 SUMMARY

This chapter presents different solution techniques that are used to solve the St. Venant equations for unsteady flow in open channels. It also gives a detailed mathematical development of three dynamic wave routing models; namely, DWOPER, EXTRAN, and ONE-D. The following conclusions can be drawn:

- Implicit schemes are more stable than explicit schemes. For implicit schemes, the time step size is selected based on accuracy requirements rather than stability requirements (Courant Criteria). However, in some instances very large time steps in the order of hours or days can lead to instability. Therefore, the selected time step should not compromise either stability or accuracy.

- DWOPER uses the "Weighted Four-Point" implicit scheme to solve the St. Venant equations. It is applicable to rivers of varying physical features. It is characterized by the ability to define the off-channel storage areas separately from the main channel flow field.

- EXTRAN uses an explicit scheme with three solution options. These options are: the "Explicit" Method, the "Enhanced Explicit" method, and the "Iterative" method. EXTRAN has the limitation on the time step size. It considers the whole channel flow field as a single unit of irregular shape.

- ONE-D uses an implicit scheme based on the principle of superposition to solve the linearized equations. It defines storage areas separate from main channel area.

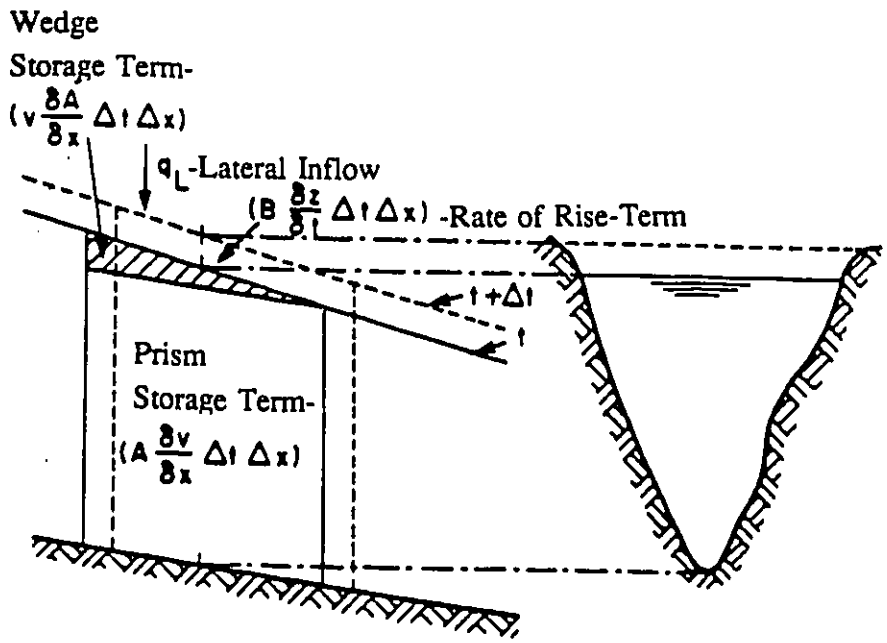

Figure 3.1 Physical Representation of Terms in the Continuity Equation.

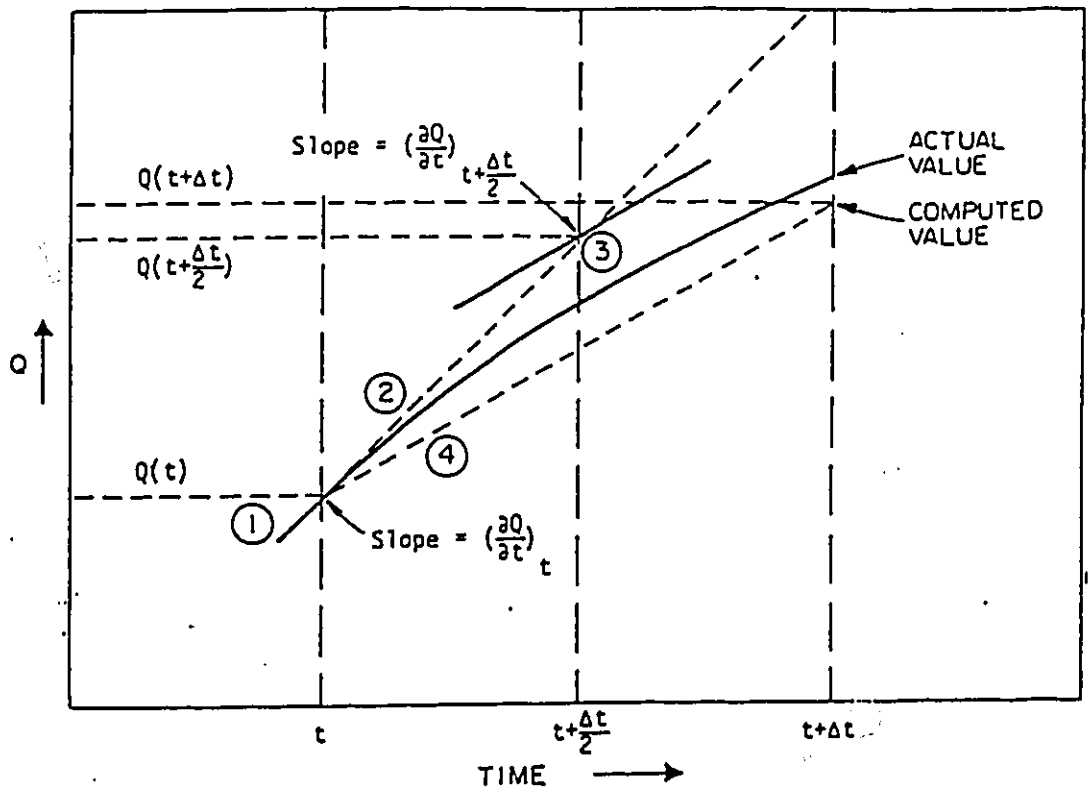

Figure 3.2 Modified Euler Solution Method for Discharge Based on Half-Step, Full-Step Projection.

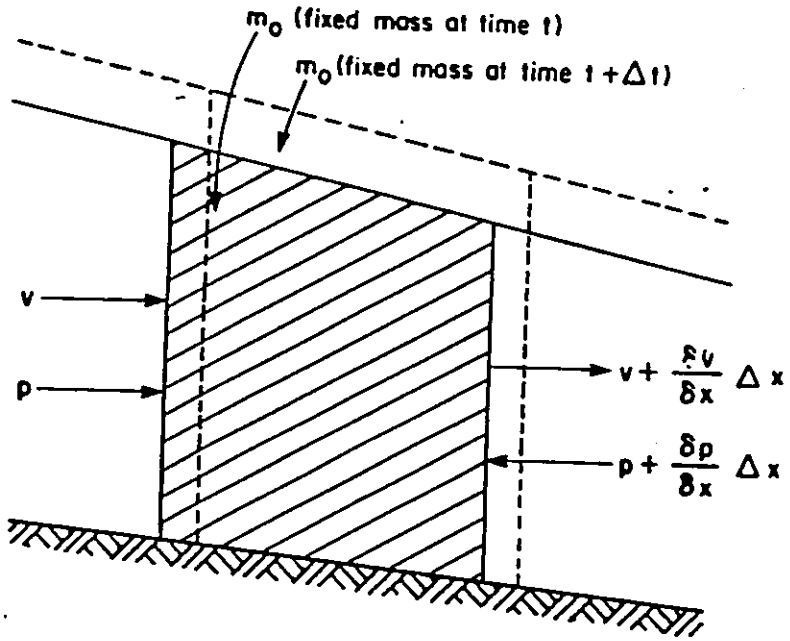

Figure 3.3 Definition Sketch of Control Volume.

CHAPTER 4

STATISTICAL CRITERIA FOR MODEL COMPARISON

4.1 INTRODUCTION

The representation of a hydraulic phenomenon by some mathematical relationships (or models) inevitably introduces some degree of inaccuracy. Other inaccuracies occur when representing the system of mathematical equations by finite differences and in producing the results. It is generally accepted that no single simulation model output will be identical in all respects to the physical phenomenon it aims to represent. However, it is required that this output be sufficiently close to its physical counterpart in order for the model simulation to be considered acceptable.

The principle of goodness-of-fit is a measure of the degree to which the output

conforms to the corresponding observed data. Goodness-of-fit techniques may range from purely subjective graphical (visual) methods to purely objective techniques using mathematical and statistical relationships. These relationships usually portray the difference between simulated and observed variables.

Prior to any calibration or model application, the user should establish criteria for comparing simulated and observed variables. However, if too many criteria are used and are frequently switched, the assessment of the model performance becomes difficult. For example, if the model is intended to design sewers, then the primary variable of interest is the peak flow and calibration would be best made on a comparison between modelled and observed peak flows. On the other hand, in designing a storm detention basin, run-off volumes and possibly the hydrograph shape are important and calibration must be based on a comparison of simulated and observed volumes and hydrograph shapes. In a hydrodynamic flood routing application, both the peak flow rates (or peak depths) and hydrograph shapes will be considered as criteria for comparison in the modelling exercise.

4.2 GRAPHICAL METHOD

Related to model simulation assessment is the graphical method for calibration. It consists of plotting the observed and simulated hydrographs on the same graph. A visual comparison is then made of peak flows and hydrograph shapes. The importance of the graphical method should not be overlooked. Although subjective, it provides a rough appreciation of the model capabilities. Johnston and Pilgrim (1976) emphasize the importance of subjective impressions, based on the fact that even the choice of the form of a statistical fitting technique is still a subjective decision.

With a good understanding of the physical problem (and the effect of each model parameter on the simulation), the user can re-adjust parameters to get a better fit. Even though time consuming, this method is very instructive to the model user and helps in

understanding the model performance under different conditions. This methodology is often used when there is only a limited number of measured events. However, it is usually thought to be highly subjective and difficult when comparing the performance of similar models. In these instances the user can only resort to statistical goodness-of-fit techniques.

4.3 STATISTICAL GOODNESS-OF-FIT TECHNIQUES

While the graphical calibration method is often referred to as a "trial and error" procedure, statistical goodness-of-fit techniques are more often associated with automatic optimization of parameters.

A statistical goodness-of-fit procedure implies a method to measure, in some way, the deviation of a simulated output to that observed; the measurement thus obtained being an end in itself. On the other hand, a statistical fitting procedure employs this measure of deviation of the simulated output to assist in the calibration process; the objective being a simulated output more closely resembling that observed.

Statistical fitting procedures were used by Dawdy and O'Donnel (1965) to demonstrate the usefulness of automatic optimization for parameter calibration. Automatic optimization means systematic adjustment of model parameters, or sets of parameters, in such a way that the corresponding model output agrees more closely with the observed data after the adjustment. In this context, the statistical goodness-of-fit equation is called an objective function. For example, let G(x) be an objective function of the error in a model prediction which results from x_1, x_2, x_3, ..., x_n model input parameters. It would be required to minimize (or optimize) the value of G(x) by assigning a suitable choice of values to the individual elements in the vector x. A search must be employed to determine the location of the overall global minimum over the surface where G(x) is defined.

Several search methods are available. Nelder and Mead (1965) used the "Direct

Search Simplex" method, whereas Fletcher and Powell (1963) used the "Steepest Descent" procedure. The optimization (or minimization) of the objective function G(x) can be achieved by changing several values of x until no significant reduction of the G(x)-value is recognized. Therefore, the goal of calibration would be to find the combination of model parameters that would minimize the objective function.

Different objective functions would ordinarily give more weight to a certain aspect of disagreement between observed and simulated results. In general, the choice and role of the objective functions are aspects which offer serious difficulties to the model user. In a comparative study, Diskin and Simon (1977) concluded that the choice of the most appropriate objective function must be based on the nature of the problem to which the model is to be applied. Furthermore, this study favoured the consideration of more than one objective function when assessing the goodness-of-fit of a particular model for a given application. Ibbitt and O'Donnell (1971) expressed similar sentiments with regard to statistical fitting procedures. Aitken (1973) stated that the simulation model should have the ability to reproduce the mean and standard deviation of the observed values.

Goodness-of-fit equations for comparing two sets of data are often manifested in the following form:

$$Residual = (Observed\ value) - (Simulated\ value) \qquad (4\text{-}1)$$

4.3.1 Sum of Squares Criteria

One of the most widely used objective functions for model comparison studies or model calibration and parameter optimization is the "sum of squares" criterion:

$$G = \sum_{i=1}^{n} [\, q_o(t) - q_s(t) \,]_i^2 \qquad (4\text{-}2)$$

where:

G = sum of squares criterion,

$q_o(t)$ = observed peak flow at time t,

$q_s(t)$ = simulated peak flow at time t, and

n = number of coordinates in the hydrograph under consideration.

Clarke (1973) criticized the use of the sum of squares criterion unless consideration was given to the statistical properties of the residuals themselves. He based his criticism on the fact that minimizing the least squares objective function was applied to simulations where the underlying assumptions, with regard to the statistical properties of the residuals, were seldom valid. In spite of the shortcomings of the sum of squares criteria, it has been widely used for model comparison and calibration.

4.3.2 Nash and Sutcliffe Method

Nash and Sutcliffe (1970) used a dimensionless objective function that measured the efficiency of a model. It has the following form:

$$R^2 = \frac{F_o^2 - F^2}{F_o^2} \qquad (4\text{-}3)$$

where:

R = model efficiency parameter,

$$F^2 = \sum_{i=1}^{n} [q_o(t) - q_s(t)]_i^2 \qquad (4\text{-}4)$$

$$F_o^2 = \sum_{i=1}^{n} [q_o(t) - \bar{q}]_i^2 \qquad (4\text{-}5)$$

and $\bar{q}$ = the mean of observed flows.

Nash and sutcliffe (1970) defined R^2 as the "index of agreement" and F_o^2 as the "initial variance". The index of agreement would have a value of one for a perfect fit. In

fact, dividing F_o^2 by the number of coordinates of the corresponding hydrograph would produce the variance of the observed data.

The criticism of the sum of squares and Nash and Sutcliffe criteria was based on the fact that a measure of accuracy should not be dependent on the number of hydrograph coordinates considered in the analysis.

4.3.3 Root Mean Square Error (RMSE)

To overcome the dilemma of the dependency of the objective function on the number of hydrograph coordinates, other accuracy measures, such as RMSE, were proposed in the literature. RMSE takes the following form:

$$RMSE = \{ \frac{1}{n} \sum_{i=1}^{n} [q_o(t) - q_s(t)]^2 \}^{\frac{1}{2}} \qquad (4-6)$$

RMSE was used by Patry and Marino (1983) to assess the performance of a non-linear functional run-off model as a criterion for comparison of hydrographs. The RMSE is a dimensional objective function with the dimensions of flow rate (or depth when comparing stage hydrographs).

4.3.4 Wood's Objective Function

Another criterion in hydrograph comparison and fitting assessment was proposed by Wood et al.(1974). His objective function has the following form:

$$G = \sum_{i=1}^{n} \{ \frac{q_o(t) - q_s(t)}{[q_o(t)]^b} \}^c_i \qquad (4-7)$$

where G = Wood's objective function and exponents b and c are referred to as "control parameters" (determined by trial and error procedures). These parameters govern the optimization strategy.

4.3.5 Standard Error of Estimate (SEE)

Another objective function was introduced which was not affected by the number of ordinates of the corresponding hydrographs or the record length. This statistic (SEE) was dimensional with the dimensions of flow rate. SEE is defined as:

$$SEE = \{ \frac{1}{n-2} \sum_{i=1}^{n} [q_o(t) - q_s(t)]^2 \}^{\frac{1}{2}} \qquad (4\text{-}8)$$

4.3.6 Reduced Error of Estimate (REE) and Proportional Error of Estimate (PEE)

REE, which was proposed by Manley (1977), has the following form:

$$REE = \{ \frac{\sum_{i=1}^{n} [q_o(t) - q_s(t)]^2}{\sum_{i=1}^{n} [q_o(t) - \overline{q}]^2} \}^{\frac{1}{2}} \qquad (4\text{-}9)$$

This method has a major drawback, in that it emphasizes errors associated with large flows more than a sequence of errors at low discharges. Manley (1978) proposed an alternative method (the PEE method), to avoid this drawback. The PEE method takes the following form:

$$PEE = \{ \frac{\sum_{i=1}^{n} [q_o(t) - q_s(t)]^2}{\sum_{i=1}^{n} [q_o(t)]^2} \}^{\frac{1}{2}} \qquad (4\text{-}10)$$

4.4 RANDOM AND SYSTEMATIC ERRORS

The goodness-of-fit criteria perviously discussed involves residuals which may be either random or systematic in form. As the name implies, random error means that the model does not show any general trend of under- or over- estimation of values. On the

other hand, a systematic error implies that the sign of the error persists over successive time intervals. Aitken (1973) was the first to recognize the importance of systematic errors in assessing model performance and that existing criteria did not account much for these errors. This meant that, while one could obtain the optimal (minimum) value of an objective function, still the model performance was not satisfactory. This would happen when large positive errors counter-balance large negative errors. Hence, the overall calibration results would be misleading.

4.5 DETECTION OF SYSTEMATIC ERRORS

4.5.1 Aitken's Methods

To overcome the aforementioned shortcoming, Aitken (1973) proposed three different methods:

1- A simple sign test which compared the number of runs of positive and negative errors to the expected number of such runs.

2- A coefficient of determination, defined as:

$$D = \frac{F_o^2 - \sum_{i=1}^{n} [\, q_o(t) - \hat{q}_s(t) \,]_i^2}{F_o^2} \qquad (4\text{-}11)$$

where:

D = coefficient of determination, and

$\hat{q}_s(t)$ = simulated flow at time t, obtained from the regression line of $q_o(t)$ on $q_s(t)$.

3- A residual mass curve coefficient defined as:

$$RMCC = \frac{\sum_{i=1}^{n} (D_c - \bar{D}_c)_i^2 - \sum_{i=1}^{n} (D_c - D_e)_i^2}{\sum_{i=1}^{n} (D_c - \bar{D}_c)_i^2} \qquad (4\text{-}12)$$

where:

RMCC = residual mass curve coefficient,

D_c = departure from the mean for the observed residual mass curve,

$\bar{D}_c$ = mean of departures from the mean for the observed mass curve, and

D_e = departure from the mean of estimated or simulated mass curve.

According to Aitken (1973), as the statistic measures the relationship between flow sequence and not simply individual flows, it should indicate the presence of systematic errors. Hughes (1982) made use of the coefficient of efficiency (Nash and Sutcliffe, 1970), the coefficient of determination, and the residual mass curve coefficient in model calibration.

4.5.2 Coefficient of Persistence

Wallis and Todini (1975) pointed out the shortcoming of RMCC and proposed the coefficient of persistence (CP) as another measure of accuracy. This coefficient is defined as:

$$CP = \sum_{i=1}^{k} \frac{A_i^2}{F^2} \qquad (4\text{-}13)$$

where:

k = number of positive and negative runs,

A = individual area of each segment of deviation, and

F^2 = as defined in eq. 4-4.

Eq. 4-13 squares areas of segments of deviation created by numbers of consecutive residuals of the same sign. Thus the resulting CP value indicates a persistent over- or under-estimation of prediction. The term "coefficient" of persistence is possibly a misnomer

as the CP value is not dimensionless, but has the dimensions of (time)^2.

4.6 SUMMARY AND RECOMMENDATIONS

When only limited data are available, the graphical calibration (trial and error) technique is fairly efficient. On the other hand, depending on the type of model application, different measures of accuracy, or deviation between simulated and observed variables, can be adopted; such as:

$$\% \textit{ Error in simulated peak flow} = \frac{q_{ps} - q_{po}}{q_{po}} \times 100 \quad (4\text{-}14)$$

where:

q_{ps} = simulated peak flow rate, and

q_{po} = observed peak flow rate.

Another criterion, based on Aitken's (1973) assertion that any model should be capable of reproducing the mean of the observed values,was considered. This was:

$$\% \textit{ Error in mean flow rate} = \frac{\overline{q}_s - \overline{q}_o}{\overline{q}_o} \times 100 \quad (4\text{-}15)$$

where:

$\overline{q}_s$ = the mean of simulated flow rates, and

$\overline{q}_o$ = the mean of observed flow rates.

When a large amount of observed data is available , a more comprehensive, systematic and detailed calibration effort is required. This form of calibration would largely depend on the choice of the objective function used in the automatic calibration process. The selection of the objective function should consider possible measures of accuracy that would not depend on the number of hydrograph ordinates considered in the analysis. This

is especially true when comparison of the performance of different models, based on a relatively large number of events, is involved.

4.6.1 Dimensional, Ordinate dependent, Shape Factors

The sum of squares and the sum of absolute residuals were considered adequate indications for comparison of simulated and observed data having the same number of ordinates. However, to compare the performance of different models, based on several events, it seemed reasonable to compare the following criteria:

1- Total overall sum of squared residuals:

$$TSSR = \sum_{j=1}^{m} \{ \sum_{i=1}^{n_j} [q_o(t) - q_s(t)]_i^2 \}_j \qquad (4\text{-}16)$$

where:

TSSR = total overall sum of squared residuals,

$q_o(t)$ = observed flow rate at time t,

$q_s(t)$ = simulated flow rate at time t,

n_j = number of ordinates in event j, and

m = number of events.

2- Total overall sum of absolute deviations:

$$TSAR = \sum_{j=1}^{m} \{ \sum_{i=1}^{n_j} | q_o(t) - q_s(t)|_i \}_j \qquad (4\text{-}17)$$

where TSAR = total overall sum of absolute deviations, and other variables are as previously defined.

In some instances, the percentage error in simulated volume may indicate good agreement between simulated and observed total volumes, whereas the shapes of the

respective hydrographs may be considerably different. This difference can be defined as:

$$\overline{A} = \sum_{i-1}^{n} \left| \frac{(Residual)_i + (Residual)_{i+1}}{2} \Delta t \right|_i \qquad (4\text{-}18)$$

where:

$\overline{A}$ = sum of absolute areas of divergence between the two hydrographs, and

Δt = time step.

3- Total overall sum of absolute ares of divergence:

$$TSAA = \sum_{j-1}^{m} \overline{A}_j \qquad (4\text{-}19)$$

where:

TSAA = total overall sum of absolute areas of divergence, and

$\overline{A}_j$ = sum of absolute areas of divergence from event j.

4.6.2 Dimensional, Ordinate Independent, Shape Factors

1- The sum of squared residuals (S^2):

$$S^2 = \frac{1}{n} \sum_{i-1}^{n} [\, q_o(t) - q_s(t) \,]_i^2 \qquad (4\text{-}20)$$

S^2 can be defined as the variance. The standard deviation is obtained by taking the square root of the variance.

2- The mean deviation for one event (MD) is defined as:

$$MD = \frac{1}{n} \sum_{i-1}^{n} | \, q_o(t) - q_s(t) \, |_i \qquad (4\text{-}21)$$

3- The sum of absolute area of divergence for one event is (A/n), where n is defined as the

number of ordinates in that event.

Because of its simplicity, the coefficient of efficiency proposed by Nash and Sutcliffe (1970) had an appealing aspect. The proportional error of estimate (Manley, 1978) is also attractive as it gives equal weight to equal proportional errors rather than to equal absolute errors.

To conclude, no single statistical goodness-of-fit criterion is sufficient to assess adequately the measure of fitness between simulated and observed hydrographs. Ultimately, the selected objective function should depend on the objective of the modelling exercise, as different criteria are weighted in favour of different hydrograph variables.

4.7 CONCLUSIONS

For the present research, different statistical goodness-of-fit techniques were employed to evaluate the performance of the three hydrodynamic models under consideration. The graphical assessment technique was employed occasionally. Simulated results were plotted on the same graph against observed data, and a visual check was performed. This method gives a good appreciation of the effect of parameter variation on model performance. However, it may be misleading on some occasions when a visual check is made for the rising and recession parts of the hydrograph. A visual check may appear to have an excellent fit, but the actual relative error at that point would rise to 30 % in some instances.

Statistical goodness-of-fit techniques used in this research to evaluate model performance included: sum of squares criteria, Nash and Sutcliffe (N & S) method, RMSE, SEE, REE, and PEE. Error in simulated peak values was checked. However, simulations show that while an excellent fit occurs around the peak value, a poor fit occurs on the rising and recession parts of the corresponding hydrograph. Thus an alternative method,

which determined the relative percent error at every point of the simulated hydrograph, was relied on. Absolute values of the corresponding relative percent errors at every point were then summed to give the total absolute percent relative error or the total absolute relative error (TARE). In general, hydrographs with the least total absolute relative errors would give the best-fit. Therefore, the goal was to minimize the objective function to get the best-fit hydrograph.

CHAPTER 5

APPLYING DWOPER TO DATA SETS

5.1 INTRODUCTION

DWOPER is a Dynamic Wave Operational routing model developed by the National Weather Service Hydrologic Research Laboratory (Fread, 1970). It is based on an implicit finite difference solution of the complete one-dimensional Saint Venant equations of unsteady flow. It is implemented where backwater effects and mild bottom slopes are most troublesome for hydrologic routing methods. DWOPER features the ability to use cross-sections spaced at irregular intervals along the river system. The model is generalized for wide applicability to rivers of varying physical features, such as irregular geometry, variable roughness parameters, lateral inflows, off-channel storage, local head losses, ...etc. In this chapter, a discussion of applying DWOPER to a laboratory data set (Treske, 1980), and a field data set (Myers, 1991) will be presented.

5.2 TRESKE'S EXPERIMENTAL CHANNELS

Treske's experimental facility, which included: (i) a straight prismatic channel; (ii) a lateral inflow channel to (i); and (iii) a meandering channel, is shown schematically in figure 5.1. In the present study, DWOPER was applied to model flow in Treske's straight prismatic channel only. Figure 5.2 shows the principal dimensions of the cross-section. The main channel was 125 cm wide by 39 cm deep and had a left flood plain 300 cm wide by 30 cm deep, and a right side flood plain 150 cm wide by 37 cm deep. The working length of the channel was 210 m, the bed slope was 0.019 %, and Manning's roughness coefficient n for the composite cross-section was estimated to be 0.012.

A head box was located at the entrance of Treske's three channels where the inflow hydrographs were controlled and measured. Two measurement stations were used. The upstream station was 14 meters downstream from the head box and the downstream station was located 210 meters from the upstream station. At each measuring station both stage and discharge hydrographs were measured for each flood event. Discharge was measured in litres per second and stage in millimetres. To each value of stage, 819 m should be added to reference it to mean sea level. Treske's data for the straight prismatic channel consisted of ten flood events, four of which were in-bank (single channel) flows and the remaining six were over-bank (composite channel) flows.

5.3 INITIAL AND BOUNDARY CONDITIONS

Initial and boundary conditions are needed to solve the Saint Venant equations.

5.3.1 Initial Conditions

Amein and Fang (1970) report that initial conditions may be given as the values of the velocity and depth at some initial time at all locations in the channel. These values may be obtained from the steady flow conditions in the channel prior to the arrival of the flood.

Input to DWOPER consisted of initial water surface elevations (YDI). If the upstream station does not have an observed hydrograph, then the YDI-value must be supplied along with all the zeros for the other YDI's. If zeros or blanks are given to all YDI's except at the downstream station of the main channel when actual YDI is read in, the program will generate the YDI's via a solution of the steady flow backwater equation. This is the case with Treske's data where the uniform flow depth of 0.212 m was the y-input for the downstream station and zeros were assigned elsewhere.

Initial discharge (QDI) should be input to DWOPER at each station. If blanks or zeros are used for all QDI-values except at the upstream station, the program will generate QDI's by summation of the flows from the upstream to the downstream boundaries, including tributary and lateral inflows. For Treske's data, 95 litre/sec (3.35 ft^3/s) was the QDI-value input at the upstream station and zeros were assigned elsewhere. This was the steady state uniform flow rate at a depth of 0.212 m.

5.3.2 Boundary Conditions

Boundary condition must be specified in order to obtain solutions for the Saint Venant equations. In fact, in most unsteady flow problems, the unsteady disturbance is introduced into the flow at the boundaries or extremities of the river system. Boundary conditions are specified at the upstream and downstream stations as input to DWOPER.

5.3.2.1 Upstream Condition

Using DWOPER, the upstream boundary condition can be either a stage or a discharge hydrograph. For Treske's data, a discharge hydrograph was used as the upstream boundary condition. The values were input in cubic metres per second (m^3/s or cms), with eight values per line (input card).

5.3.2.2 **Downstream Condition**

With DWOPER, the downstream boundary condition can be one of the following:

i- a stage hydrograph,
ii- a discharge hydrograph,
iii- a single value rating curve of discharge as a function of stage,
iv- a loop rating curve, or
v- normal flow computed from Manning's equation (with the channel bottom slope used as the energy slope).

In the case of Treske's data, a rating curve was not available, however, both stage and discharge hydrographs were measured at the downstream station. A linear regression analysis was performed on the data of flood event No.10 using the observed stages and discharges at the corresponding times. The downstream stage-discharge values were sorted in ascending order then subdivided into two data sub-sets; the first including the depths up to a maximum of 0.39 m (corresponding to the maximum in-bank channel depth), and the second including the remaining (over-bank) depths. Figure 5.3 shows a plot of the rating curve along with the equations developed by the linear regression analysis. These equations have the following form:

$$y = 1.287\,Q + 0.093\,, \quad for\ y < 0.39\ m \quad and$$
$$y = 0.593\,Q + 0.255\,, \quad for\ y > 0.39\ m \qquad (5\text{-}1)$$

where y = flow depth in meters, and Q = flow rate in m^3/s.

5.4 TIME STEP AND THE IMPLICIT METHOD

DWOPER features the ability to use large time steps for slowly varying floods. The implicit formulation of the basic dynamic wave computational element allows the time step

size to be selected according to accuracy requirements rather than numerical stability considerations. This factor makes DWOPER very efficient in the use of computer time. Computational requirements are approximately 0.004 sec./time step/distance step. Efficiency due to the implicit formulation compared to the explicit finite difference models is greatest for slowly varying transients in large rivers and decreases as the transient being modeled becomes more rapidly varying.

Amein and Fang (1970) reported that the implicit method can handle varying channel geometry even where the changes from section to section and in the bottom slope are quite significant. They concluded that the implicit method provides fast and accurate solutions of the unsteady flow equations. They stated two factors that work in favour of the implicit method. First, the method is stable for large time steps; thus, time steps many times larger than the explicit method, with no loss of accuracy, can be used. Second, although the system of equations may contain a large number of unknowns, each equation by itself contains at most only four unknowns.

For the case of Treske's data, a time step of one minute (0.0166 hour) was chosen based on the fact that the observed stage and discharge hydrographs were measured on a 1-minute basis. Three different time steps (18 sec., 60 sec., and 180 sec.) were chosen for flood event case 10 to detect the effect of the time step change on the accuracy of the simulated hydrographs. Figure 5.4 (and table 5.1) shows that varying the time step within reasonable ranges did not affect, to any significant degree, the simulated hydrographs.

5.5 MODEL INPUT DATA

Data was input to DWOPER in the following manner : the channel was subdivided into fifteen stations, spaced 15 m apart, with gauging stations located at the upstream and downstream ends of the channel. Since the observed hydrographs were measured at one minute intervals, and since DWOPER is an implicit model, a time step of 1 minute (0.0166 hour) was used. According to DWOPER input criteria, the depth tolerance in Newton's

iteration should range between 0.000305 to 0.305 m (0.001-1.0 ft) with a preferred value of 0.01524 m (0.05 ft). However, with Treske's data, the depths were relatively small, and a smaller tolerance value of 0.00305 m (0.01 ft) was selected in this instance.

The discharge tolerance should range between 0.283 and 283.17 m^3/s (10-10000 ft^3/s). Since the actual discharge values for Treske's data ranged between 0.095 and 0.40 m^3/s (3 and 14 ft^3/s), a smaller tolerance of 0.000283 m^3/s (0.01 ft^3/s) was adopted. The acceleration factor ranged between 0.5 and 1.0, with a chosen value of 0.55.

A weighting factor was introduced to approximate the spatial derivatives by a finite difference quotient positioned between two adjacent time lines. Amein and Chu (1975) and Baltzer and Lai (1968) used a weighting factor of 1.0, which resulted in the formation of a fully implicit scheme. Amein and Fang (1970) used a weighting factor of 0.5, which led to a box scheme. Fread (1974) examined the influence of the weighting factor on the stability and convergence properties. He concluded that the accuracy decreases as the weighting factor departs from 0.5 and approaches 1.0, and this effect becomes more pronounced as the time step size increases. A value of 0.55 is often used to minimize loss of accuracy while avoiding weak or pseudo instability, as reported by Baltzer and Lai (1968) and Fread (1975) when a weighting factor of 0.5 is used. Four values of top widths versus elevations were used at each station to define the main channel cross-sectional geometry and the off-channel storage sections. Table 5.2 shows the effect of the weighting factor variation on the simulated hydrographs for Treske's data, case 10.

5.6 MODEL CALIBRATION AND MODIFICATION

In open-channel flows, Manning's n is used to describe the resistance to flow due to channel roughness caused by bed forms, bank vegetation and obstructions, and eddy losses. In DWOPER, Manning's n is defined for each channel reach bounded by gauging stations. n is specified as a function of either stage or discharge according to a piece-wise linear relation, with both n and the independent variable (y or Q) read in DWOPER in

tabular form. Linear interpolation is then used to obtain intermediate values.

A critical task in the application of one-dimensional hydrodynamic models in natural rivers is the determination of the roughness parameter in the friction slope term of the momentum equation. Simulation results are often very sensitive to Manning's n. While in the absence of necessary data (observed stages and discharges), n can be estimated. Best results are obtained when n is adjusted to reproduce historical observations of stage and discharge. The adjustment process is referred to as calibration. Fread (1987) reports that the calibration process may be either a trial-error process or an automatic iteration procedure available within DWOPER.

Since Treske's channel was a smooth experimental channel containing flood plains built of the same material as the main channel, Manning's n was a constant with a value of 0.012. However, DWOPER was developed to simulate large river systems where flow depths are typically much smaller than channel widths. For such a condition, the top width of flow may be assumed to be approximately equal to the wetted perimeter. This assumption was adopted in the development of the DWOPER input data file. Since Treske's channel was "narrow" with a width of 1.25 m for the main channel, 4.5 m for the overall flood plain width, and with flow depths varying from 0.2 m to 0.6 m, the true wetted perimeter is significantly greater than the top width which DWOPER treats as the wetted perimeter. An equation was derived to modify Manning's roughness coefficient to compensate for the under-estimation of the wetted perimeter (or the corresponding over-estimation of the hydraulic radius).

Based on Manning's equation:

$$Q_A = \frac{A\,R^{\frac{2}{3}}\,S^{\frac{1}{2}}}{n} \qquad (5\text{-}2)$$

where:

Q_A = actual flow, (m^3/s),

A = cross-sectional area, (m^2),

R = hydraulic radius, (m)

S = friction slope, and

n = actual Manning's coefficient.

Also:

$$Q_{eq} = \frac{A\, R_{eq}^{\frac{2}{3}}\, S^{\frac{1}{2}}}{n_{eq}} \tag{5-3}$$

where:

Q_{eq} = flow rate calculated by DWOPER,

R_{eq} = hydraulic radius calculated by DWOPER, and

n_{eq}= equivalent Manning's roughness coefficient.

According to the conservation of mass principle (continuity equation):

$$Q_A = Q_{eq} \tag{5-4}$$

Equating eqs. 5-2 and 5-3 and simplifying:

$$n_{eq}\, R^{\frac{2}{3}} = n\, R_{eq}^{\frac{2}{3}} \tag{5-5}$$

R is defined as:

$$R = \frac{A}{P} \tag{5-6}$$

where: P = wetted perimeter (m).

Since DWOPER assumes the top width to be wetted perimeter then:

$$R_{eq} = \frac{A}{W} \tag{5-7}$$

where: W = channel top width (m).

Substituting eqs. 5-6 and 5-7 in eq. 5-5 and rearranging:

$$\frac{n_{eq}}{n} = \left(\frac{P}{W} \right)^{\frac{2}{3}} \tag{5-8}$$

Therefore:

$$n_{eq} = n \left(\frac{P}{W} \right)^{\frac{2}{3}} \tag{5-9}$$

For a simple rectangular channel:

$$P = 2y + W \tag{5-10}$$

Substitute eq. 5-10 in eq. 5-9 and simplify to get:

$$n_{eq} = n \left(1 + \frac{2y}{W}\right)^{\frac{2}{3}} \tag{5-11}$$

Accordingly, in the present study, different values of y were assumed and the corresponding n_{eq}-values computed. A table of Manning's n as a function of depth y was input to DWOPER. DWOPER was run for Treske's flood events 1 to 4 (representing in-bank flows). Results of this exercise are shown in figures 5.5 to 5.8.

5.7 OFF-CHANNEL STORAGE

DWOPER features the ability to deal with dead storage areas wherein the flow velocity in the x-direction is considered negligible relative to the velocity in the active area of the cross-section. Such a dead area does not convey flow, but serves mainly to store it. Another effective use of off-channel storage is to model a heavily rough flood plain which stores a portion of the flood water passing through the channel. The off-channel storage cross-sectional properties are described in the same way as the active cross-sectional areas, i.e., for each station, a table of top widths and elevations is read in along with the area associated with the lowest elevation.

5.7.1 Defining Off-Channel Storage Areas

In analyzing flow through open channels of regular cross-sectional shape and hydraulic roughness it is sufficient, in general, to use the overall hydraulic radius as the parameter which best characterizes the properties of the cross-section. However, if the cross-sectional shape is irregular, this approach can introduce considerable error. Treske's compound channel consisted of a relatively deep main channel flanked by shallow flood plains. The velocity difference between the main channel and the flood plain flows resulted in lateral transfer of momentum from the relatively fast main channel flow to the much slower flood plain flows. The high longitudinal shear stresses arising in the interface zones (and consequent energy losses) tend to reduce the discharge capacity of the compound section; (Wormleaton, 1982).

The most commonly used and expedient methods for calculating discharge in compound channels are based on the concept of splitting the cross-section into hydraulically homogeneous subdivisions. The discharges for each subdivision are calculated individually and then summed to give the overall section discharge. Different methods based on this concept were introduced by various investigators. However, they only differ in the assumptions made regarding the location and nature of the imaginary interface planes separating the main channel and flood plain zones. Wright and Carstens (1970) proposed that such interfaces be included in the wetted perimeter calculation for the main channel subdivision only. Wormleaton (1982) examined the relative effectiveness of the different types of imaginary interface planes commonly used; namely, horizontal, vertical, and diagonal planes. He noted that the most commonly used method of calculating discharge in rectangular compound channels adopts a vertical interface plane. He also stated that, when compared to vertical planes, using horizontal or (inward) diagonal interface planes, in general, gave better results for low flood plain depths.

Yen and Overton (1973) found an empirical relationship between the angle of

inclination of (inward) diagonal interface planes and the depth of flow on the flood plain. The angle of inclination to the horizontal increased with flood plain depth. Moreover, they suggested that the interfaces could be reasonably closely approximated by lines drawn from the main channel/flood plain junction to a point on the water surface at the main channel centre line. These interfaces were referred to as diagonal interfaces; (figure 5.9).

5.7.2 Interface Planes

Three different options were selected to define the flood plain flow fields or the flood plain conveyance. First, for large flood plain depths, conveyance throughout the entire cross-section was assumed, i.e. flood plains contribute fully to system conveyance. In this instance the compound channel is treated hydraulically as a "single" unit. Second, for moderated flood plain depths, flood plains are contributing partly to system conveyance and outward-facing diagonal interface plains are employed. Lastly, for very small flood plain depths, flood plains are viewed as "storage" zones only and vertical interface plains are employed, (figure 5.10).

Vertical imaginary interfaces were applied to Treske's data. The corresponding simulated depth and discharge hydrographs were deemed satisfactory, see figures 5.11 to 5.16. Clearly, as indicated by these figures, viewing the flood plain zones as purely "storage" areas did not introduce significant error in the modelling exercise. However, because Treske's channel boundaries were uniformly "smooth", the flood plain zones should contribute some flow, even for small flood plain depths. Therefore, another approach was considered. In this instance storage areas were not assumed and the entire cross-section was viewed as single unit with irregular shape. Inconsistencies were also noted in this approach in the output hydrographs, especially at the bank-full stage where the top width changes dramatically. Comparing simulated and observed depth hydrographs for any flood event, a significant difference between the two hydrographs occurs in the vicinity of the "bank-full" stage (0.39 m). For example, figures 5.17 to 5.22 show that with an increase in time, the flow depth remains the same or even reduces slightly at the 0.39

m level. This continues for a certain period until the two hydrographs, once again, match reasonably well. This phenomenon can be explained by supposing there is a certain portion of the compound channel that serves as storage and does not contribute to system conveyance. This storage area can be rectangular, triangular, parabolic, or any other shape. To reduce the effect of the abrupt increase in the wetted perimeter at the junction between the main channel and the flood plains, the rectangular "storage" area (vertical interface planes) was not used. Also, applying a parabolic (or any other mathematically defined area) would be tedious and the calculations would be cumbersome.

5.7.3 Diagonal Interface Planes

In an attempt to improve the overall simulation, a hypothetical triangular-shaped "storage" area was identified in the DWOPER input data. This area was the triangular-shaped portion of the flood plain flow field below a sloping line, extending upwards from the junction point J (between main channel and flood plain zone) to point X (where the line intersects the outer flood plain boundary), figure 5.23. Thus, if θ is the angle this sloping line makes with the horizontal, then:

$$\theta = \arctan\left(\frac{b}{B}\right) \qquad (5\text{-}12)$$

where:

b = vertical height of X above J, and

B = horizontal distance between J and X.

Applying this hypothetical storage component to different flood events in Treske's data gave rather good results. The simulated hydrographs were very sensitive to any variation of θ. Varying θ by only 4 % produced a significant change in the simulated hydrographs. Different θ-values ranging between 5.3° and 8.6° were investigated for each flood event. The simulated stage and discharge hydrographs were then plotted separately for every θ-value used and for each flood event; refer to figures 5.24 to 5.51. Some

analysis was performed to determine the θ-value that produced the best-fitting hydrographs. Clearly, matching peak depths or discharges was very important in deciding whether the simulated results were acceptable or not. However, matching peak values was not the only criterion involved in determining the "best-fit". Comparison between other portions of corresponding hydrographs was also necessary. In this exercise, the % relative error between observed and simulated values (points on the respective hydrographs) was calculated as follows:

$$\% \ error = \frac{observed - simulated}{observed} \times 100 \qquad (5\text{-}13)$$

The values obtained were then summed to identify the hydrograph variation giving the minimum absolute total relative % error, (refer to chapter 4 for detailed statistical procedures involved). Based on the Inland Water Directorate (Environment Canada), applying the one-dimensional flood routing model ONE-D to river systems (St. Lawrence, Fraser, St. Croix, ...etc.) was capable of reproducing depths within 0.061 m (0.2 ft) and discharges within 4 to 7 % of the actually measured. The figures are those verified by Water Survey of Canada using conventional and moving-boat, discharge measurement techniques in the Port Mann to Mission section of the Fraser River. In addition to statistical goodness-of-fit techniques, these limiting values were used to choose the "best" θ-value for a certain flood event. Table 5.3 shows the optimal θ-values selected for each flood event for a certain d/D where d is the flood plain depth and D is the total depth at the peak flow for each flood event.

Consequently, θ was calculated along with d/D. d/D vs. θ was plotted and a linear regression analysis was applied to the data to get a best-fit line. This resulted in a correlation coefficient $r^2 = 0.91$. Another method used a second degree polynomial function which also gave a good fit, figure 5.52. The best-fit equation takes the following form:

$$\theta = 27.813 \left(\frac{d}{D}\right)^2 + 2.646 \left(\frac{d}{D}\right) + 6.673 \qquad (5\text{-}14)$$

5.8 MYERS' DATA SET

Previously, DWOPER was applied to a prismatic, straight, laboratory channel data set (Treske, 1980). In this section, a discussion on the application of DWOPER to a non-prismatic, natural channel data set (Myers, 1991) will be presented.

5.8.1 Myers' Experimental channel

Myers' data was obtained from an 800 m-long experimental reach of the River Main in N. Ireland. This experimental reach was non-prismatic. The cross-sectional dimensions for 3 stations were given; i.e., (i) at the upstream end of the reach (section 14), (ii) at the downstream end of the reach (section 6), and (iii) at a station mid-distance between the upstream and downstream stations (section 10). Stages were measured at sections 6 and 14 on a continuous basis. Stages were recorded as depth-probe transducer readings, measured in millivolts (mV) and converted to depth above probe in millimeters (mm) using the following equations:

$$\begin{aligned} &\textit{For section } 6, \quad h = 187.3219\, Pr - 216.253 \text{ , } \textit{and} \\ &\textit{for section } 14, \quad h = 191.1804\, Pr - 36.946 \end{aligned} \qquad (5\text{-}15)$$

where :

h = depth above probe in mm, and

Pr = probe reading in mV.

To convert these "depths" into true river depths, it was necessary to add the vertical distance between the probe and the channel bed level. Levels above datum of depth probes at section 14 and section 6 were 36.75 m and 34.29 m respectively.

The principal dimensions of the channel at sections 6, 10 and 14 are given in figures 5.53, 5.54, and 5.55 respectively. Myers (1991) supplied a graph (figure 5.56) showing the variation of Manning's n with depth at different flow levels. He reported a minimum value of 0.03 at a depth of 1.5 m and a maximum of 0.05 at a depth of 0.4 m.

5.8.2 Initial and Boundary Conditions

Input to DWOPER consisted of the initial water surface elevation of 1.085 m (specified at the downstream station of Myers' reach) and zeros were assigned elsewhere. Also the initial discharge was input to DWOPER at each station. A value of 16.7 m^3/s (591 ft^3/s) was input at the upstream station and zeros were assigned elsewhere. These initial conditions were the steady flow depth and discharge respectively.

At the upstream station, a stage hydrograph was used as the boundary condition and a single value rating curve was used as the downstream boundary condition. An equation representing the rating curve was derived based on regression analysis applied to the measured stage-discharge values at the upstream and downstream stations, see figures 5.57 and 5.58. The upstream rating curve can be expressed as:

$$Q = 23.19\,H - 848.90 \quad \textit{for } H < 37.43\text{ , and}$$
$$Q = 51.05\,H - 1892.44 \quad \textit{for } H > 37.43 \qquad \text{(5-16)}$$

where Q = flow rate in m^3/s and H = water surface elevation in m. On the other hand, the downstream rating curve can be expressed as:

$$Q = 25.02\,H - 859.82 \quad \textit{for } H < 35.12\ m\text{ , and}$$
$$Q = 36.84\,H - 1274.55 \quad \textit{for } H > 35.12\ m \qquad \text{(5-17)}$$

Using these equations, discharge hydrographs were obtained from measured stage

hydrographs.

5.8.3 Time Step

Myers' stages were measured at five-minute intervals. However, although DWOPER has no limitations on the time step size used, it has some limitations on the total dimensions of the input system. Thus the observed stage hydrograph was taken based on a 40 minute interval, and a graphical check was made to ensure that accuracy was not compromised and peak values missed. Using a 40-minute time step resulted in an out message indicating that the time step size had to be reduced. Accordingly the input hydrograph was read in DWOPER based on a 2-hour interval. A time step of 30 minutes was selected and DWOPER run; however, there was a phase lag of about 6 hours (3 measuring intervals) between the downstream observed and simulated stage hydrographs, (figure 5.59). Analysis confirmed that the time step used (30 minutes) was not small enough to provide the required accuracy, and a smaller time step had to be used.

In an attempt to reduce the time step size and solve the total dimension limitation problem, the input hydrograph was divided into 4 components and DWOPER was run separately for each component. In this exercise, the last value in each component was taken as the "initial condition" for the subsequent run. Hydrographs were simulated satisfactorily with no lagging time or phase shift. In this instance, a time step of 8 minutes was adopted.

5.8.4 Model Input Data

Data was input to DWOPER in the following manner: the channel was subdivided by 3 stations, spaced 400 m apart, with gauging stations located at the upstream and downstream ends of the channel. A time step of 8 minutes was used. A depth tolerance of 0.001524 m (0.005 ft) was selected, and a discharge tolerance of 0.000141 m^3/s (0.005 ft^3/s) was adopted. A value of 0.55 was used for both the acceleration factor and the

weighting factor. Refer to section 5.8.6 for details on the cross-sectional data input.

5.8.5 Model Calibration

In general, model simulation results are often very sensitive to any variation in Manning's n. In his data set, Myers supplied 4 independent curves describing the variation of n with respect to y (where y = flow depth) for different flow categories; namely, "in-bank" flow, "over-bank" flow, "main- channel" flow, and "flood-plain" flow; (figure 5.56). Initially, an attempt was made to use readings from this figure to produce a single curve of "composite" n (for the compound section) versus y to be used as input to DWOPER. However, the n-values were fairly high for a natural channel, in that some values exceeded 0.05. According to Chow (1959) a value n = 0.05 (at in-bank flow depth) would indicate that the channel bed had irregularly-shaped stones with some weeds and large vegetation cover.

Meyers and Schultz (1940) studied the variation of n with y in connection with the design of the Panama Canal. In their study, they concluded that the n-value for a river channel is minimum when the stage is at or somewhat above normal bank-full stage and tends to increase for both higher and lower stages. They also found that the bank-full n-value does not vary greatly for rivers and canals in different kinds of material and in widely separated locations. Based on these observations and on the Nishnabutna River Study, Iowa (1954), a value of 0.03 would appear to be a reasonable bank-full n-value. However, Myers' bank-full n-value was 0.042, which is relatively high given the aforementioned studies. Nevertheless, several factors are involved in estimating Manning's n for a river, not the least of which is personal judgment. Ven Te Chow (1959) stated: "To select a value of n actually means to estimate the resistance to flow in a given channel, which is really a matter of intangibles. To veteran engineers, this means the exercise of sound engineering judgment and experience; for beginners, it can be no more than a guess, and different individuals will obtain different results".

To resolve the problem of the variation of Manning's n with depth, a model calibration had to be performed adjusting Manning's n to reproduce historical observations of both stage and discharge. A trial and error process was used in the calibration where part of the observed stage hydrograph was input into DWOPER and n-values were changed arbitrarily (trial and error) in the model input data till optimum values were obtained.

5.8.6 Off-Channel Storage Areas

Several options were tried to define the off-channel storage area in DWOPER input for Myers' data set. First, the irregular-shaped cross-section was assumed a single hydraulic unit contributing all the flow, (i.e. no off-channel storage areas were assumed). Using this approach, six values of top width versus elevation were input to DWOPER. Inconsistencies were noted in the simulated stage hydrograph. For example, the peak stage was found to be 21.3 % in error, (see figure 5.60). Because of the poor performance of this approach, another method, where imaginary vertical interface planes separated the main channel and flood plain zones, was tested. Three values of top width versus elevation were used at each station to define the main channel cross-sectional geometry and six values of top width versus elevation were used to specify the off-channel storage sections. While inconsistencies were also noted using this approach, the simulations were improved over those obtained using the "no-storage" approach. For example, as shown in figure 5.61, the simulated peak depth was over-estimated by only 5.23 %.

In an attempt to further improve the overall model simulation, a hypothetical triangular-shaped storage area was included in the DWOPER input data. This storage area was defined based on figure 5.50 developed for Treske's data to define off-channel storage area; (refer to section 5.7.3). Good results were obtained using this approach. Peak stage was under-estimated by only 1.55 %, which is an acceptable relative error in a computer simulation, figure 5.62. For more details on the goodness of fit of simulated hydrographs and the criteria used to choose the best-fit, refer to chapter 4.

5.9 CONCLUSIONS

DWOPER was applied successfully to model flow in a straight experimental prismatic channel and in a compound non-prismatic river channel. The following main conclusions can be drawn:

1- Time step size is based on accuracy rather than stability in an implicit scheme. However, instability can occur when selecting a "large" time step.

2- Changing the weighting factor did not significantly improve the simulated hydrographs of Treske's data.

3- DWOPER assumes the top width as the wetted perimeter. This assumption is not valid for modelling Treske's data. Thus an equation was derived to compensate for the under-estimation of the wetted perimeter.

4- For both data sets assuming an irregular channel cross-section with no storage did not produce satisfactory simulations. This may be due to the fact that depths over the flood plains are small and thus the flood plain roughness would have considerable impact on conveyance. In addition, the wetted perimeter changes dramatically at the bank-full depth.

5- Introducing (imaginary) vertical and outward-facing diagonal interface planes, to separate the main channel and flood plain zones of compound channels, gave generally good results.

6- Compared to diagonal interface planes, vertical interface planes produced smaller overall error in the simulated hydrographs for Treske's laboratory data but were less successful when applied to Myers' field data.

7- The inclination of the diagonal interface planes to the horizontal θ was adjusted to reflect changing hydraulic conditions. An equation was developed to define the flood plain hydraulic boundaries. This equation relates the variation of θ with the ratio of the flood plain depth to the total flow depth.

Table 5.1 Effect of Time Step Variation on the Simulated Depths Using DWOPER, Treske's Data, Case 10.

Time (min)	Observed Depth (m)	Simulated Depth (m)	Simulated Depth (m)	Simulated Depth (m)
Time	Step	t=18 sec	t=60 sec	t=180 sec
0	0.215	0.213	0.216	0.216
9	0.217	0.216	0.216	0.219
18	0.250	0.244	0.244	0.247
27	0.292	0.283	0.280	0.283
36	0.330	0.323	0.323	0.323
45	0.367	0.363	0.363	0.363
54	0.394	0.393	0.393	0.393
63	0.406	0.405	0.405	0.405
72	0.426	0.424	0.421	0.424
81	0.447	0.439	0.439	0.439
90	0.468	0.457	0.457	0.460
99	0.486	0.475	0.475	0.475
108	0.487	0.482	0.482	0.482
117	0.478	0.475	0.475	0.475
126	0.464	0.463	0.466	0.463
135	0.448	0.448	0.451	0.448
144	0.430	0.433	0.433	0.433
153	0.411	0.415	0.415	0.415
162	0.393	0.396	0.399	0.396
171	0.338	0.344	0.351	0.347
180	0.287	0.287	0.290	0.290
189	0.240	0.241	0.247	0.244
198	0.225	0.226	0.226	0.226
207	0.220	0.219	0.219	0.219
216	0.217	0.219	0.219	0.219
219	0.217	0.219	0.219	0.219

Table 5.2 Effect of Weighting Factor Variation on the Simulated Depths Using DWOPER, Treske's Data, Case 10.

Time (min)	Observed Depth (m)	Simulated Depth (m)	Simulated Depth (m)	Simulated Depth (m)	Simulated Depth (m)
Weighting	Factor	0.50	0.55	0.75	1.00
0	0.215	0.216	0.216	0.216	0.216
9	0.217	0.219	0.219	0.219	0.219
18	0.250	0.247	0.247	0.247	0.247
27	0.292	0.283	0.283	0.283	0.283
36	0.330	0.323	0.323	0.323	0.323
45	0.367	0.363	0.363	0.363	0.363
54	0.394	0.393	0.393	0.393	0.393
63	0.406	0.405	0.405	0.405	0.405
72	0.426	0.424	0.424	0.424	0.424
81	0.447	0.439	0.439	0.439	0.439
90	0.468	0.460	0.460	0.460	0.460
99	0.486	0.475	0.475	0.475	0.475
108	0.487	0.482	0.482	0.482	0.482
117	0.478	0.475	0.475	0.475	0.475
126	0.464	0.463	0.463	0.463	0.463
135	0.448	0.448	0.448	0.448	0.448
144	0.430	0.433	0.433	0.433	0.433
153	0.411	0.415	0.415	0.415	0.415
162	0.393	0.396	0.396	0.396	0.396
171	0.338	0.347	0.347	0.347	0.347
180	0.287	0.290	0.290	0.290	0.290
189	0.240	0.244	0.244	0.244	0.244
198	0.225	0.226	0.226	0.226	0.226
207	0.220	0.219	0.219	0.219	0.219
216	0.217	0.219	0.219	0.219	0.219
219	0.217	0.219	0.219	0.219	0.219

Table 5.3 Optimal Θ-value for a Certain d/D for Each Flood Event of Treske's Data Using DWOPER.

Flood Event Case #	d/D	Optimal Value of Θ
5	0.0394	6.8427
6	0.0909	7.0937
7	0.1196	7.3443
8	0.1522	7.8447
9	0.1892	8.0944
10	0.2008	8.3439

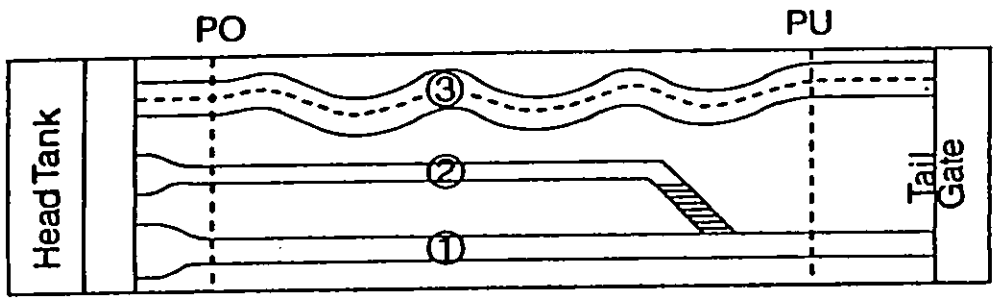

Figure 5.1 Schematic Representation of Treske's Experimental Facility.

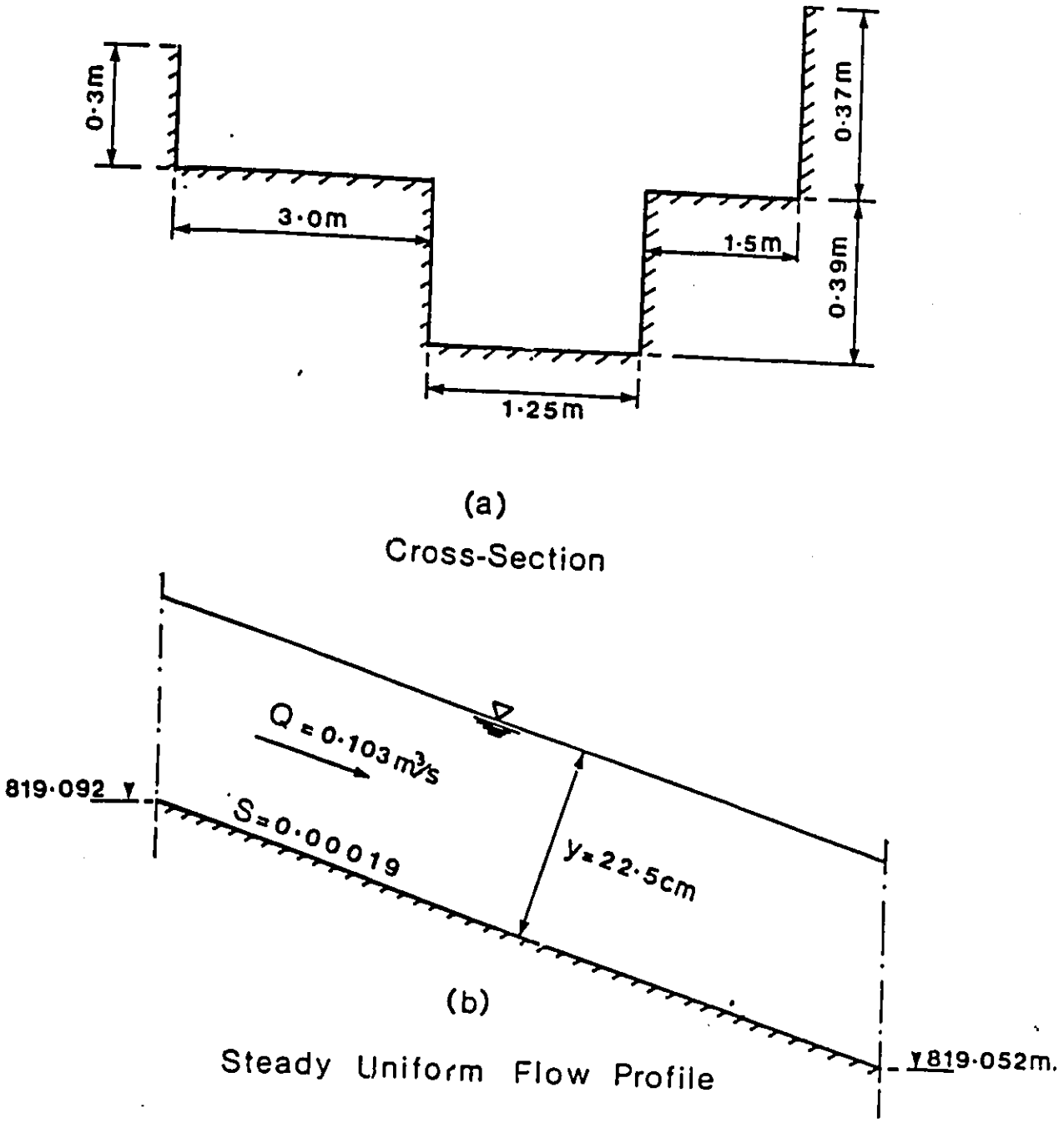

Figure 5.2 Principal Dimensions of Treske's Straight Prismatic Channel.

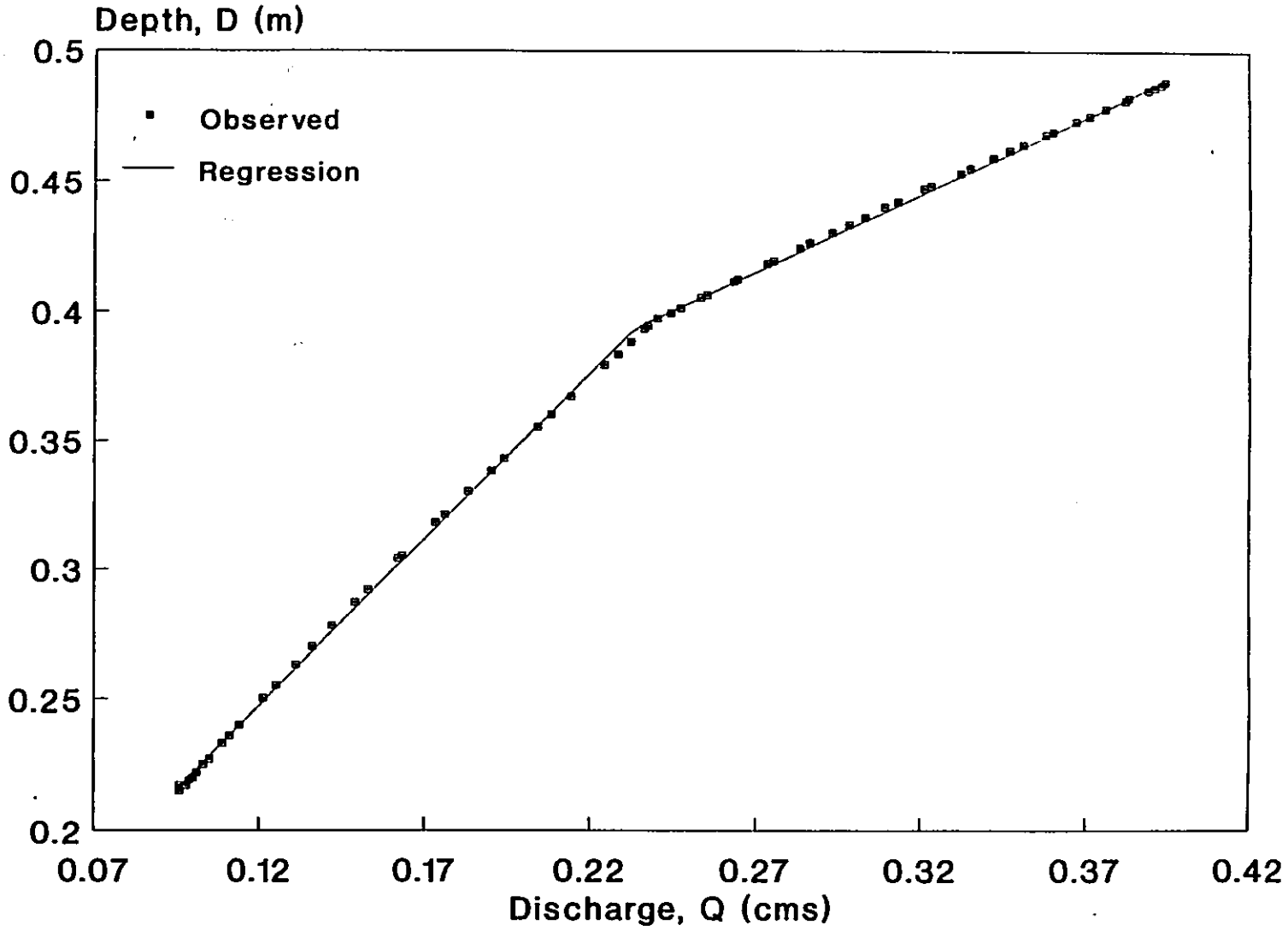

Figure 5.3 Depth-Discharge Relationship for Treske's Straight Prismatic Channel.

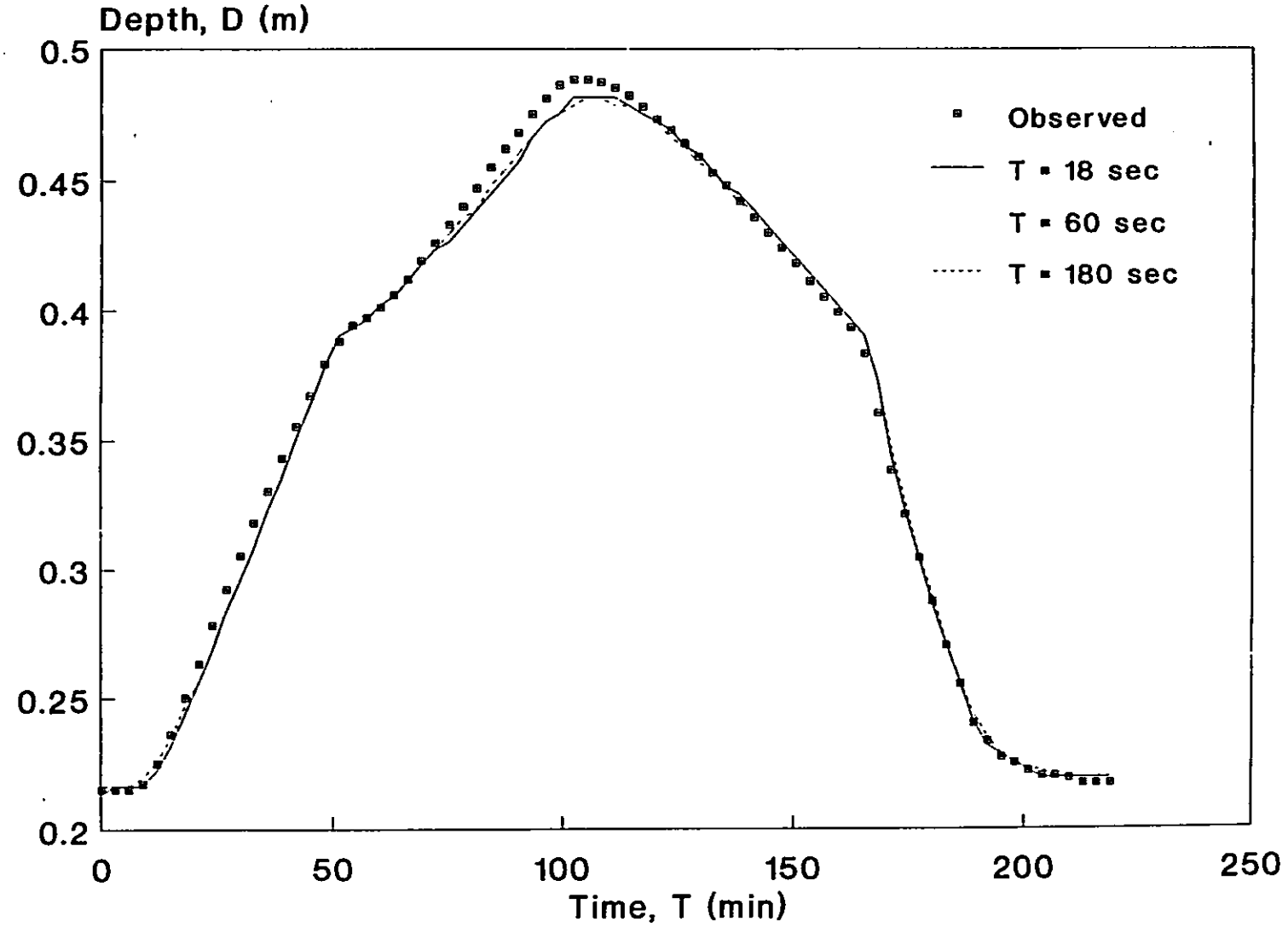

Figure 5.4 Effect of Time Step Variation on the Simulated Depth:Hydrograph Using DWOPER, (Treske's Data, Case 10).

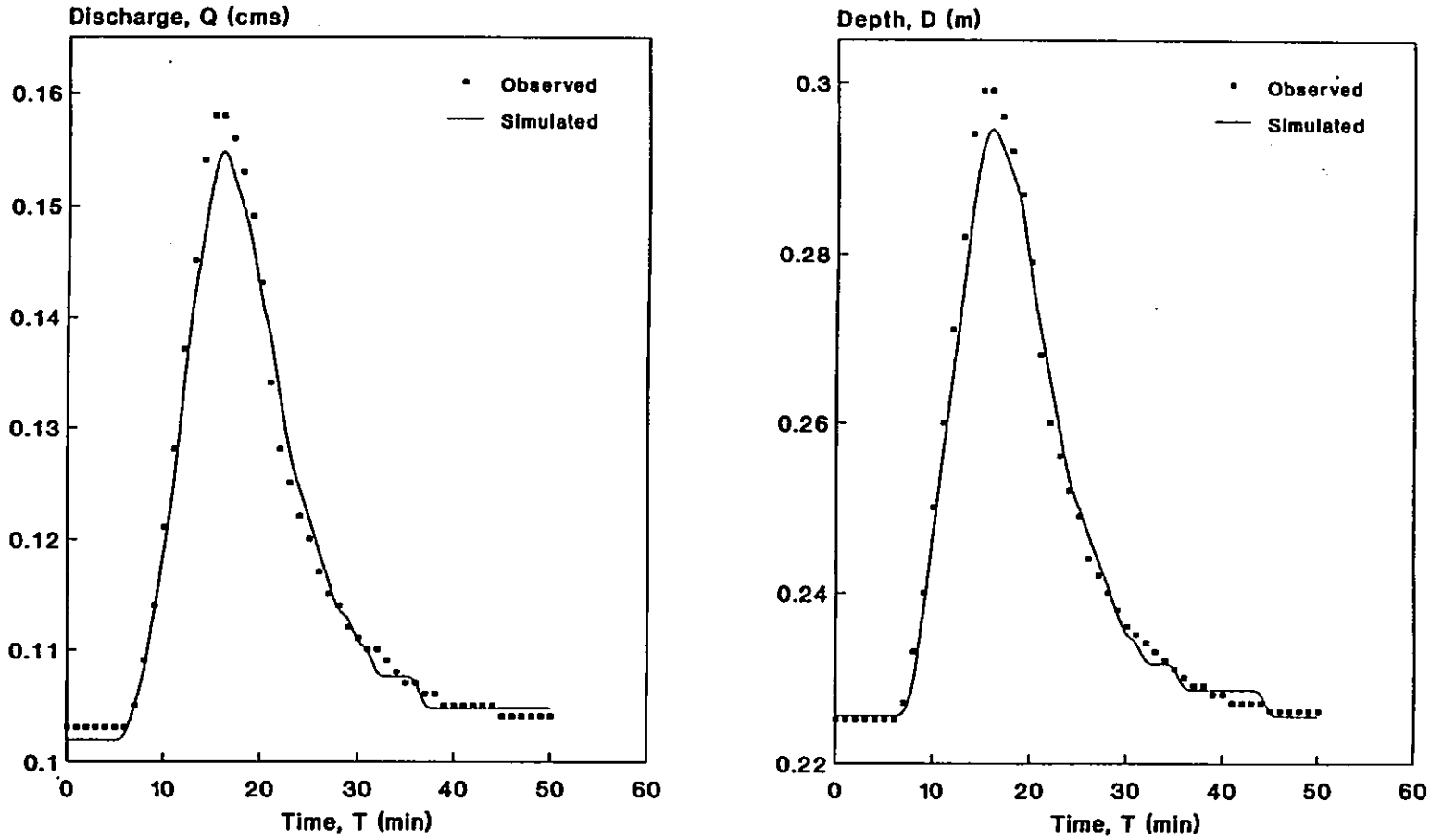

Figure 5.5 Simulated vs. Observed Discharge and Depth Hydrographs Using DWOPER, (Treske's Data, Case 1).

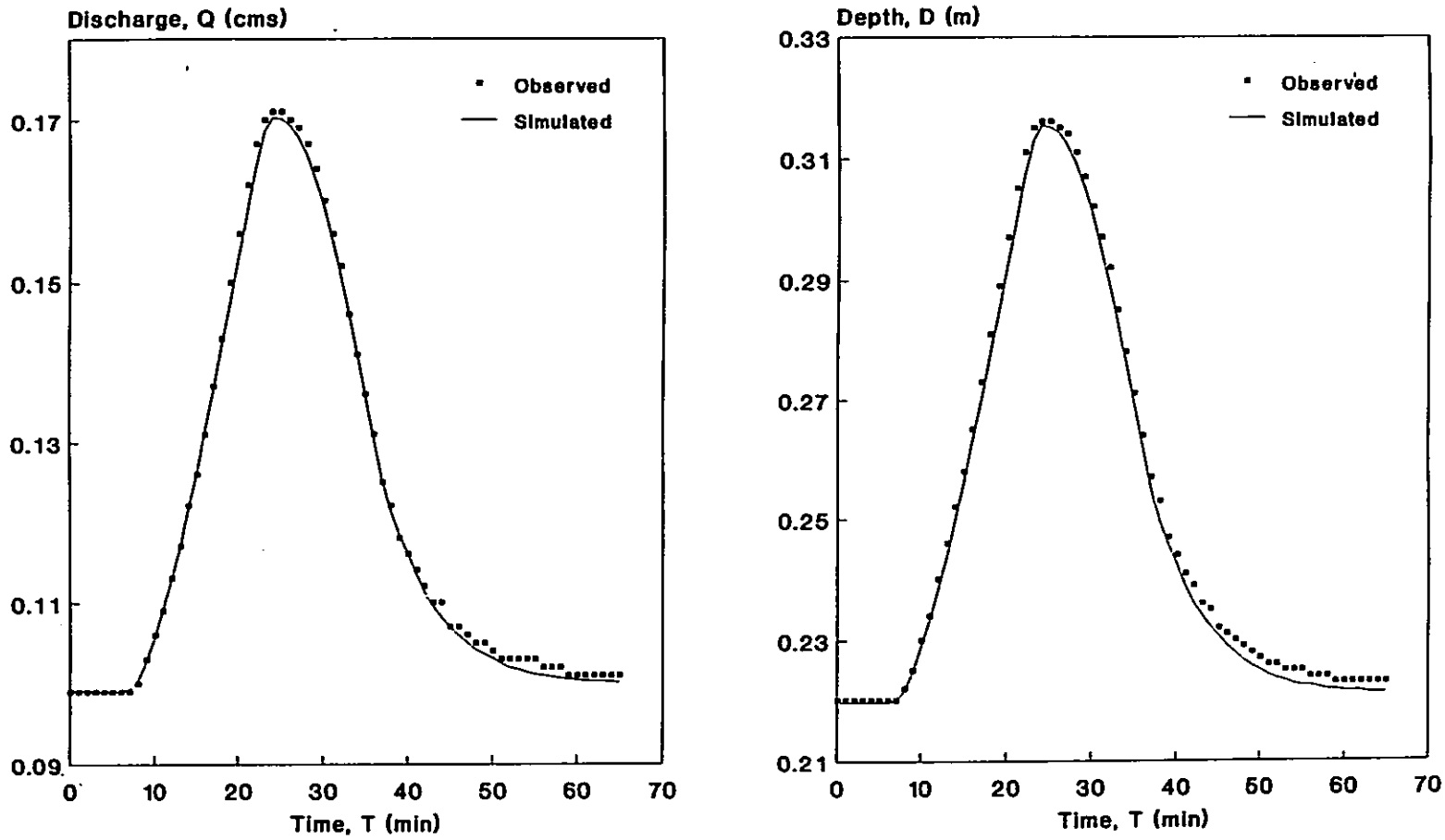

Figure 5.6 Simulated vs. Observed Discharge and Depth Hydrographs Using DWOPER, (Treske's Data, Case 2).

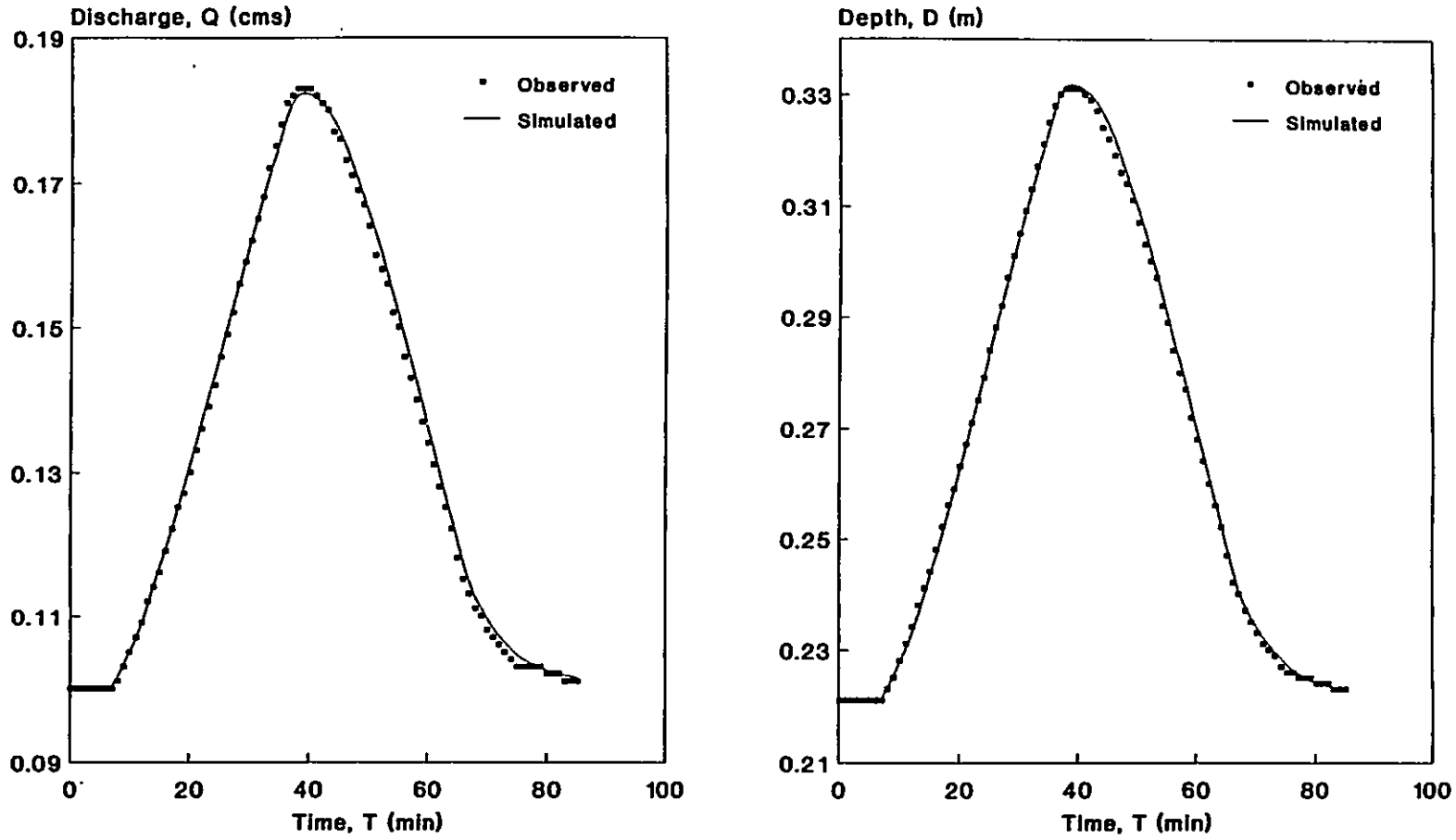

Figure 5.7 Simulated vs. Observed Discharge and Depth Hydrographs Using DWOPER, (Treske's Data, Case 3).

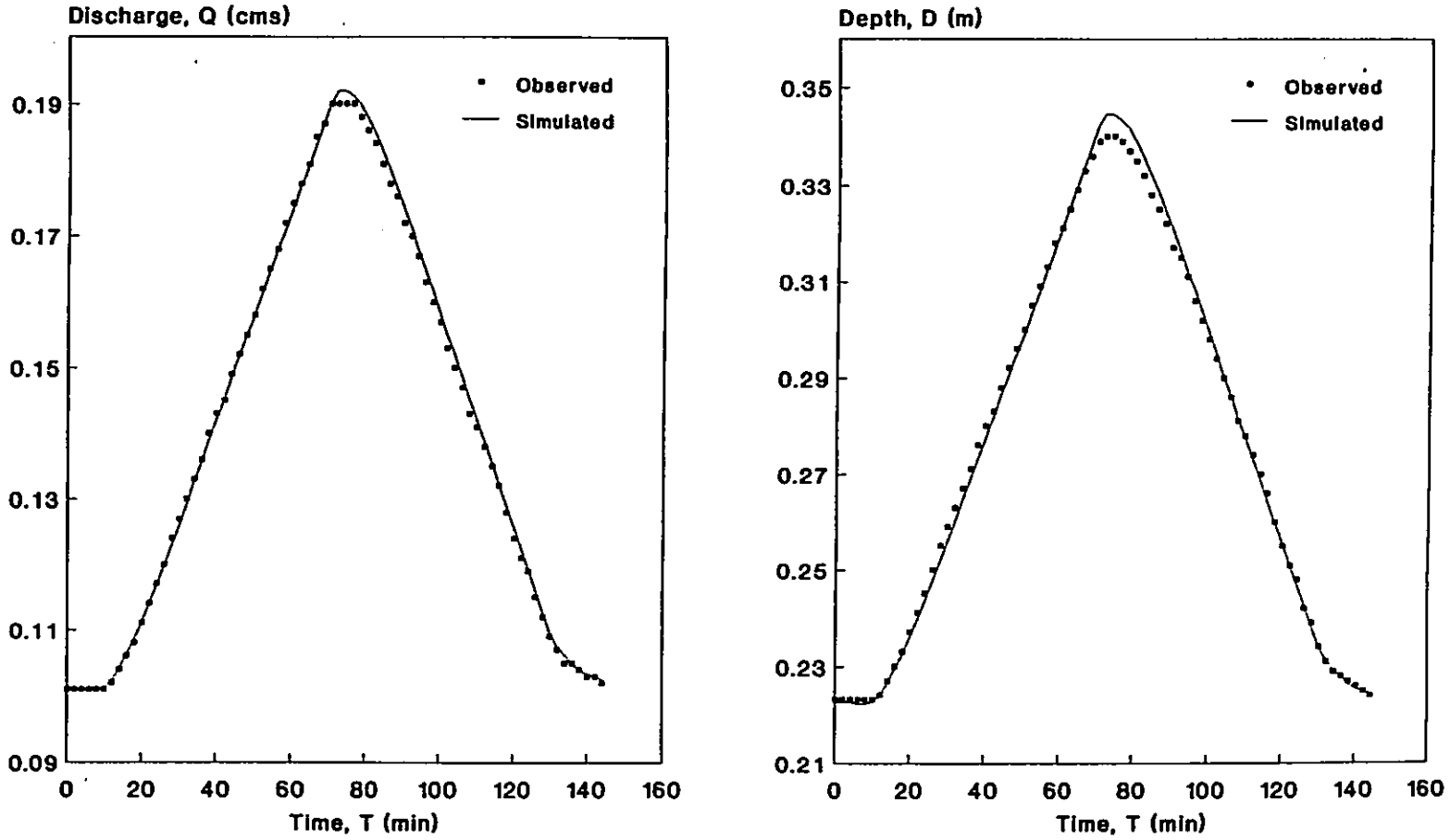

Figure 5.8 Simulated vs. Observed Discharge and Depth Hydrographs Using DWOPER, (Treske's Data, Case 4).

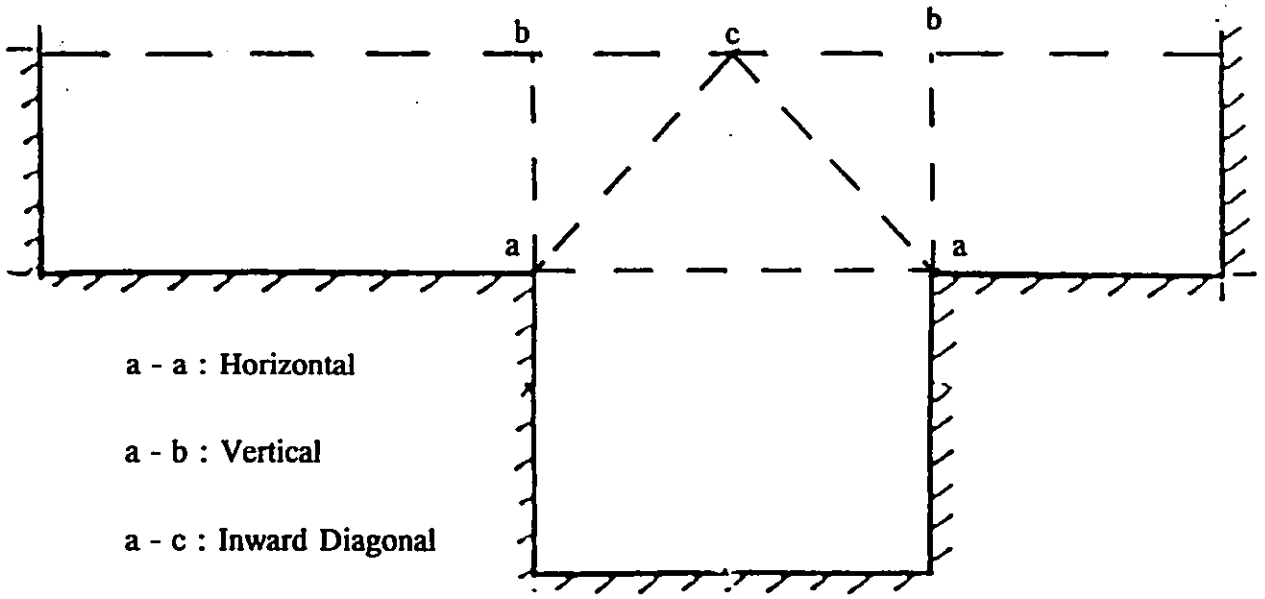

Figure 5.9 Vertical, Horizontal, and Diagonal interface planes, (After Wormleaton, 1982).

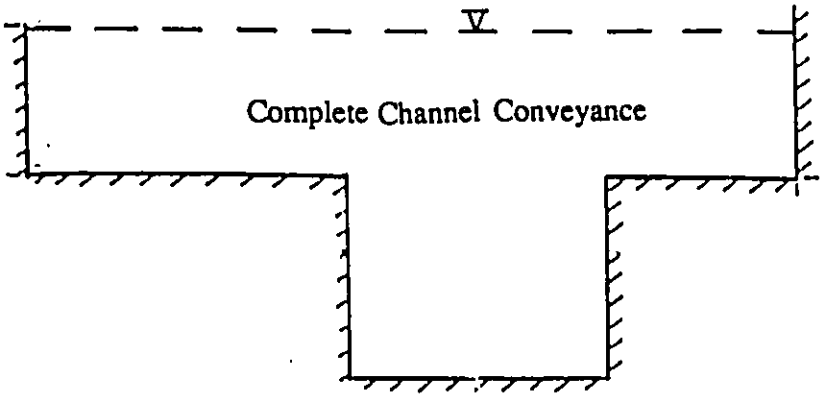

(a) No-Storage Areas.

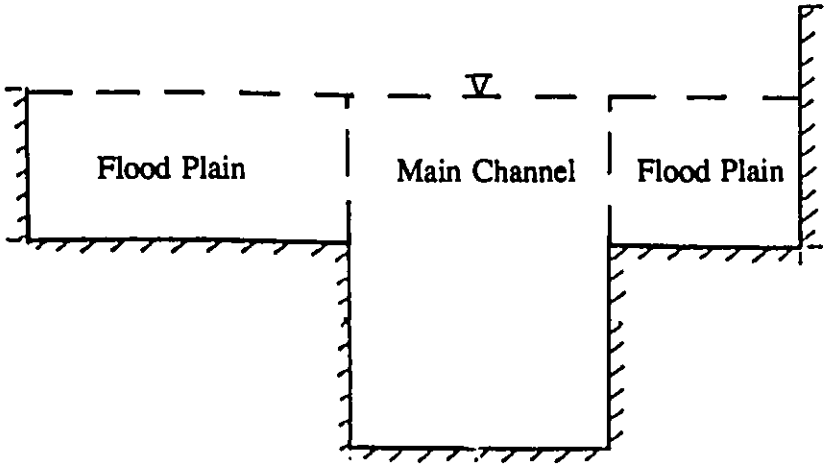

(b) Vertical Interface Planes.

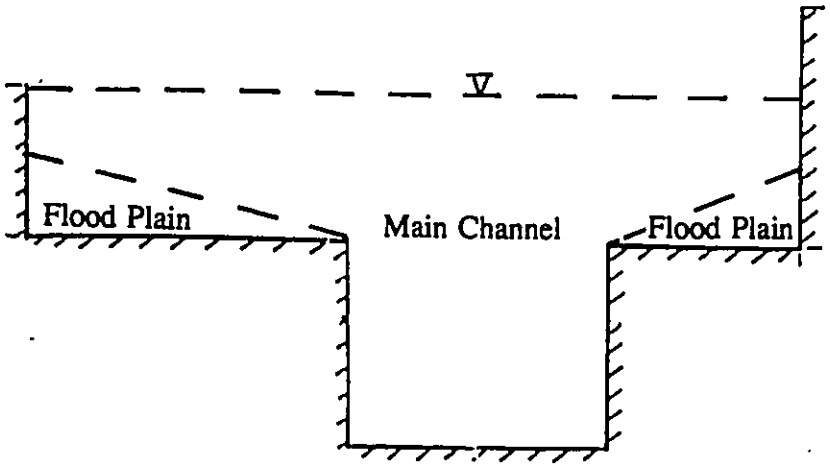

(c) Diagonal Interface Planes.

Figure 5.10 Schematic Representation of Different Interface Planes Applied to DWOPER.

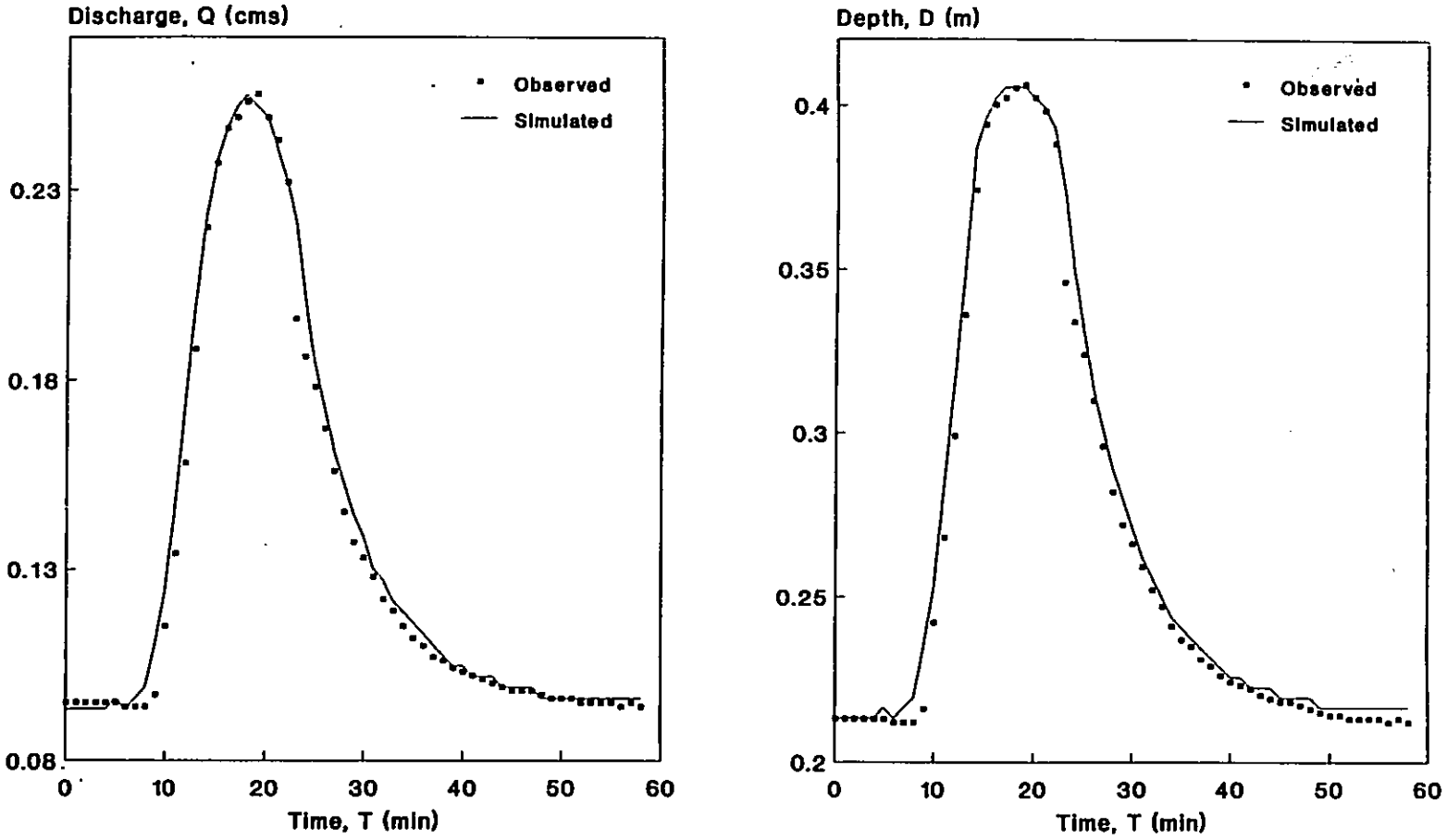

Figure 5.11 Simulated vs. Observed Discharge and Depth Hydrographs with Vertical interface planes applied to DWOPER, (Treske's data, case 5).

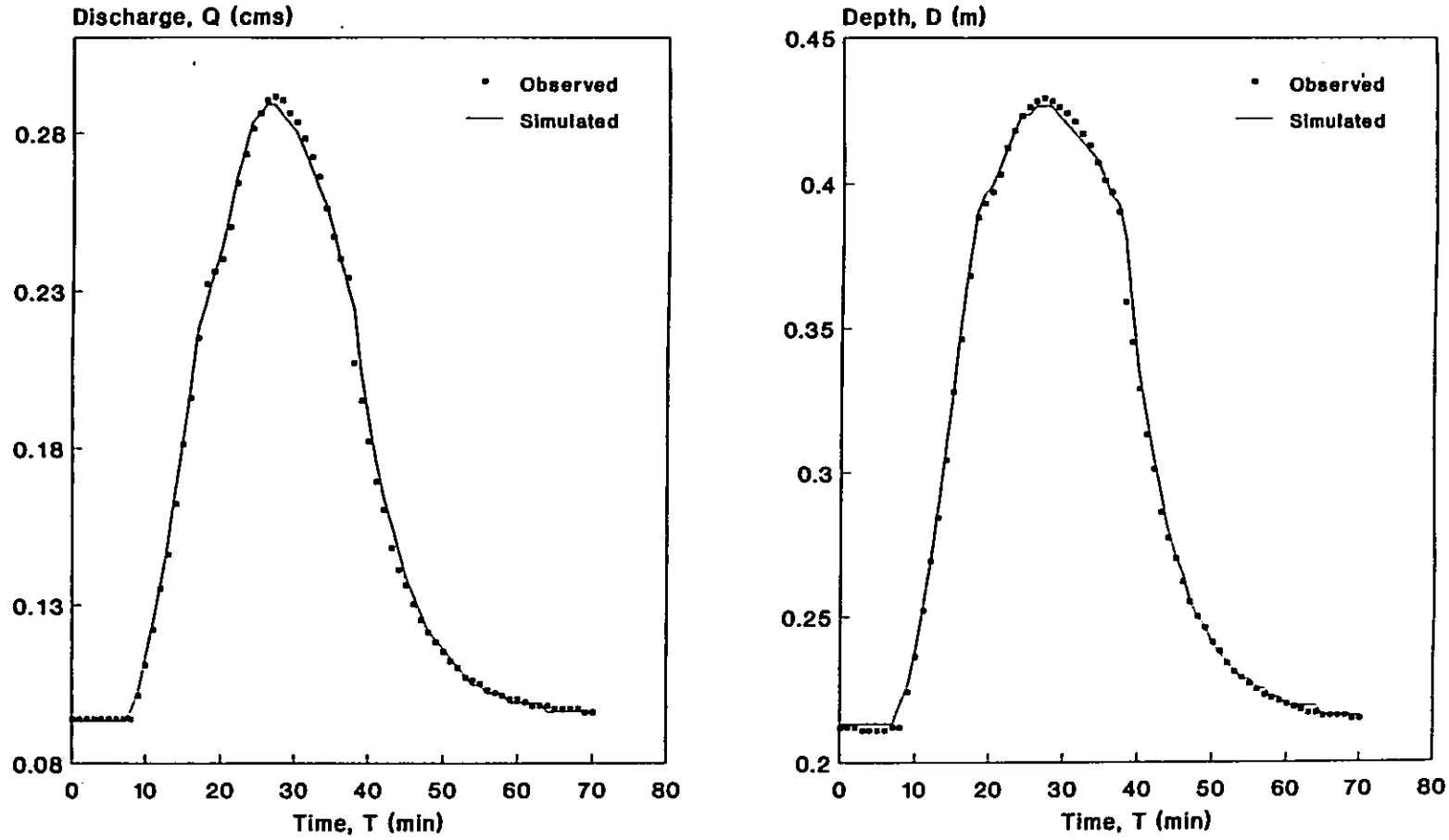

Figure 5.12 Simulated vs. Observed Discharge and Depth Hydrographs with Vertical interface planes applied to DWOPER, (Treske's data, case 6).

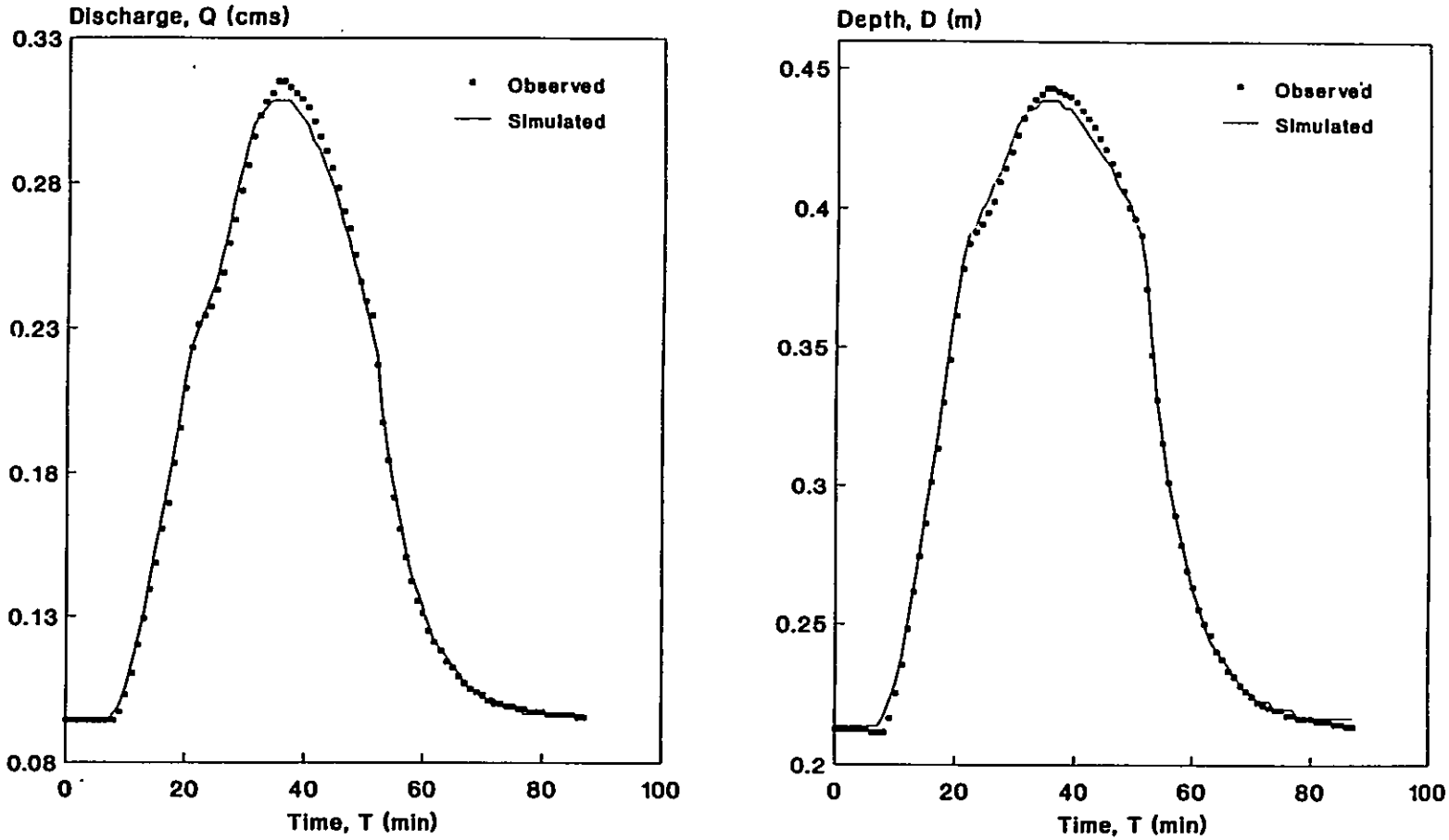

Figure 5.13 Simulated vs. Observed Discharge and Depth Hydrographs with Vertical interface planes applied to DWOPER, (Treske's data, case 7).

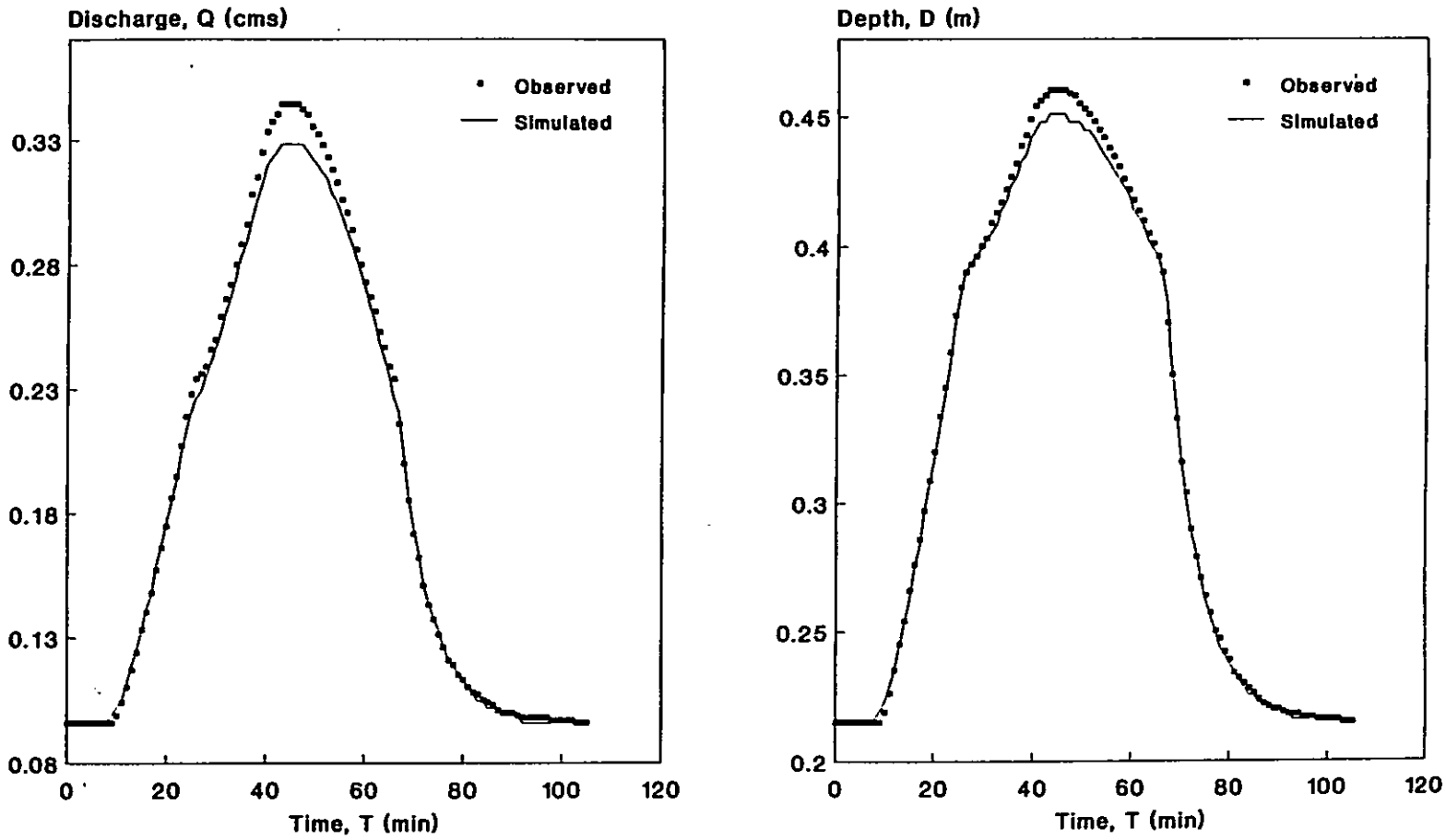

Figure 5.14 Simulated vs. Observed Discharge and Depth Hydrographs with Vertical interface planes applied to DWOPER, (Treske's data, case 8).

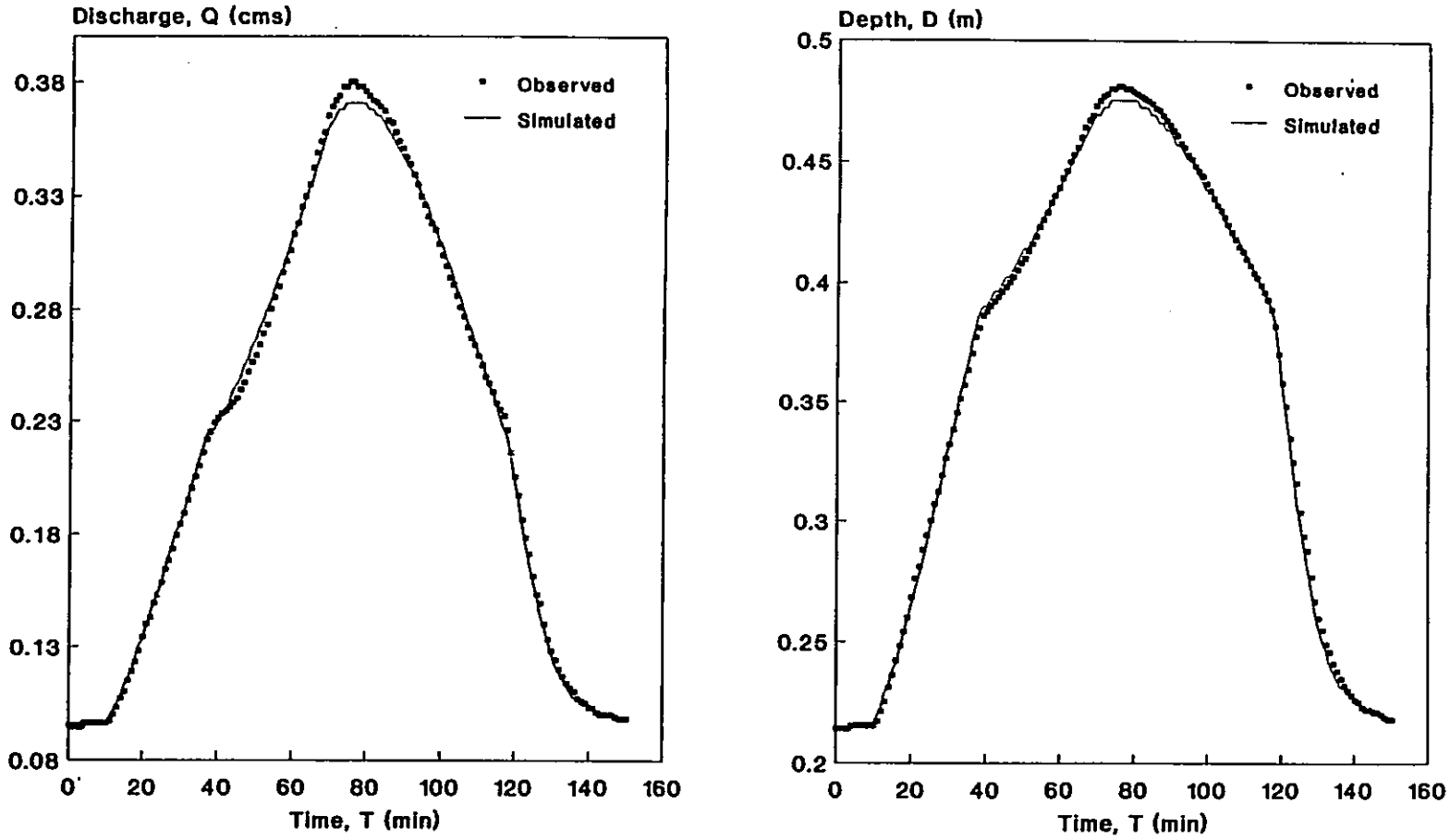

Figure 5.15 Simulated vs. Observed Discharge and Depth Hydrographs with Vertical interface planes applied to DWOPER, (Treske's data, case 9).

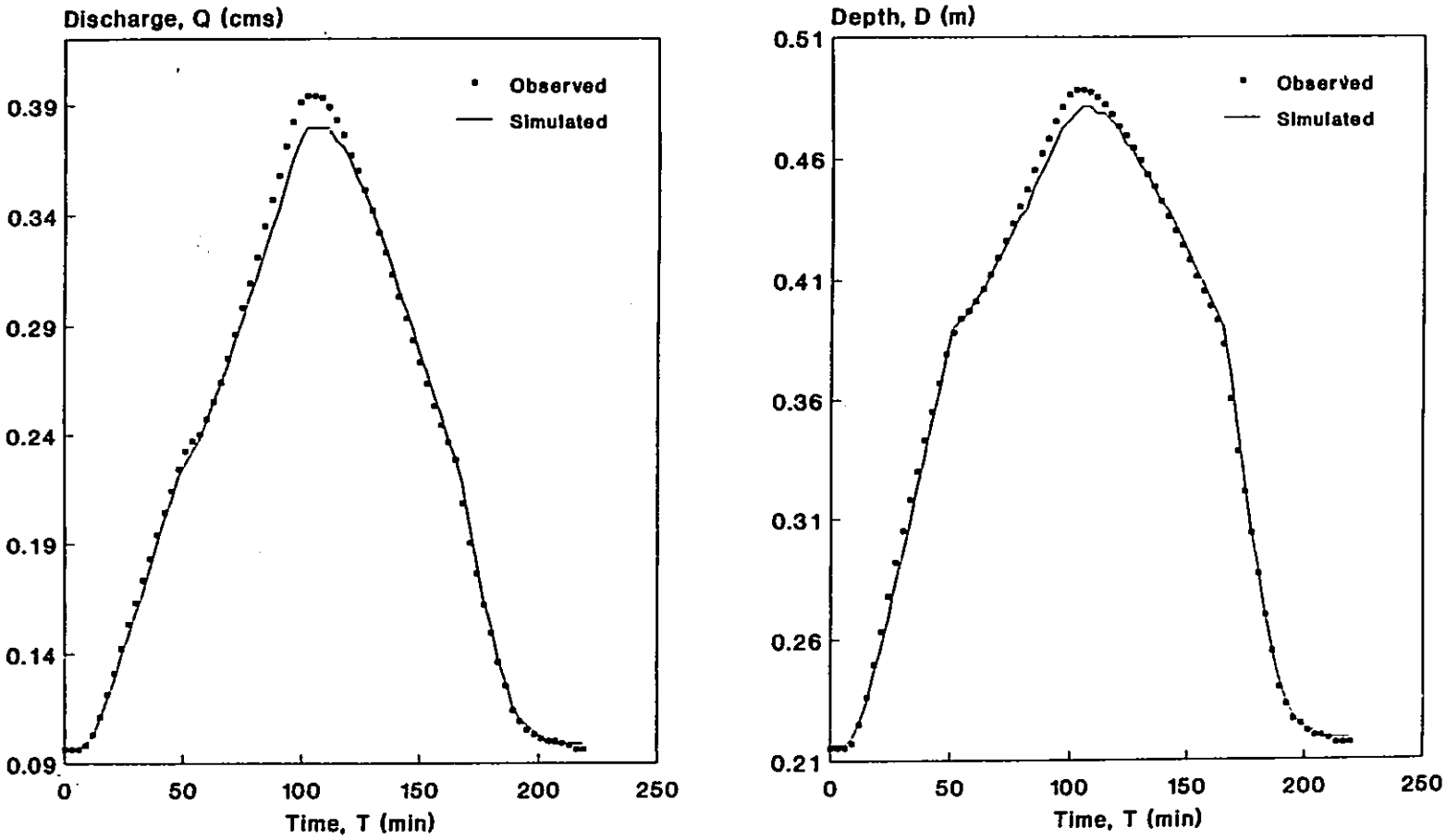

Figure 5.16 Simulated vs. Observed Discharge and Depth Hydrographs with Vertical interface planes applied to DWOPER, (Treske's data, case 10).

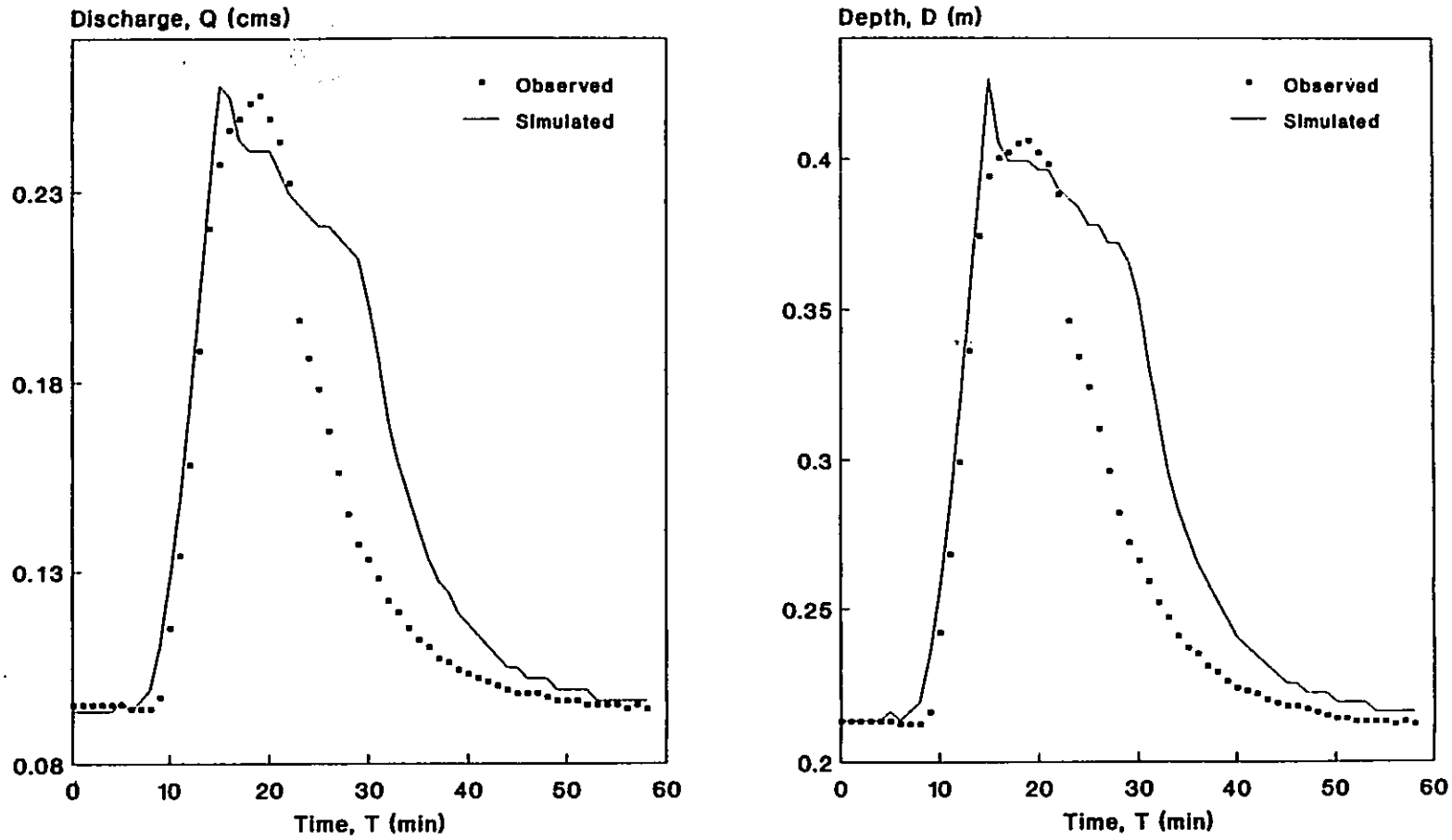

Figure 5.17 Simulated vs. Observed Discharge and Depth Hydrographs with No Off-Channel Storage Areas applied to DWOPER, (Treske's data, case 5).

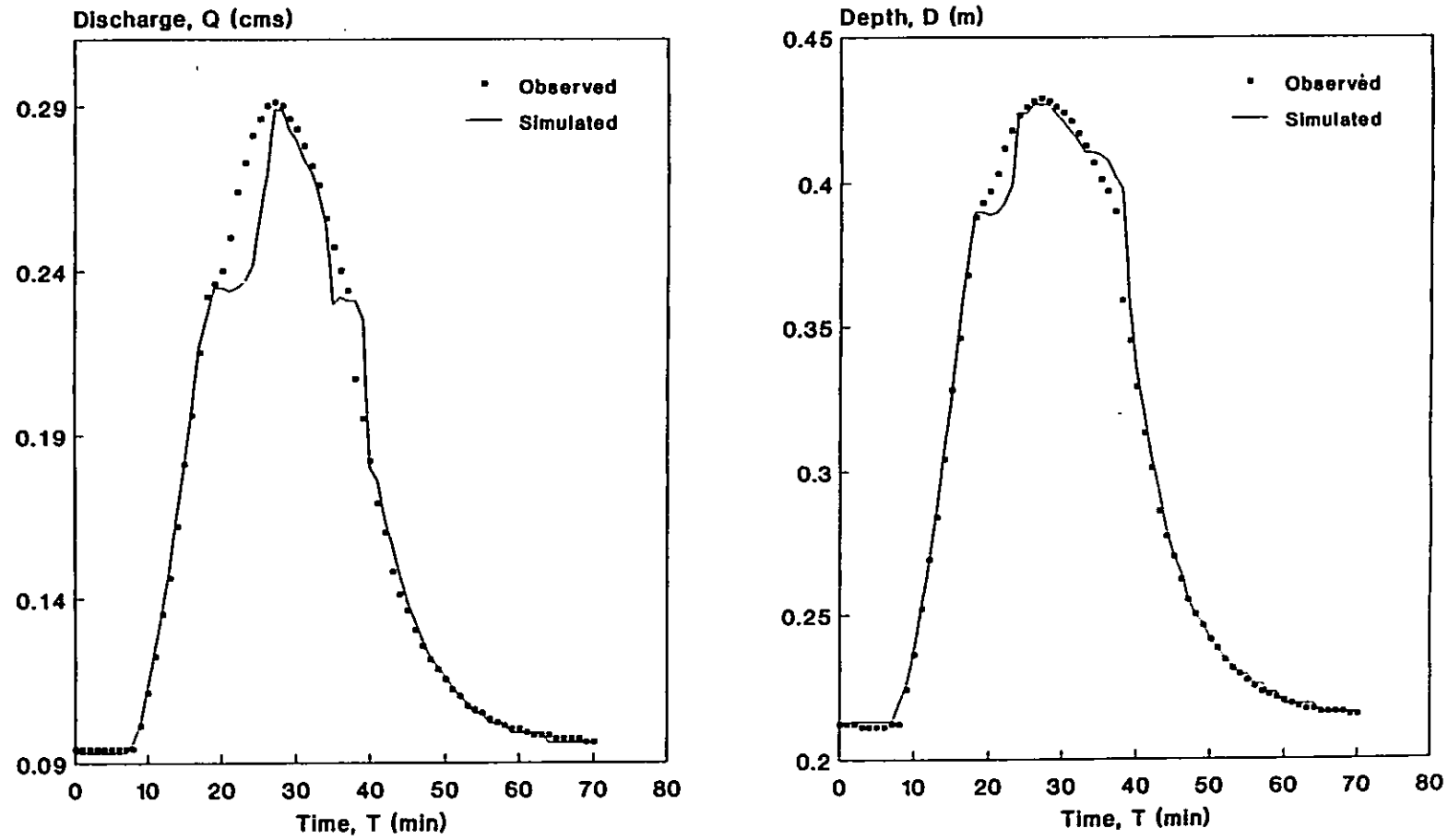

Figure 5.18 Simulated vs. Observed Discharge and Depth Hydrographs with No Off-Channel Storage Areas applied to DWOPER, (Treske's data, case 6).

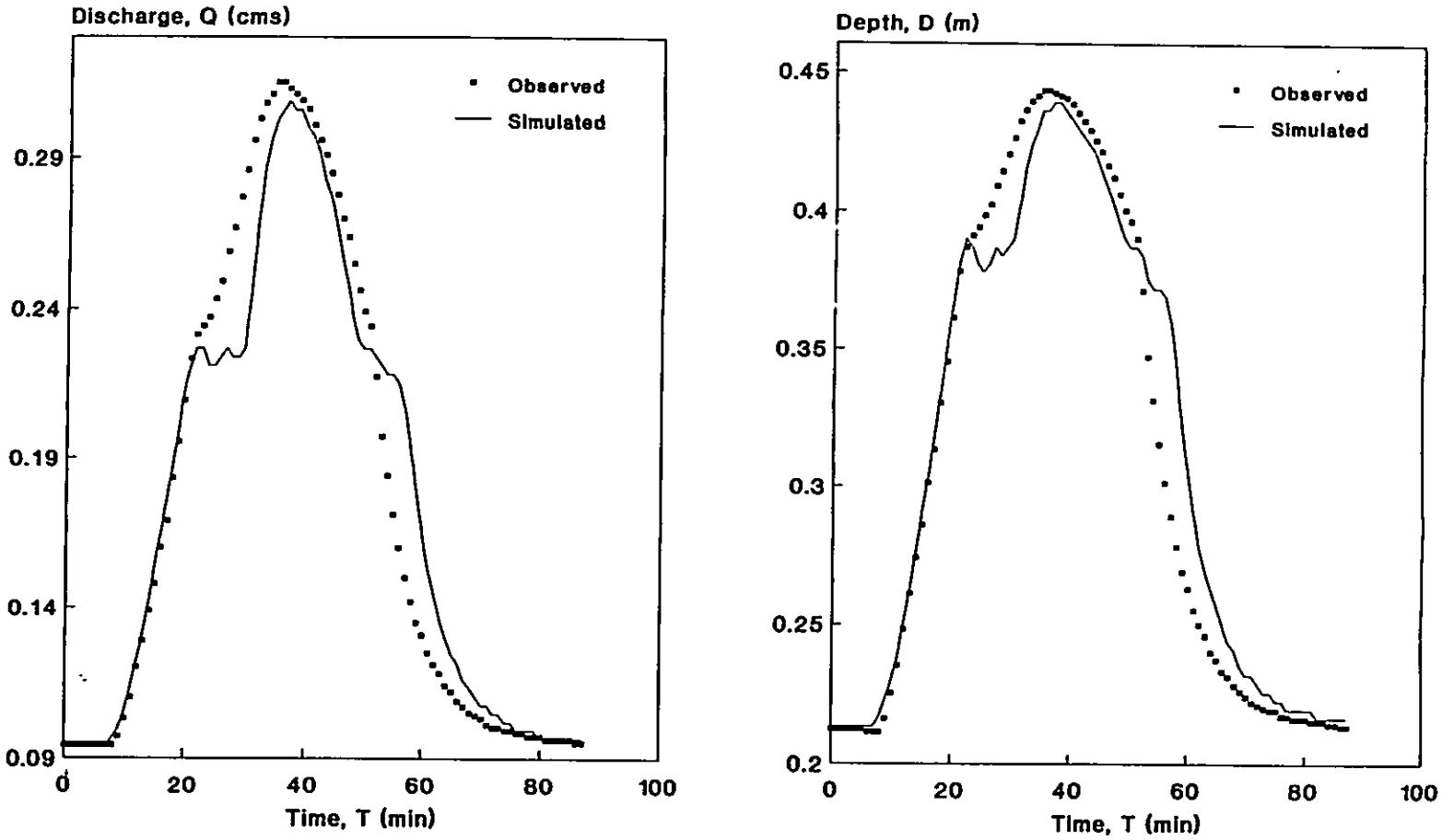

Figure 5.19 Simulated vs. Observed Discharge and Depth Hydrographs with No Off-Channel Storage Areas applied to DWOPER, (Treske's data, case 7).

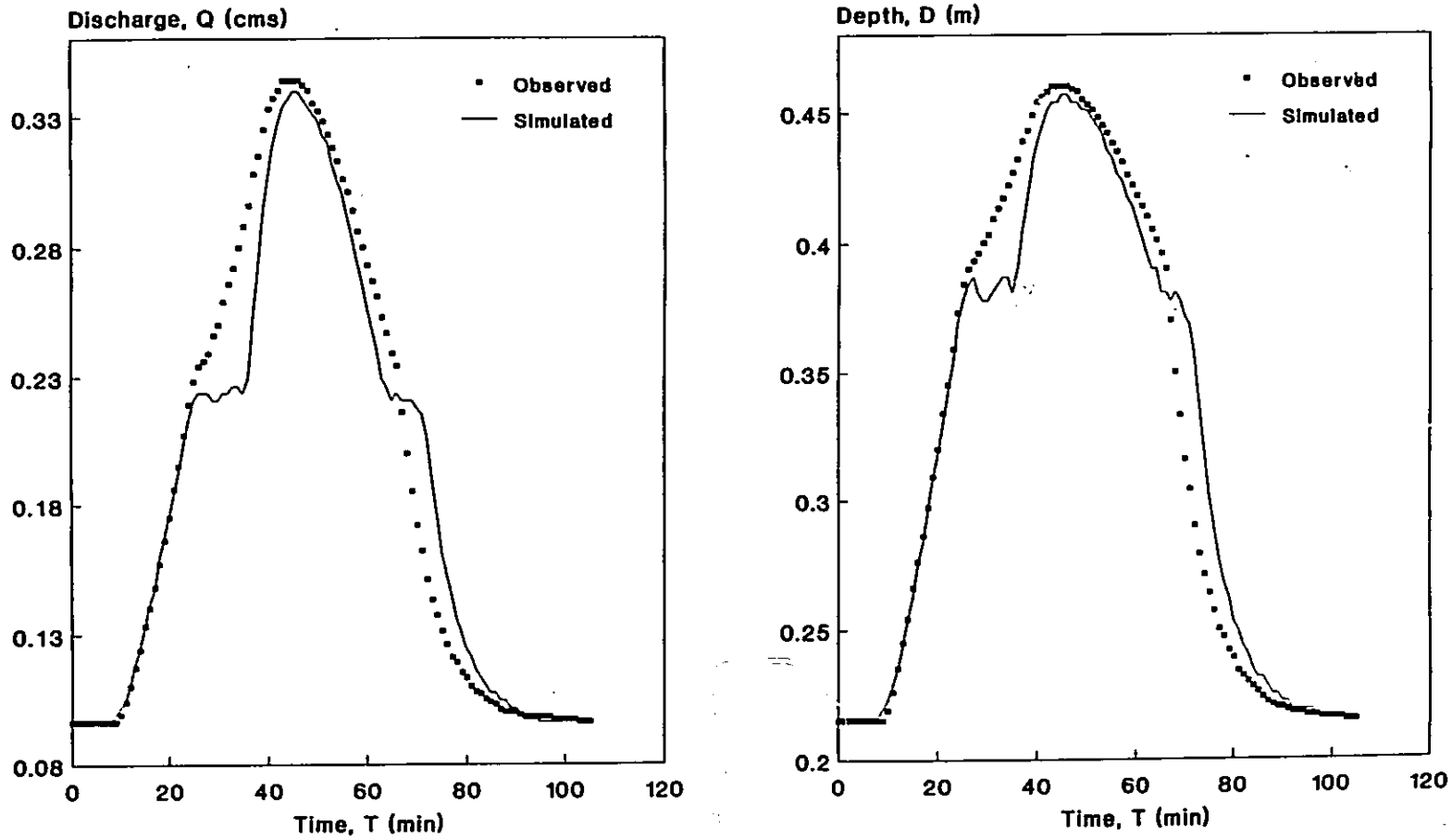

Figure 5.20 Simulated vs. Observed Discharge and Depth Hydrographs with No Off-Channel Storage Areas applied to DWOPER, (Treske's data, case 8).

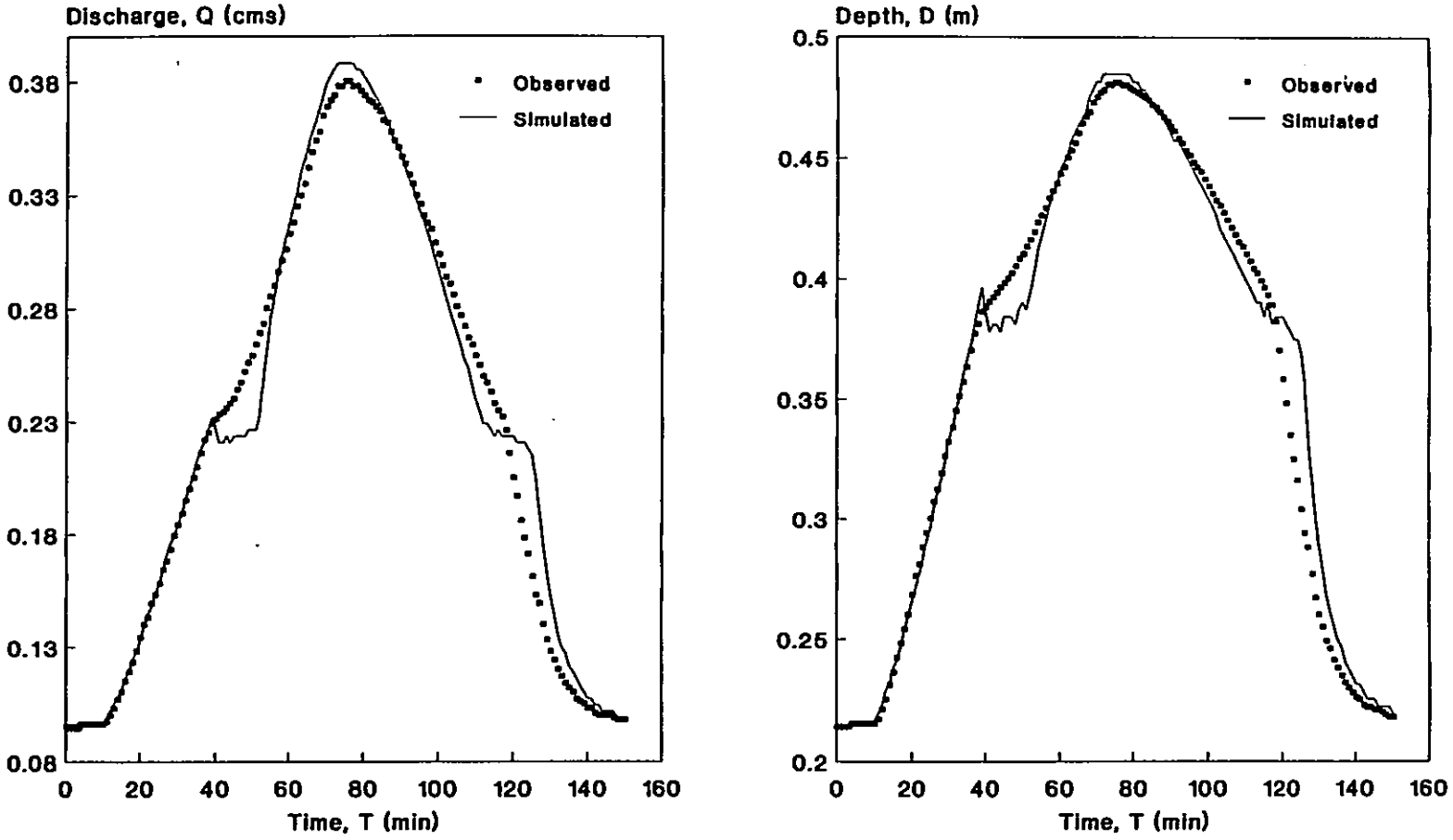

Figure 5.21 Simulated vs. Observed Discharge and Depth Hydrographs with No Off-Channel Storage Areas applied to DWOPER, (Treske's data, case 9).

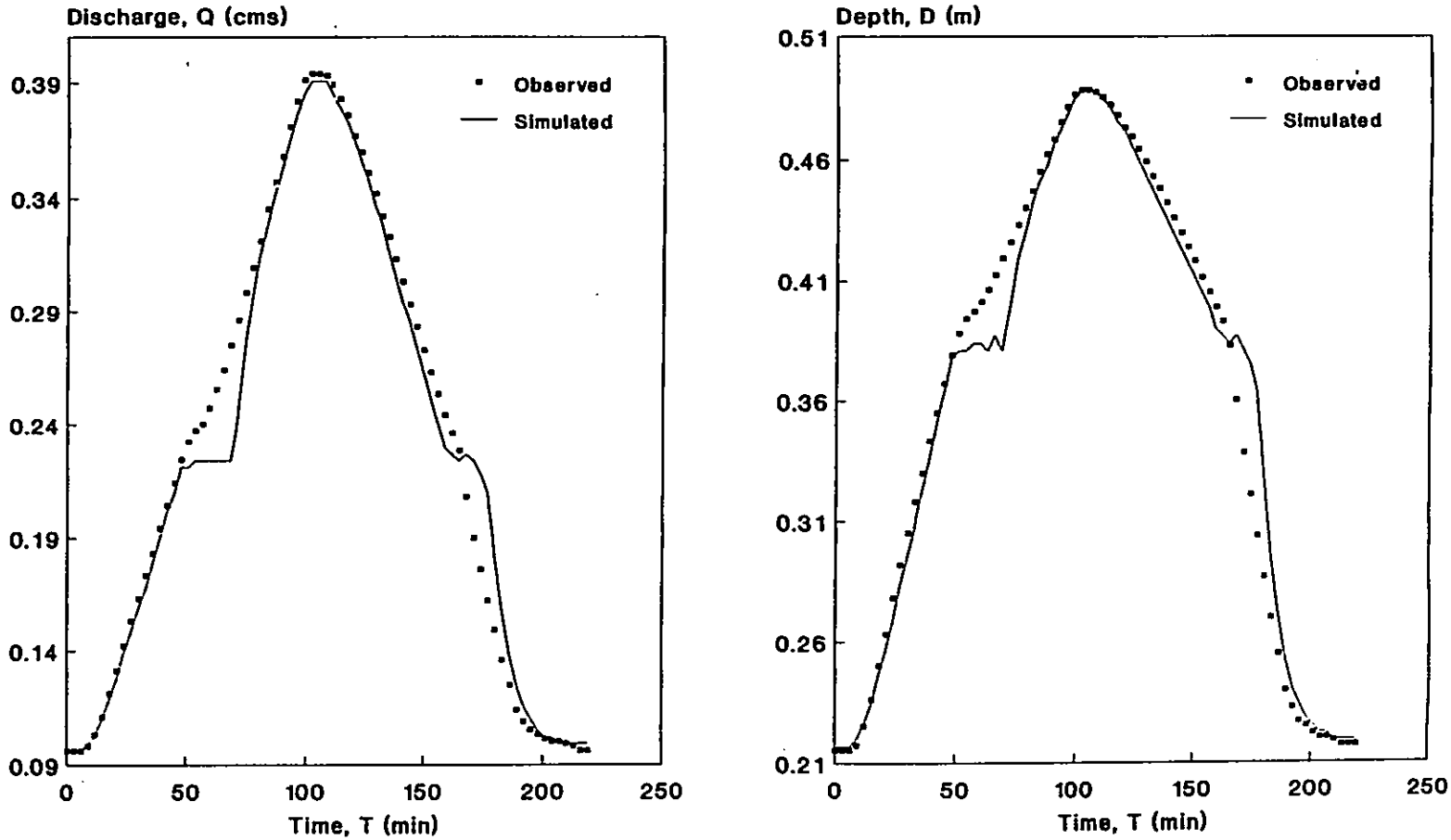

Figure 5.22 Simulated vs. Observed Discharge and Depth Hydrographs with No Off-Channel Storage Areas applied to DWOPER, (Treske's data, case 10).

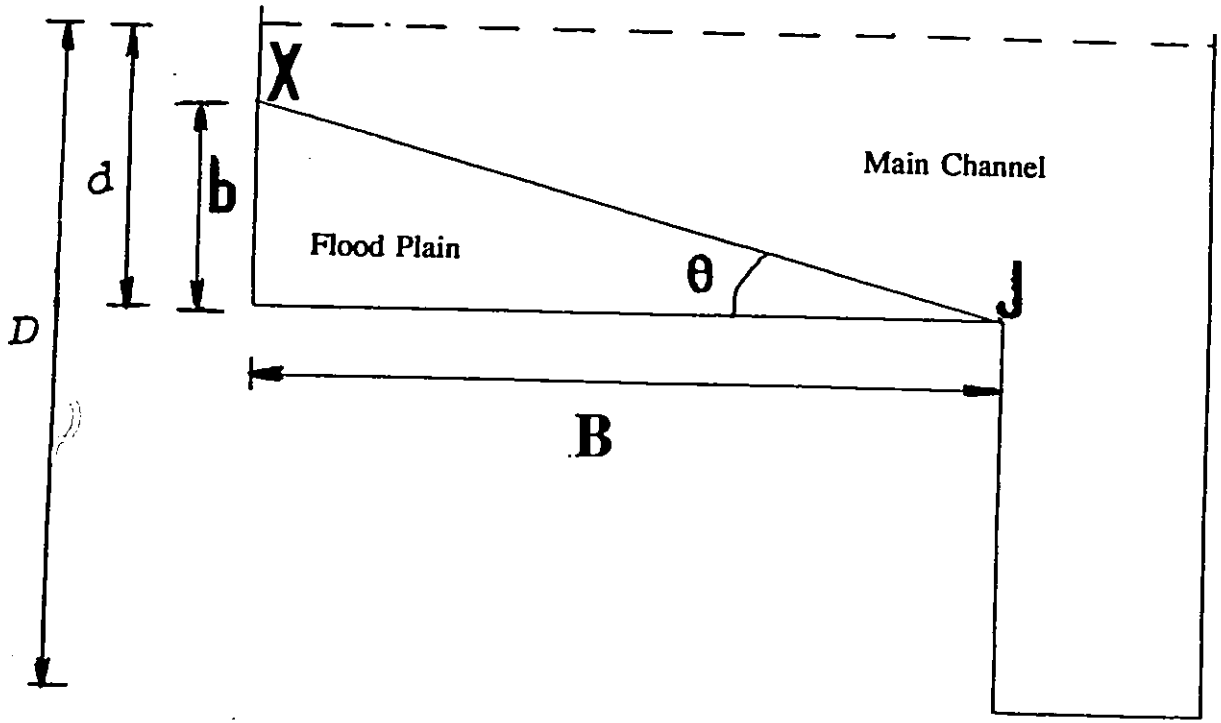

$$\theta = 27.813\ (d/D)^2 + 2.646\ (d/D) + 6.673$$

Figure 5.23 Defining the Diagonal Interface Planes Applied to DWOPER.

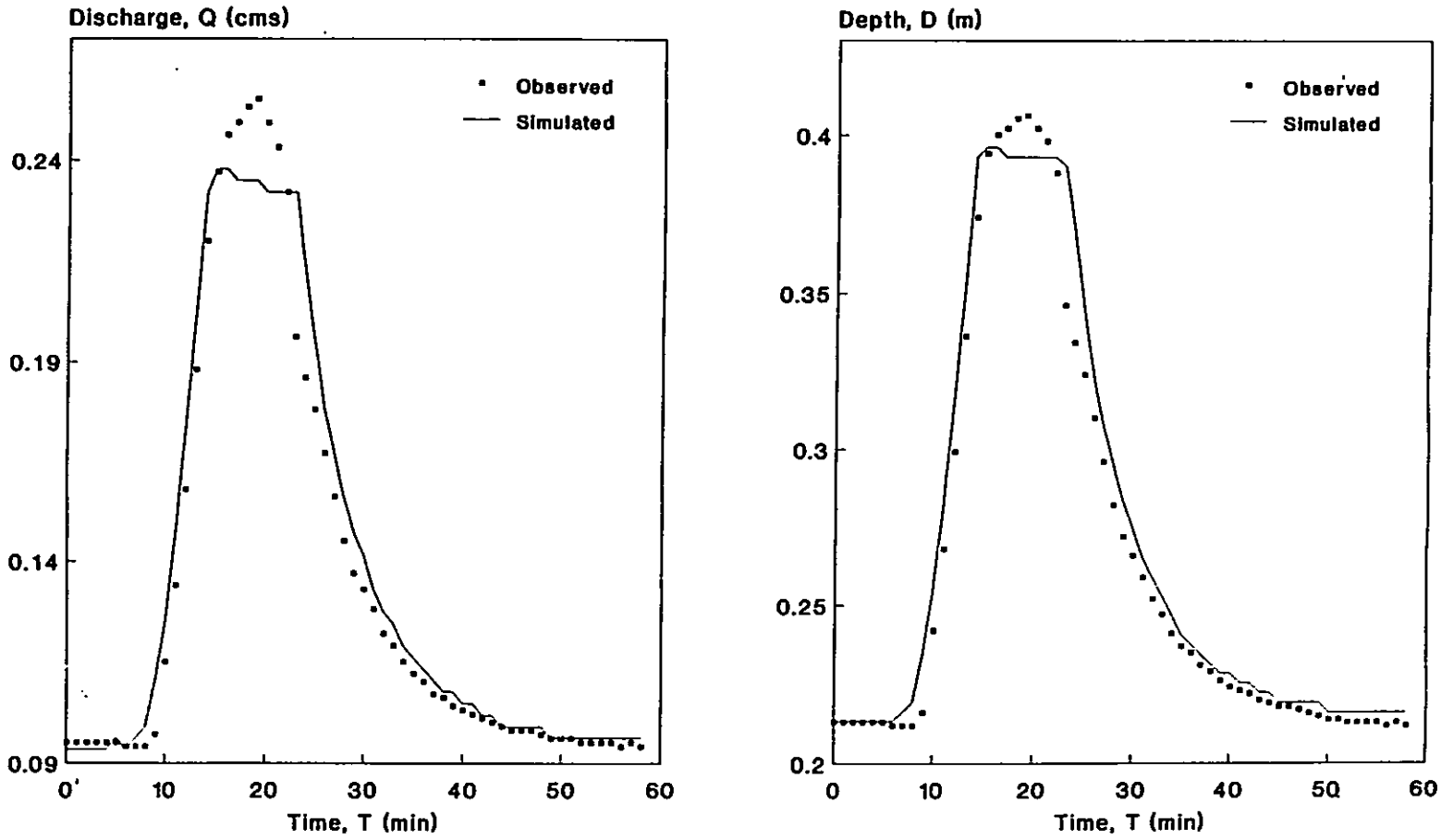

Figure 5.24 Simulated vs. Observed Discharge and Depth Hydrographs with Diagonal Interface Planes applied to DWOPER, (Θ = 5.33°, Treske's Data, Case 5).

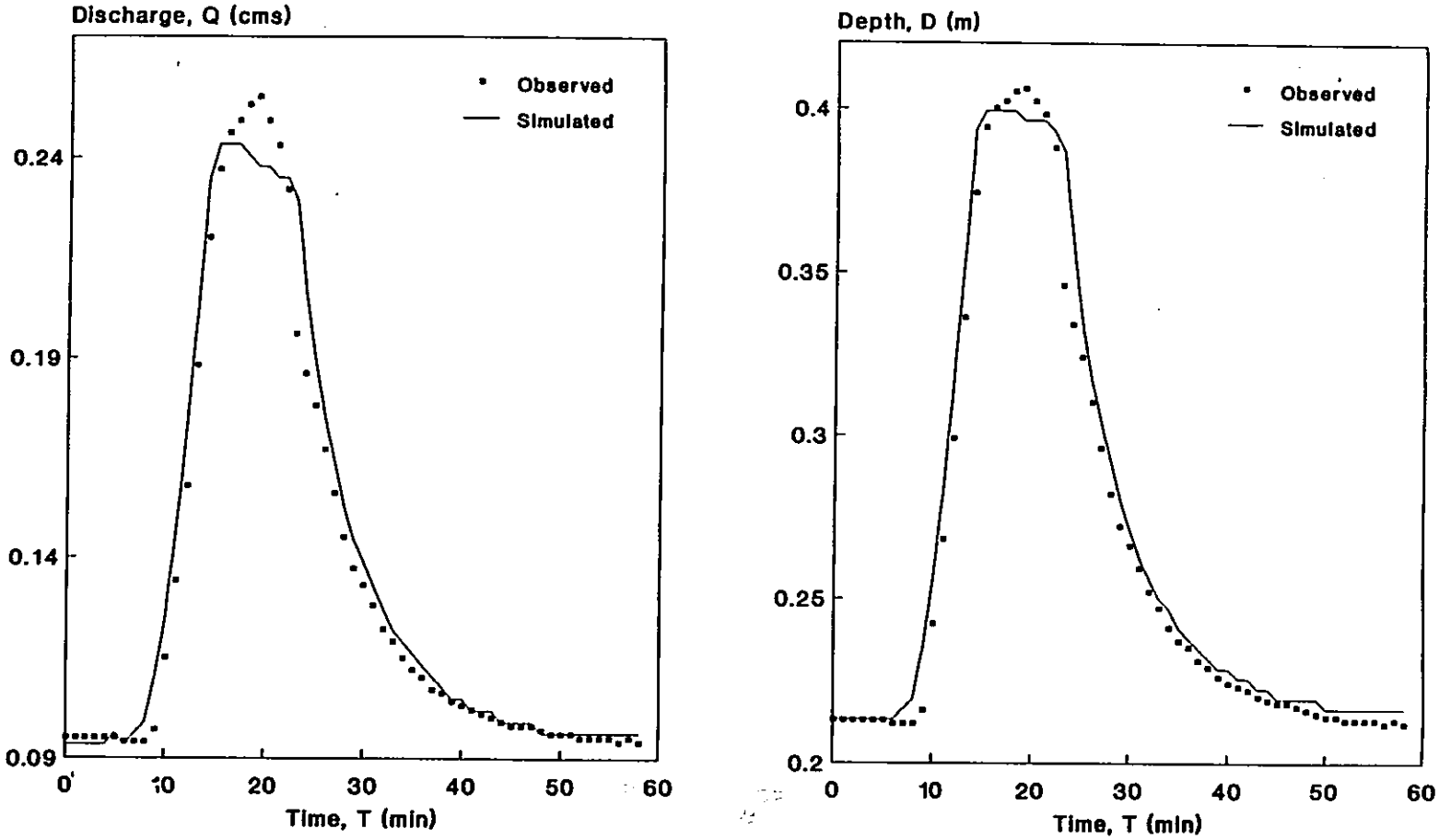

Figure 5.25 Simulated vs. Observed Discharge and Depth Hydrographs with Diagonal Interface Planes applied to DWOPER, (Θ = 5.58°, Treske's Data, Case 5).

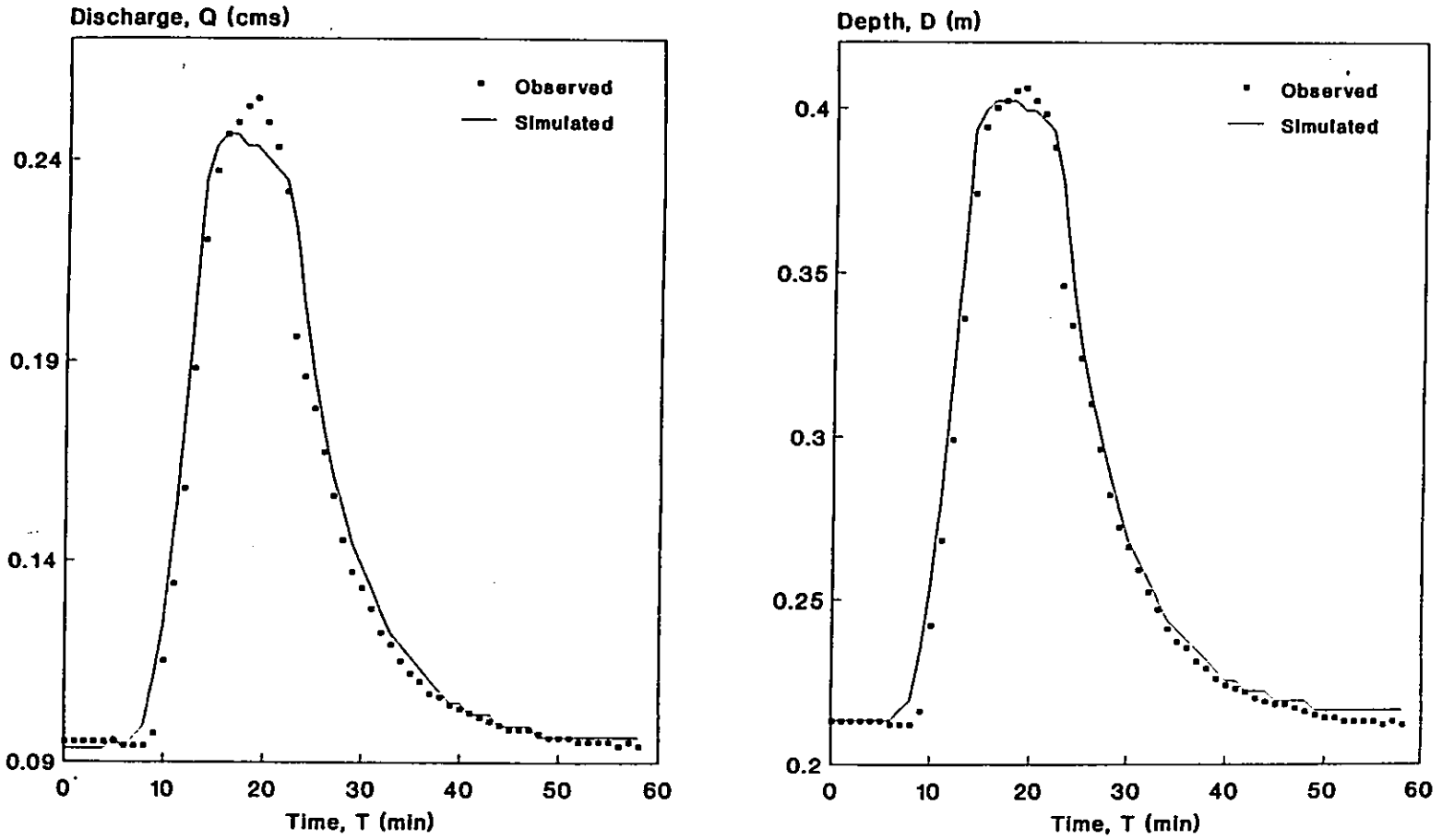

Figure 5.26 Simulated vs. Observed Discharge and Depth Hydrographs with Diagonal Interface Planes applied to DWOPER, (Θ = 5.71°, Treske's Data, Case 5).

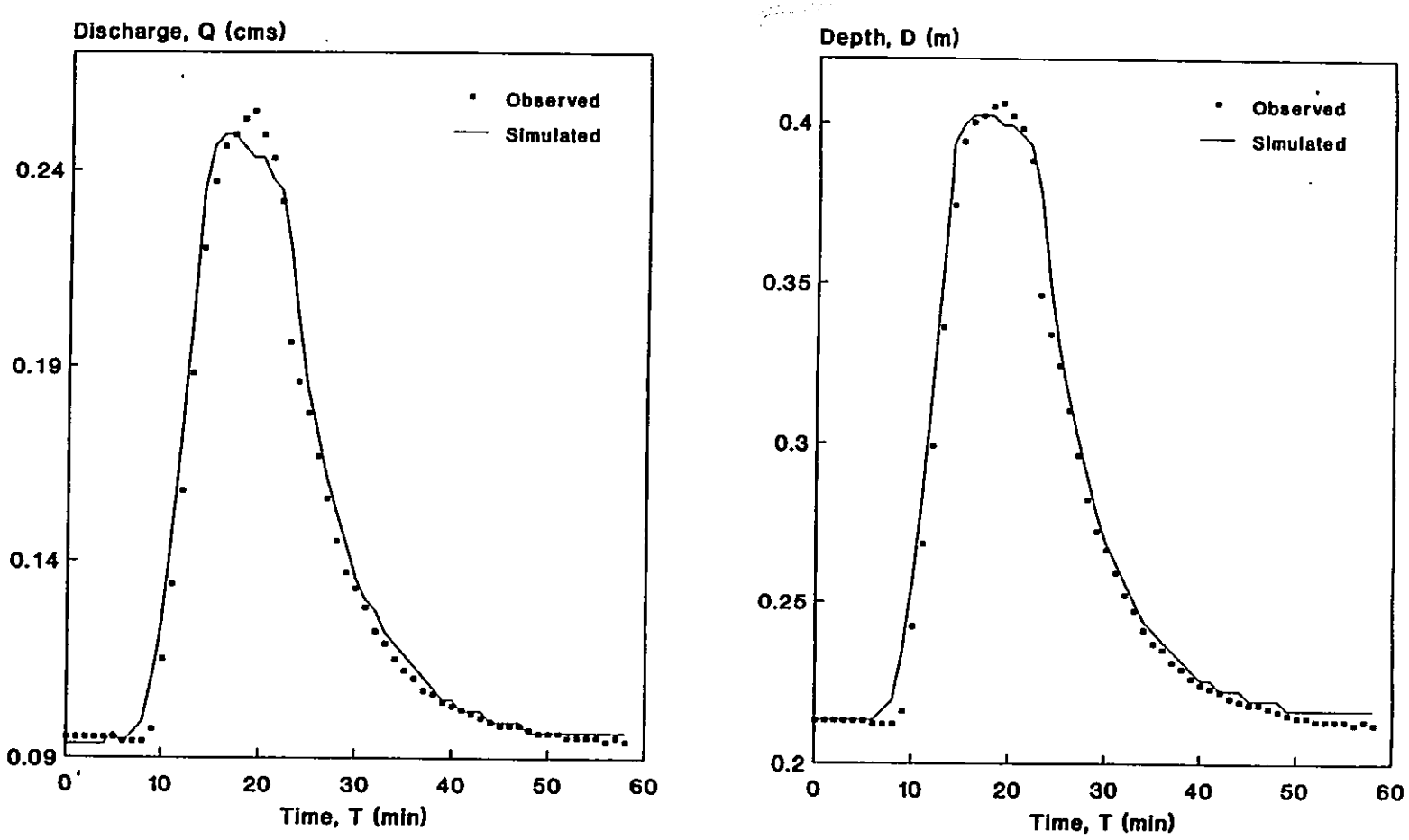

Figure 5.27 Simulated vs. Observed Discharge and Depth Hydrographs with Diagonal Interface Planes applied to DWOPER, (Θ = 5.84°, Treske's Data, Case 5).

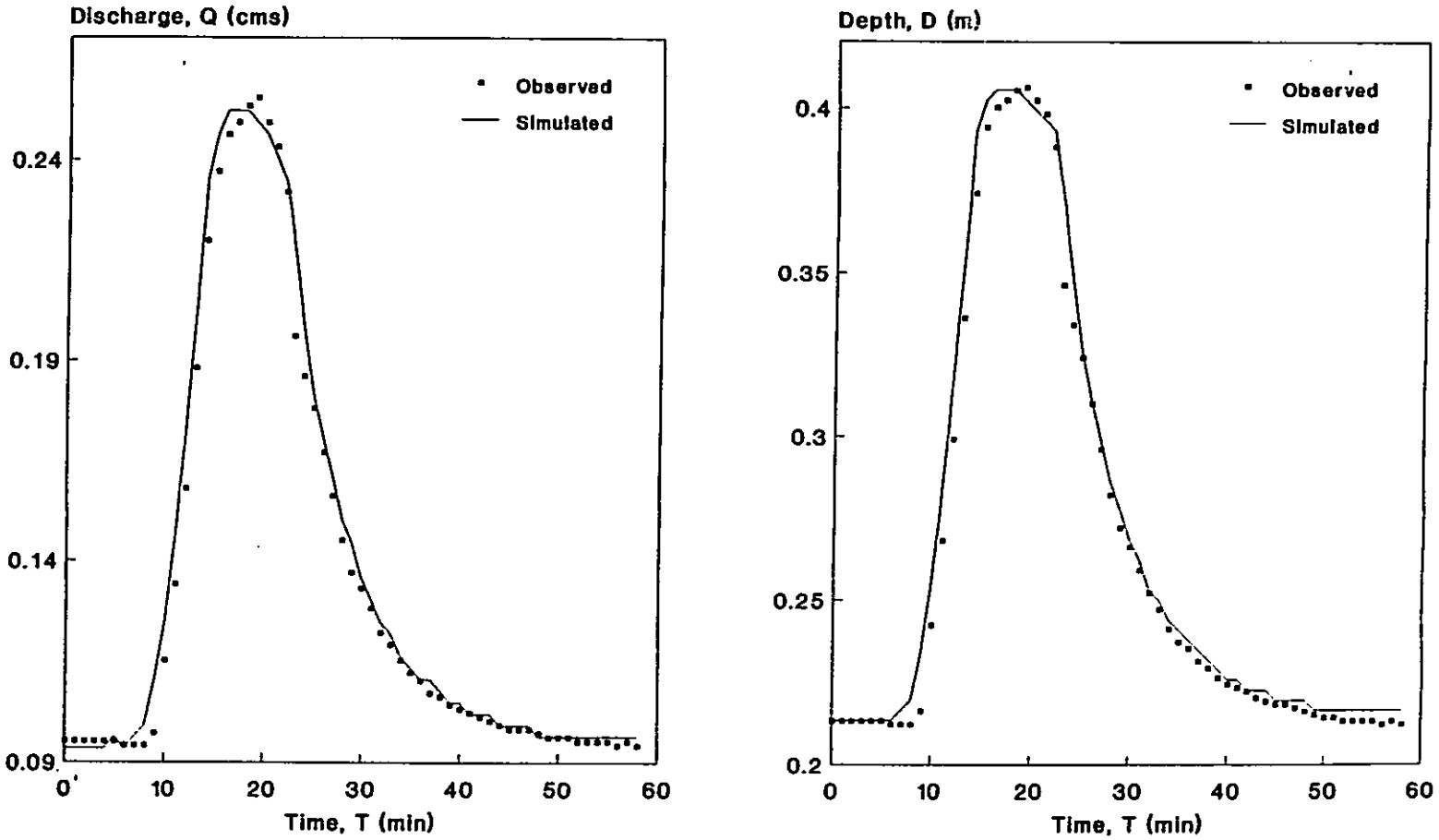

Figure 5.28 Simulated vs. Observed Discharge and Depth Hydrographs with Diagonal Interface Planes applied to DWOPER, (Θ = 6.09°, Treske's Data, Case 5).

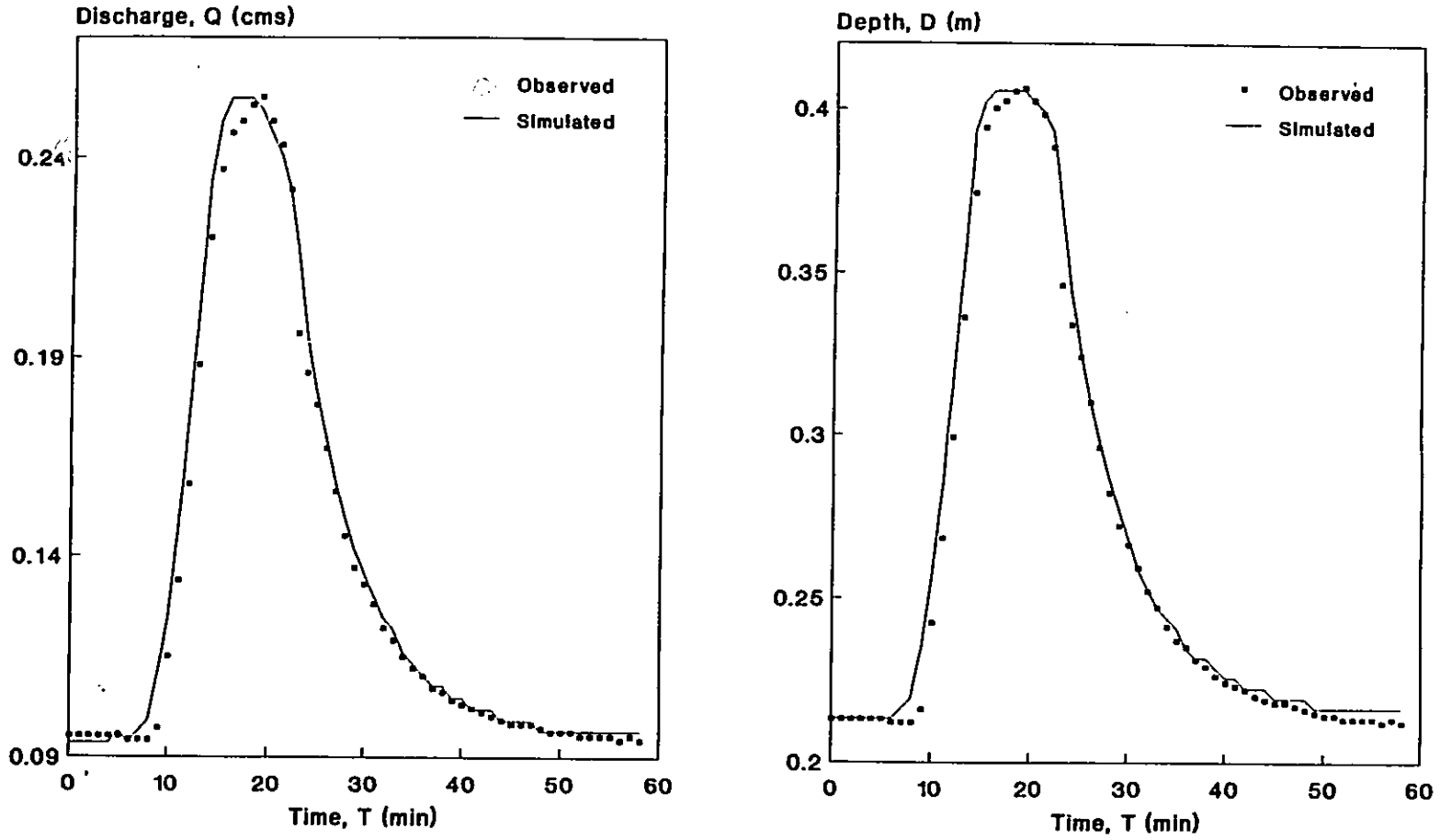

Figure 5.29 Simulated vs. Observed Discharge and Depth Hydrographs with Diagonal Interface Planes applied to DWOPER, (Θ = 6.34°, Treske's Data, Case 5).

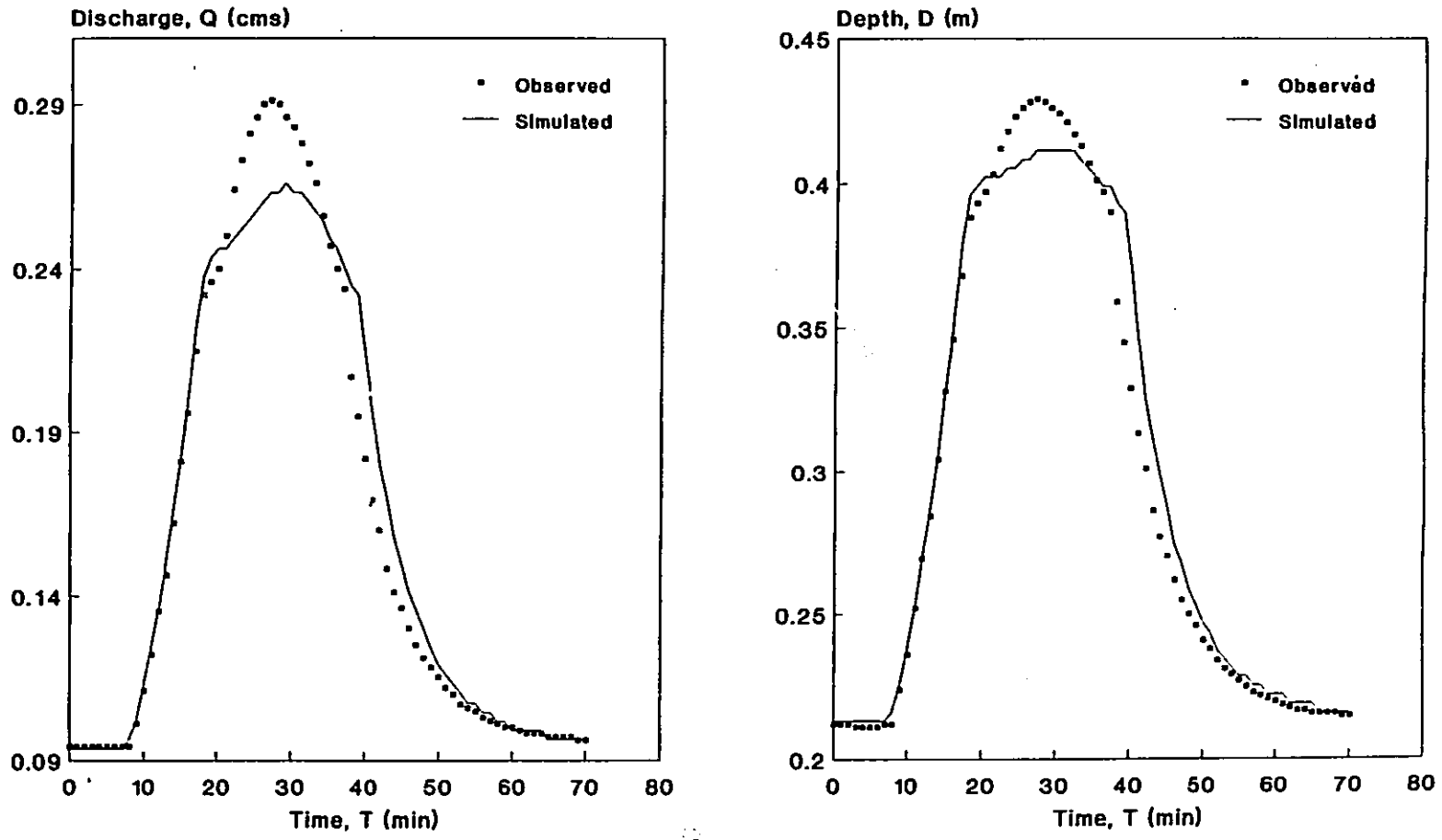

Figure 5.30 Simulated vs. Observed Discharge and Depth Hydrographs with Diagonal Interface Planes applied to DWOPER, (Θ = 5.84°, Treske's Data, Case 6).

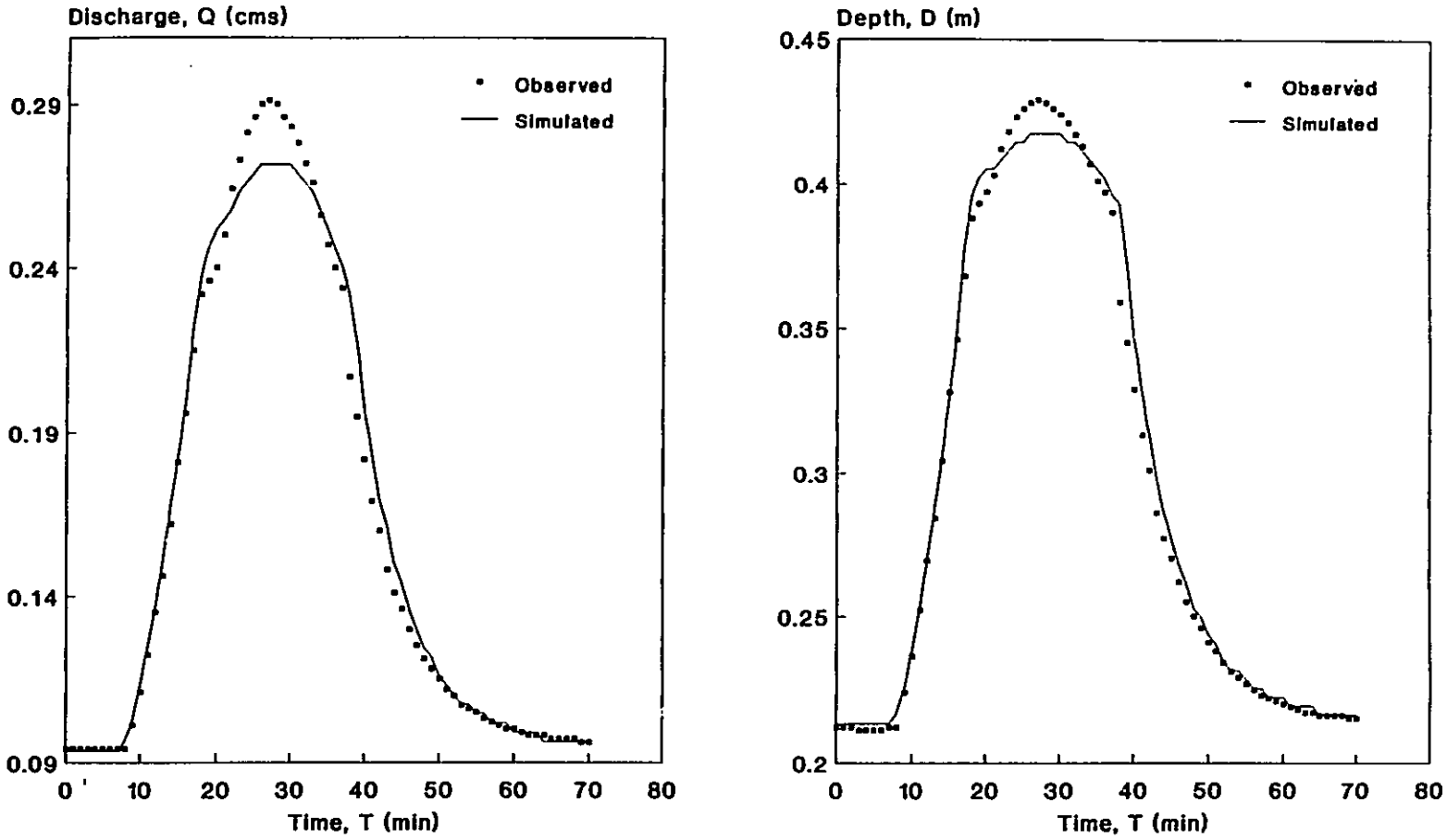

Figure 5.31 Simulated vs. Observed Discharge and Depth Hydrographs with Diagonal Interface Planes applied to DWOPER, (Θ = 6.34°, Treske's Data, Case 6).

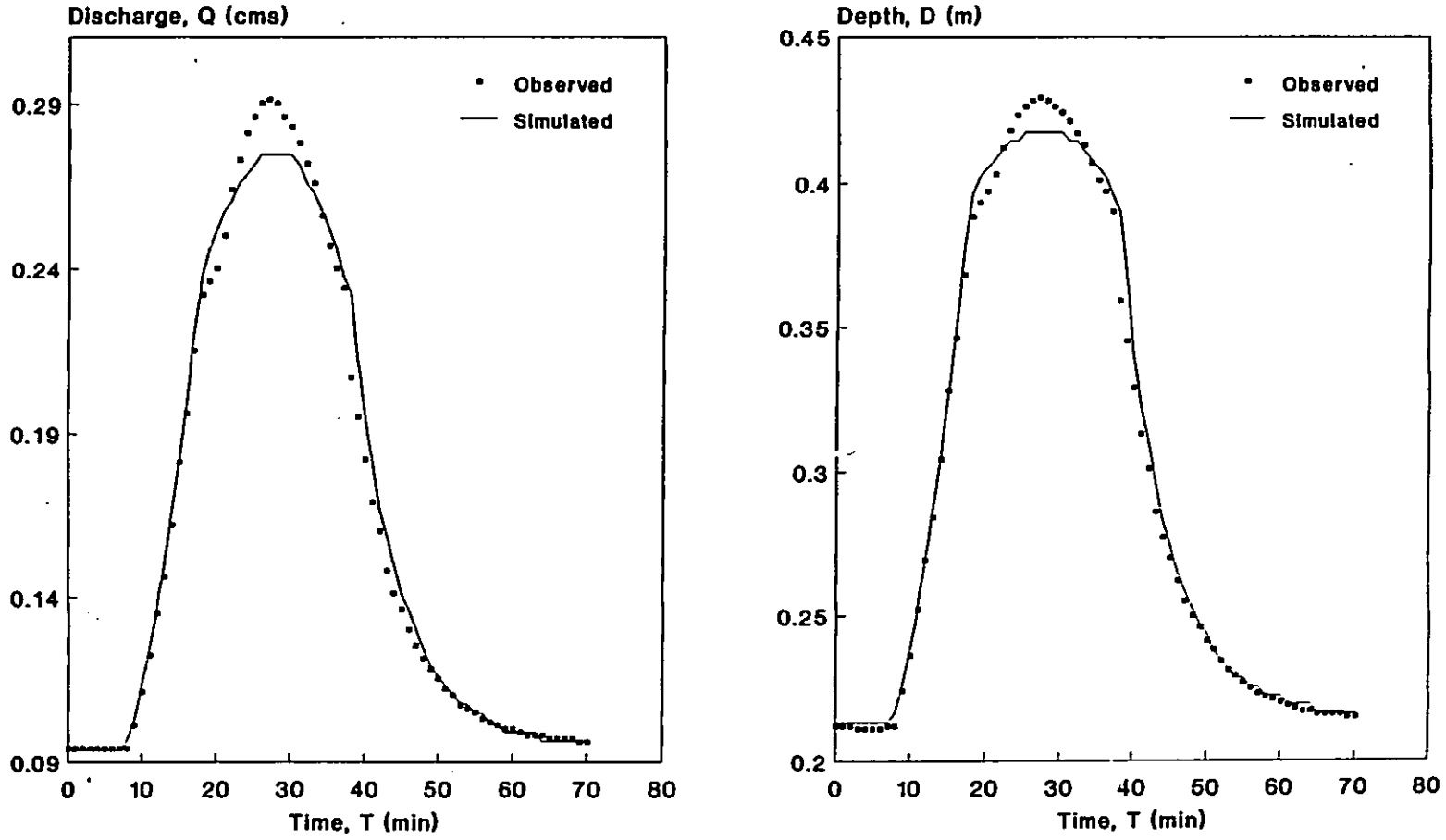

Figure 5.32 Simulated vs. Observed Discharge and Depth Hydrographs with Diagonal Interface Planes applied to DWOPER, (Θ = 6.59°, Treske's Data, Case 6).

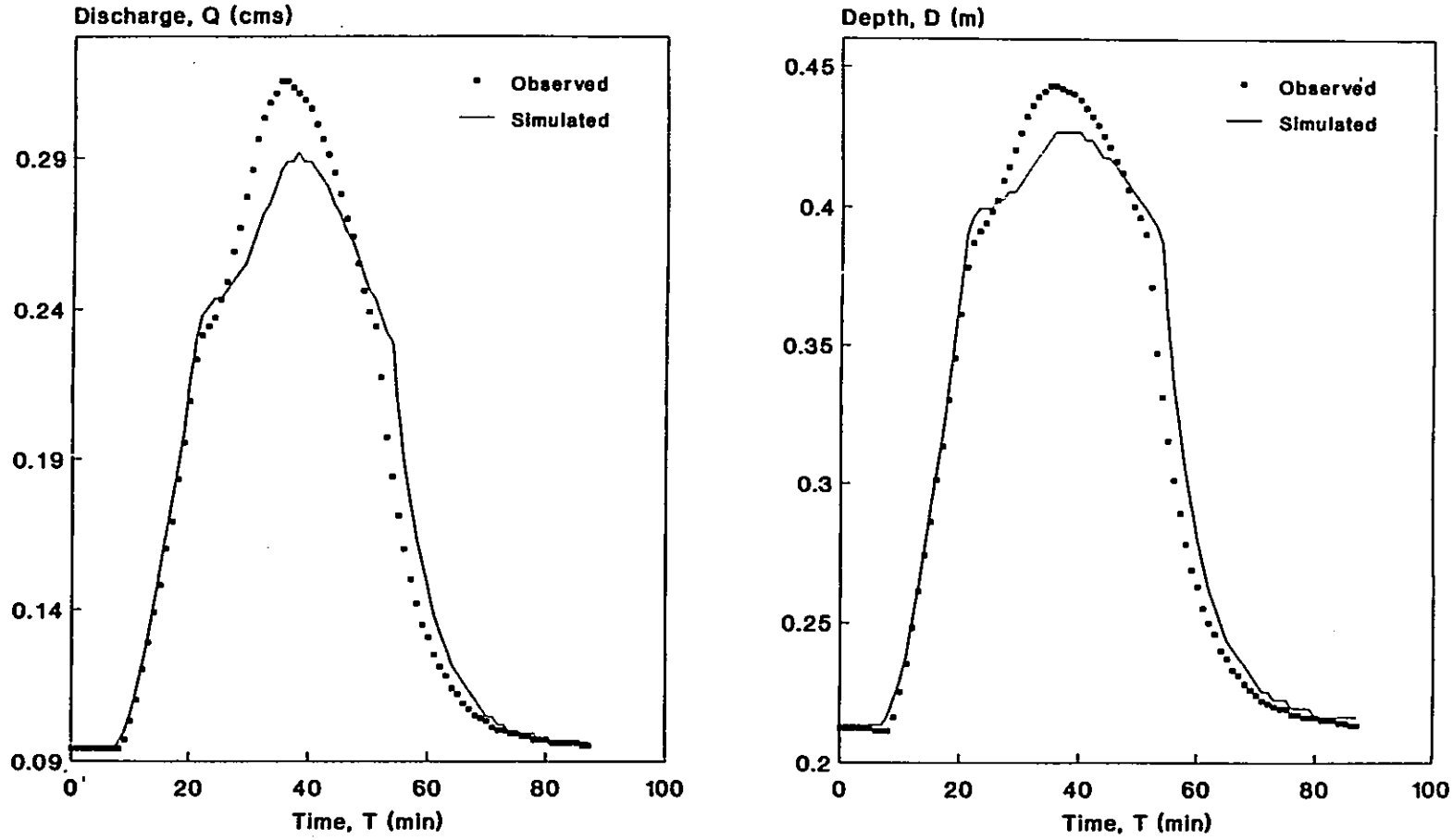

Figure 5.33 Simulated vs. Observed Discharge and Depth Hydrographs with Diagonal Interface Planes applied to DWOPER, (Θ = 5.84°, Treske's Data, Case 7).

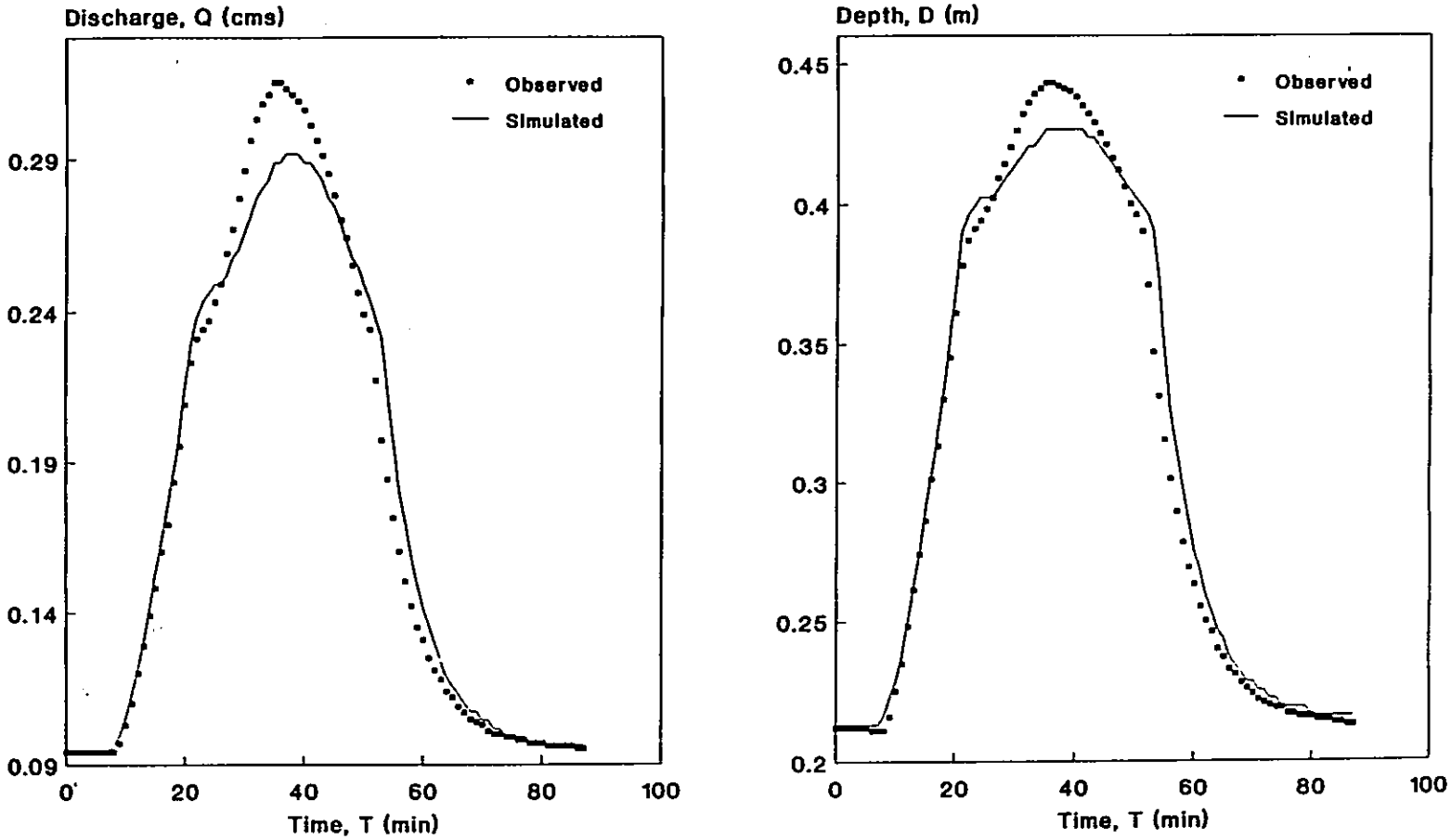

Figure 5.34 Simulated vs. Observed Discharge and Depth Hydrographs with Diagonal Interface Planes applied to DWOPER, (Θ = 6.09°, Treske's Data, Case 7).

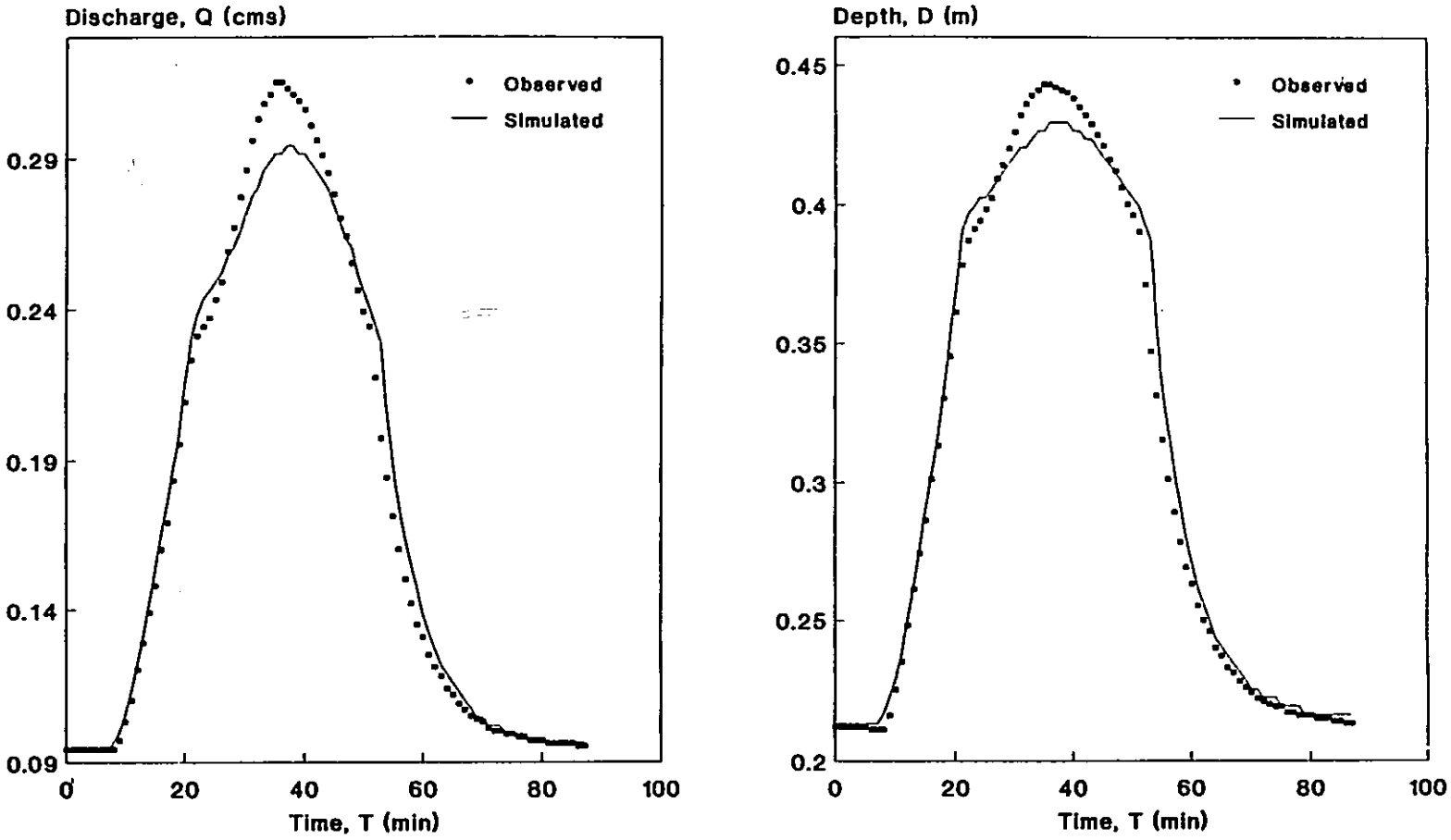

Figure 5.35 Simulated vs. Observed Discharge and Depth Hydrographs with Diagonal Interface Planes applied to DWOPER, (Θ = 6.34°, Treske's Data, Case 7).

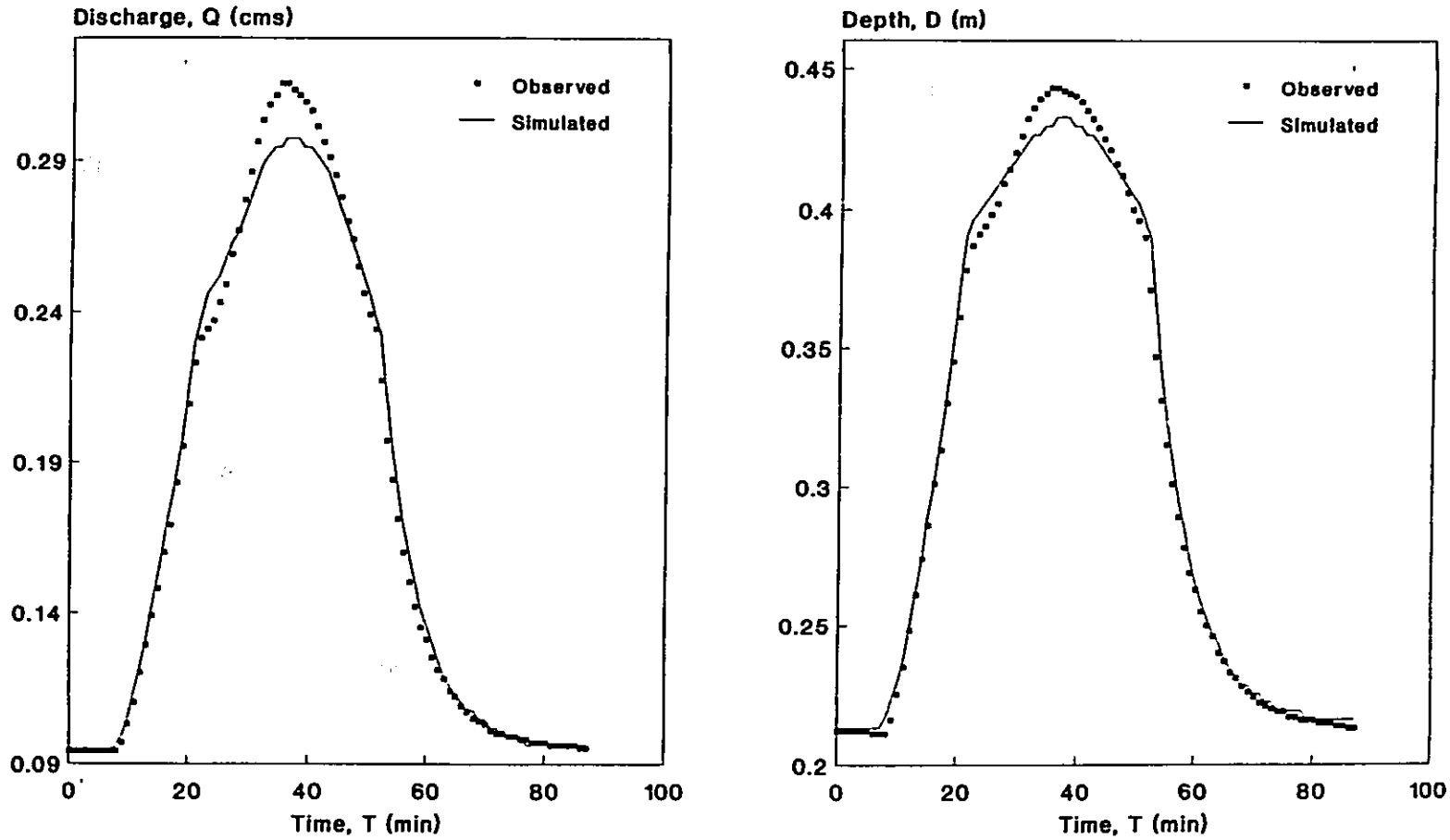

Figure 5.36 Simulated vs. Observed Discharge and Depth Hydrographs with Diagonal Interface Planes applied to DWOPER, (Θ = 6.84°, Treske's Data, Case 7).

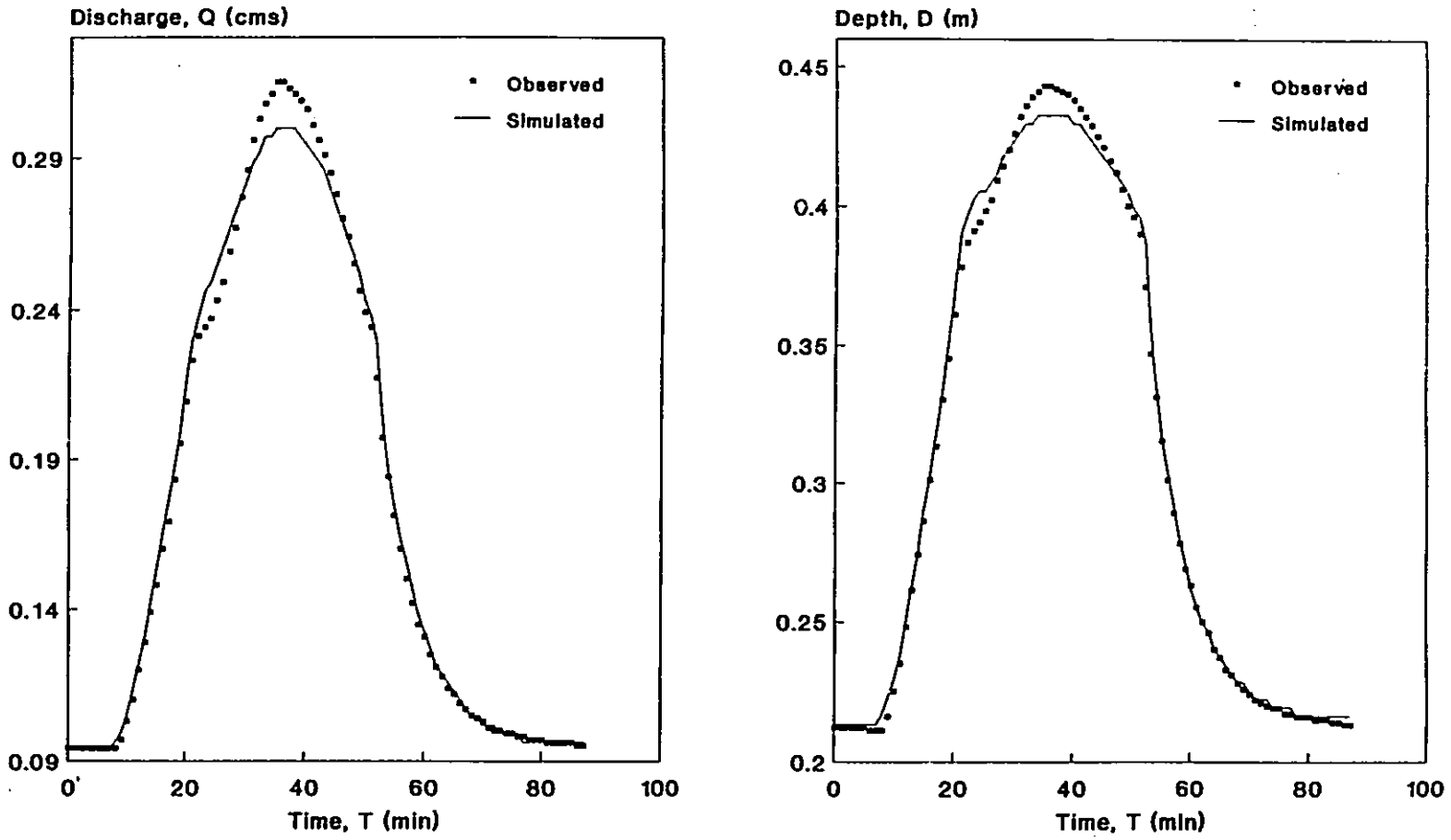

Figure 5.37 Simulated vs. Observed Discharge and Depth Hydrographs with Diagonal Interface Planes applied to DWOPER, (Θ = 7.34°, Treske's Data, Case 7).

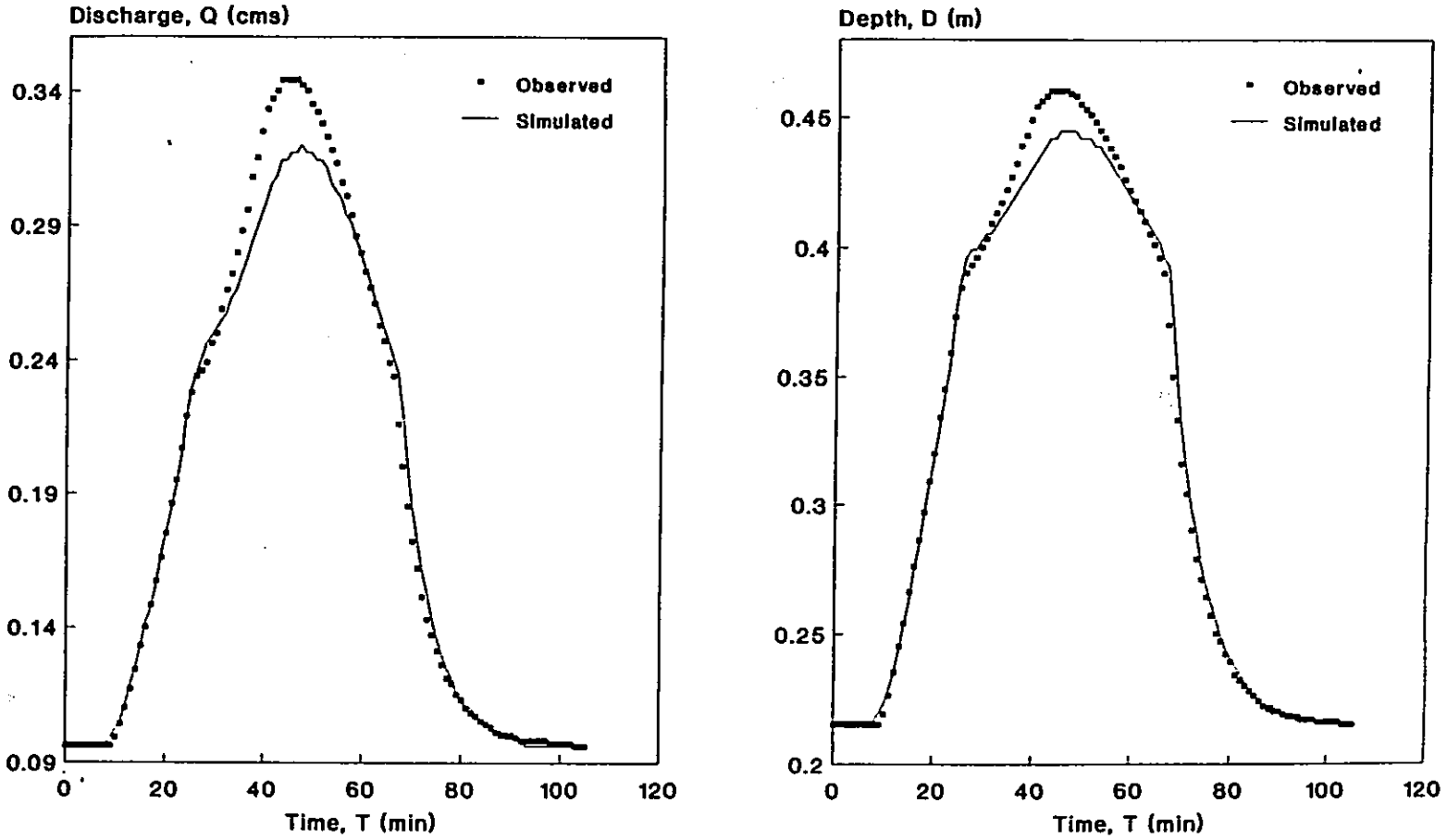

Figure 5.38 Simulated vs. Observed Discharge and Depth Hydrographs with Diagonal Interface Planes applied to DWOPER, (Θ = 6.84°, Treske's Data, Case 8).

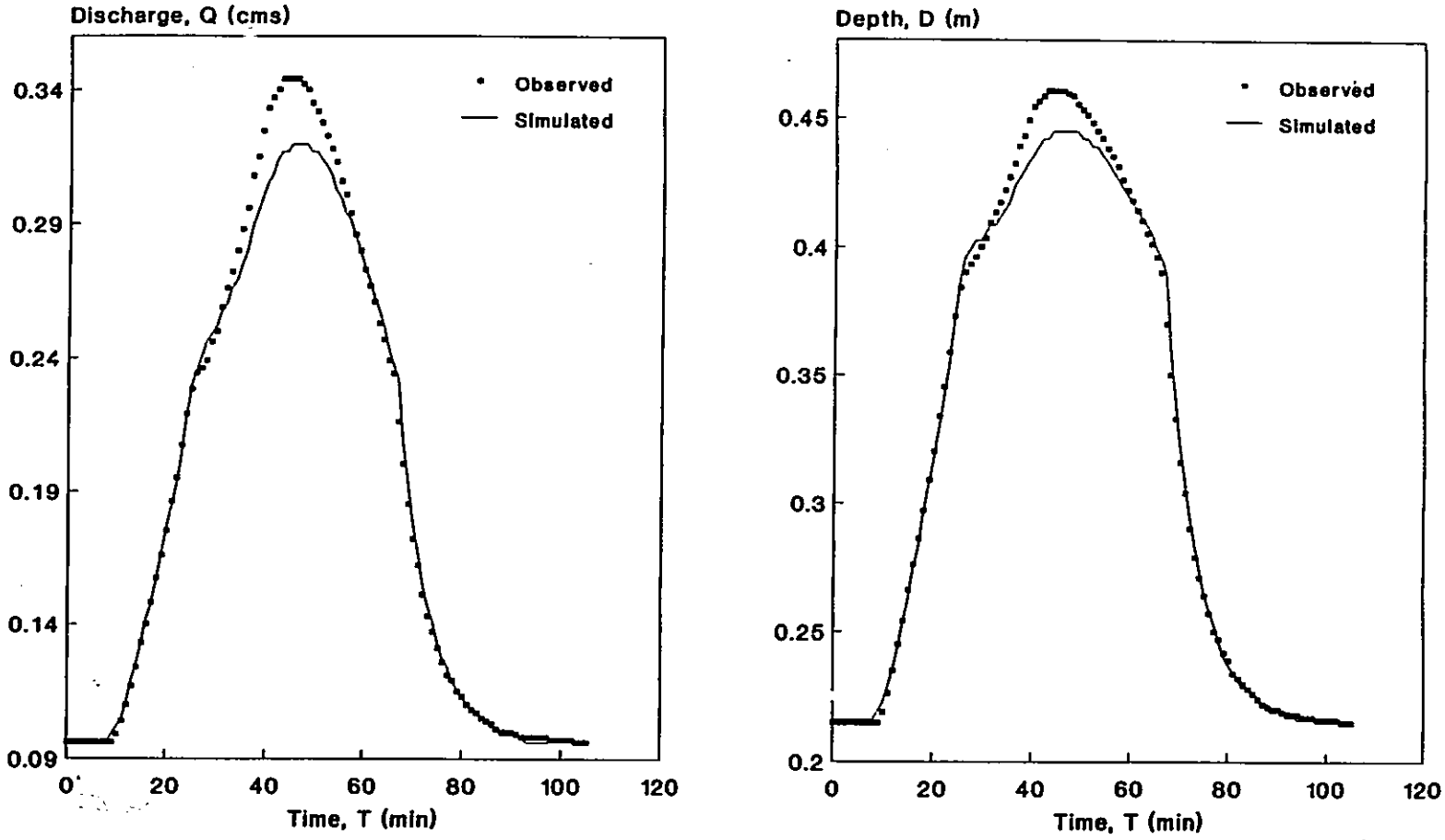

Figure 5.39 Simulated vs. Observed Discharge and Depth Hydrographs with Diagonal Interface Planes applied to DWOPER, (Θ = 7.34°, Treske's Data, Case 8).

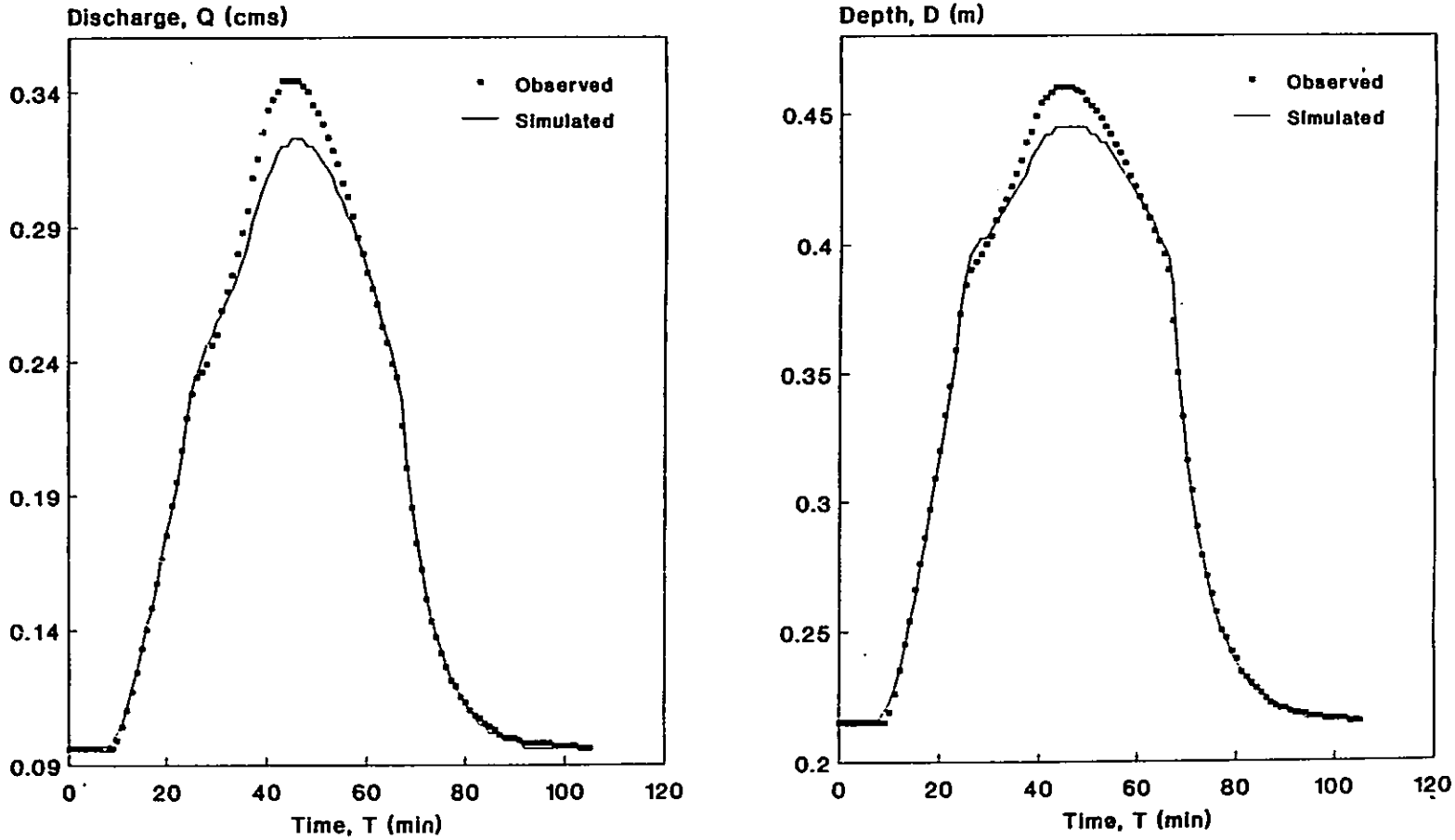

Figure 5.40 Simulated vs. Observed Discharge and Depth Hydrographs with Diagonal Interface Planes applied to DWOPER, (Θ = 7.84°, Treske's Data, Case 8).

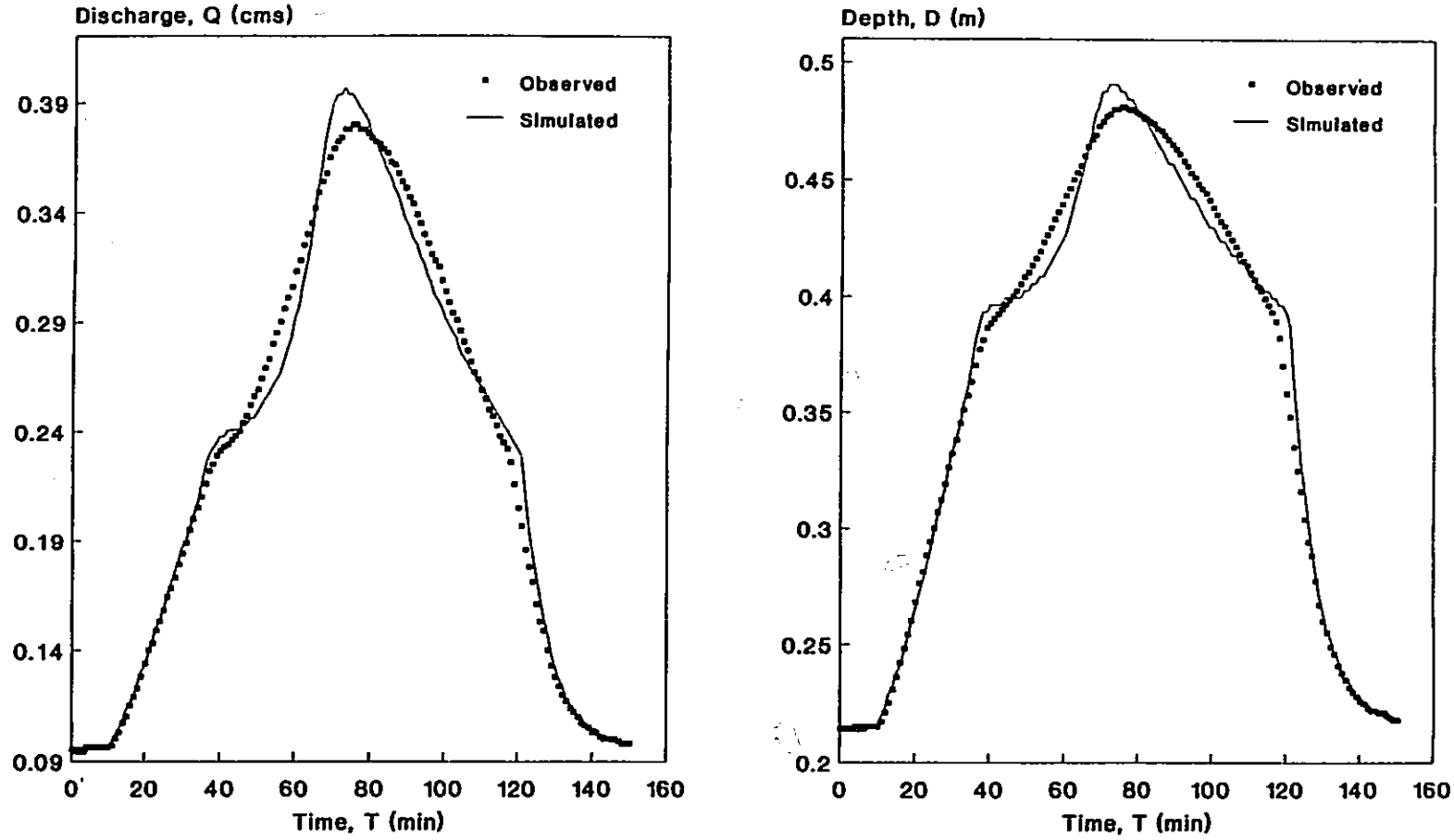

Figure 5.41 Simulated vs. Observed Discharge and Depth Hydrographs with Diagonal Interface Planes applied to DWOPER, (Θ = 5.84°, Treske's Data, Case 9).

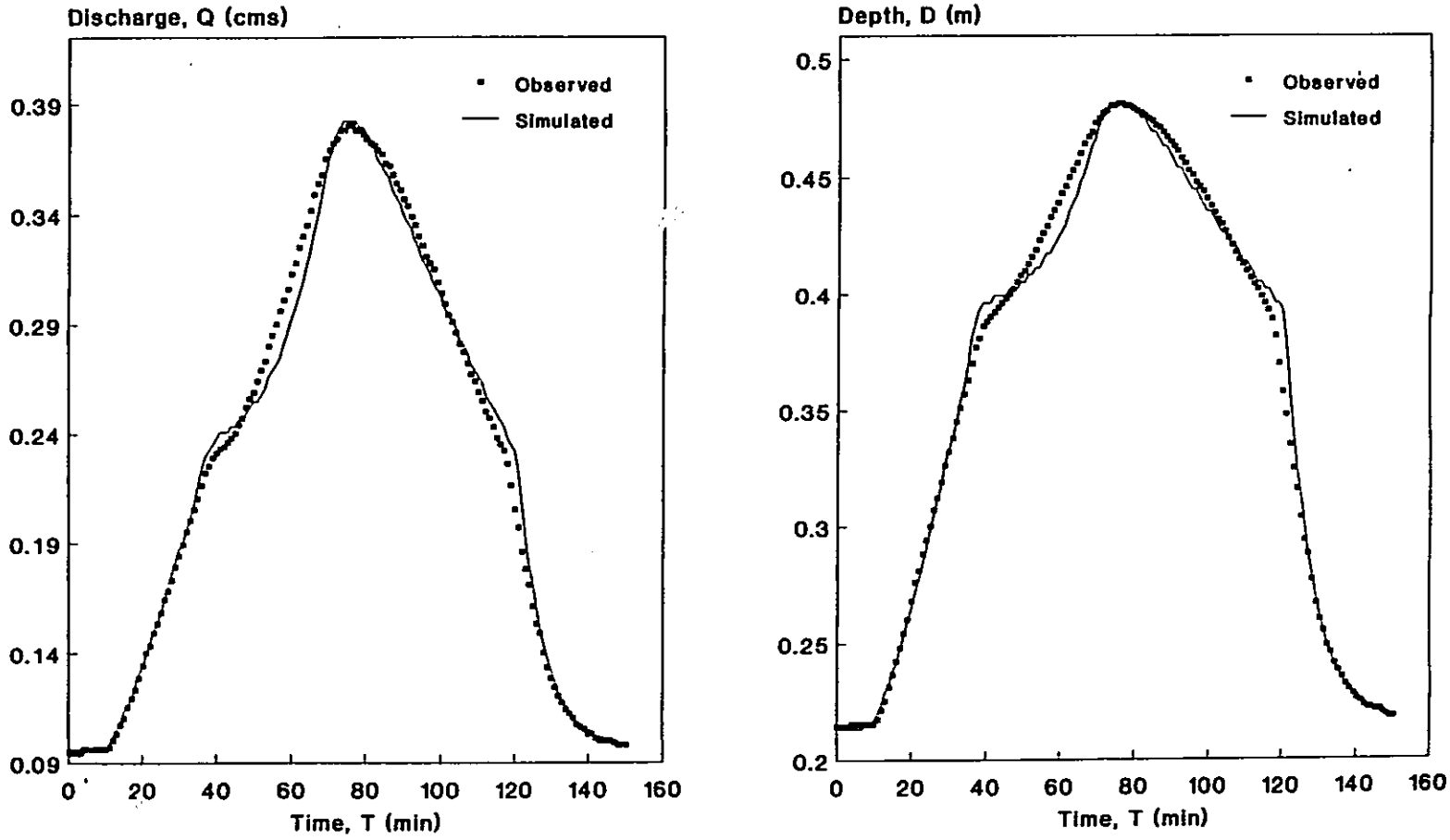

Figure 5.42 Simulated vs. Observed Discharge and Depth Hydrographs with Diagonal Interface Planes applied to DWOPER, (Θ = 6.09°, Treske's Data, Case 9).

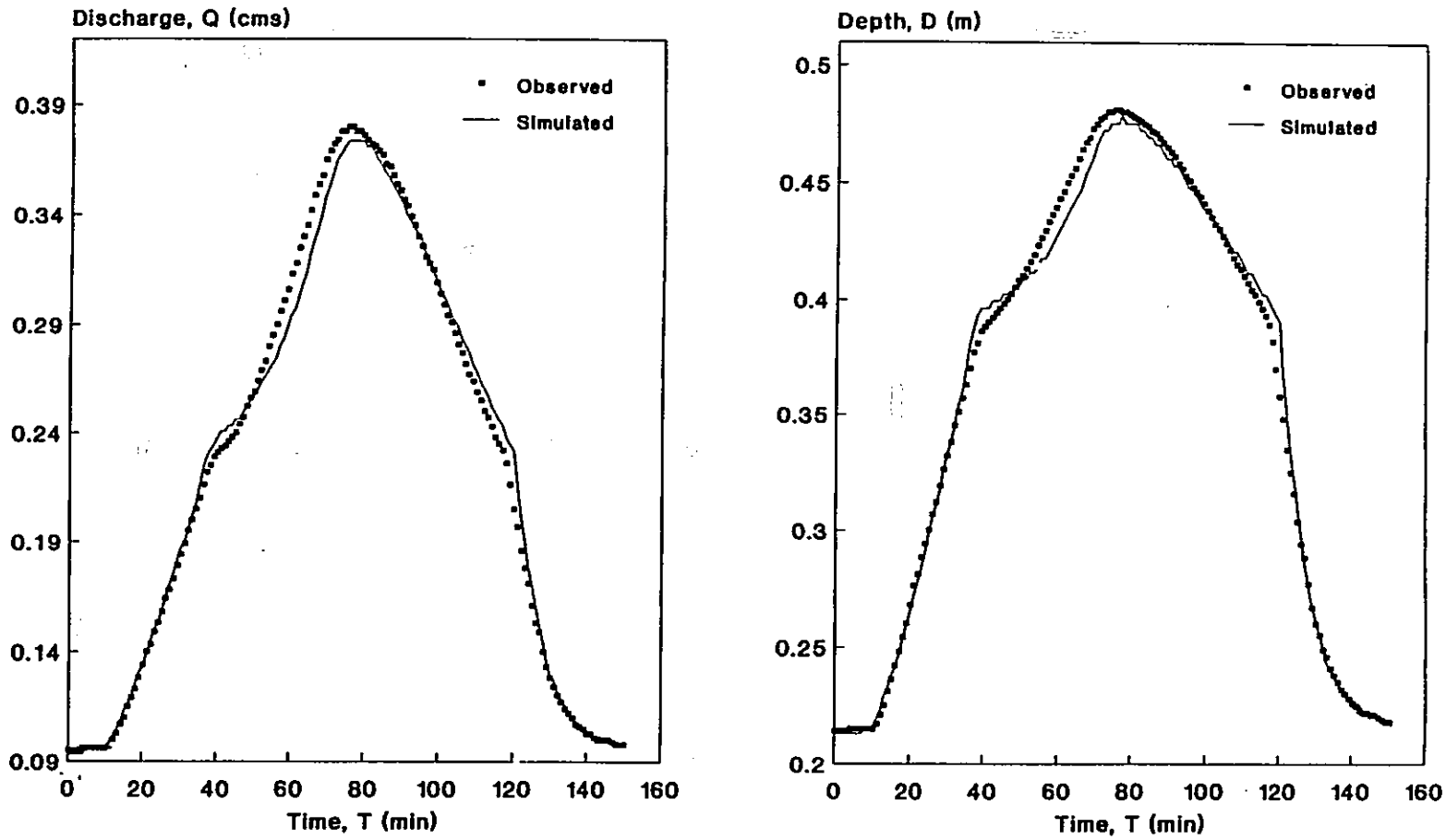

Figure 5.43 Simulated vs. Observed Discharge and Depth Hydrographs with Diagonal Interface Planes applied to DWOPER, (Θ = 6.34°, Treske's Data, Case 9).

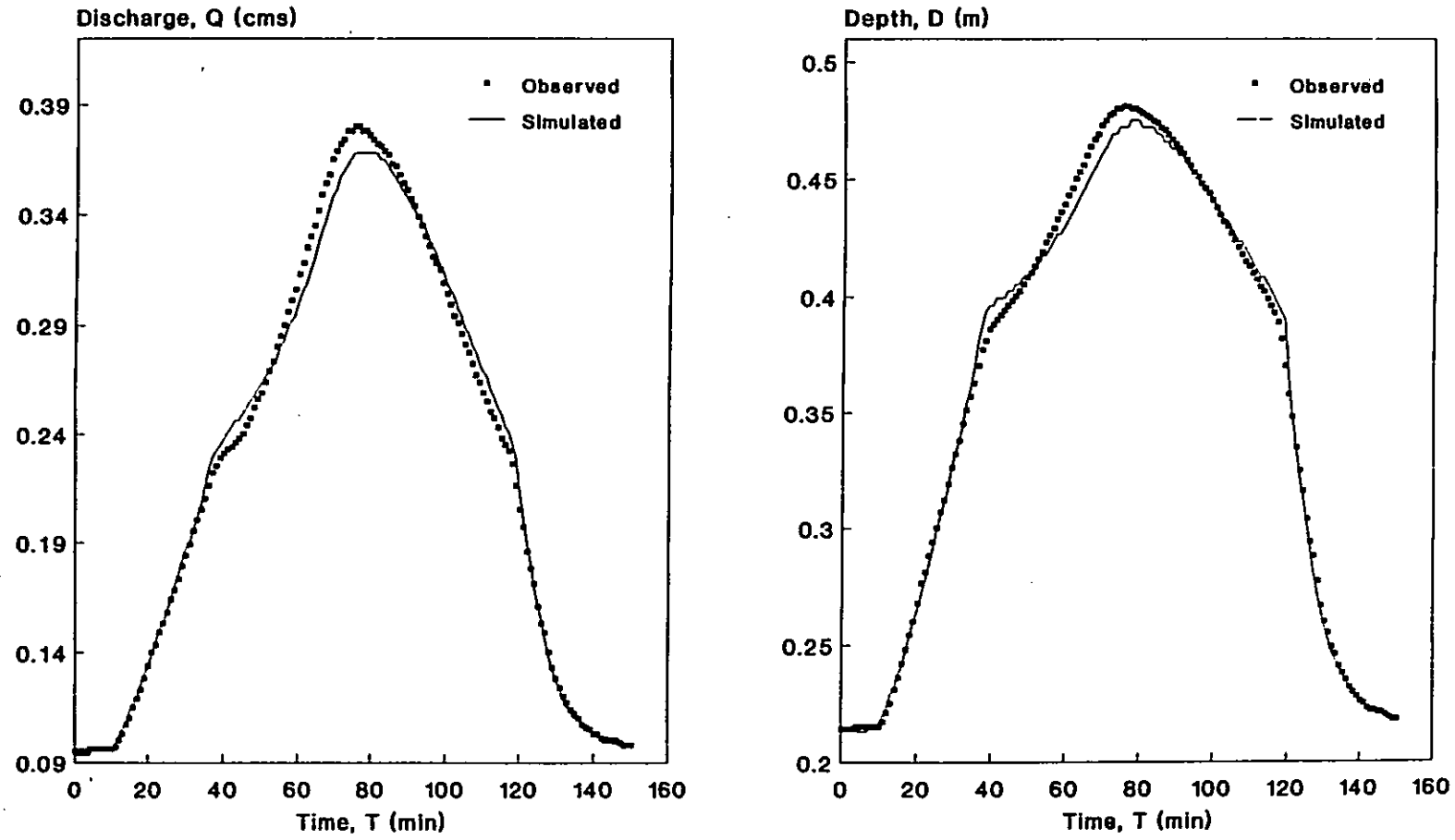

Figure 5.44 Simulated vs. Observed Discharge and Depth Hydrographs with Diagonal Interface Planes applied to DWOPER, (Θ = 7.09°, Treske's Data, Case 9).

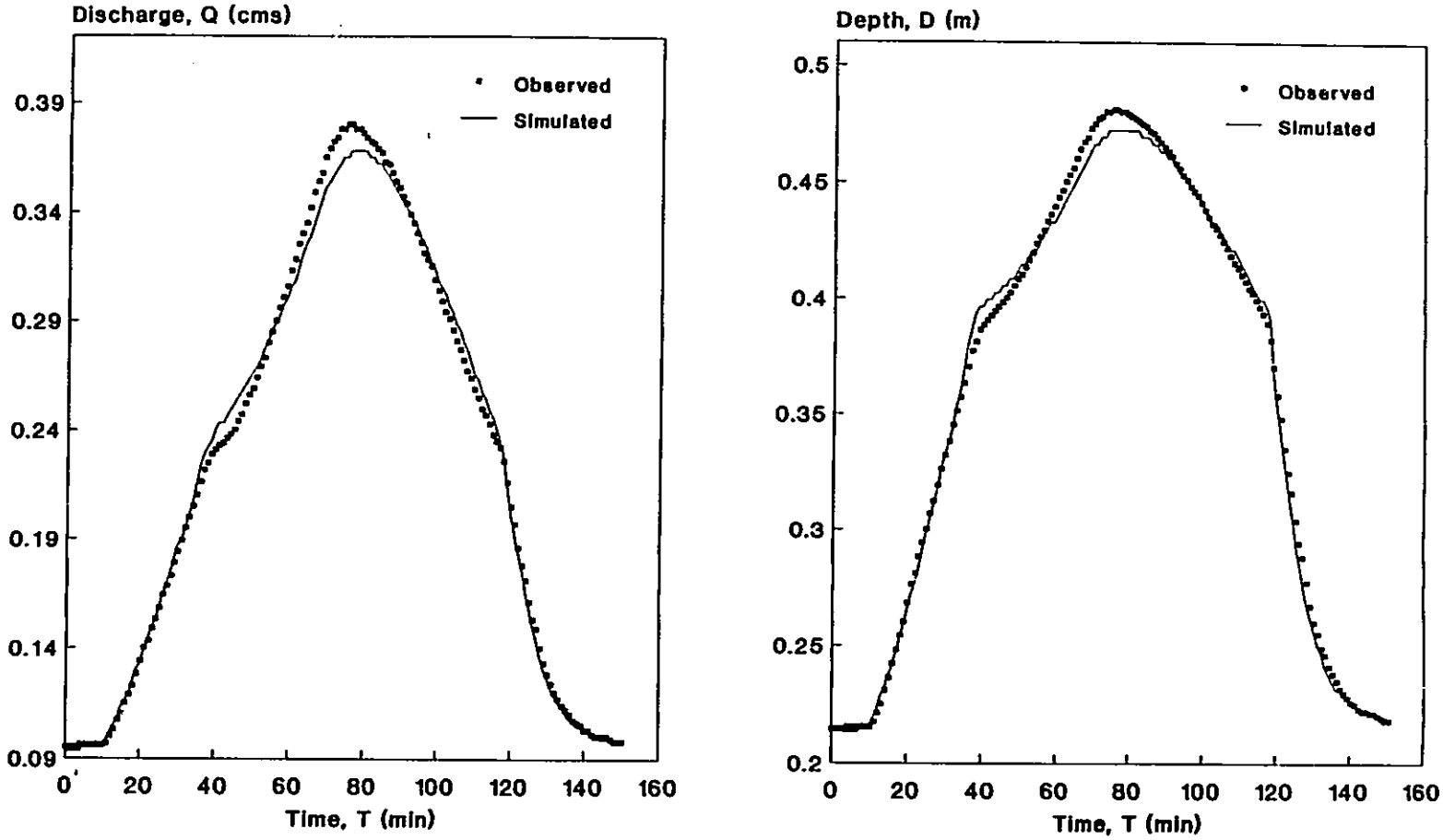

Figure 5.45 Simulated vs. Observed Discharge and Depth Hydrographs with Diagonal Interface Planes applied to DWOPER, (Θ = 8.09°, Treske's Data, Case 9).

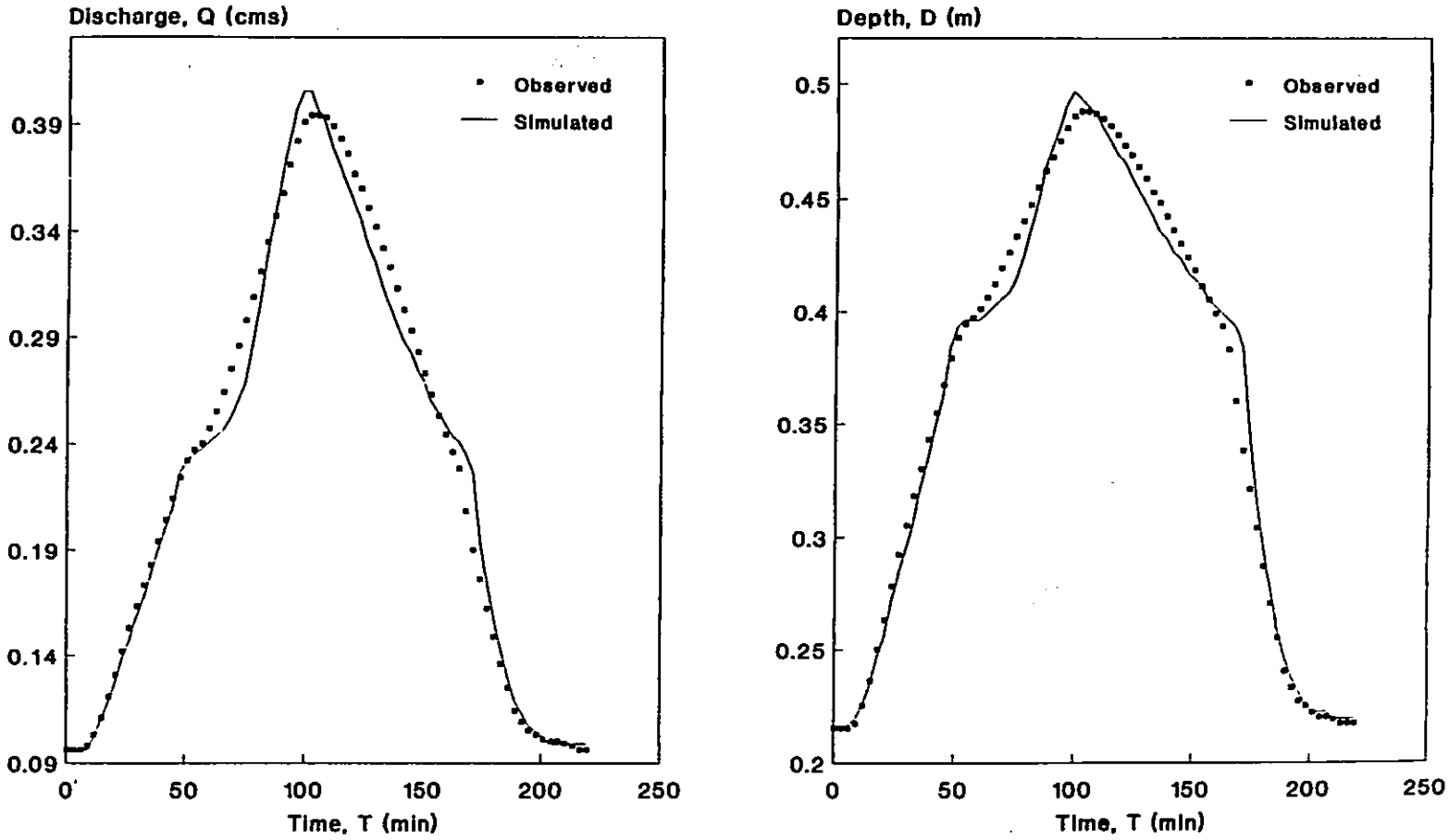

Figure 5.46 Simulated vs. Observed Discharge and Depth Hydrographs with Diagonal Interface Planes applied to DWOPER, (Θ = 5.71°, Treske's Data, Case 10).

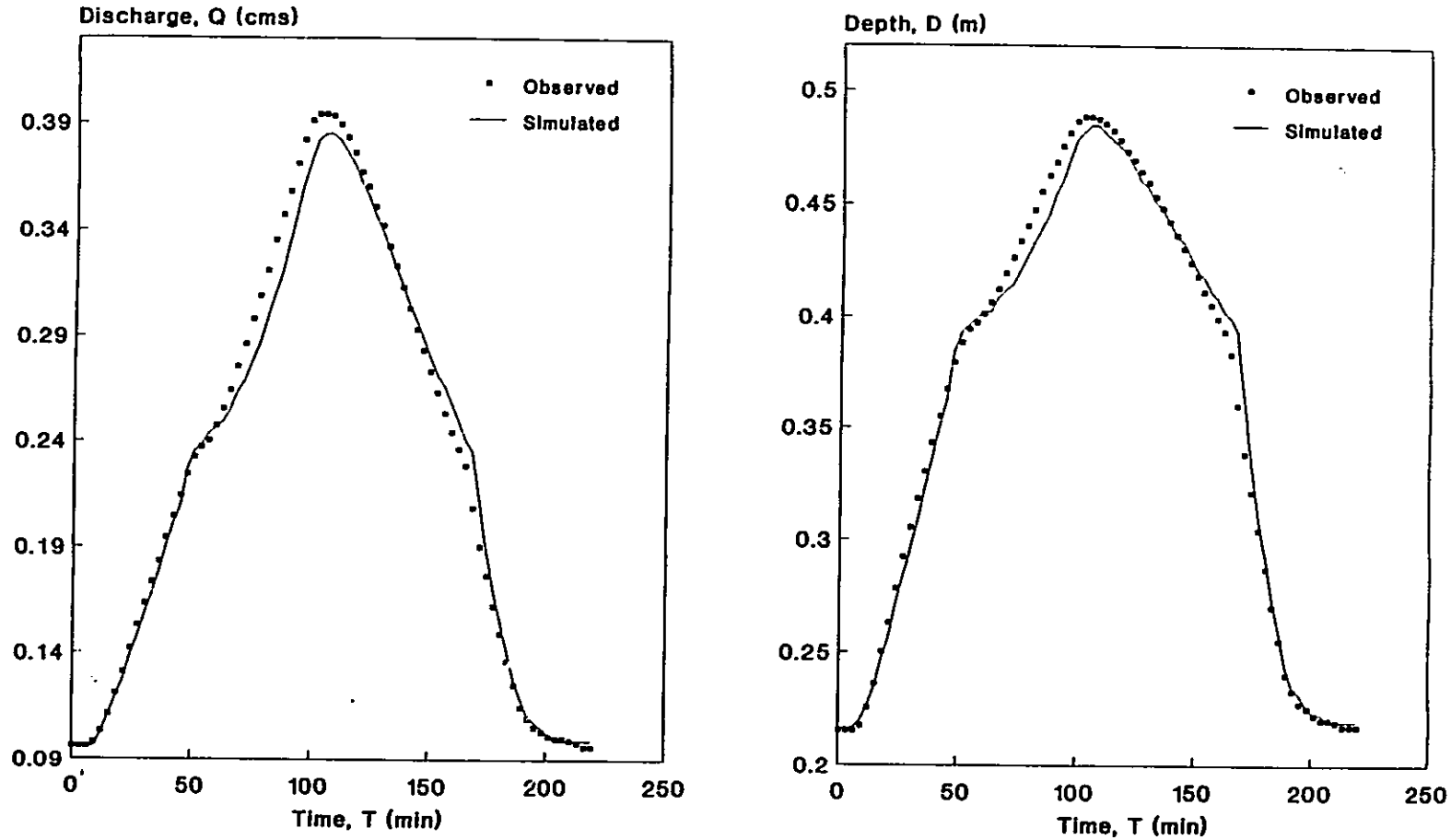

Figure 5.47 Simulated vs. Observed Discharge and Depth Hydrographs with Diagonal Interface Planes applied to DWOPER, (Θ = 5.84°, Treske's Data, Case 10).

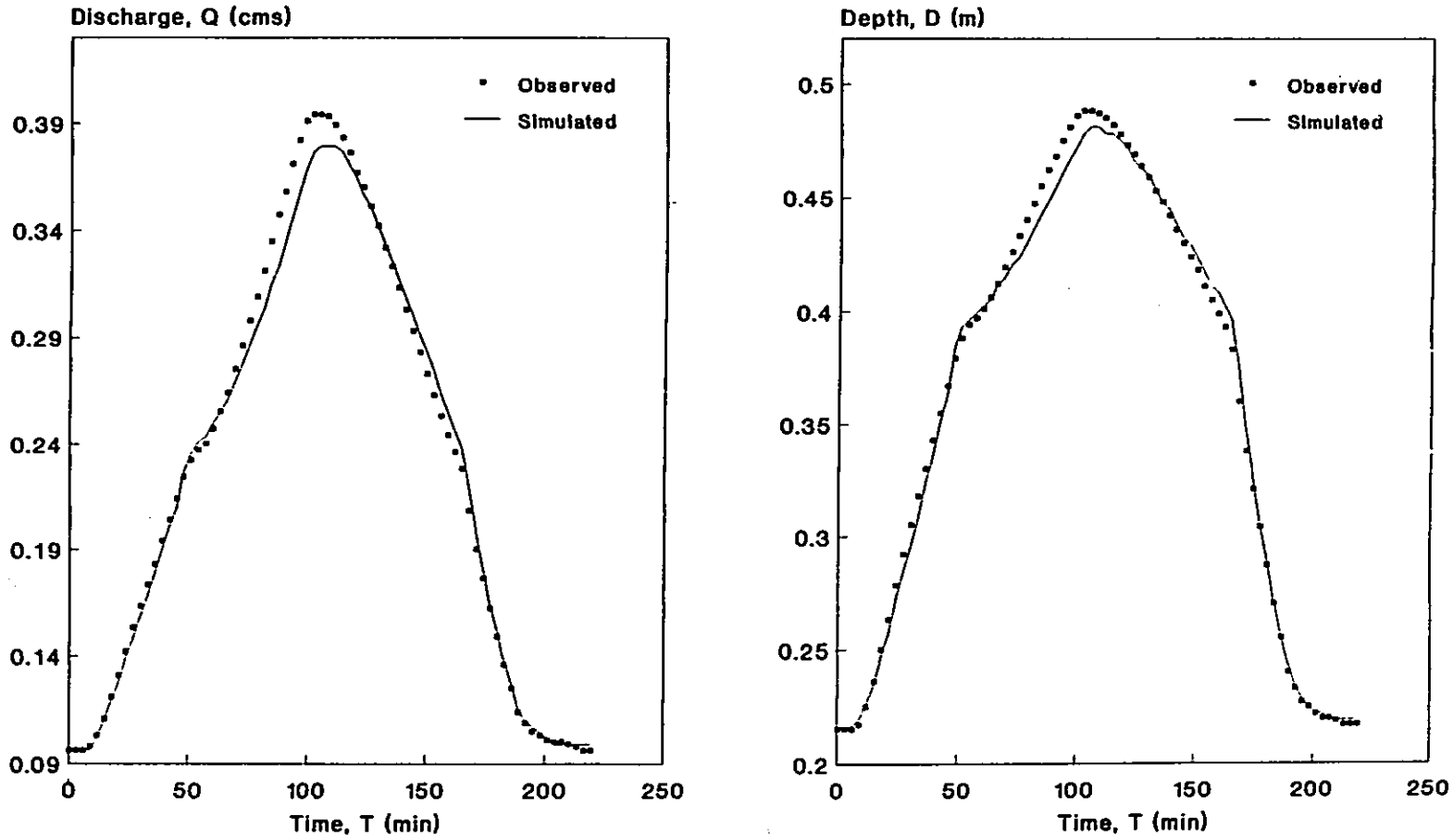

Figure 5.48 Simulated vs. Observed Discharge and Depth Hydrographs with Diagonal Interface Planes applied to DWOPER, (Θ = 6.34°, Treske's Data, Case 10).

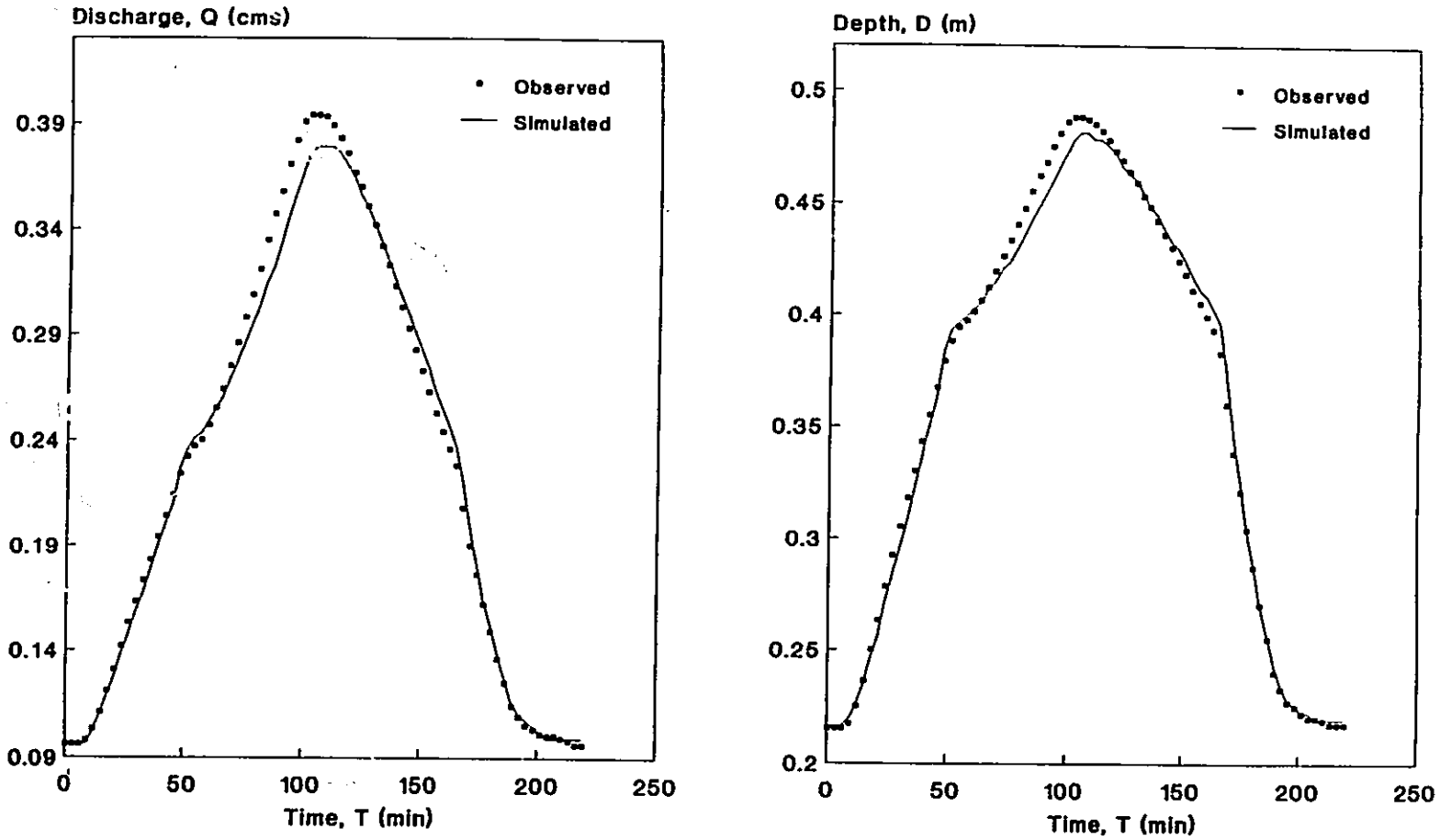

Figure 5.49 Simulated vs. Observed Discharge and Depth Hydrographs with Diagonal Interface Planes applied to DWOPER, (Θ = 7.34°, Treske's Data, Case 10).

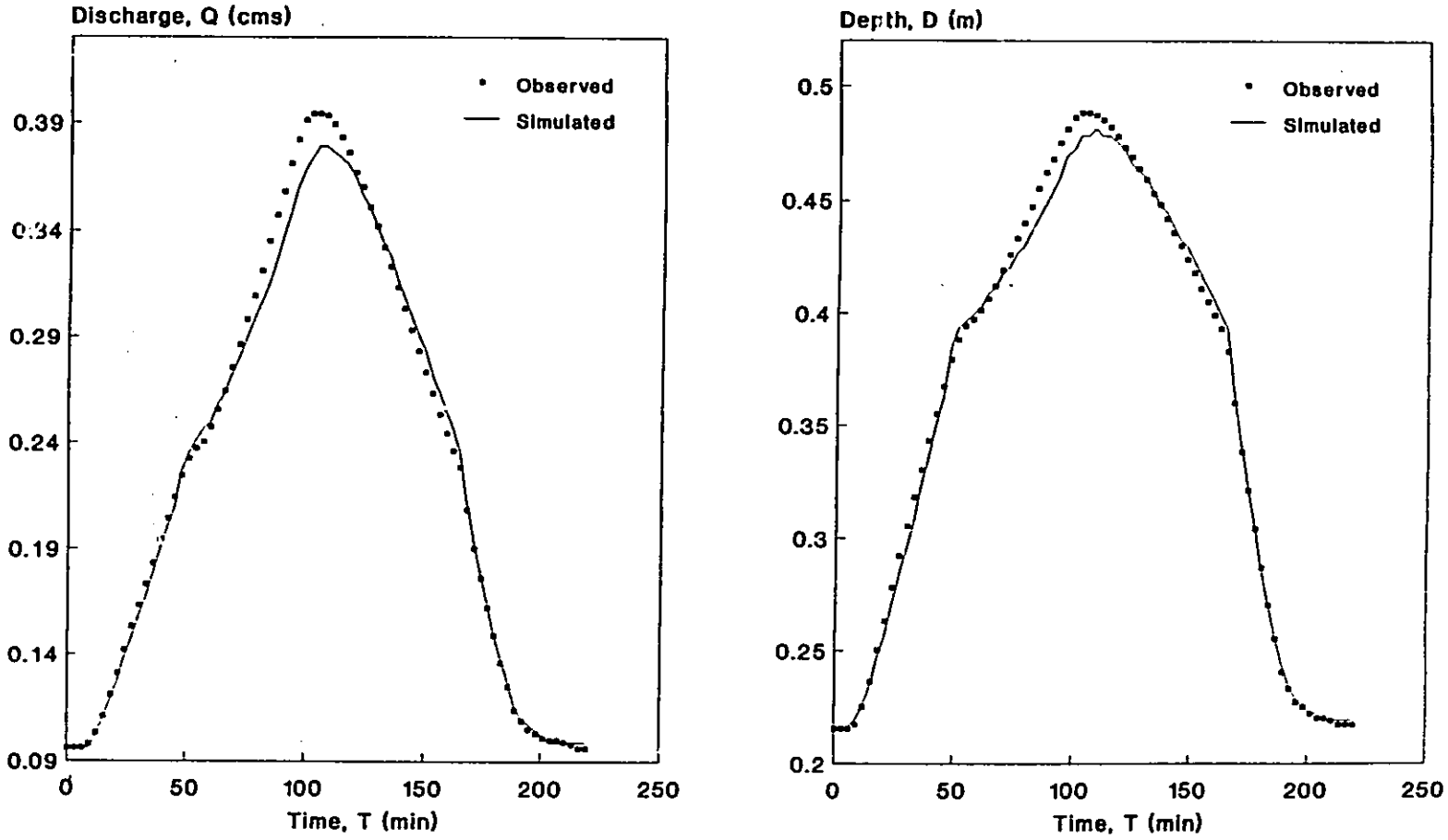

Figure 5.50 Simulated vs. Observed Discharge and Depth Hydrographs with Diagonal Interface Planes applied to DWOPER, (Θ = 8.09°, Treske's Data, Case 10).

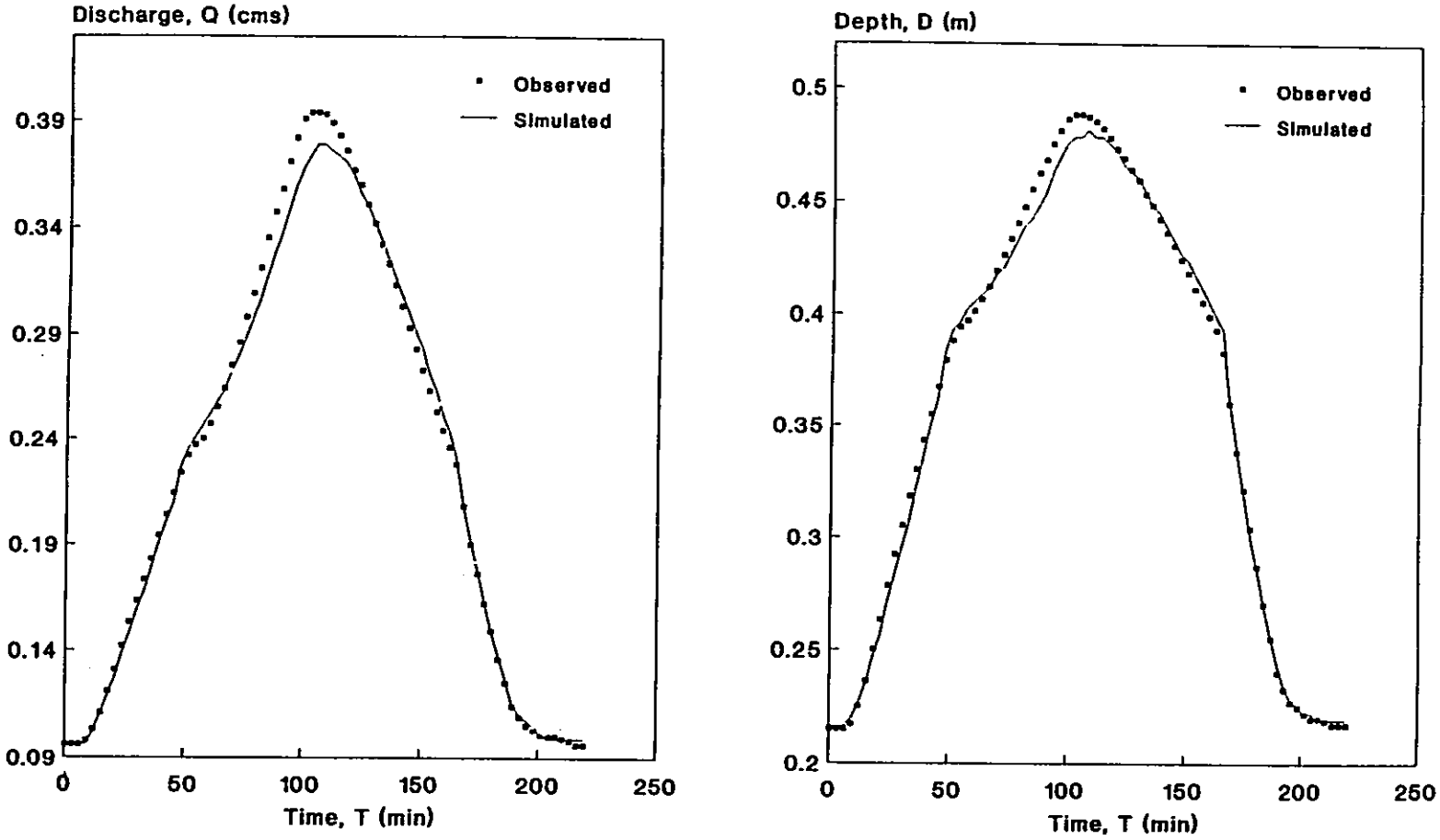

Figure 5.51 Simulated vs. Observed Discharge and Depth Hydrographs with Diagonal Interface Planes applied to DWOPER, (Θ = 8.59°, Treske's Data, Case 10).

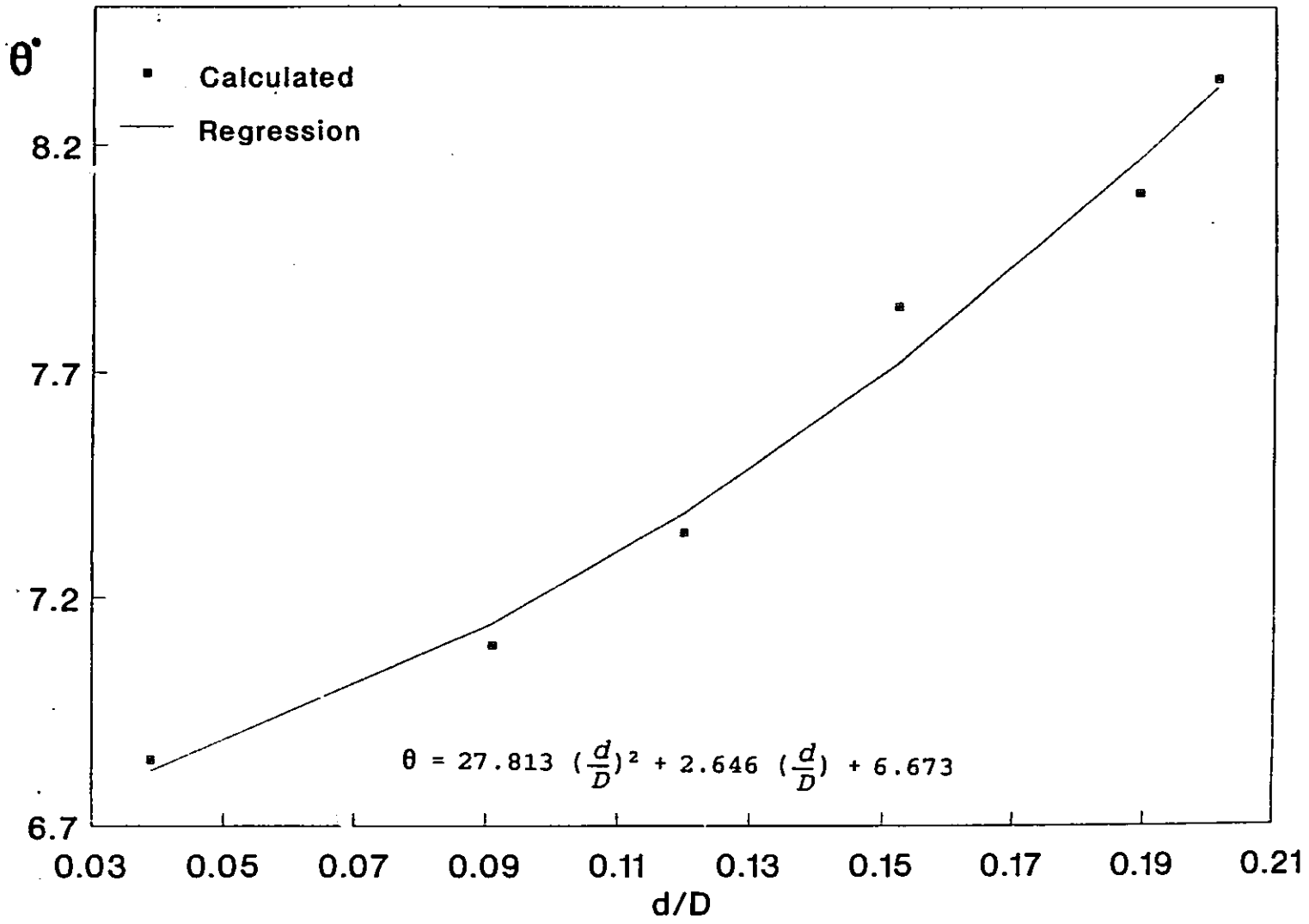

Figure 5.52 Variation of the Angle the Diagonal Interface Plane Makes with the Horizontal (Θ) with the Ratio of the Depth of Flood Plain Flow to the Total Channel Depth (d/D).

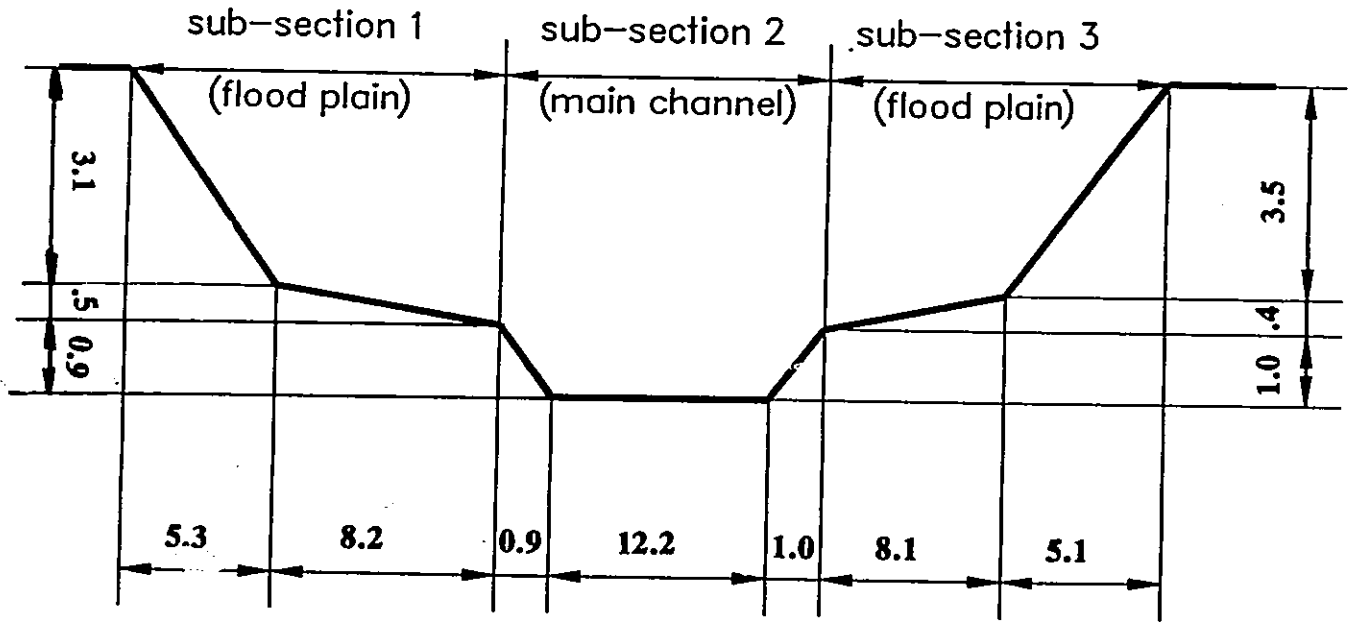

Figure 5.53 Principal Dimensions of the Upstream Cross-section of Myers' Experimental Reach, River Main, N. Ireland.

all Dimensions in Meters

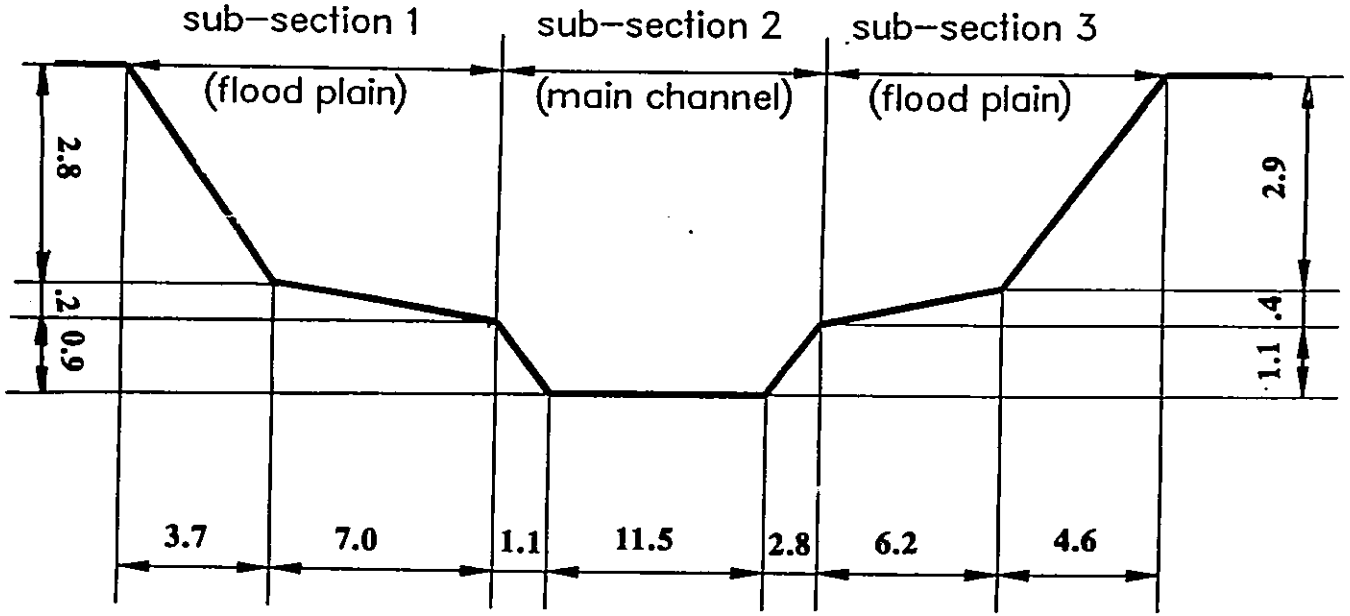

Figure 5.54 Principal Dimensions of the Mid-way Cross-section of Myers' Experimental Reach, River Main, N. Ireland.

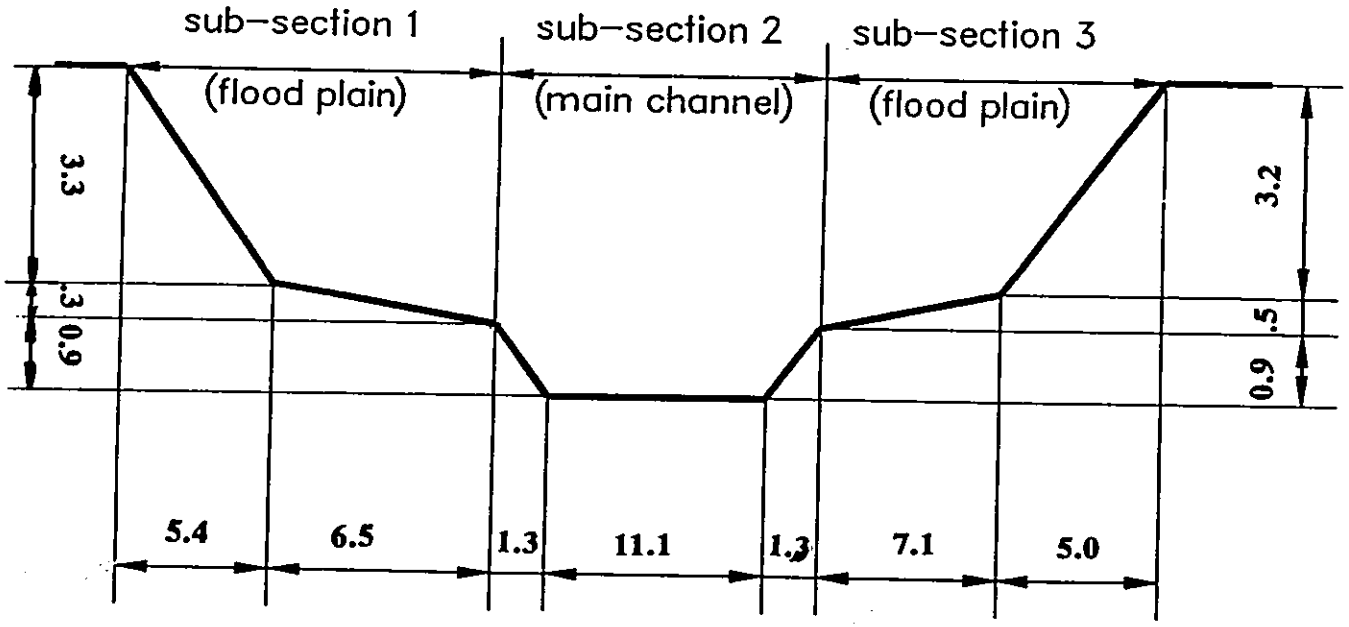

Figure 5.55 Principal Dimensions of the Downstream Cross-section of Myers' Experimental Reach, River Main, N. Ireland.

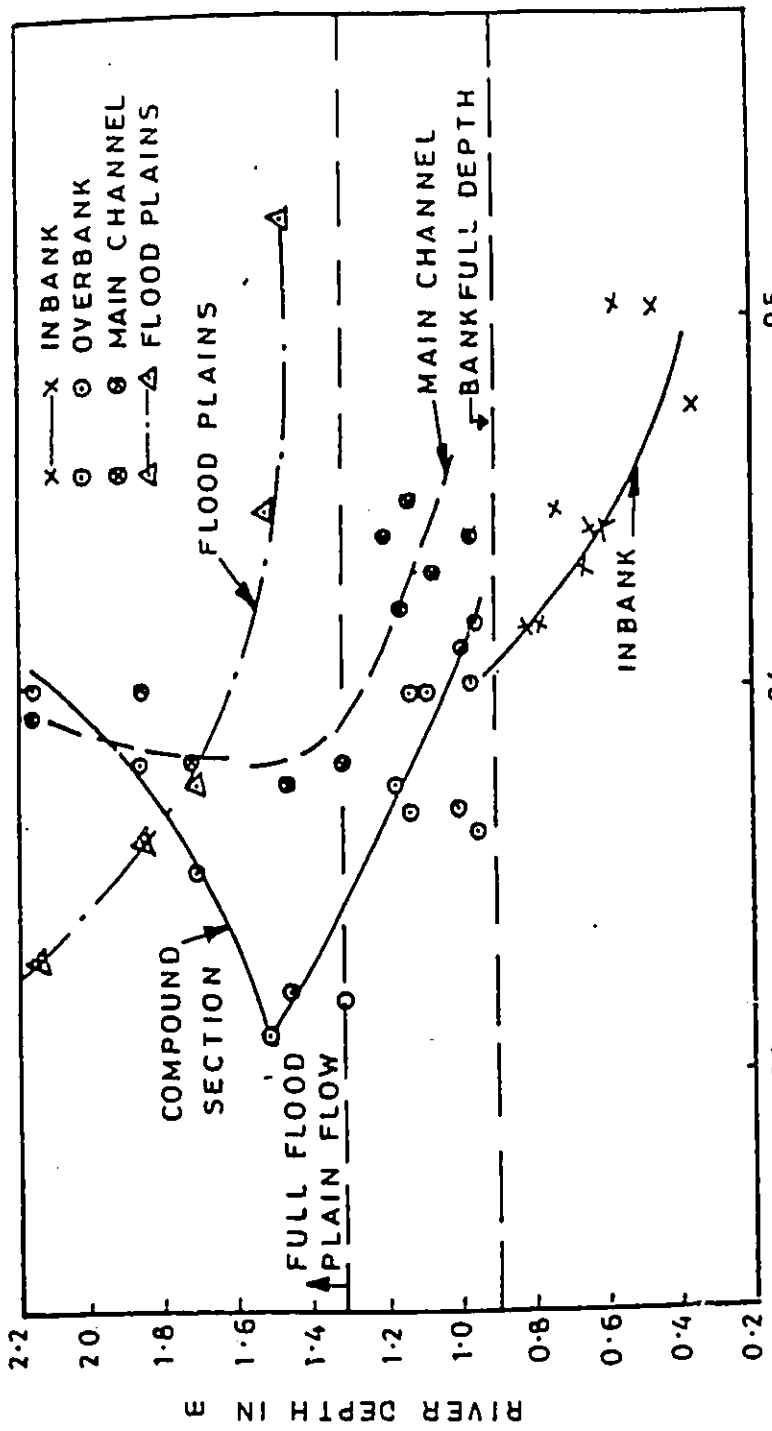

Figure 5.56 Variation of Manning's Roughness coefficient n with Flow Depth for Myers' Data set.

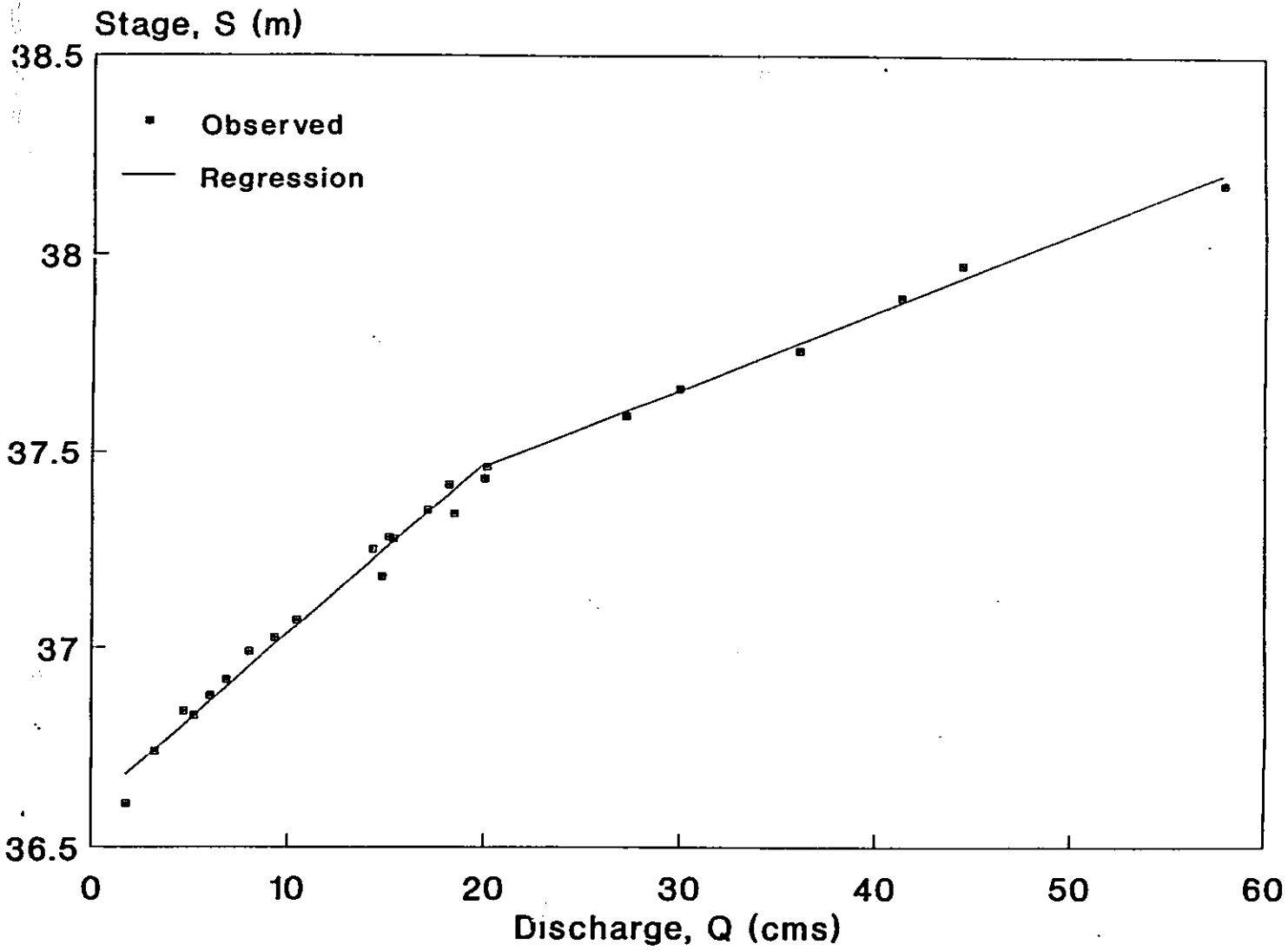

Figure 5.57 Stage-Discharge Variation for Myers' Experimental Reach at the Upstream Cross-section (Rating Curve).

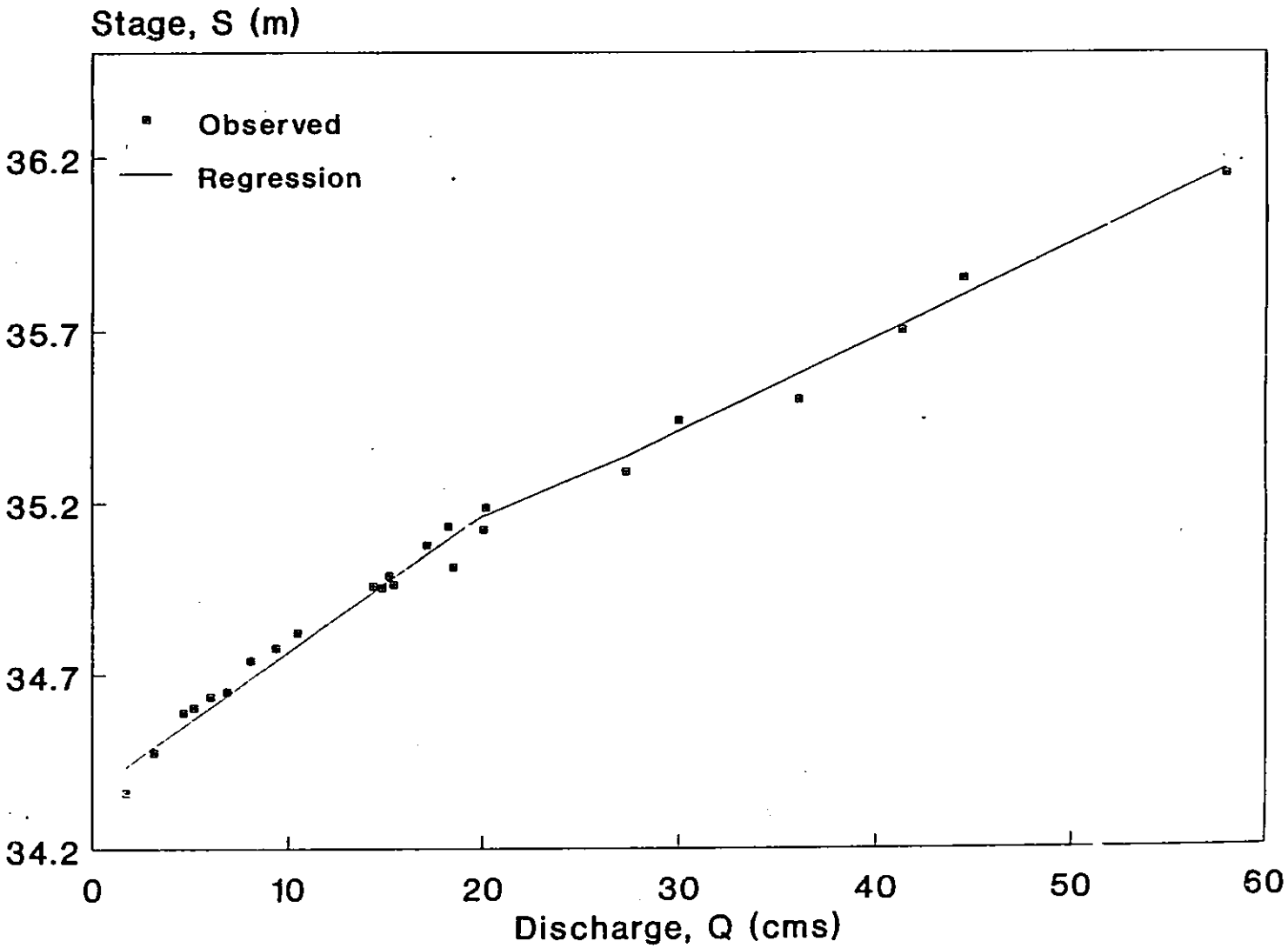

Figure 5.58 Stage-Discharge Variation for Myers' Experimental Reach at the Downstream Cross-section (Rating Curve).

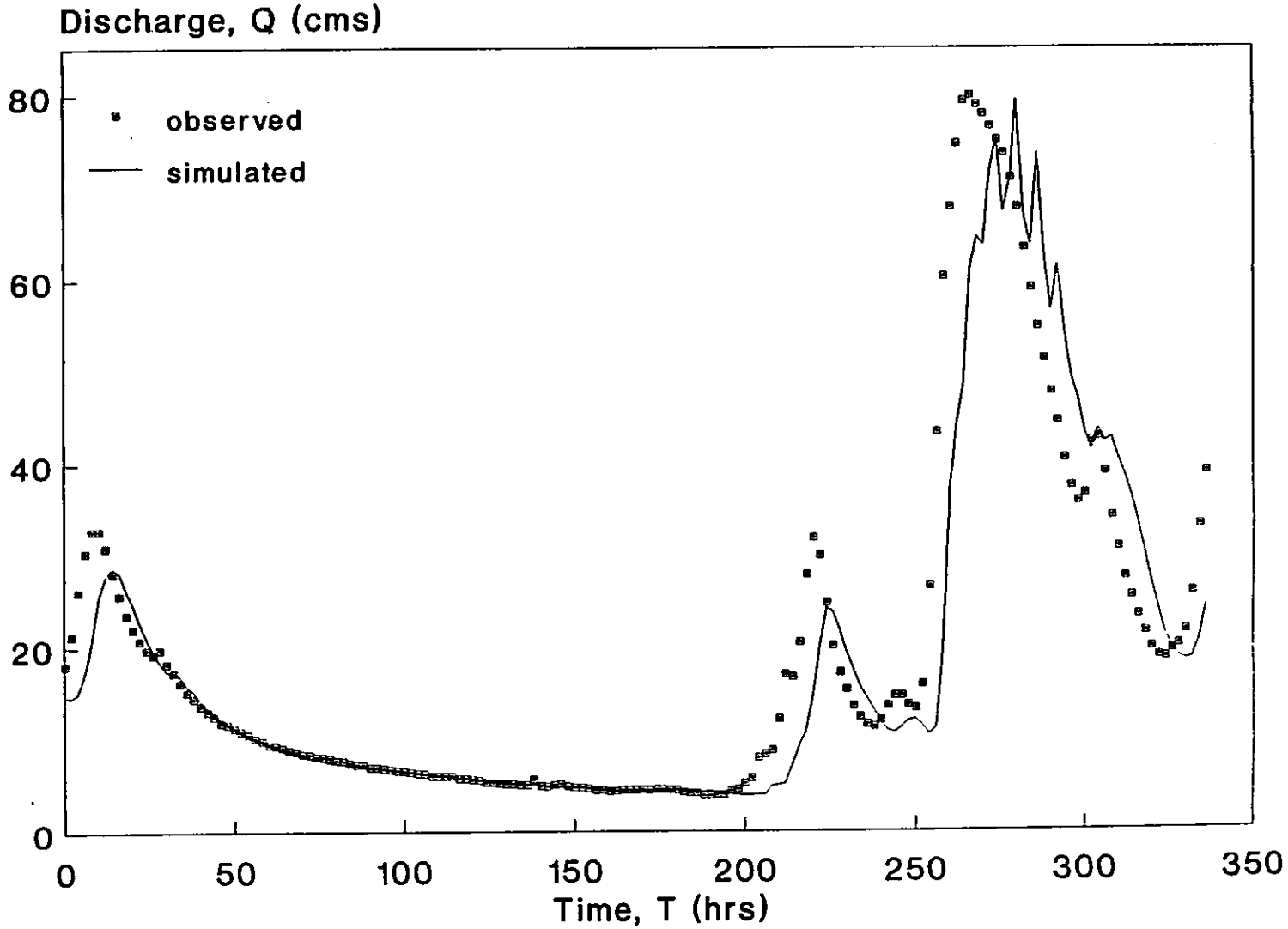

Figure 5.59 Effect of a Large Time Step (30 minutes) on the Stability and Accuracy of the Simulated Discharge Hydrograph for Myers' Data using DWOPER.

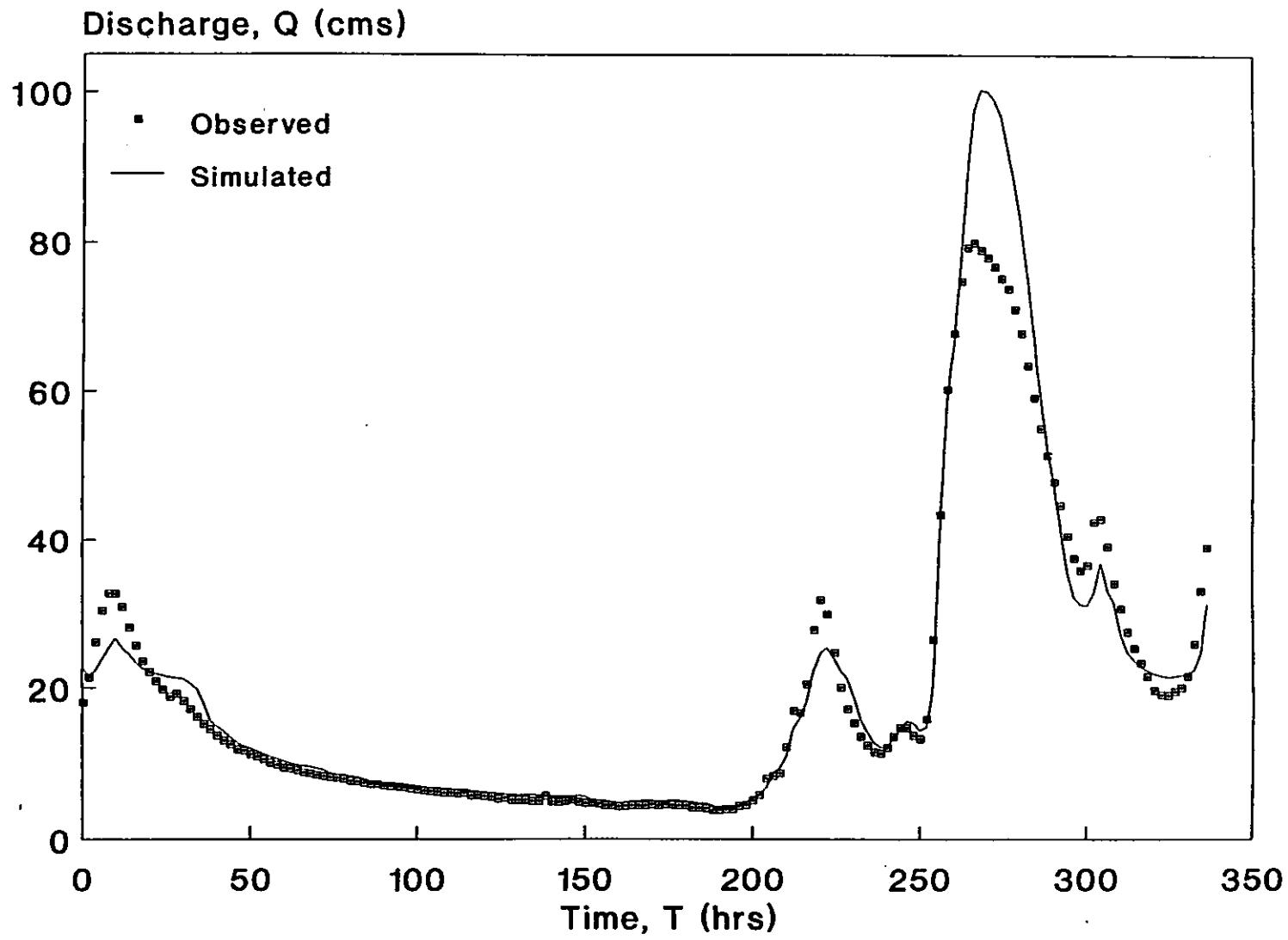

Figure 5.60.a Simulated vs. Observed Discharge Hydrograph with No Off-Channel Storage Areas applied to DWOPER for Myers' Data Set.

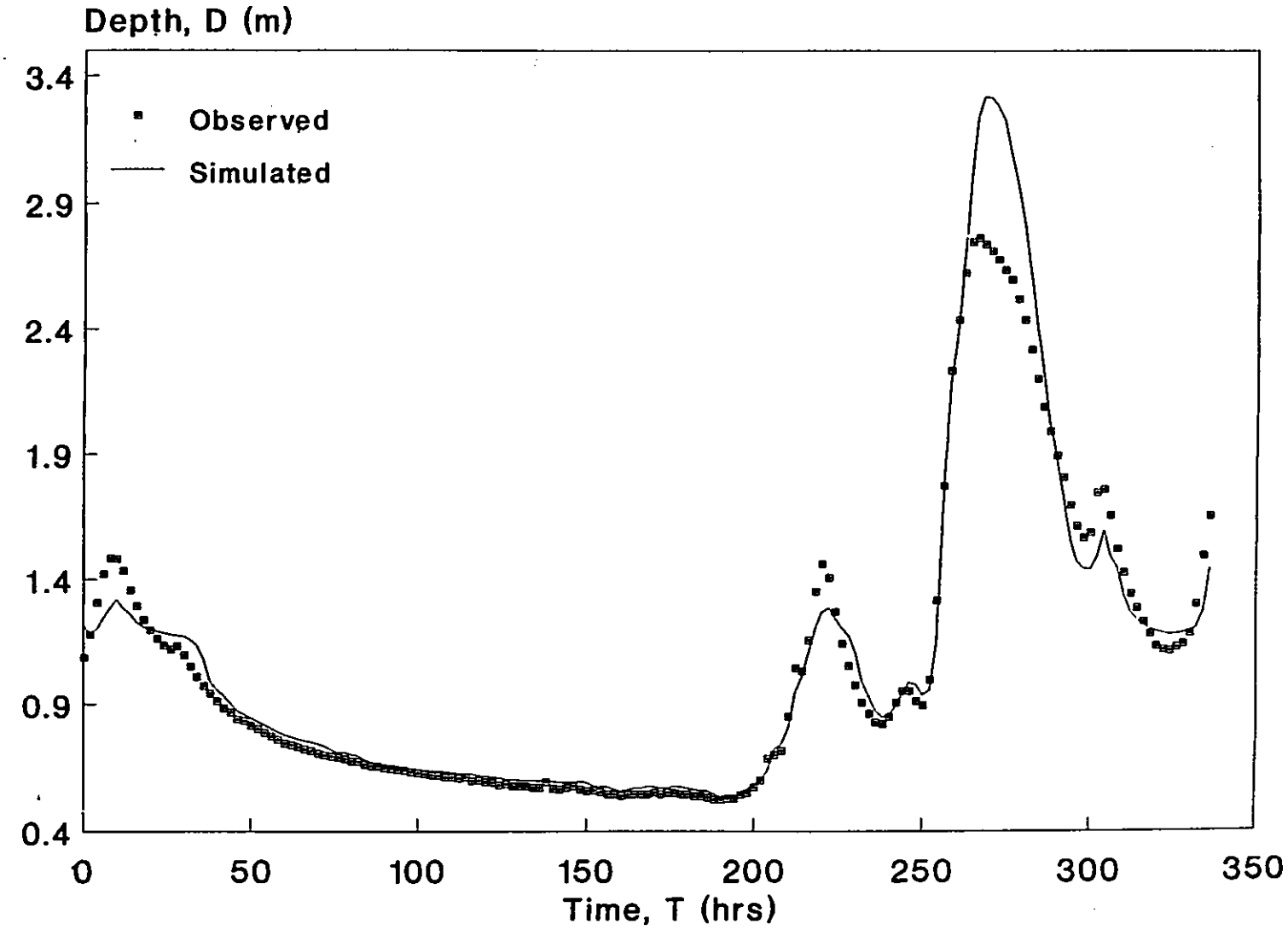

Figure 5.60.b Simulated vs. Observed Depth Hydrograph with No Off-Channel Storage Areas applied to DWOPER for Myers' Data Set.

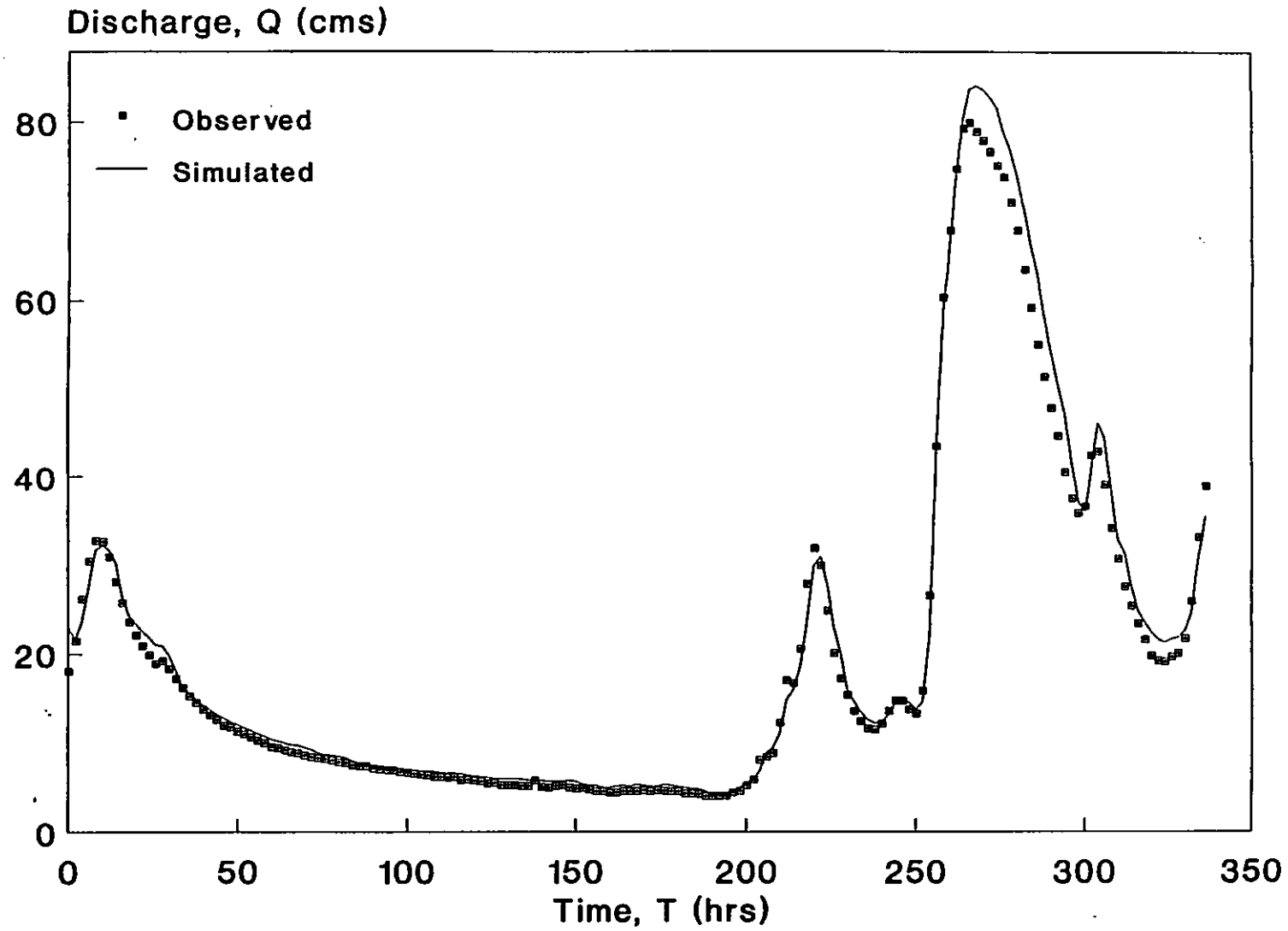

Figure 5.61.a Simulated vs. Observed Discharge Hydrograph with Vertical interface planes applied to DWOPER for Myers' Data Set.

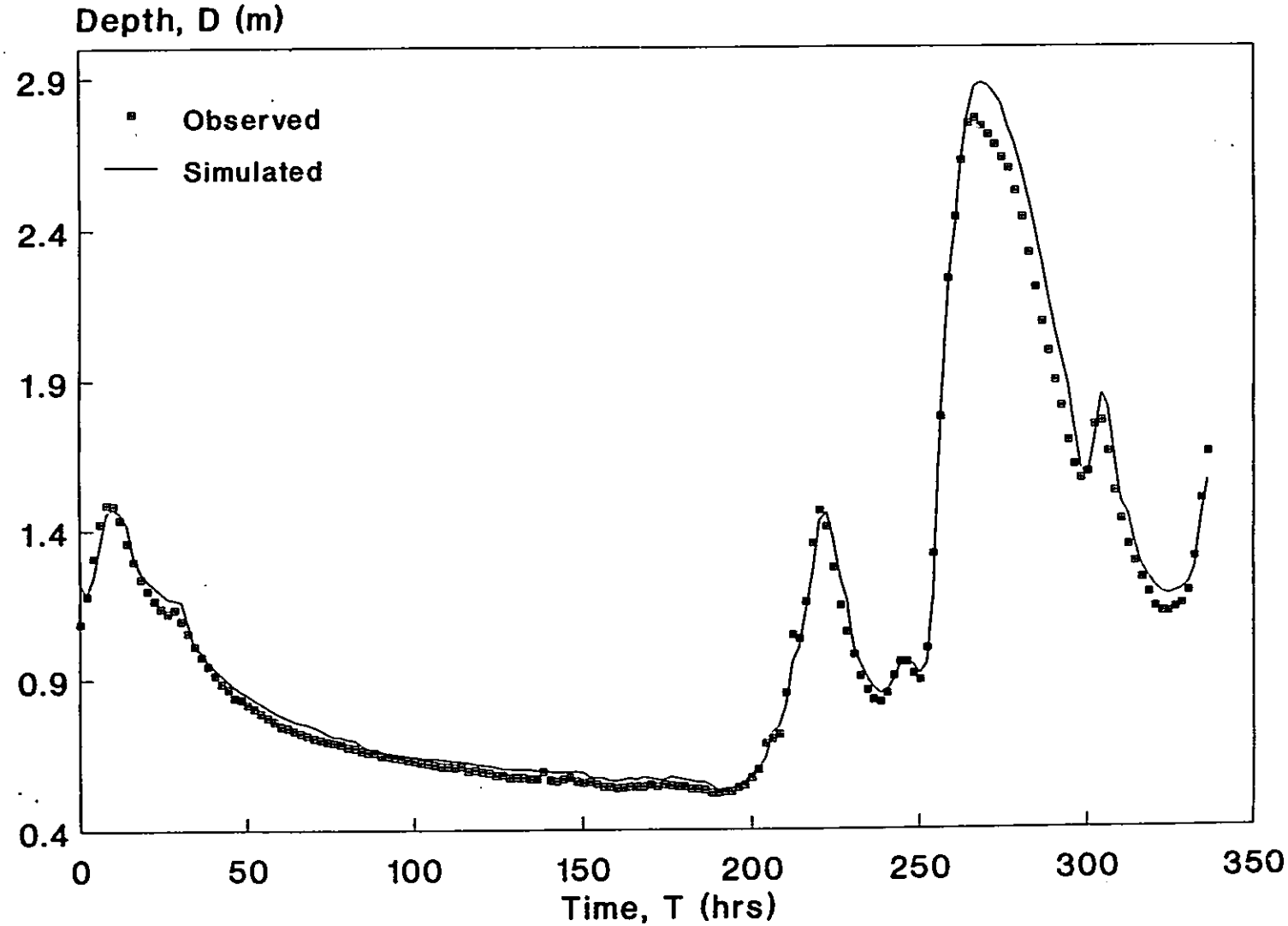

Figure 5.61.b Simulated vs. Observed Depth Hydrograph with Vertical interface planes applied to DWOPER for Myers' Data Set.

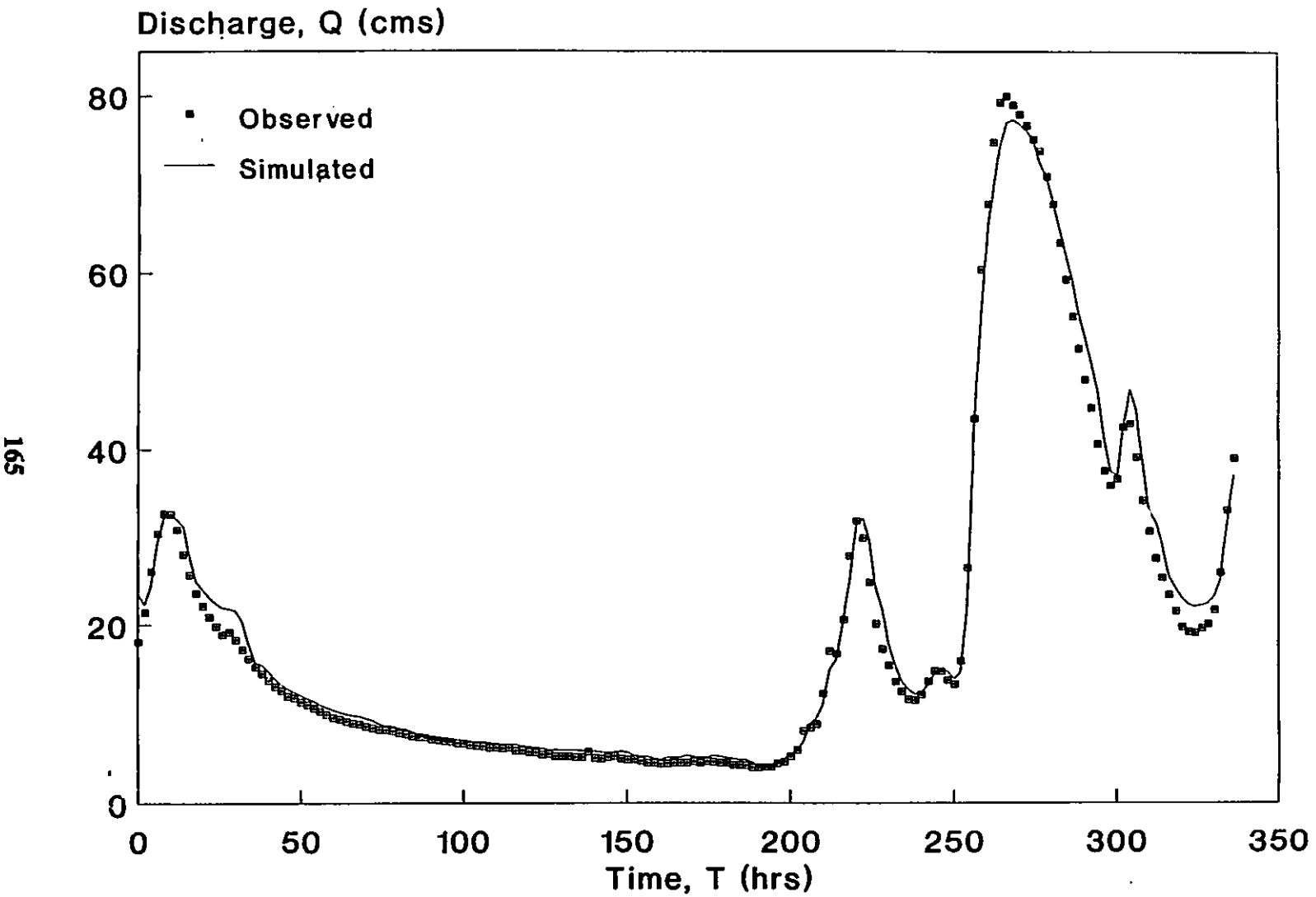

Figure 5.62.a Simulated vs. Observed Discharge Hydrograph with Diagonal interface planes applied to DWOPER for Myers' Data Set.

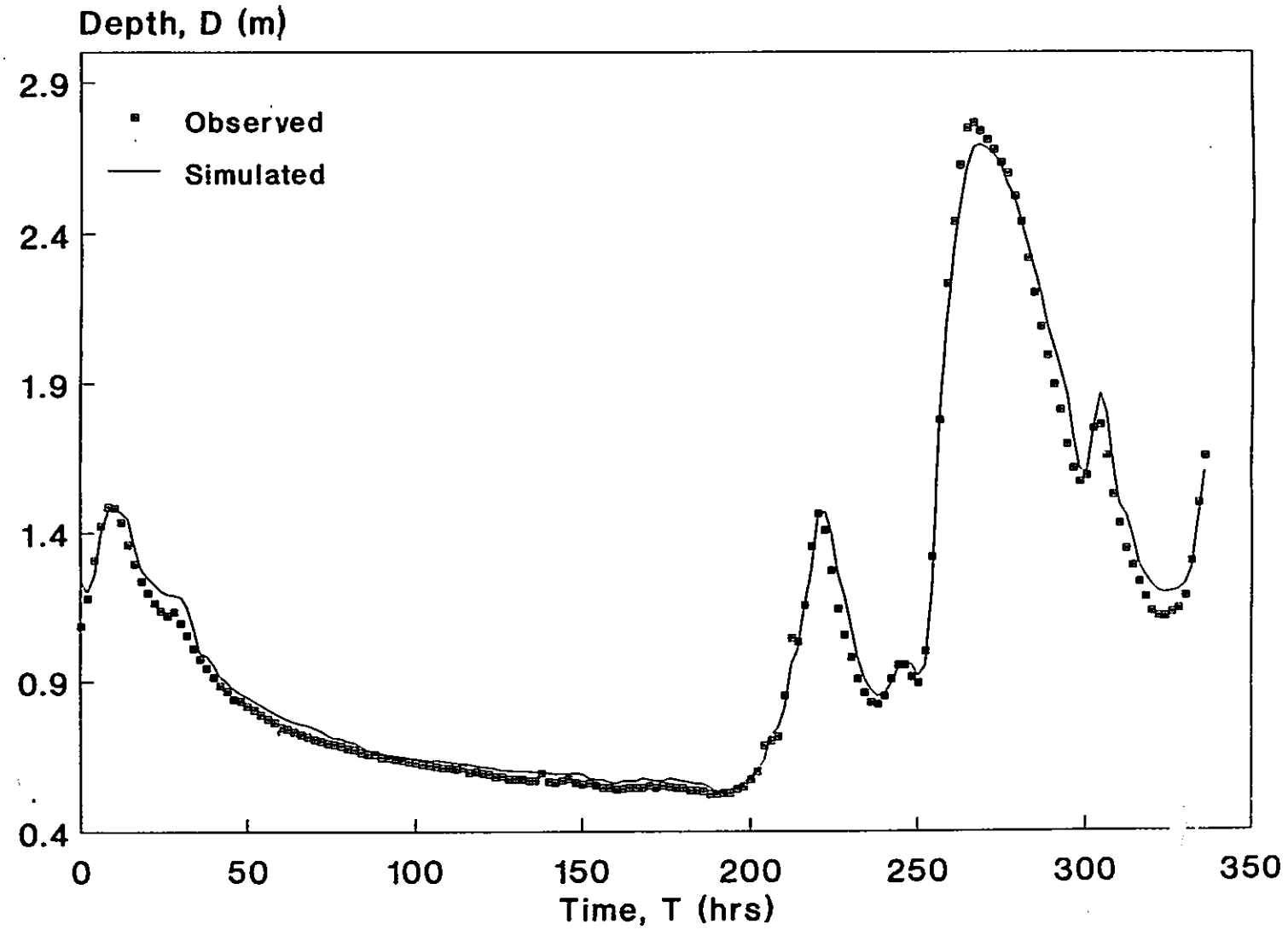

Figure 5.62.b Simulated vs. Observed Depth Hydrograph with Diagonal interface planes applied to DWOPER for Myers' Data Set.

CHAPTER 6

APPLYING EXTRAN TO DATA SETS

6.1 INTRODUCTION

EXTRAN, or Extended Transport Block of the U.S. Environmental Protection Agency (EPA) Storm Water Management Model (SWMM), is an explicit dynamic flow routing model that routes hydrographs through open channels and/or closed conduit systems experiencing unsteady flow (time history of flows and heads), (EXTRAN, 1973). EXTRAN was primarily developed for use in urban drainage combined and separate systems. It can also be used for stream channels involving arbitrary cross-sections that can be adequately represented by a trapezoidal cross-section. EXTRAN solves the full dynamic Saint Venant equations for gradually varied flow using an explicit solution technique to step forward in time. As a result, the solution time-step is governed by the wave celerity in the shorter channels or conduits in the system.

EXTRAN was developed in 1973 for the city of San Francisco. At that time it was called the San Francisco Model or more properly the WRE Transport Model. In 1974, EPA acquired this model and incorporated it into the SWMM package. It was called the extended transport model to distinguish it from the Transport Block developed by the University of Florida as a part of the original SWMM package. EXTRAN represents the drainage system as links and nodes, allowing simulation of parallel or looped pipe networks; weirs, orifices, and pumps; and system surcharges. EXTRAN is used most efficiently when applied to those parts of the drainage system that cannot be simulated accurately by simpler, less costly models.

6.2 INPUT DATA GUIDELINES

EXTRAN is format free. Input is not restricted to fixed columns but at least one space should separate each data field. No decimal places are allowed in integer data fields. A variable is real if it has a 0.0 in the default column. Also character data has to be enclosed by single quotation marks.

6.3 ROUTING OPTIONS

EXTRAN includes three options for solving the gradually varied, one dimensional unsteady flow equations for open channels. The solution options are called using the ISOL parameter on data group B0. ISOL = 0 represents the explicit method, ISOL = 1 the enhanced explicit method, and ISOL = 2 the iterative method. This data group (B0) was not a requirement and may be omitted.

The following are two significant differences between the explicit and the enhanced explicit solutions:

1- The $d(Q^2/A)/dx$ term in the momentum equation (eq. 3-23) has a different

derivation, and

2- An additional Q_{t+dt} is factored out of the momentum-continuity equation. Refer to chapter-3 for the theoretical development and formulation.

The main consequence of these differences occurs during the rising and falling portion of the hydrograph. During steady flow conditions the momentum equation reduces to a balance of hydraulic head slope and friction slope. However, as the flow is increasing or decreasing the enhanced explicit solution allows substantially longer time steps than the explicit solution. The iterative solution option is based on using appropriate weighting coefficients where values of velocity, hydraulic radius and area are weighted averages of the conduit upstream, middle, and downstream values at time t and/or t+dt. Numerical integration of the equations is accomplished by using an under-relaxation iterative matrix solution. An under-relaxation factor of 0.75 is used for the first iteration and 0.50 for subsequent iterations where these two values were found by trial end error. The iterative method uses a variable time step.

For the case of Treske's data set, different optional routing solution control parameters were used. The solution technique parameters selected were ISOL = 0, 1, and 2. Table 6.1 (and figure 6.1) shows the effect of varying ISOL on the downstream simulated depth hydrograph as compared to the observed hydrograph. Investigating the simulated results leads to the conclusion that the iterative explicit solution gave the best-fit hydrographs in comparison with the explicit solution and the enhanced explicit solution.

6.4 TIME STEP AND THE EXPLICIT METHOD

EXTRAN is an explicit model for solving unsteady flow problems. The explicit method was applied by Stoker et al (1957) to river flow problems. The method is subject to a stringent stability condition that imposes a limiting value for the time step in relation with the distance step. This limitation does not pose much difference for modelling short-

term flows; however, it becomes cumbersome and inefficient for long-term flows such as floods in large rivers. In the explicit method, the momentum equation is applied to discharge in each link and the continuity equation to head at each node. It is well known that explicit methods involve fairly simple arithmetic and require little storage space compared to implicit methods. However, they are generally less stable and often require very short time steps.

The time step (DELT) is most critical to the cost and stability of the EXTRAN model run and must be selected carefully. The time step should not be longer than the time it takes for a dynamic wave to travel the length of the shortest conduit in the transport system. According to the EXTRAN data input manual, a 10-second time step is recommended for most wet-weather runs, whereas a 45-second time step is used satisfactorily for most dry-weather conditions.

The choice of the time step is controlled by the wave celerity in the system. To estimate the time step DELT is computed for wide channels or circular pipes, based on the following equation:

$$\Delta t_c = \frac{L}{(g\,D)^{\frac{1}{2}}} \qquad (6\text{-}1)$$

where:

Δt_c = time, in seconds, for a surface wave to travel from one end of a conduit to the other,

L = conduit length, in meters,

D = diameter or depth, in meters, and

g = gravitational acceleration, in meter per square seconds.

Or compute DELT for a general open channel or conduit cross-section, using the following

equation:

$$\Delta t_c = \frac{L}{\left(\frac{g A}{T}\right)^{\frac{1}{2}}} \qquad (6\text{-}2)$$

where:

A = maximum cross-sectional area, in square meters, and

T = full flow top width, in meters.

The Courant number (C), in seconds, is an important criterion for stability. It is defined as:

$$C = \frac{L}{\left(V + \frac{g A}{T}\right)^{\frac{1}{2}}} \qquad (6\text{-}3)$$

where V = average conduit velocity, in meters per seconds.

The time step can usually exceed Δt_c by a factor of 1.5 to 2.0 for a few widely separated conduits. However, a time step of 60 to 90 seconds should not be exceeded even in large open channel systems where the celerity criterion is not violated with a large time step.

For the case of Treske's data set, the channel was subdivided into 14 conduits each 15 m long. Based on the stability criterion (eqs. 6-2 and 6-3), a time step of up to 7 seconds can be used; however, a time step of 2 seconds was adopted in this instance. The choice of the time step was arbitrary as long as it satisfies the Courant criteria for stability. In addition, several time steps other than 2 seconds were selected to check the effect of the time step variation on the simulated hydrographs, (table 6.2 and figure 6.2).

6.5 INITIALIZATION OF FLOW

Frequently, it is desired to initialize the system with starting flow values. These initial conditions represent either the dry weather or antecedent flow conditions just prior to the storm to be simulated. Initial flows will in turn be used to estimate initial depths. This is accomplished by computing the normal depth in each conduit. Initial depths may also be entered and the model will begin the simulation based on these values. However, unless these values are taken from a prior run, depths and flows input in this manner may not be consistent, leading to irregular output during the first few time steps.

For the case of Treske's data, a value of $0.095\,m^3/s$ was specified as the initial discharge at the upstream station of the channel and zeros were assigned elsewhere. In addition, a value of 0.212 m was the initial depth input at the downstream station. These initial values represent the steady flow conditions for the channel before the occurrence of the flood.

6.6 BOUNDARY CONDITIONS

Boundary conditions should be specified at the upstream and downstream stations of the channel.

6.6.1 Upstream Condition

EXTRAN provides up to 65 inflow hydrographs as input data lines in cases where it is desirable to run the model alone without prior use of an upstream block or additional input hydrographs, either at the same or different nodes, to those computed by an upstream block. The upstream boundary condition is a discharge hydrograph specified at any convenient time (not necessarily evenly spaced) as long as a value is included for each junction. Then hydrographs at each time step are formed by linear interpolation between

consecutive input values of the time series.

A discharge hydrograph is the upstream boundary condition with time increments input in decimal hours and flow rates in m^3/s.

6.6.2 Downstream Condition

The downstream boundary conditions can be described by up to five sets of data groups. They may be applied to any outfall with or without flap gates. The downstream boundary condition can be either one of the following:

i- no water surface at the outfall (pipe or weir discharge above any tailwater),

ii- a water surface at constant elevation,

iii- a tide whose period and amplitude are described by user-supplied tide coefficients,

iv- a tide given by the following equation:

$$HTIDE = A_1 + A_2 \sin wt + A_3 \sin 2wt + a_4 \sin 3wt + A_5 \cos wt + A_6 \cos 2wt + A_7 \cos 3wt \qquad (6\text{-}4)$$

where:

HTIDE = elevation of outfall water surface in meters,

t = current time in hours,

w = angular frequency $2\pi/W$, in radians/hour,

W = tidal period, in hours, and

A_1--A_7 = coefficients in meters.

(Coefficients for equation 6-4 will be computed by EXTRAN based on a specified number of stage-time points describing a single tidal cycle), or

v- a user-input time series of tail water elevations with linear interpolation between values.

Investigating the aforementioned types of downstream boundary conditions, one can eliminate the possibility of using types ii, iii, and iv for Treske's straight prismatic channel. The controlling water surface elevation at the downstream outfall station is not at constant elevation. Also using the tide option does not apply to the case under consideration. Type 5 means that the user is supplying EXTRAN with a stage hydrograph at the downstream end and is asking the program to compute the stage and discharge hydrographs. If the downstream stage hydrograph was known, the discharge hydrograph would be computed using the rating curve equation. Thus, the modelling exercise would be illogical and there would be no need to use a dynamic model.

6.7 MODIFYING THE CHANNEL

Therefore, "no water surface" at outfall was the most logical and suitable condition for the present application. However, the downstream end of Treske's channel was not a "free fall" outlet. Thus, a modification was applied to the channel input data. The channel was artificially elongated to avoid the occurrence of critical flow depth at the free outfall. Different percentages of the original length were applied to elongate the channel, and an optimal value of 210 m (one channel length) was determined based on comparing simulated and observed hydrographs. In addition, backwater computations were performed for the channel to determine the length at which uniform flow occurred; (Table 6.3). Therefore, the free outfall option was selected as the downstream boundary condition for the artificially elongated channel. The simulated hydrographs were calculated and plotted at a station 210 m from the upstream extremity of the channel.

6.8 STORAGE AREAS

Input to EXTRAN includes specification for conduits including shape, size, length, hydraulic roughness, connecting junctions, initial flow and invert distances referenced from the junction invert.

Unlike DWOPER, EXTRAN does not have the ability to specify part or all of the flood plain flow as separate off-channel storage areas. However, channels with flood plains are entered as one unit cross-section using the irregular cross-section data option. For non-prismatic channels, irregular cross-sections may be mixed with regular cross-sections, but the data for the irregular sections are grouped together after all the regular section data input is done. Usually, a trapezoidal-shaped cross-section approximation may not be appropriate for many natural channels; (figure 6.3). Elevations are used only to determine the shape of the cross-section. Irregular cross-section details are input by entering coordinates of contour points (or end points of inflections). These coordinates are measured with respect to a system of axes located at the left side of the channel cross-section. Total depth in a cross-section is computed as the difference between the highest and lowest contour points on the cross-section.

6.9 MODEL INPUT DATA

Data was input to EXTRAN in the following manner: Treske's straight prismatic channel was subdivided into 14 conduits, each 15 m long, or 15 junctions numbered from the upstream end and proceeding to the downstream junction or station. No modification to the conduit lengths was considered using equivalent-conduit option provided by EXTRAN to ease time step limitations within certain limits. However, the channel was subdivided in several ways to check the effect of the distance step size on the accuracy of the simulated stage and discharge hydrographs. Table 6.4 and figure 6.4 show the effect of varying the distance step between 70 m and 210 m on simulated hydrographs. Choosing a smaller distance step would result in a very small time step.

An initial flow rate of $0.095 m^3/s$ was assigned at the upstream junction and zeros were assigned elsewhere. An irregular (natural) cross-section was specified by defining 8 contour points (points of inflection). These points were input based on a coordinate system of axes with the origin located at the left extremity of the channel cross-section.

As an EXTRAN requirement, data input to define an irregular-shaped cross-section should include:

1- Total number of stations or contour points,
2- Station (or z-distance from the origin) from the left bank of the channel,
3- Station from the right bank of the channel,
4- Length of channel,
5- Elevation (y) of cross-section at station n (may be positive or negative), and
6- Station (z) of cross-section at station n.

6.10 MODEL CALIBRATION

EXTRAN data input requires a value of Manning's roughness coefficient n to be specified. In addition to reflecting the degree of boundary roughness, this n-value must also account for entrance, exit, expansion, and contraction losses. It must be specified for the main channel, left over-bank, and right-over bank flows.

For the case of Treske's data set, n was given as 0.012 for the entire compound channel. However, adopting this n-value for EXTRAN input data did not produce good agreement between observed and simulated hydrographs. Thus, a model calibration had to be performed. Different n-values ranging between 0.012 and 0.022 were applied to flood event #1 (in-bank flow) and an optimum value of 0.020 was obtained. This n-value was then verified through simulations for flood events 2, 3, and 4 (all in-bank flows). Then a model calibration procedure had to be performed for Treske's compound channel data (Flood events 5, 6, 7, 8, 9, and 10). A trial and error procedure was applied and an optimal n-value of 0.019 was obtained. This n-value was used for the main channel as well as the flood plains. In addition, selecting a different n-value for the flood plains did not introduce considerable improvements on the simulated hydrographs as table 6.5 shows, (figure 6.5). Finally, this optimal n-value (0.019) was successfully applied for simulating flood events

5 to 10 of Treske's data set. Figures 6.6 to 6.15 show the simulated via observed discharge and depth hydrographs using EXTRAN after calibration. Also, table 6.6 shows the percentage deviation of simulated peak values from those observed.

6.11 ROUND-OFF ERRORS

Round-off errors represent an important cause of discrepancies resulting when EXTRAN was applied to Treske's data set. Treske's data was measured on an experimental laboratory channel. The dimensions were very small compared to those of a natural channel for which most of the hydrodynamic models were developed. Treske's flows and depths were having values read to three significant figures. However, EXTRAN produced the simulated results with two significant figures exhibiting some round-off errors. For example, a measured discharge of Q = 0.104 m^3/s would by reported by EXTRAN as Q = 0.10 m^3/s. This rounding-off significant figures results in up to 4 % relative error. Also, it results in a step-wise simulated hydrograph rather than a smooth curve. Figure 6.16 shows the effect of plotting two observed discharge hydrographs of Treske's data (cases 1 and 4) using two and three significant figures.

6.12 MYERS' DATA SET

This section deals with the application of EXTRAN to a non-prismatic natural channel data set (Myers, 1991).

6.12.1 Initial and Boundary Conditions

Input to the model consisted of an initial water surface elevation of 1.085 m specified at the downstream station of the river reach, and zeros assigned elsewhere. Also, initial discharge Q_i was input to EXTRAN at each station. A value of 16.7 m^3/s (591 ft^3/s) was the Q_i-input at the upstream station. These initial values represent the steady uniform

flow conditions before the flood occurred.

While EXTRAN requires a discharge hydrograph for the upstream boundary condition, it should be noted that Myers supplied only a stage hydrograph at the upstream and downstream stations. However, Myers also supplied a single-value rating curve at the upstream and downstream stations of the river reach. This rating curve relation was used to obtain a discharge hydrograph from the corresponding measured depth hydrograph. The upstream rating curve can be expressed as follows:

$$Q = 23.19\,H - 848.90 \quad for\ H < 37.43\ m\ ,\ and$$
$$Q = 51.05\,H - 1892.44 \quad for\ H > 37.43\ m \qquad (6\text{-}5)$$

where Q = flow rate in m^3/s and H = water surface elevation in m. The corresponding expression for the downstream rating curve is:

$$Q = 25.02\,H - 859.82 \quad for\ H < 35.12\ m\ ,\ and$$
$$Q = 36.84\,H - 1274.55 \quad for\ H > 35.12\ m \qquad (6\text{-}6)$$

Based on the discussion in sections 6.6 and 6.7, a "no water surface at the outfall" boundary condition was used in this instance at the downstream station. However, the channel was hypothetically elongated by 800 m (equal to one channel length) to avoid the occurrence of critical flow at or near the free outfall. This elongation was more than that obtained using backwater computation. Simulated downstream hydrographs were plotted at a section located 800 m down from the channel entrance; i.e. in the middle of the hypothetically elongated channel.

6.12.2 Time Step

An 8-minute time step was adopted for the DWOPER application. This value was small enough to satisfy accuracy and stability requirements in the DWOPER implicit

formulation, and resulted in a total of 729 time steps. However, the 8-minute time step was considered too large to satisfy the Courant criteria in the explicit formulation of EXTRAN. In EXTRAN, the time step is governed by the wave celerity in the shorter channels or conduits in the system. For this reason time steps between 5 and 60 seconds are typically used. This would mean that the computer time is a significant consideration in the use of this explicit model. Therefore, applying EXTRAN limitations on the time step, a 30-second time step was small enough to satisfy Courant criteria for a 266.67 m distance increment. This value resulted in a total of 40 400 time steps in the simulation exercise. By comparison, using a 10-second time step would result in 121 200 time steps which is time consuming for a simulation process. The same purpose would be achieved faster using an implicit technique for solving the St. Venant equations of unsteady flow.

6.12.3 Model Calibration

In general, model simulation results are often very sensitive to any variation in Manning's n. Based on the discussion in section 5.8.5, Myers' bank-full n-value was relatively high. Thus, a model calibration had to be performed based on a trial and error procedure. The calibration process was performed for a part of the observed hydrograph to reproduce measured observations of both stage and discharge. The n-value obtained by the calibration process was adopted in data input to EXTRAN. In general, good simulation results were obtained and an optimum value of $n = 0.033$ was reached for the main channel flow and $n = 0.045$ was adopted for the flood plain flows.

6.12.4 Model Input Data

Data was input to EXTRAN in the following manner: Myers' non-prismatic channel was subdivided into 3 sub-reaches, each 266.67 m long. Myers' reach was hypothetically elongated by 800 m to avoid the occurrence of critical flow at or close to the free outfall boundary condition. Thus, 4 reaches were used to represent the elongated channel. A time

step of 30 seconds was adopted, which resulted in a total of 40 400 time steps in the modelling exercise for each run.

Using EXTRAN, it is not possible to define off-channel storage areas separately. However, the channel cross-section, at each station or junction, was defined as an irregular cross-section using a cartesian system of coordinates. Eight contour points were used to define each cross-section, and five values of station (Z) and elevation (Y) were input per data card.

Figures 6.17 and 6.18 show the simulated depth and discharge hydrographs resulting from the application of EXTRAN to Myers' data set.

6.13 CONCLUSIONS

EXTRAN was applied to model flow in a laboratory prismatic rectangular channel (Treske, 1981), and a non-prismatic natural channel (Myers, 1991). Being an explicit model, for reasons of numerical stability, EXTRAN has a restriction on the size of the computational time step. The stability criterion (eqs. 6-2 and 6-3) indicates that the computational time step is substantially reduced as the hydraulic depth (A/B) increases. Therefore, small time steps, in the order of few minutes or seconds, are used even though flood waves may have a duration in the order of a few weeks.

In general, EXTRAN produced good simulations. However, some discrepancies appear at various points on the simulated hydrographs. In addition, careful choice of the time step and the distance step should be made to ensure a successful run.

To conclude, the explicit method is very inefficient in the use of computer time. Fread (1981) identified another disadvantage of explicit solution schemes which is the requirement of equal distance step size. He suggested a remedy in that this requirement can

be relaxed somewhat by using weighting factors. Nevertheless, his main conclusion is that: "Explicit schemes are quite disadvantageous for modelling flows in natural waterways".

Table 6.1 Effect of Solution Technique Parameter Variation on Simulated Discharges using EXTRAN, (Treske's Data, Case 10).

Time	Observed Discharge	Simulated Discharge	Simulated Discharge	Simulated Discharge
(min)	(cms)	ISOL = 0	ISOL = 1	ISOL = 2
0	0.096	0.100	0.100	0.100
9	0.098	0.100	0.100	0.100
18	0.121	0.120	0.120	0.120
27	0.153	0.150	0.150	0.150
36	0.183	0.190	0.190	0.190
45	0.214	0.220	0.220	0.220
54	0.237	0.240	0.240	0.240
63	0.255	0.270	0.270	0.260
72	0.286	0.300	0.300	0.290
81	0.321	0.330	0.330	0.330
90	0.358	0.360	0.360	0.360
99	0.391	0.390	0.390	0.400
108	0.393	0.390	0.390	0.390
117	0.376	0.370	0.370	0.370
126	0.351	0.340	0.340	0.340
135	0.323	0.310	0.310	0.310
144	0.293	0.280	0.280	0.280
153	0.263	0.250	0.260	0.250
162	0.236	0.230	0.220	0.220
171	0.190	0.170	0.170	0.170
180	0.149	0.140	0.140	0.140
189	0.114	0.110	0.110	0.110
198	0.103	0.100	0.100	0.100
207	0.100	0.100	0.100	0.100
216	0.096	0.100	0.100	0.100
219	0.096	0.100	0.100	0.100
Total % Relative	Absolute Error	84.047	84.482	82.912

Table 6.2 Effect of Time Step Variation on Simulated Discharges using EXTRAN, (Treske's Data, Case 10).

Time (min)	Observed Discharge	Simulated Discharge	Simulated Discharge	Simulated Discharge
	(cms)	dt=1 sec	dt=5 sec	dt=10 sec
0	0.096	0.100	0.100	0.100
9	0.098	0.100	0.100	0.100
18	0.121	0.120	0.120	0.120
27	0.153	0.150	0.150	0.150
36	0.183	0.190	0.190	0.190
45	0.214	0.220	0.220	0.220
54	0.237	0.240	0.240	0.240
63	0.255	0.270	0.270	0.270
72	0.286	0.300	0.300	0.300
81	0.321	0.330	0.330	0.330
90	0.358	0.360	0.360	0.360
99	0.391	0.390	0.390	0.390
108	0.393	0.390	0.390	0.390
117	0.376	0.370	0.370	0.370
126	0.351	0.340	0.340	0.340
135	0.323	0.310	0.310	0.310
144	0.293	0.280	0.280	0.280
153	0.263	0.260	0.260	0.260
162	0.236	0.220	0.220	0.220
171	0.190	0.170	0.170	0.170
180	0.149	0.140	0.140	0.140
189	0.114	0.110	0.110	0.110
198	0.103	0.100	0.100	0.100
207	0.100	0.100	0.100	0.100
216	0.096	0.100	0.100	0.100
219	0.096	0.100	0.100	0.100
Total % Relative	Absolute Error	230.564	230.564	230.564

Table 6.4 Effect of Distance Step Variation on Simulated Discharges using EXTRAN, (Treske's Data, Case 10).

Time (min)	Observed Discharge	Simulated Discharge	Simulated Discharge	Simulated Discharge
	(cms)	dx=70 m	dx=105 m	dx=210 m
0	0.096	0.120	0.100	0.100
9	0.098	0.110	0.100	0.100
18	0.121	0.120	0.120	0.130
27	0.153	0.140	0.150	0.160
36	0.183	0.180	0.190	0.190
45	0.214	0.210	0.220	0.230
54	0.237	0.230	0.240	0.260
63	0.255	0.250	0.270	0.290
72	0.286	0.270	0.300	0.320
81	0.321	0.300	0.330	0.350
90	0.358	0.330	0.360	0.380
99	0.391	0.370	0.390	0.410
108	0.393	0.380	0.390	0.390
117	0.376	0.370	0.370	0.360
126	0.351	0.350	0.340	0.320
135	0.323	0.330	0.310	0.290
144	0.293	0.310	0.280	0.260
153	0.263	0.280	0.260	0.220
162	0.236	0.250	0.220	0.200
171	0.190	0.220	0.170	0.160
180	0.149	0.160	0.140	0.130
189	0.114	0.120	0.110	0.100
198	0.103	0.110	0.100	0.100
207	0.100	0.100	0.100	0.100
216	0.096	0.100	0.100	0.100
219	0.096	0.100	0.100	0.100
Total % Relative	Absolute Error	149.438	84.482	203.882

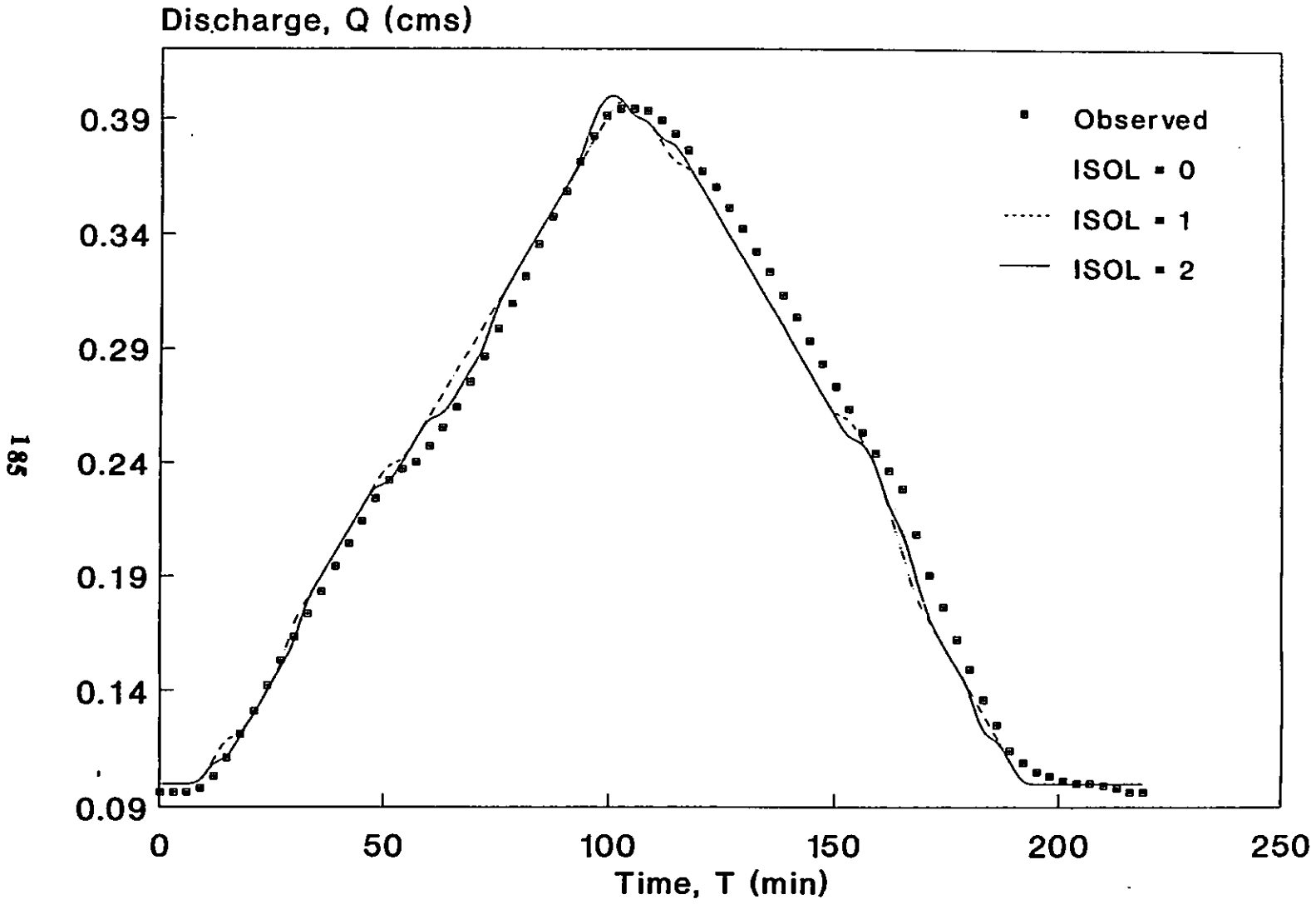

Figure 6.1 Effect of Solution Technique Parameter Variation on the Simulated Depth Hydrograph Using EXTRAN, (Treske's Data, Case 10).

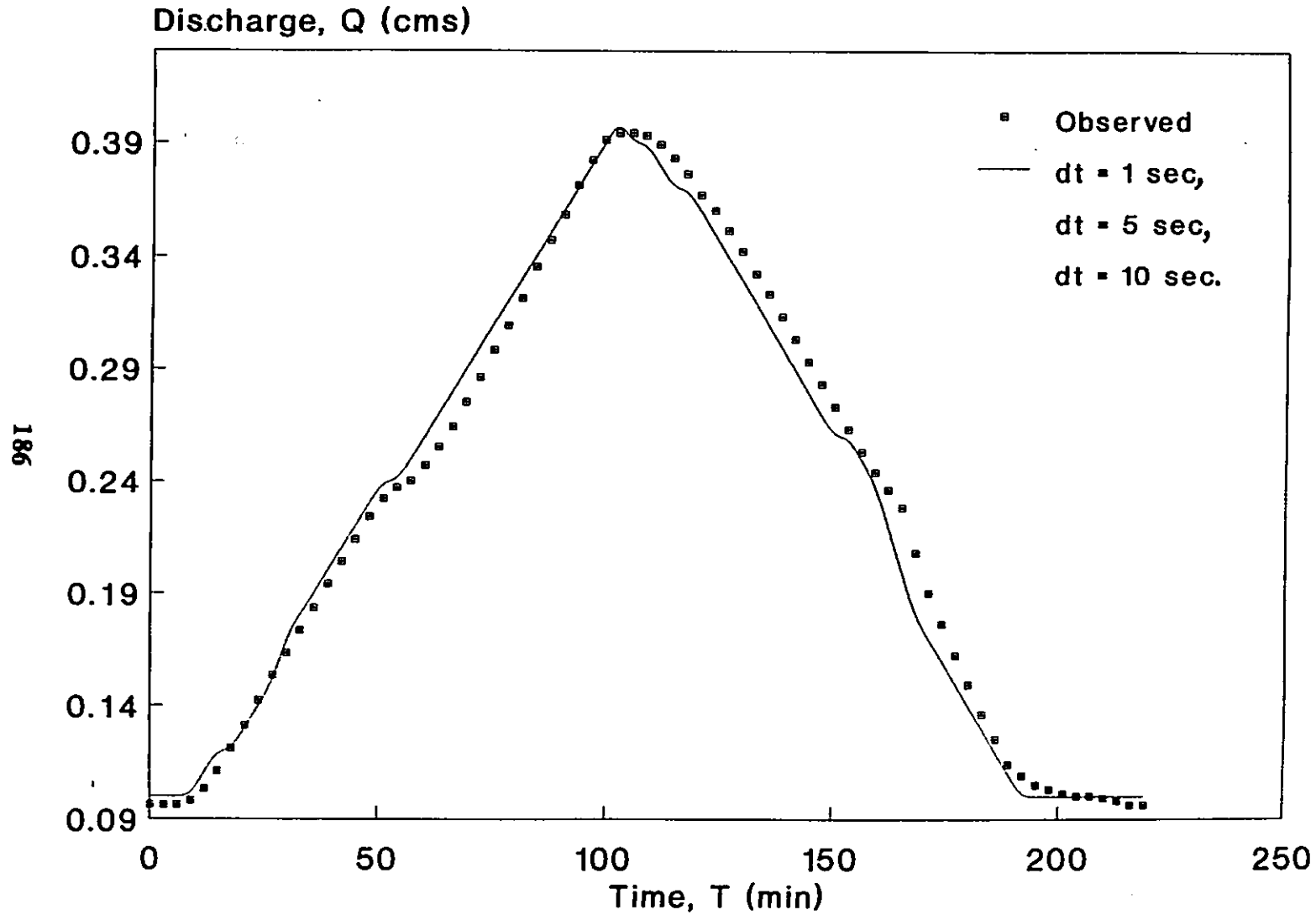

Figure 6.2 Effect of Time Step Variation on the Simulated Depth Hydrograph Using EXTRAN, (Treske's Data, Case 10).

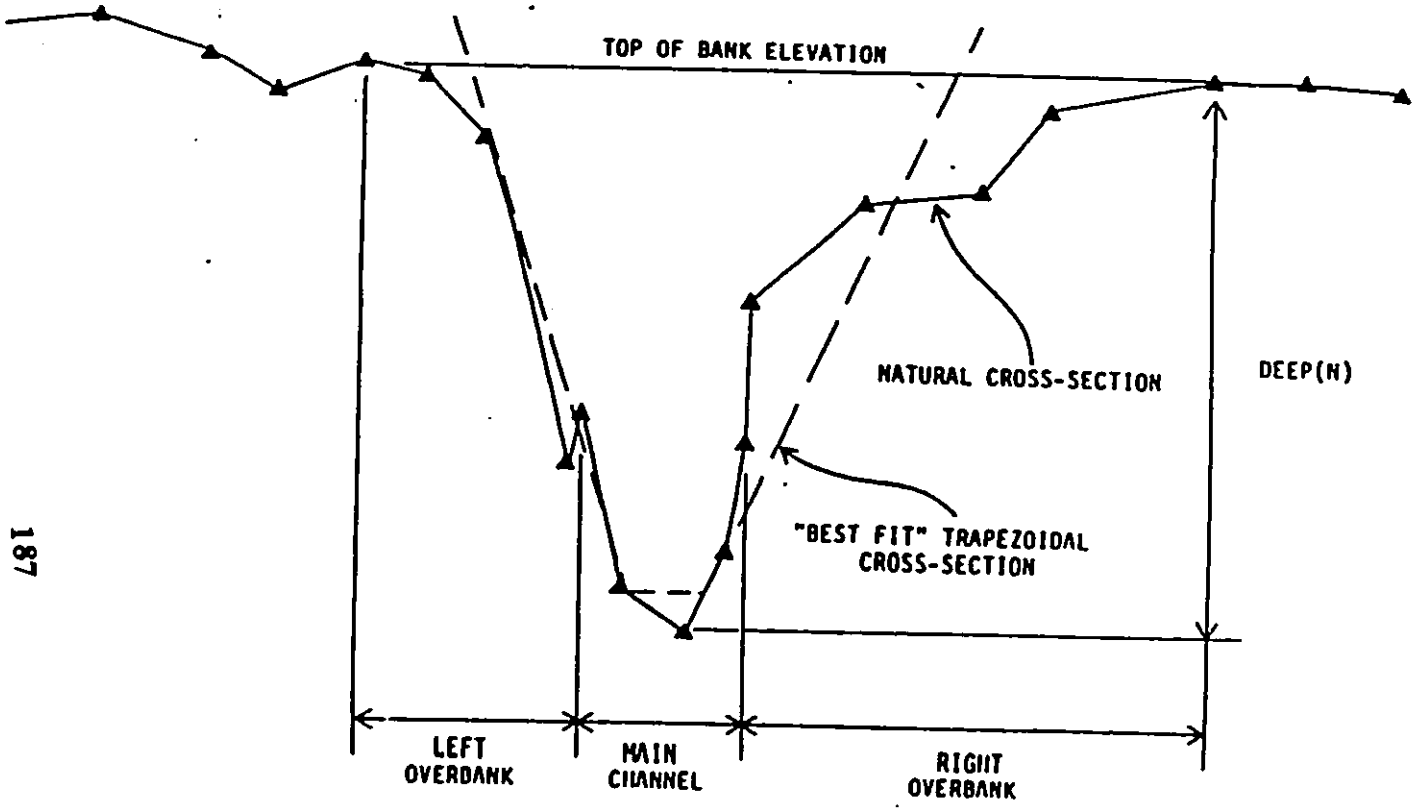

Figure 6.3 Definition Sketch of an Irregular Cross-Section.

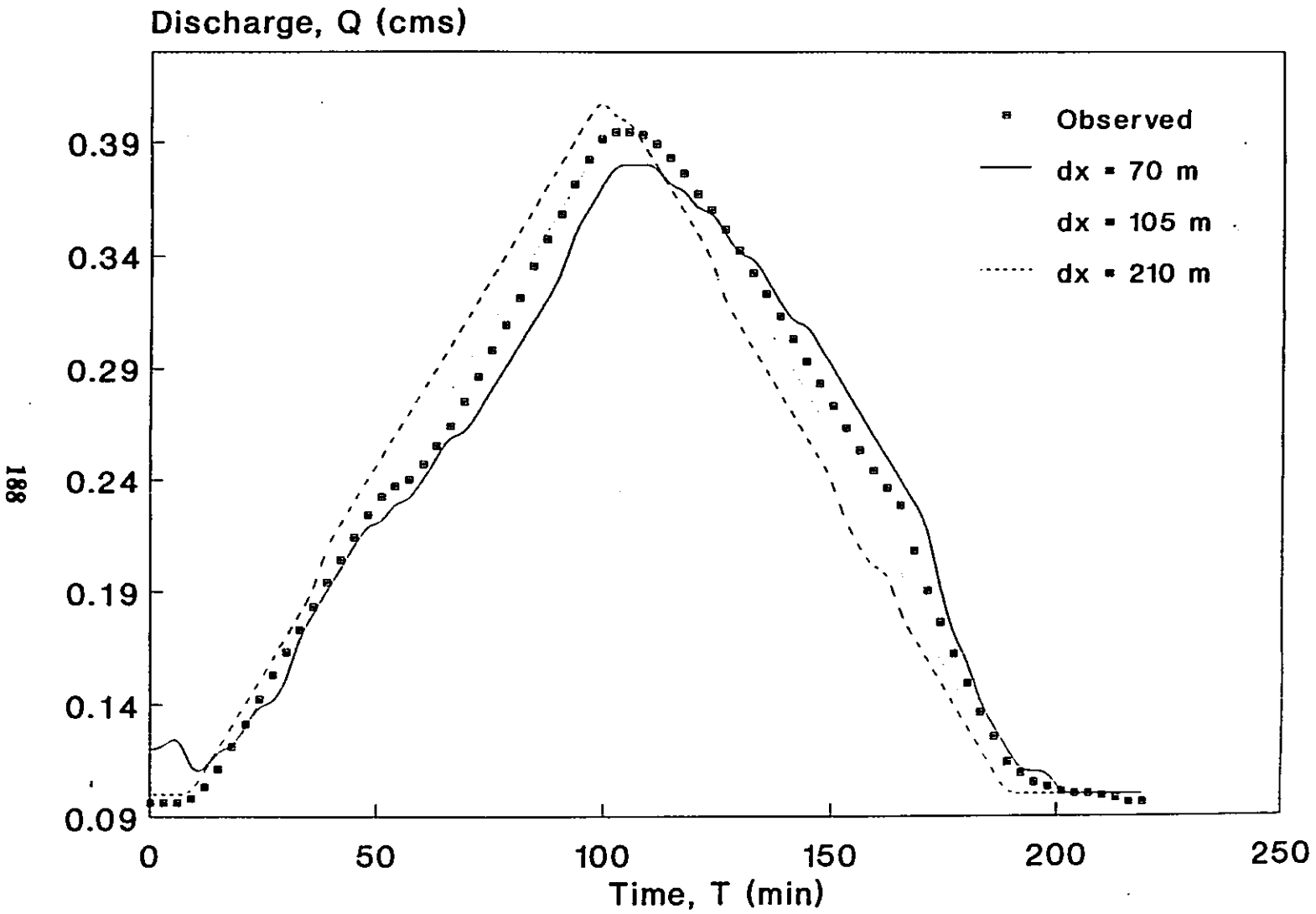

Figure 6.4 Effect of Distance Step Variation on the Simulated Depth Hydrograph Using EXTRAN, (Treske's Data, Case 10).

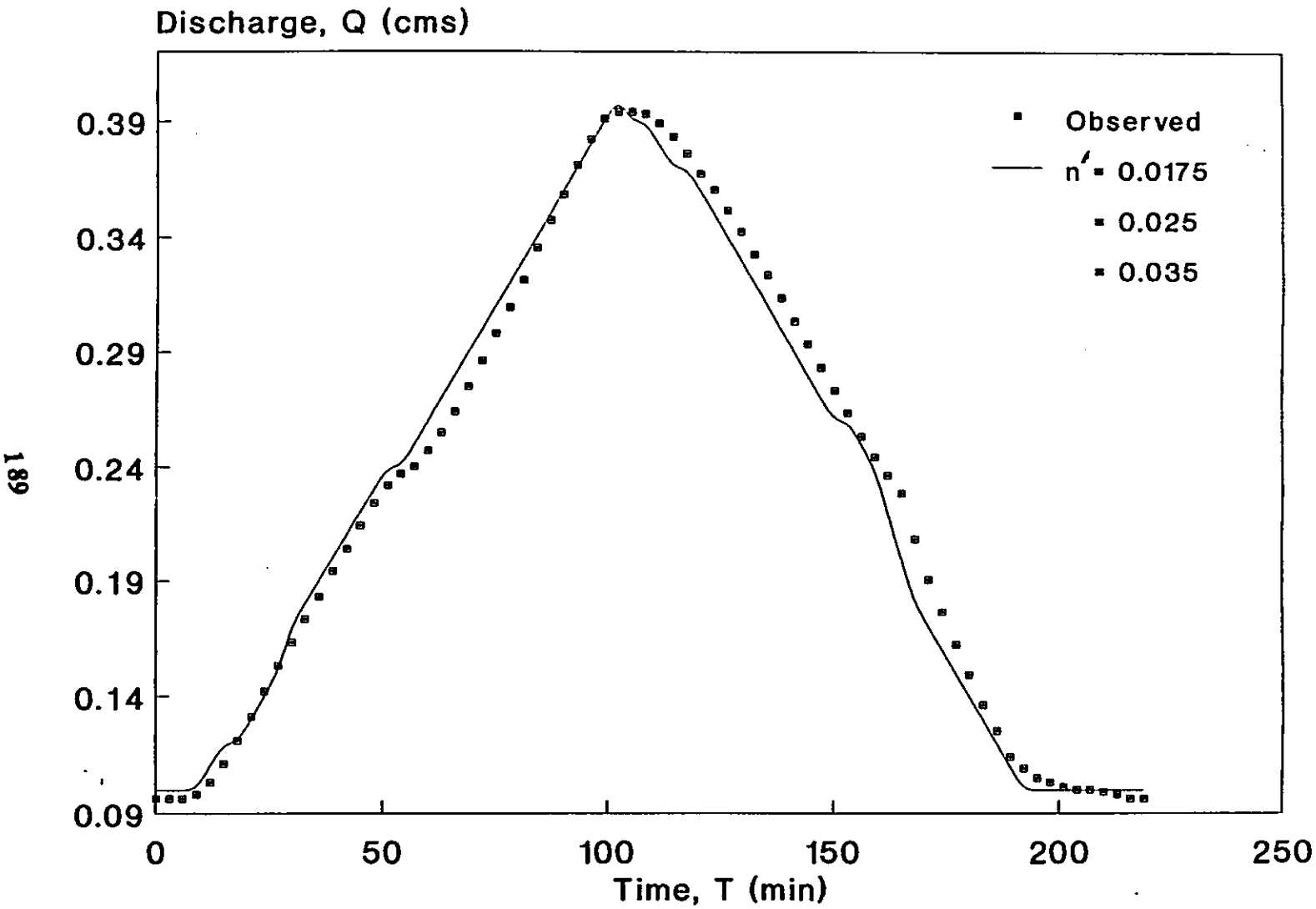

Figure 6.5 Effect of Calibrating the Flood Plain n Keeping the Main Channel n Constant.

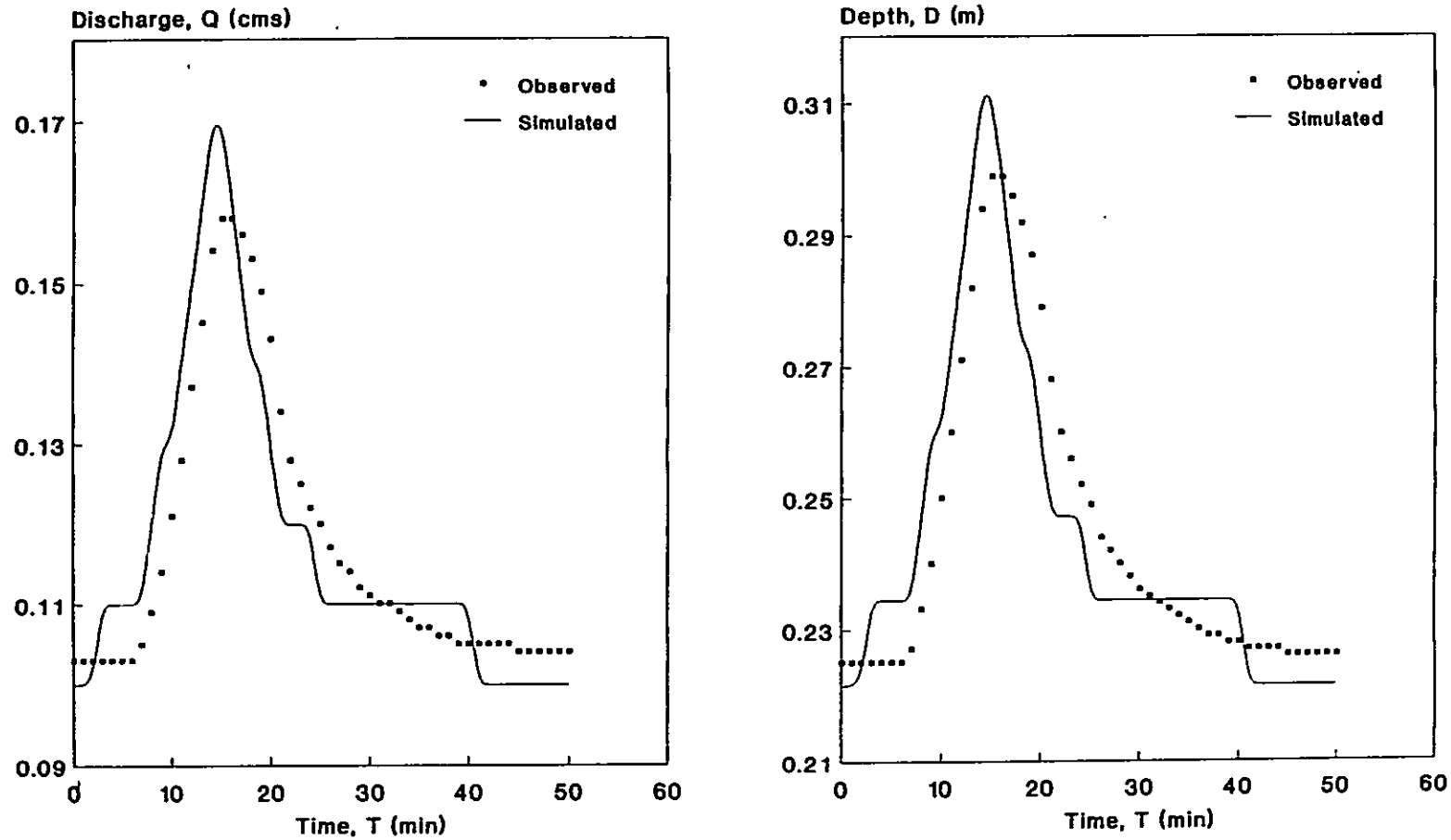

Figure 6.6 Simulated vs. Observed Discharge and Depth Hydrographs using EXTRAN, (Treske's data, case 1).

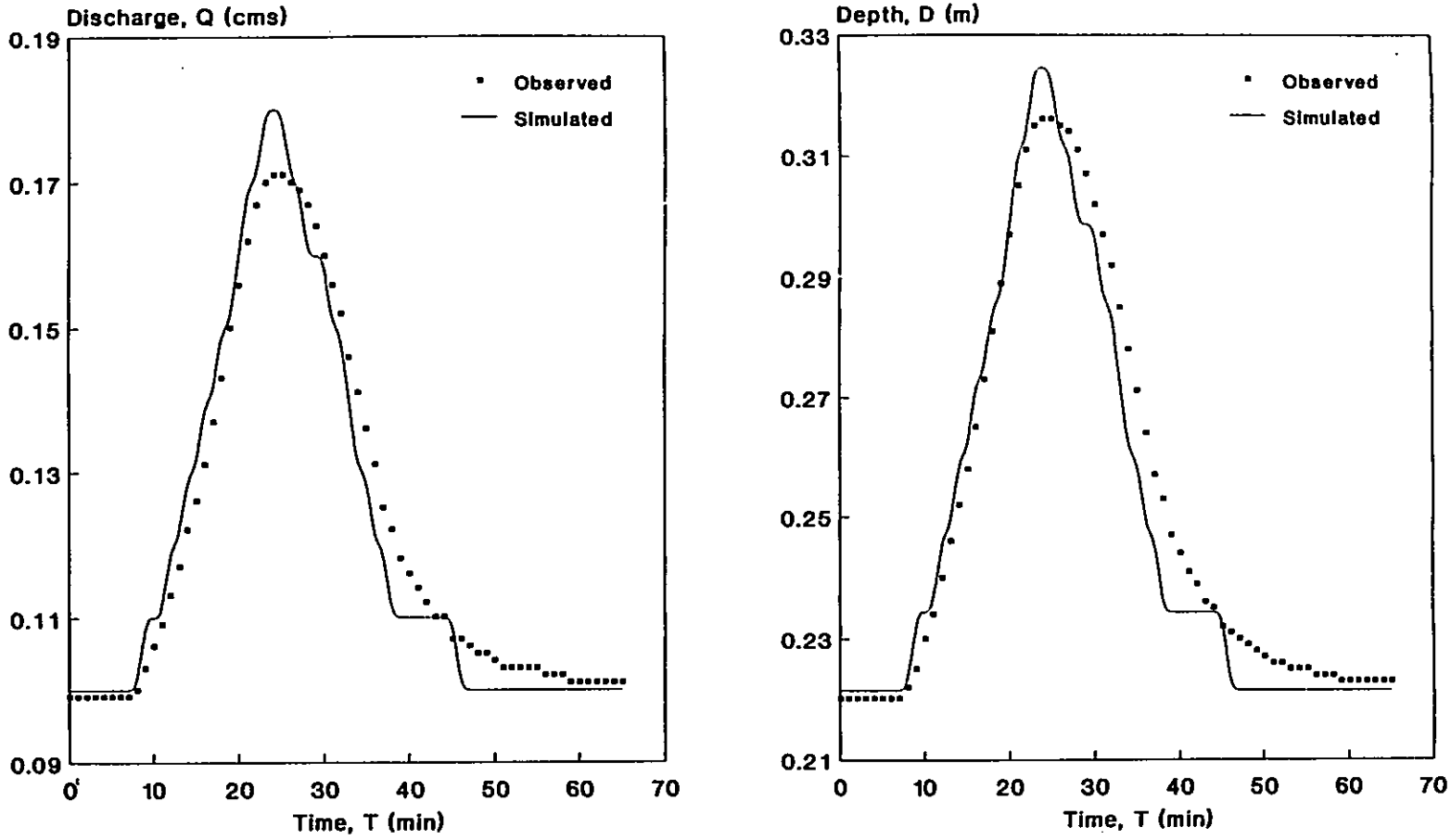

Figure 6.7 Simulated vs. Observed Discharge and Depth Hydrographs using EXTRAN, (Treske's data, case 2).

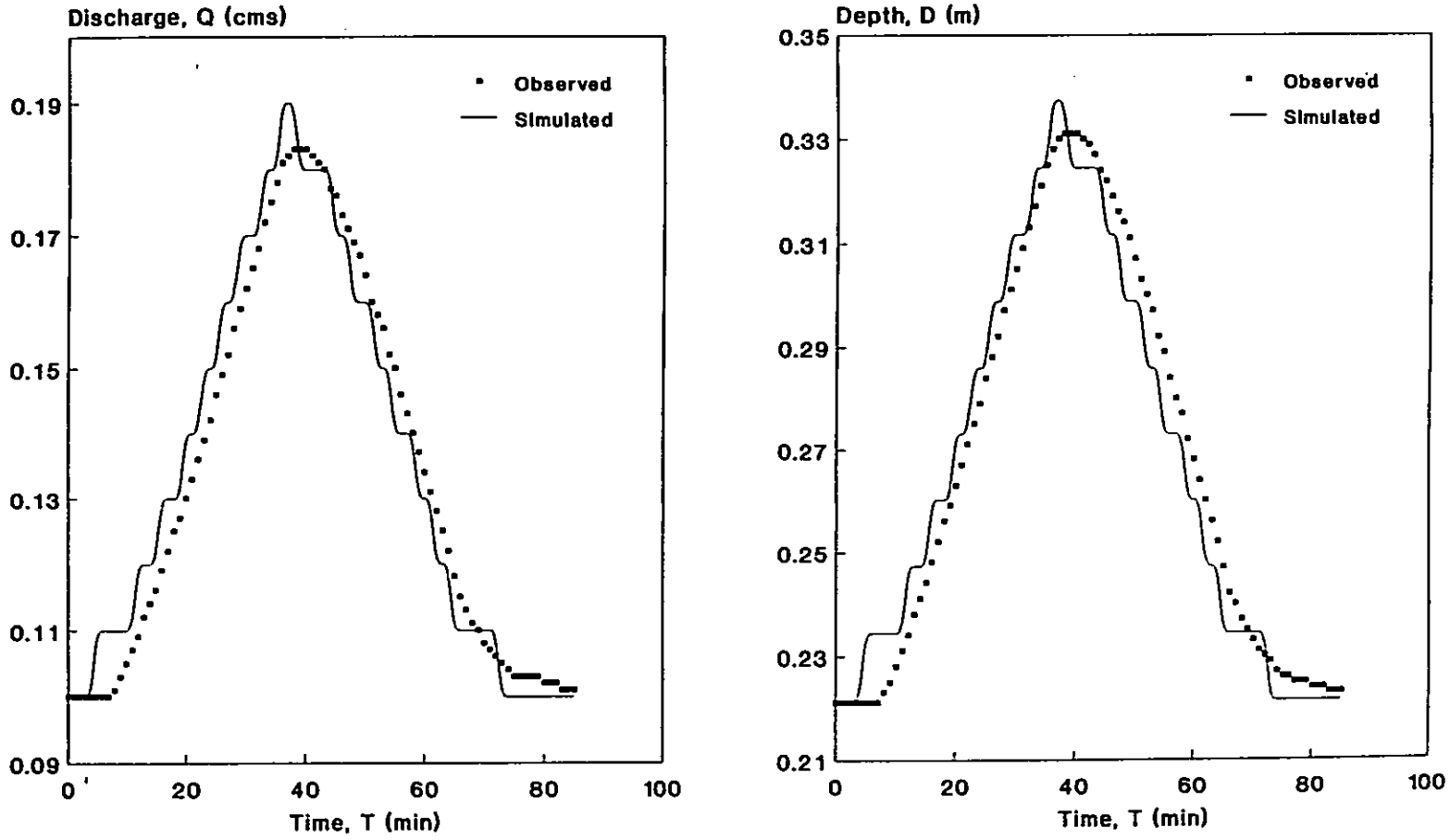

Figure 6.8 Simulated vs. Observed Discharge and Depth Hydrographs using EXTRAN, (Treske's data, case 3).

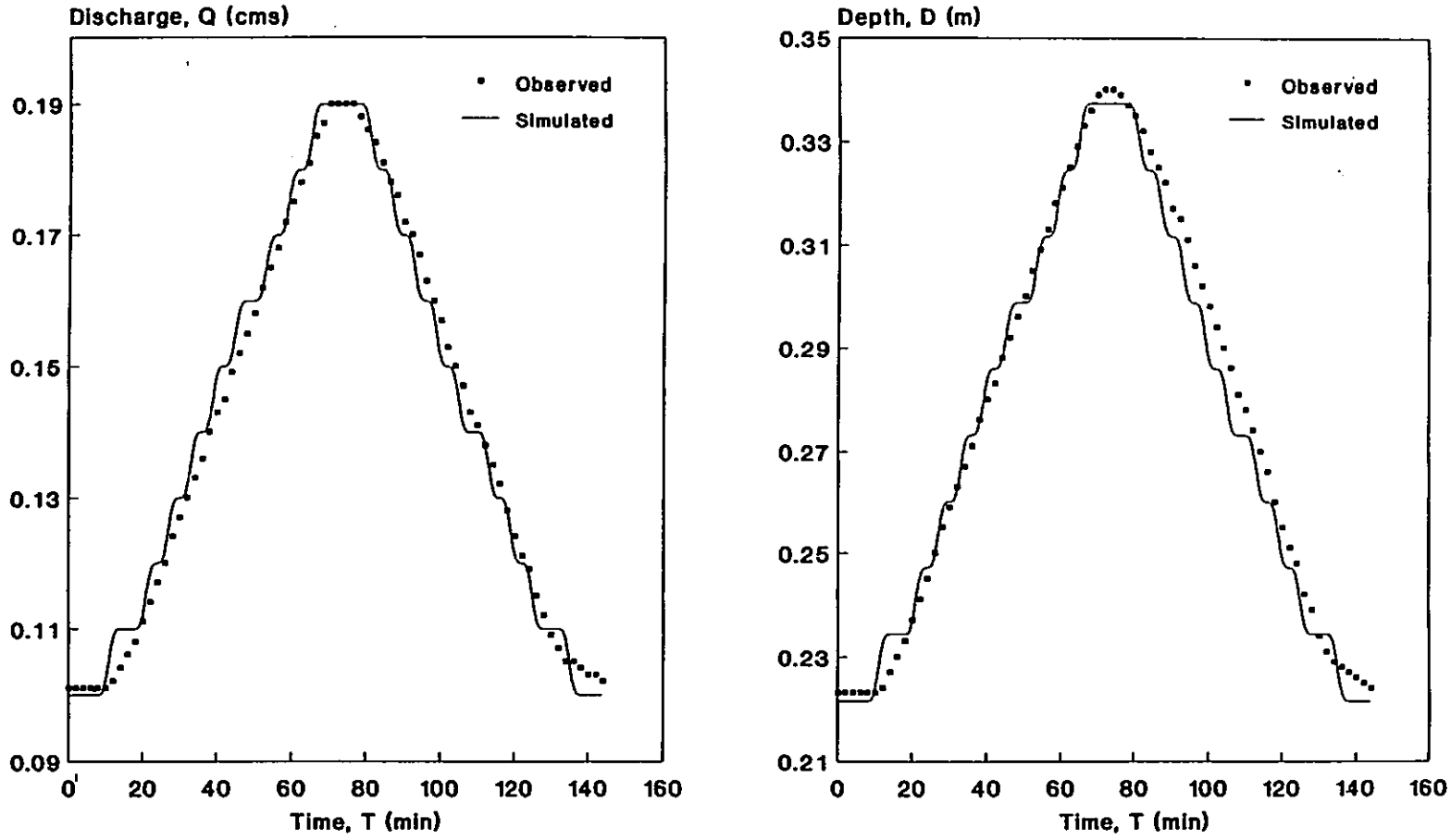

Figure 6.9 Simulated vs. Observed Discharge and Depth Hydrographs using EXTRAN, (Treske's data, case 4).

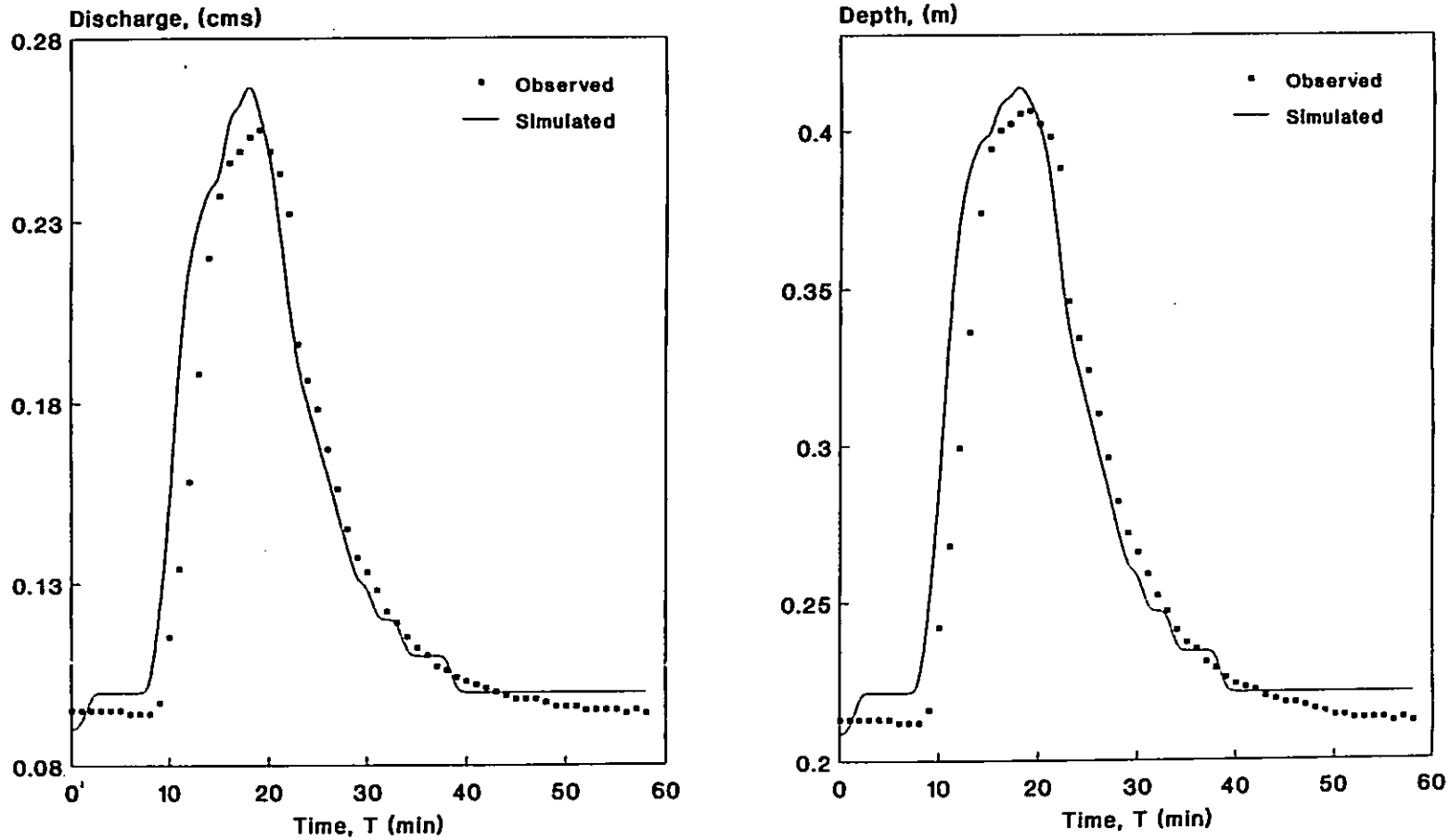

Figure 6.10 Simulated vs. Observed Discharge and Depth Hydrographs using EXTRAN, (Treske's data, case 5).

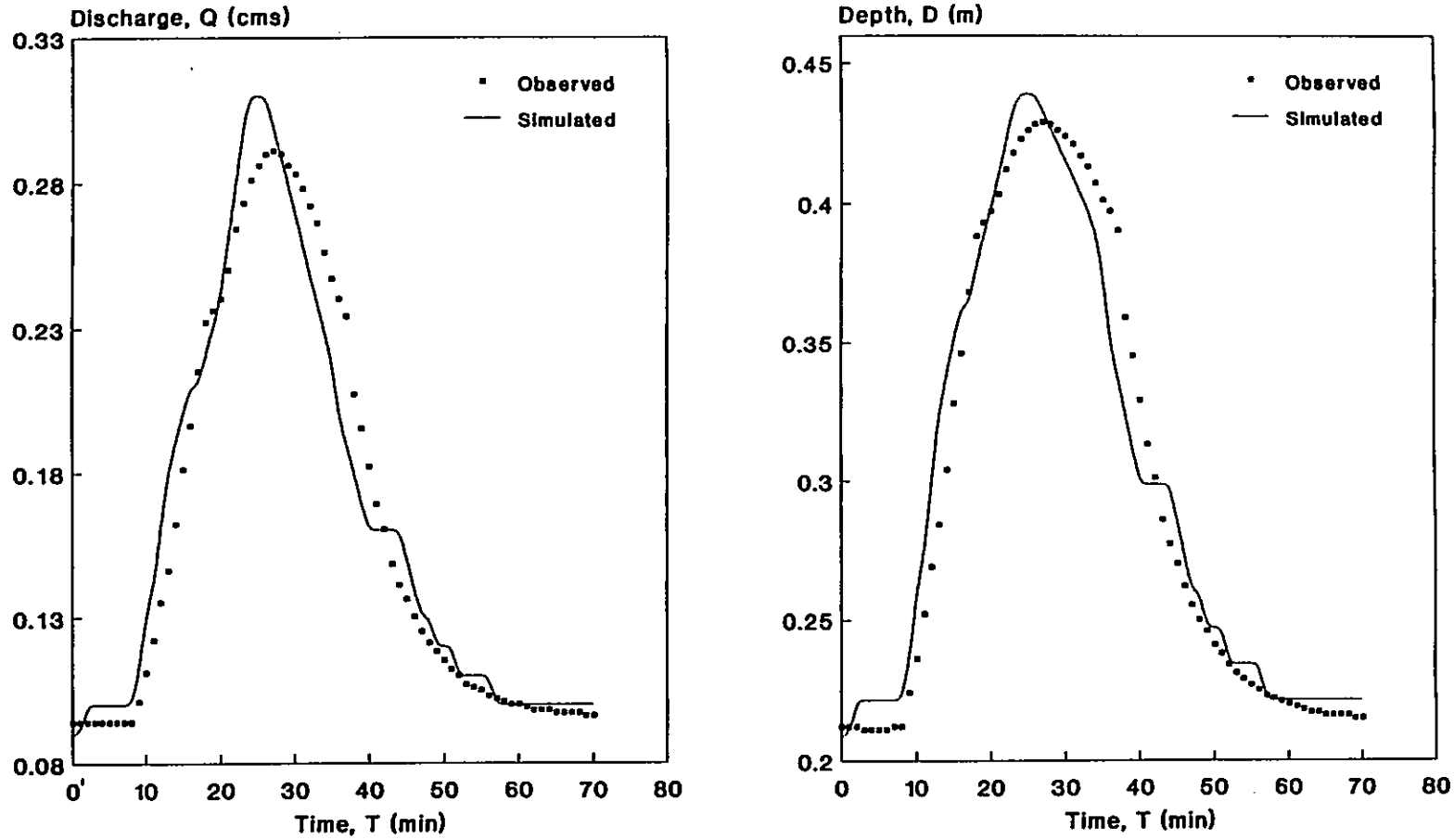

Figure 6.11 Simulated vs. Observed Discharge and Depth Hydrographs using EXTRAN, (Treske's data, case 6).

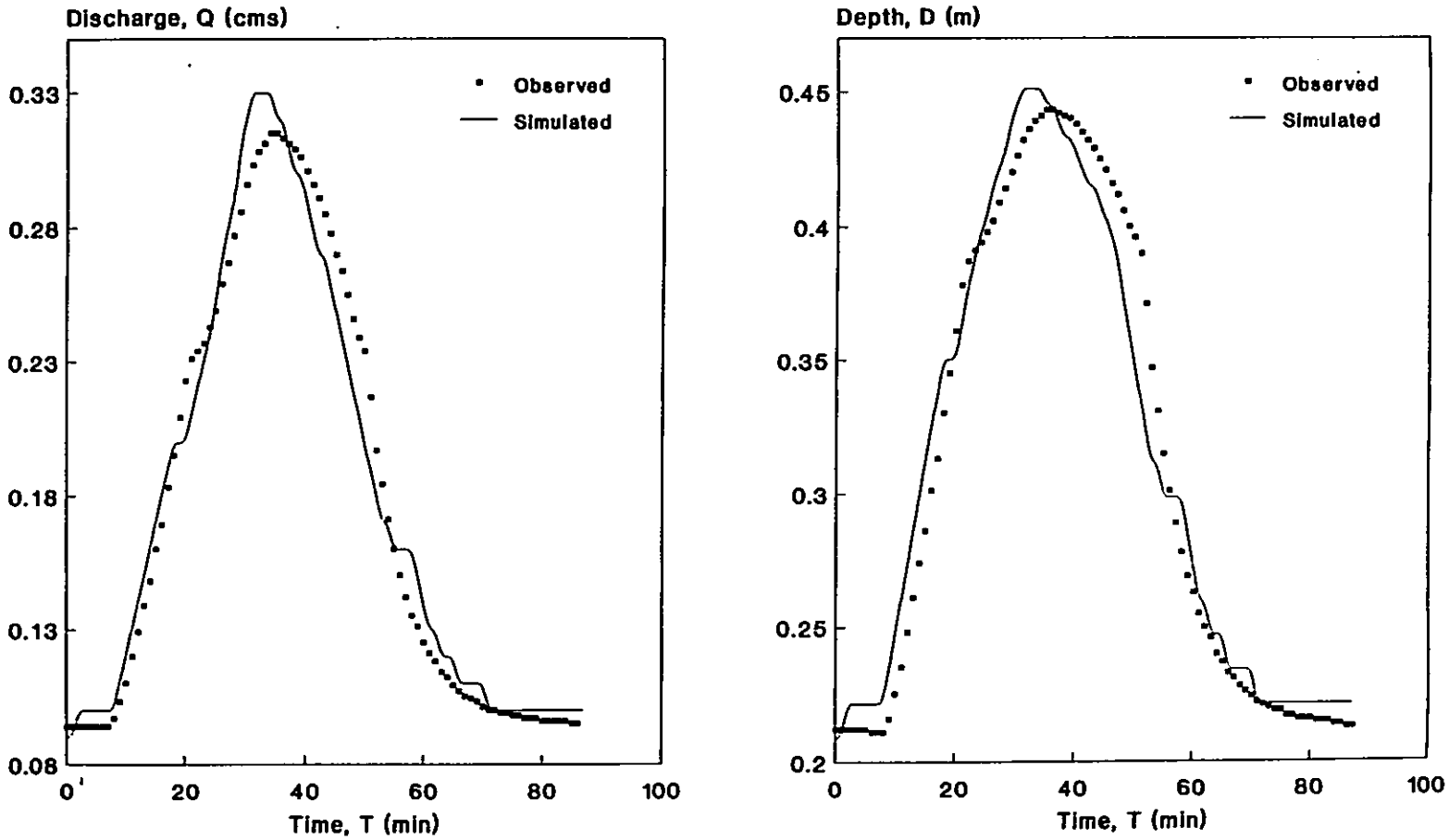

Figure 6.12 Simulated vs. Observed Discharge and Depth Hydrographs using EXTRAN, (Treske's data, case 7).

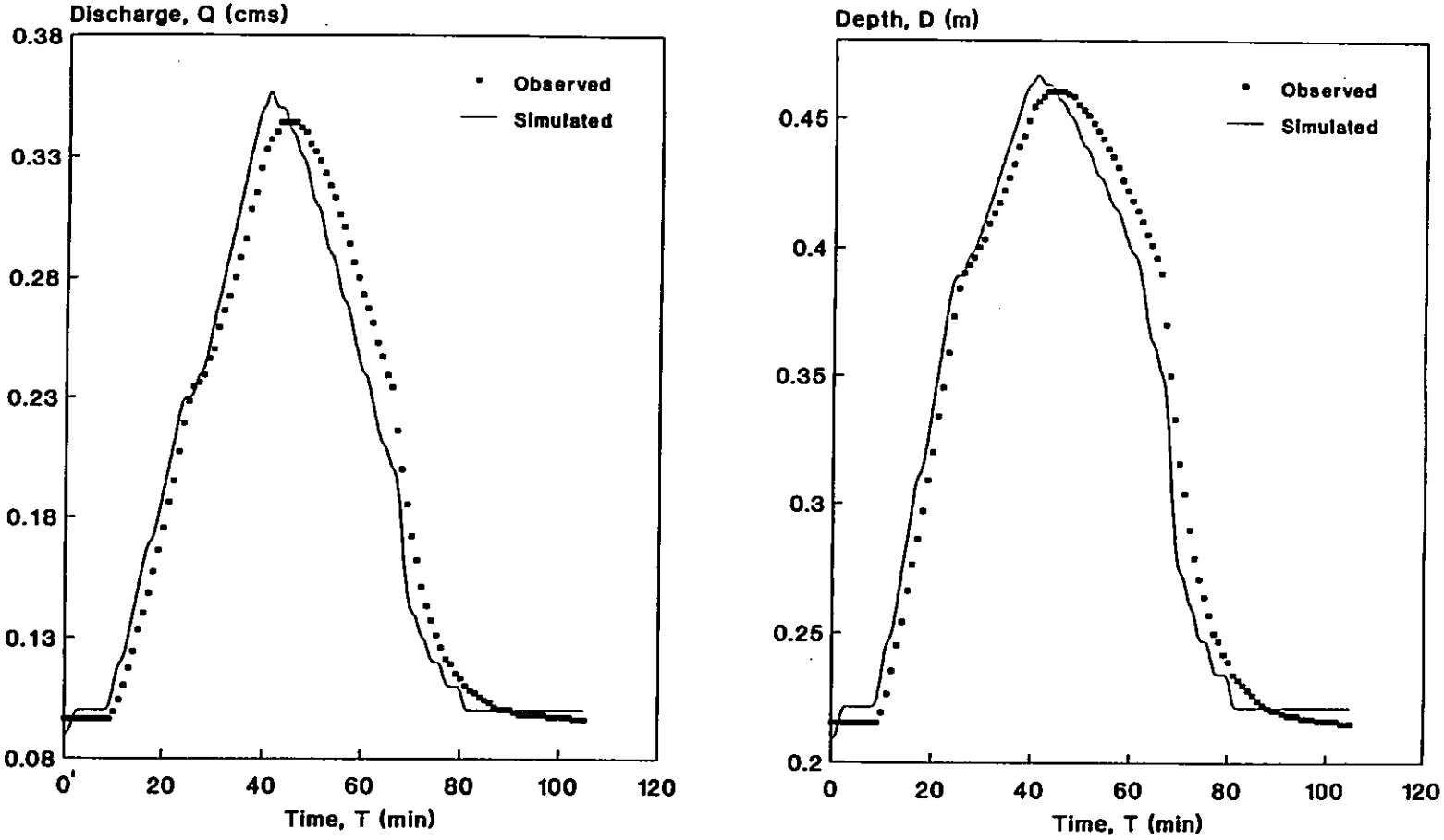

Figure 6.13 Simulated vs. Observed Discharge and Depth Hydrographs using EXTRAN, (Treske's data, case 8).

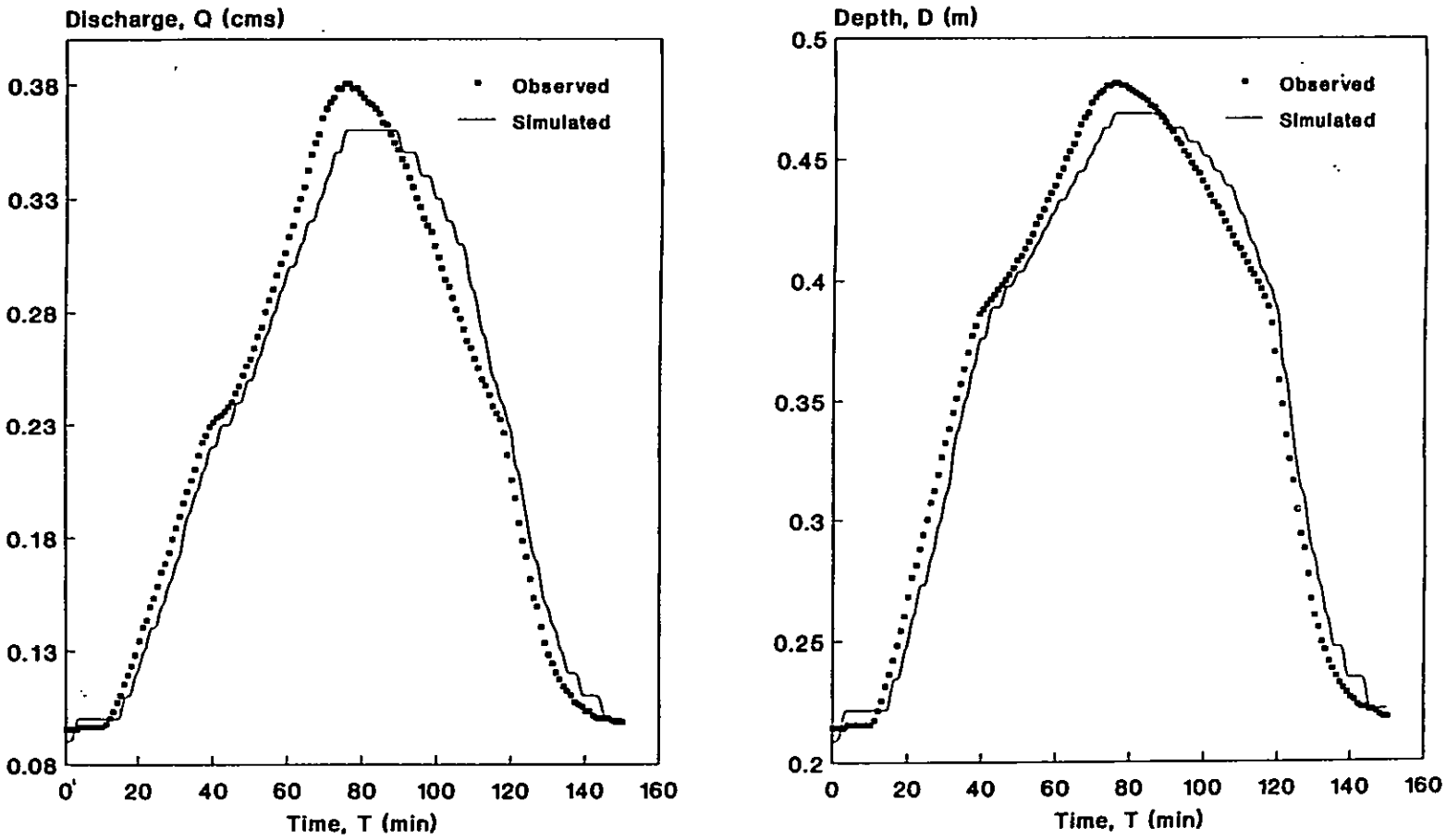

Figure 6.14 Simulated vs. Observed Discharge and Depth Hydrographs using EXTRAN, (Treske's data, case 9).

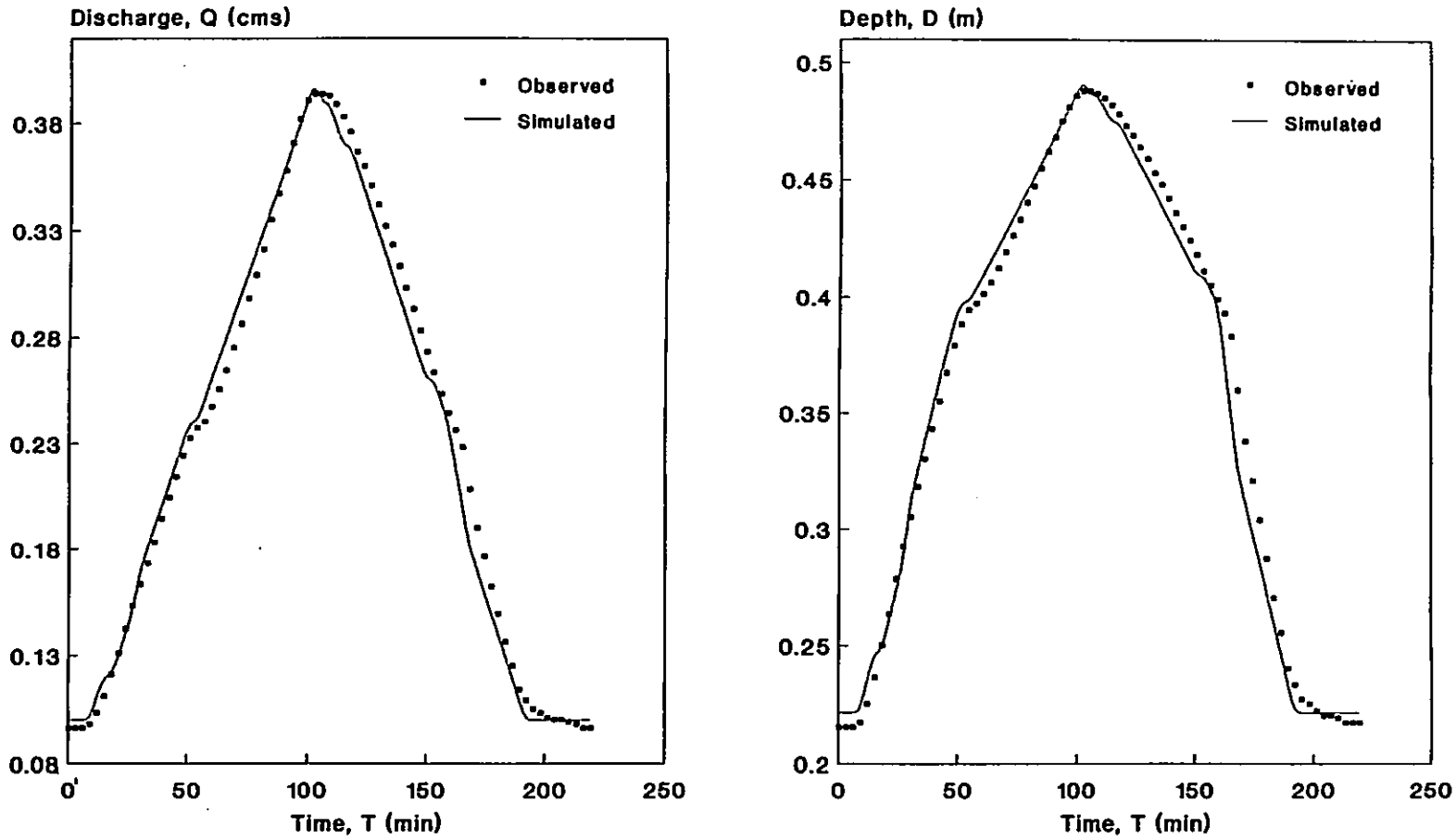

Figure 6.15 Simulated vs. Observed Discharge and Depth Hydrographs using EXTRAN, (Treske's data, case 10).

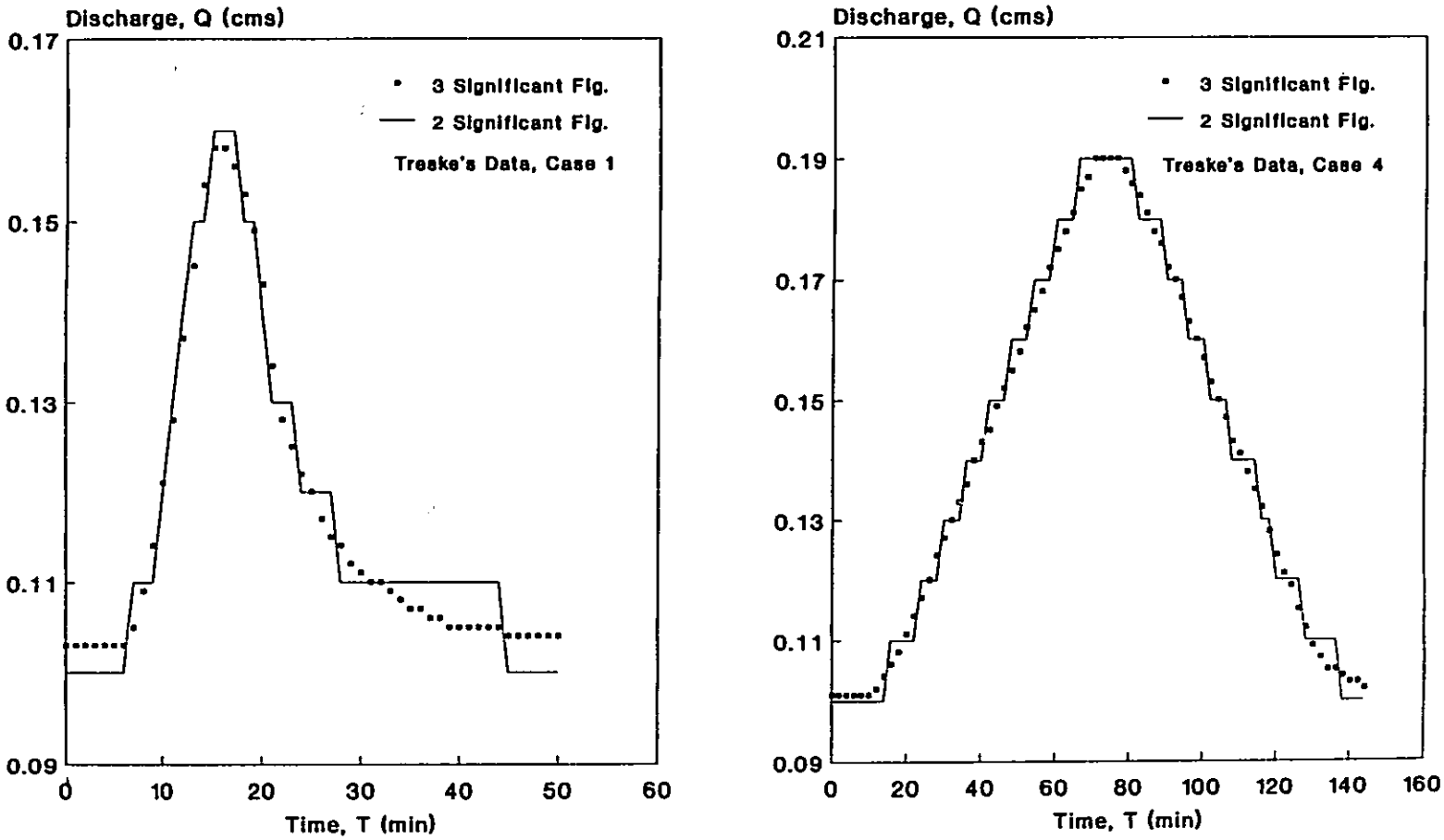

Figure 6.16 Effect of Rounding-Off Significant Figures on the Observed Hydrographs, (Treske's Data, Cases 1 & 4).

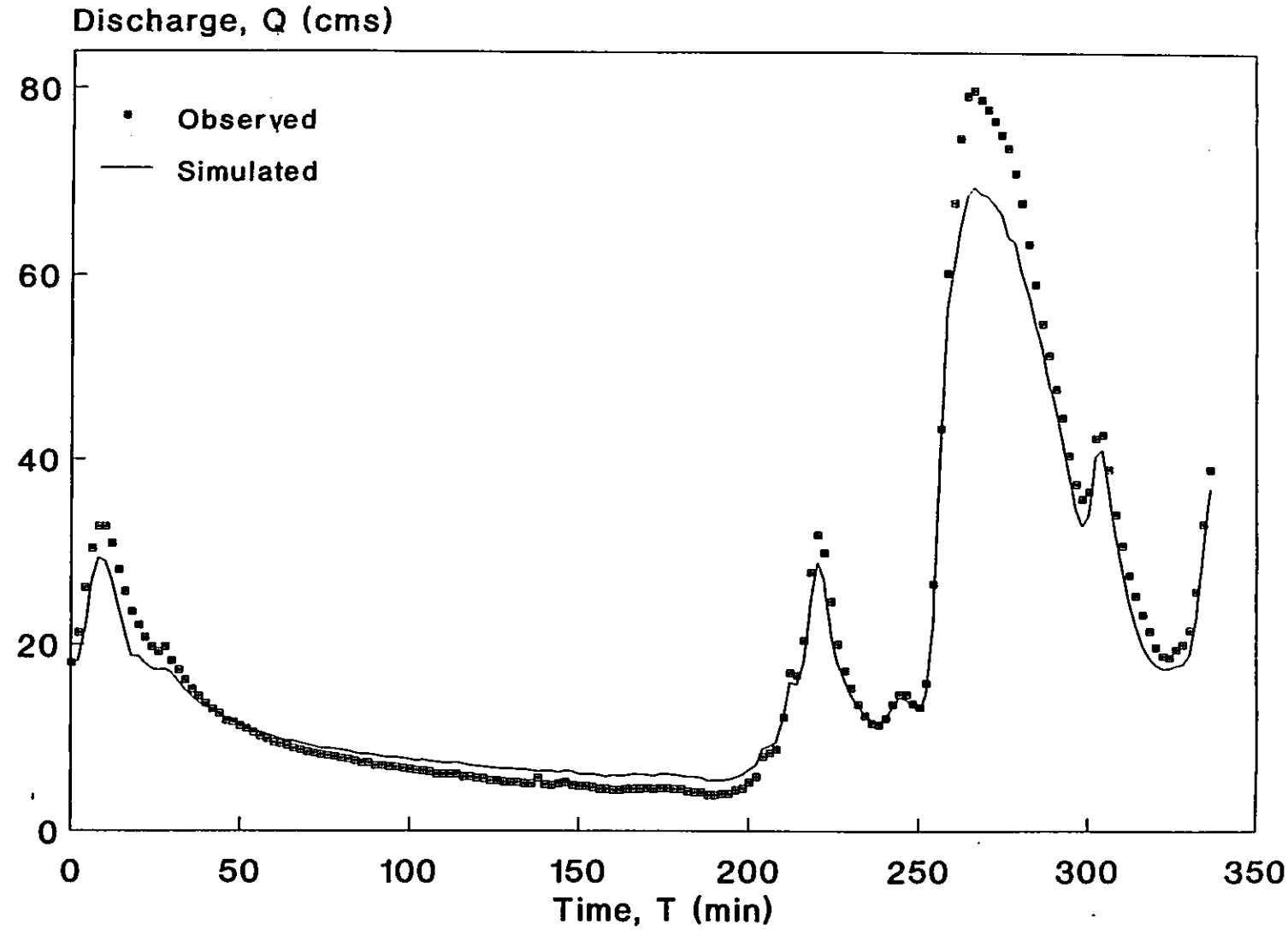

Figure 6.17 Simulated vs. Observed Discharge Hydrograph with EXTRAN Applied to Myers' Data Set.

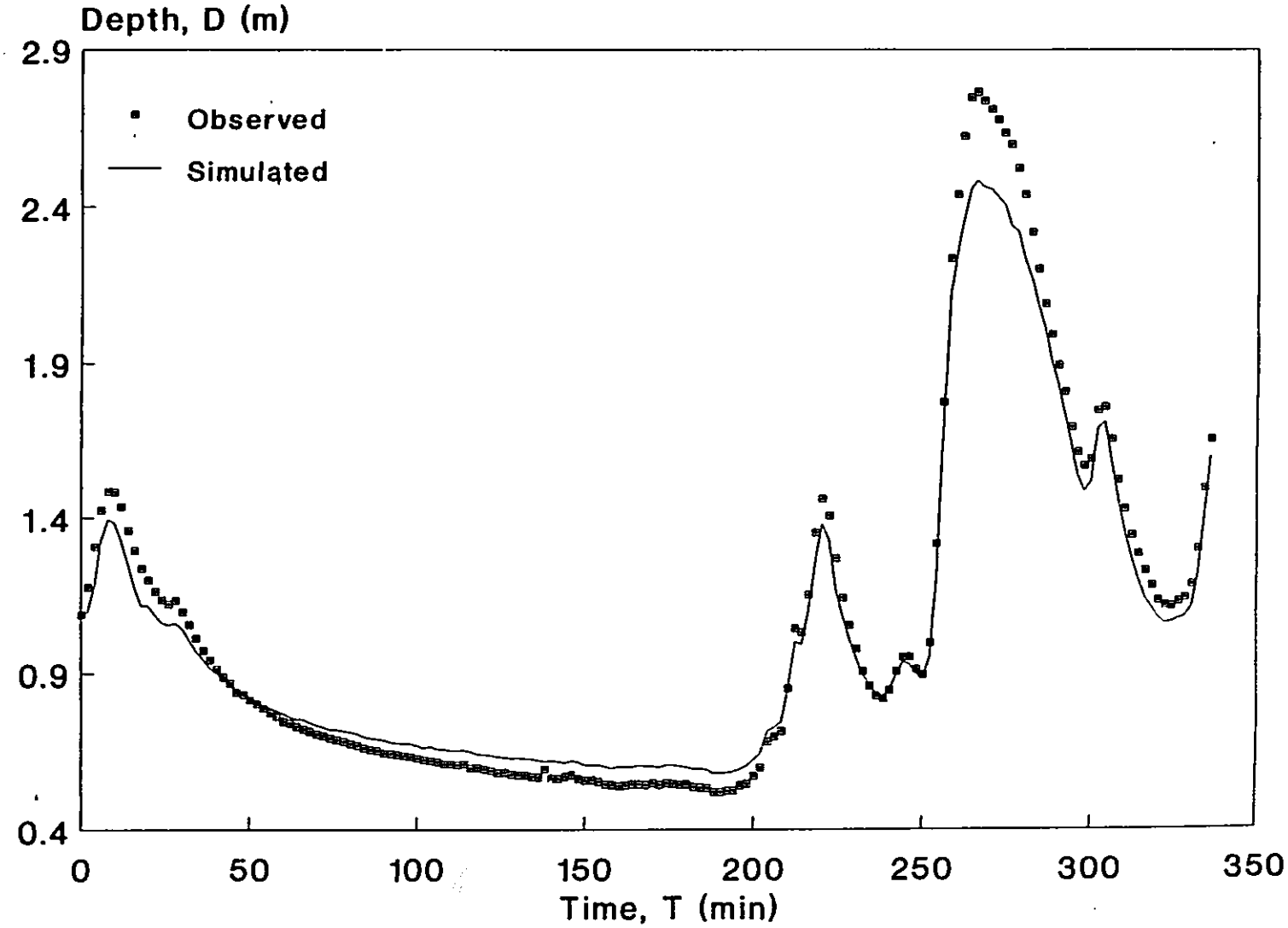

Figure 6.18 Simulated vs. Observed Depth Hydrograph with EXTRAN Applied to Myers' Data Set.

CHAPTER 7

APPLYING ONE-D TO DATA SETS

7.1 INTRODUCTION

ONE-D, or the one-dimensional hydrodynamic model, is a dynamic flow routing model that solves transient flow conditions in rivers and tidal estuaries. An important attribute of ONE-D is the fact that, unlike most other steady-state routing models, it can handle divided flows, (channels networks). The model, which was developed at the Massachusetts Institute of Technology (Harleman, 1974), is used by many North American agencies including the Water Planning Management Branch, Inland Water Directorate, Environment Canada.

ONE-D adopts an implicit finite-difference scheme to integrate the Saint Venant equations over a wide range of transient flows and conditions. It uses the Galerkan techniques of weighted residuals in solving the linearized Saint Venant equations. The model can be applied to simulate steady-state flows as well as transient conditions. ONE-D was successfully applied in several Canadian case studies (Fraser, Red, St.Croix Rivers) to

reproduce stage hydrographs within 0.061 meters (0.2 ft) accuracy over a daily tidal cycle and, at the same time, instantaneous discharges within 4 to 7 % accuracy of the measured flows. These figures were verified by Water Survey of Canada (WSC) using conventional and moving-boat discharge measurement techniques in the Port Mann to Mission section of the Fraser River. Using ONE-D, rectangular, circular, trapezoidal, as well as completely irregular channel geometry may be fully described. Like DWOPER and unlike EXTRAN, ONE-D permits the differentiation between areas that actively convey water and those off-channel storage areas that do not contribute to the channel flow. ONE-D can simulate rapids through the use of stage-discharge rating curves or stage-routing boundary conditions; however, the model is not able to simulate supercritical flow regimes.

ONE-D has been successfully applied to a wide variety of river networks. Applications include the Fraser River multi-channel and tidal reaches; (Sydor et al., 1989), the Truro River (including a very complex channel network system where channels are interconnected by dykes and culverts), the Red River (flood plain zones are inundated during spring run-off; (Morasse, 1985).

7.2 DATA PREPARATION PROGRAMS

As an input requirement to ONE-D, a river system is characterized by a network of reaches inter-connected by nodes. Each reach is represented by a group of cross-sections. Two FORTRAN computer programs: COORD1 and COORD2, were developed to fulfil this purpose. These programs generate the cross-sectional data used in Card Group B in the ONE-D input data file.

7.2.1 COORD1 PROGRAM

COORD1 is a FORTRAN program that uses the cross-sectional data in order to prepare a data set that will be further processed by COORD2. COORD1 has the ability to plot cross-sections of any reach to check visually the accuracy of the data prepared. The

program can deal with different reaches at the same time, resulting in a run-time reduction.

Coordinates should be used to define completely the geometry of the channel cross-section. Three coordinates are used per input cross-sectional data card, and repeated as many times as required to fully describe the cross-section (up to 300 coordinate points per cross-section). Separate scale factors are introduced to the program to compute coordinates in the vertical and horizontal directions. The origin can be defined at a convenient location satisfying the following restriction: within a reach, the relation between the origins of all cross-sections must be linear, forming the relative datum. This relative datum is referenced later to some standard datum, (figure 7.1).

Also, the values for the left- and right-bank slopes are input to the program. COORD1 sets the maximum bank height equal to 10 times the difference between the highest and lowest points of the cross-section. Therefore, the user has to do a schematizing process to define all the reaches, nodes, and cross-sectional data that will fully represent the actual geometry of the channel. Finally, an accuracy check is done by investigating the plots of the cross-sections to avoid any error in COORD2 input data.

2.7.2 COORD2 PROGRAM

COORD2 is a FORTRAN program used to determine the channel hydraulic parameters that are used in ONE-D input data. These parameters include area, wetted perimeter, top width, core top width, core area, total area, ...etc.

Similar to COORD1, COORD2 can handle several reaches at the same time. Vertical coordinates are referenced with respect to the standard datum. The output of COORD2 is used by ONE-D to generate tables of hydraulic parameters for cross-sections that are interpolated over a space increment Δx. These interpolated cross-sections, and not the actual, are used in the flow computation processes.

7.3 INITIAL CONDITIONS

Input to ONE-D should include the specification of the initial conditions of H and Q known at all computational points. In the absence of any knowledge of these conditions, some approximate values should be estimated. The accuracy of these conditions helps in reducing the computer time for each simulation. In routing unsteady flows, it is recommended to "lead-in" to the initial time of the transient study by a previous run based on a steady-state or a transient flow condition of shorter duration. This "lead-in" process will help in the correct estimation of the initial conditions and thus enhance the possibility of convergence.

For the case of Treske's data, 0.095 m^3/sec was used as the initial discharge value at the upstream and downstream stations of the channel. In addition, 0.212 m was specified as the initial water depth at both extremities of the channel.

7.4 BOUNDARY CONDITIONS

The initial and boundary conditions should be specified in the ONE-D input data to get a unique solution of the complete St. Venant equations. These conditions are input at each boundary of the channel. For sub-critical flow in ONE-D, the upstream and downstream boundary conditions could be either one of the following:

1- Time history specification of the discharge (discharge hydrograph),

2- Time history specification of the surface elevation (stage hydrograph),

3- Stage-routing boundary condition,

4- Specification of a relation between stage and discharge (a single-value or loop-rating curve).

Henderson (1966) shows that a loop-rating curve can be defined by the following equation, (figure 7.2):

$$Q = C_z A \left[R \left(S_o - \frac{\partial H}{\partial x} - \frac{V}{g}\frac{\partial V}{\partial x} - \frac{1}{g}\frac{\partial V}{\partial t}\right)\right]^{\frac{1}{2}} \qquad (7\text{-}1)$$

where:

C_z = the Chezy coefficient,

R = hydraulic radius of the cross-section under consideration,

S_o = channel bed slope,

t = time,

x = distance along the channel,

A = cross-sectional area,

H = water surface elevation referenced to a datum,

V = velocity of flow, and

g = gravitational acceleration.

The Chezy coefficient C_z, can be expressed in terms of Manning's roughness coefficient using the following relation:

$$C_z = \frac{R^{\frac{1}{6}}}{n} \qquad (7\text{-}2)$$

For the conditions of uniform flow in straight channels or for flood routing techniques, the terms $V\partial V/g\partial x$ and $\partial V/g\partial t$ are much smaller than 1 and so can be neglected due to their minimal effects. Therefore, eq. 7-1 reduces to:

$$Q = C_z A \left[R \left(S_o - \frac{\partial H}{\partial x}\right)\right]^{\frac{1}{2}} \qquad (7\text{-}3)$$

This equation defines the relationship between discharge and stage for a loop-rating curve, (figure 7.2). Several previous attempts were made to approximate the loop-rating curve by a single-value rating curve using a linearization technique. Gunaratnam and Perkins (1970) expanded the discharge in a Taylor series in time using an approximated line for the rating

curve as a basis for the expansion. They then derived a relationship to represent the variation of stage and discharge.

For the case of Treske's data set, a discharge hydrograph was used as the upstream boundary condition. Time increments were specified in seconds and flows in m^3/sec. Furthermore, a single-value rating curve was used to represent the downstream boundary condition. The related equations were obtained, based on linear regression analysis applied to Treske's flood event case 10. They define the depth-discharge (rating curve) variation for in-bank and over-bank flow fields as follows:

$$y = 1.287\ Q + 0.093\ , \quad for\ y < 0.39\ m\ , \ and$$
$$y = 0.593\ Q + 0.255\ , \quad for\ y > 0.39\ m. \qquad (7\text{-}4)$$

7.5 ACCURACY OF INITIAL CONDITION ESTIMATION

Initial conditions (H and Q) should be specified at every computational station at time t = 0. In the absence of such detailed knowledge approximate values should be used. Convergence depends on the initial condition approximation. The better the initial condition approximation the sooner convergence is obtained, with a corresponding saving in computer time. It is usually advisable to start the transient run based on steady-state initial conditions. Examining the simulated hydrographs would indicate that ONE-D was not truly steady state at start up. Therefore, it retained flow in storage at the beginning of the run. This is noted in the depth increase within the first few minutes of the depth hydrograph.

7.6 DETAILED REPRESENTATION OF INFLOW HYDROGRAPH

Based on discussions with personnel of the Inland Water Directorate (Environment Canada), the inflow hydrograph can be represented by only a few points rather than inputing all the observed points. In this case, a third degree parabolic interpolating function should be used. A data file for Treske's data case 1 (lowest in-bank flow depth) was prepared by inputting only five points out of fifty measured time increments to represent

the inflow hydrograph, with a third degree parabolic interpolating function. Good simulations were obtained, (figure 7.3). However, this raises the issue of checking this phenomenon, i.e. the effect of the detailed representation of the inflow hydrograph on the simulated downstream hydrograph with a different type of interpolating function. Observed data was measured on a 1-minute basis. However, several time increments were used to define the inflow hydrograph at the upstream boundary. In this instance, half the number of points were input for the inflow hydrograph of Treske's data case 3. In this context a linear interpolating function was selected to interpolate between inflows. Then, an evaluation was made based on accuracy requirements and goodness-of-fit techniques for the simulated hydrographs using a linear interpolating function with the two cases of defining the inflow hydrograph (half and all number of coordinates), (figures 7.4 and 7.5). It was concluded that linear interpolating functions are recommended when the inflow hydrograph is fully described with an ample number of coordinates. In other cases, it would be preferable to use a third degree parabolic interpolation function.

7.7 MODEL INPUT DATA

Data was input to ONE-D in the following manner: Treske's straight prismatic channel was divided into 22 sub-reaches with 10 meters as an initial estimate of the mesh spacing in the reach. Then a final value of 9.16 m was computed by the program to ensure the total length is divided into equal increments. No modification to the channel or channel data was introduced, except for a minor change in Manning's n (0.0116) as a result of model calibration. An initial flow of 0.095 m^3/sec was selected and an initial depth of 0.212 m was adopted in this instance. These values represent the uniform steady flow conditions prior to the onset of the flood wave.

Being an implicit finite difference model, ONE-D does not exhibit a strict limitation on the time step size. The time step is selected based on an accuracy requirement rather than stability requirements (Courant Criteria). The computational time step was reduced to 10 sec to allow the model to follow more precisely the inflow hydrograph and predict more

accurately the output. Several options were available to interpolate the inflow. These included:

- Linear interpolation of variable boundary condition data,
- Cosine interpolation of variable boundary condition data, and
- Parabolic interpolation using a third degree parabolic interpolation procedure.

However, compared to other options, the third degree parabolic interpolation option gave the best results.

7.8 MODEL CALIBRATION

For Treske's data set the Manning's roughness coefficient n was 0.012. This n-value produced relatively good simulations when applied to model the different flood events using ONE-D. However, a model calibration was performed in an attempt to further improve the simulations. The model was calibrated for flood event case 10 and an optimum n-value of 0.01165 was obtained. This n-value was slightly less than the given value; however, it resulted in improved simulations. Figures 7.6 to 7.9 show the ONE-D simulations to in-bank flow depths in Treske's simple rectangular channel.

7.9 OFF-CHANNEL STORAGE AREAS

Like DWOPER and unlike EXTRAN, ONE-D has the ability to distinguish between off-channel storage areas or flood plain flow fields and the main channel flow area. The cross-sectional geometry is defined in the following manner:

- The water surface elevation entry I for cross-section J in reach K, where I ranges from 1 to the number of entries in elevation tables of geometric parameters,

- Total top width for entry I,

- Core width for entry I,

- Core area for entry I,

- Wetted perimeter of core area for entry I, and

- Total cross-sectional area for entry I (core and storage).

The aforementioned parameters should be repeated for every cross-section in the reach.

For Treske's case 5 data, two different options were used to define the off-channel storage areas in the ONE-D input data file. The first option, which involved the application diagonal interface planes , did not produce a good match between observed and simulated hydrographs, (figure 7.10). The diagonal interface planes were defined based on the equation derived while applying DWOPER to Treske's data set, (eq. 5-14). This particular form of interface planes was not as successful as when applied in the DWOPER application. This can be explained by the fact that the two models (DWOPER and ONE-D) have different representation of the off-channel storage areas in the momentum equation. In general, some modifications would suit some models but would fail to apply to others. An example is the fact that an n-value of 0.01165 successfully predicted the downstream stage and discharge hydrographs. However, because of the DWOPER formulation, an equation was derived for Manning's n to account and compensate for the under-estimation of the wetted perimeter. Moreover, a different n-value was used to obtain successful runs using EXTRAN.

The other option for defining storage areas as input to ONE-D involved the application of vertical interface planes. The corresponding simulated depths and discharges were deemed satisfactory, see figures 7.11 to 7.16. Thus, viewing the flood plain zones as purely "storage" did not introduce significant errors in the modelling exercise.

7.10 MYERS' DATA SET

Previously, ONE-D was applied to a prismatic, straight, laboratory channel data set, (Treske, 1980). In this section, discussion will centre on the application of ONE-D to a non-prismatic, natural channel data set (Myers, 1991).

7.10.1 COORD Programs

COORD1 and COORD2 were applied to determine the channel hydraulic parameters to be used in the ONE-D input file. These parameters include area, wetted perimeter, total top width, core top width, core area, total area, ...etc. The channel was considered as a single reach with stations located at the upstream, midway, and downstream extremities of the reach. For each cross-section coordinates were input as station and elevation relative to a certain datum (bed of the channel). Eight contours (points of inflection) were needed to define each cross-sectional geometry, with three points input per data line, and fifteen data entries (elevations) selected in this instance. Manning's n was input at the maximum and minimum water levels based on figure 5.56. The two Fortran programs were run, and a file was ready for use in ONE-D input data file.

7.10.2 Initial and Boundary Conditions

Input to ONE-D should include the specification of the initial conditions of H and Q at all computational points. These values can be approximated in the absence of precise (known) values. Another option involves getting the initial conditions from a steady-state run of ONE-D before the onset of the flood. A value of 16.70 m^3/s was input as the initial discharge at the upstream, midway, and downstream extremities of the channel. Also, 3.48 m, 2.28 m, and 1.09 m were specified as the respective initial water surface elevations at these three stations.

At the upstream station, a discharge hydrograph was the boundary condition, where

time increments were input in seconds and flow rates in m^3/s. A single value rating curve was used as the downstream boundary condition, (refer to section 5.8.2 for equations representing the rating curve).

7.10.3 Model Input Data

Data was input to ONE-D in the following manner: Myers' non-prismatic reach was divided into 10 sub-reaches, with 80 m as an initial estimate of the mesh spacing in the reach. No major modification to the channel or channel data was introduced except for Manning's roughness coefficient as a result of model calibration. An initial flow of 16.70 m^3/s was input and an initial water depth of 1.085 m was adopted in this instance. These values represent the uniform steady flow conditions prior to the onset of the flood.

Being an implicit model that uses Galerkan techniques of weighted residuals in solving the linearized St. Venant equations, ONE-D does not have a strict limitation on the time step size. Based on the Courant criteria, a time step of 60 sec can be used in this instance. However, the ONE-D manual allows selecting the time step up to 15 times the allowable. In this exercise a time step of 5 minutes was adopted. The selection of the time step size is arbitrary as long as accuracy of simulated hydrographs is not compromised. A linear interpolating function was selected to interpolate the inflow. Finally, storage areas were defined in ONE-D input using vertical interface planes. This was done automatically using the COORD2 program by specifying the distances to the left and right edges of the conveyance area measured from the origin of axis, (figure 7.17).

7.10.4 Model Calibration

In general, model simulations are often very sensitive to variations in Manning's n. Based on the discussion in section 5.8.5, Myers' bank-full n-value might be considered high. A model calibration was performed for a part of the observed hydrograph to reproduce measured observations of both stage and discharge. The n-value obtained by this

calibration was then adopted in data input to ONE-D. In general, good simulation results were obtained and an optimum value of 0.03 was obtained. Figures 7.18 and 7.19 present the simulated discharge and depth hydrographs resulting from the application of ONE-D to Myers' data set.

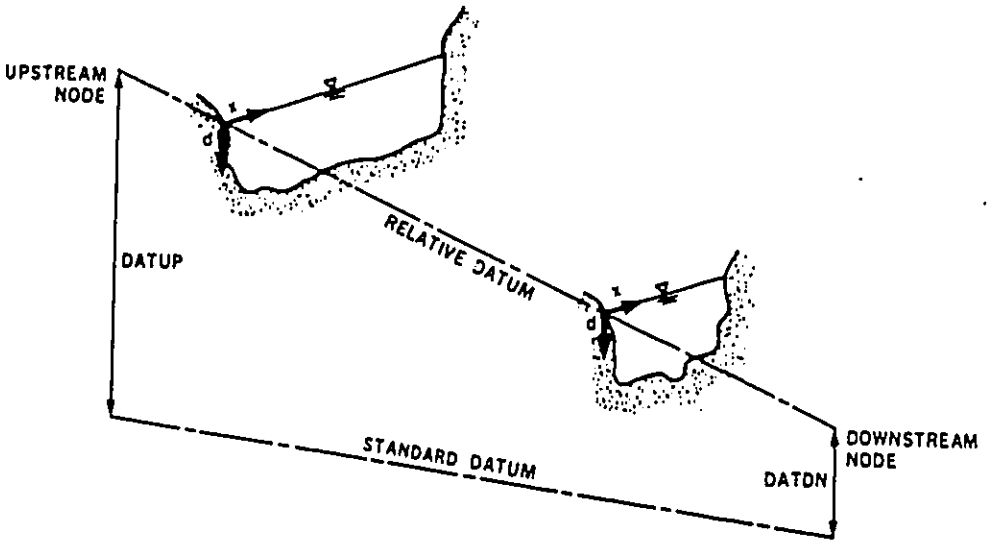

Figure 7.1 Definition Sketch of a Reach with the Corresponding Datums and Origins.

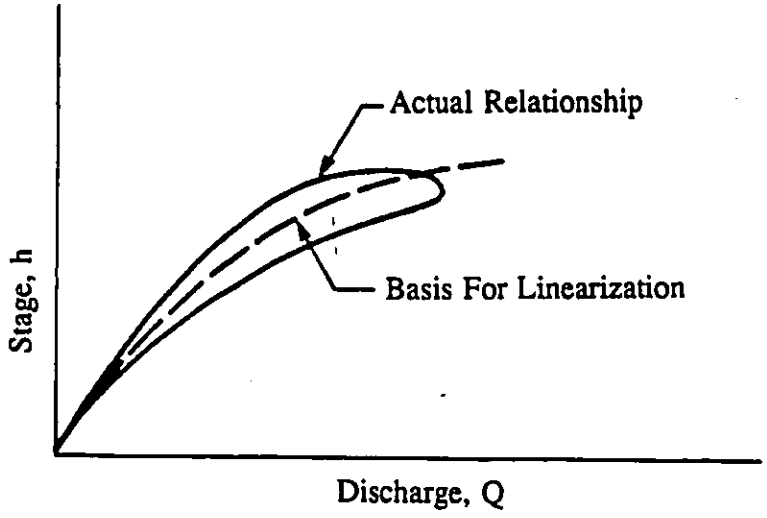

Figure 7.2 Definition Sketch of a Stage-Discharge Loop Rating Curve.

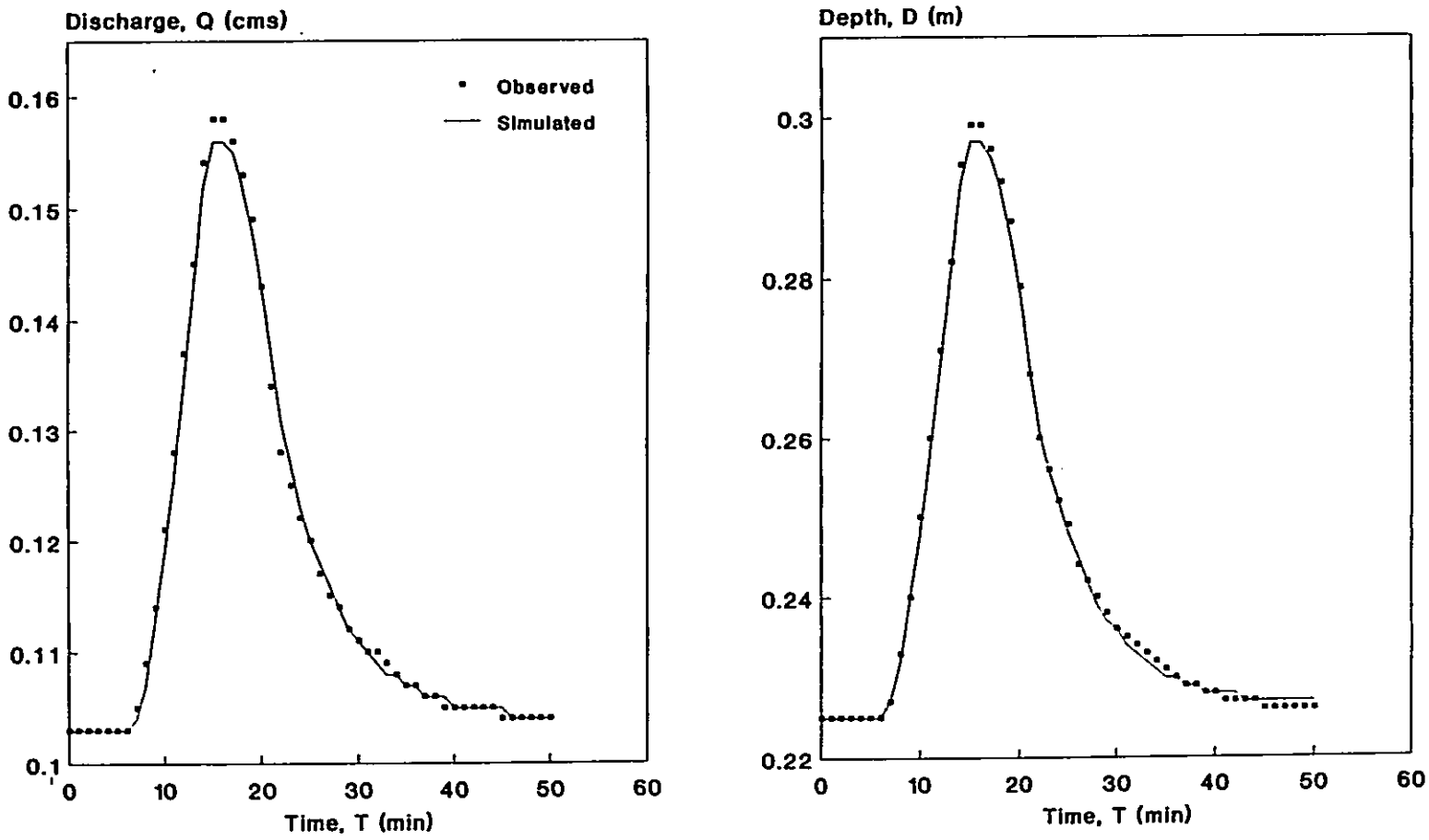

Figure 7.3 Simulated vs. Observed Discharge and Depth Hydrographs Using Third-Degree Parabolic Interpolation Function in ONE-D, (Treske's Data, Case 1)

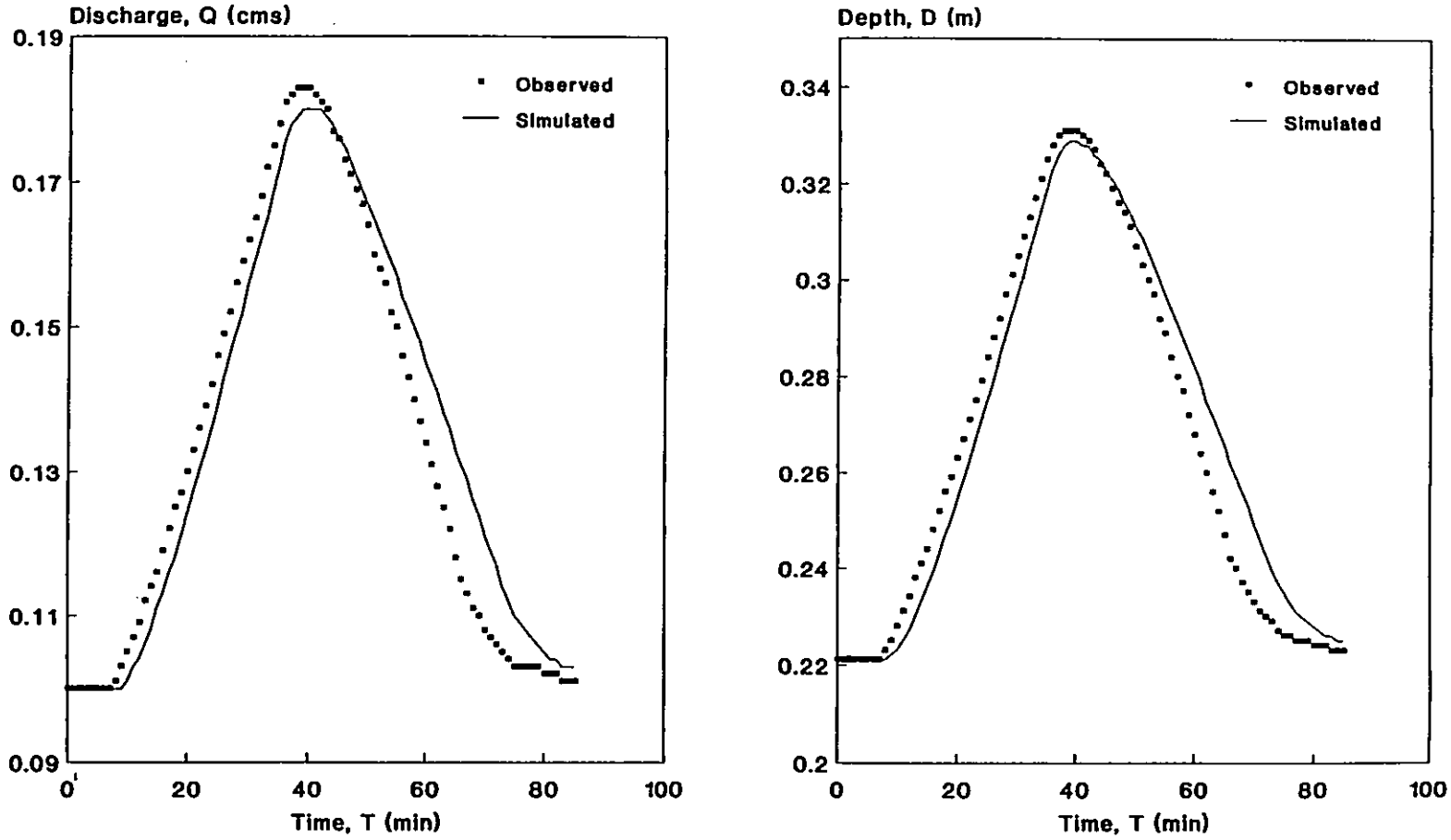

Figure 7.4 Simulated vs. Observed Discharge and Depth Hydrographs Using a Non-Detailed Representation of Inflow Hydrograph in ONE-D, (Treske's Data, Case 3)

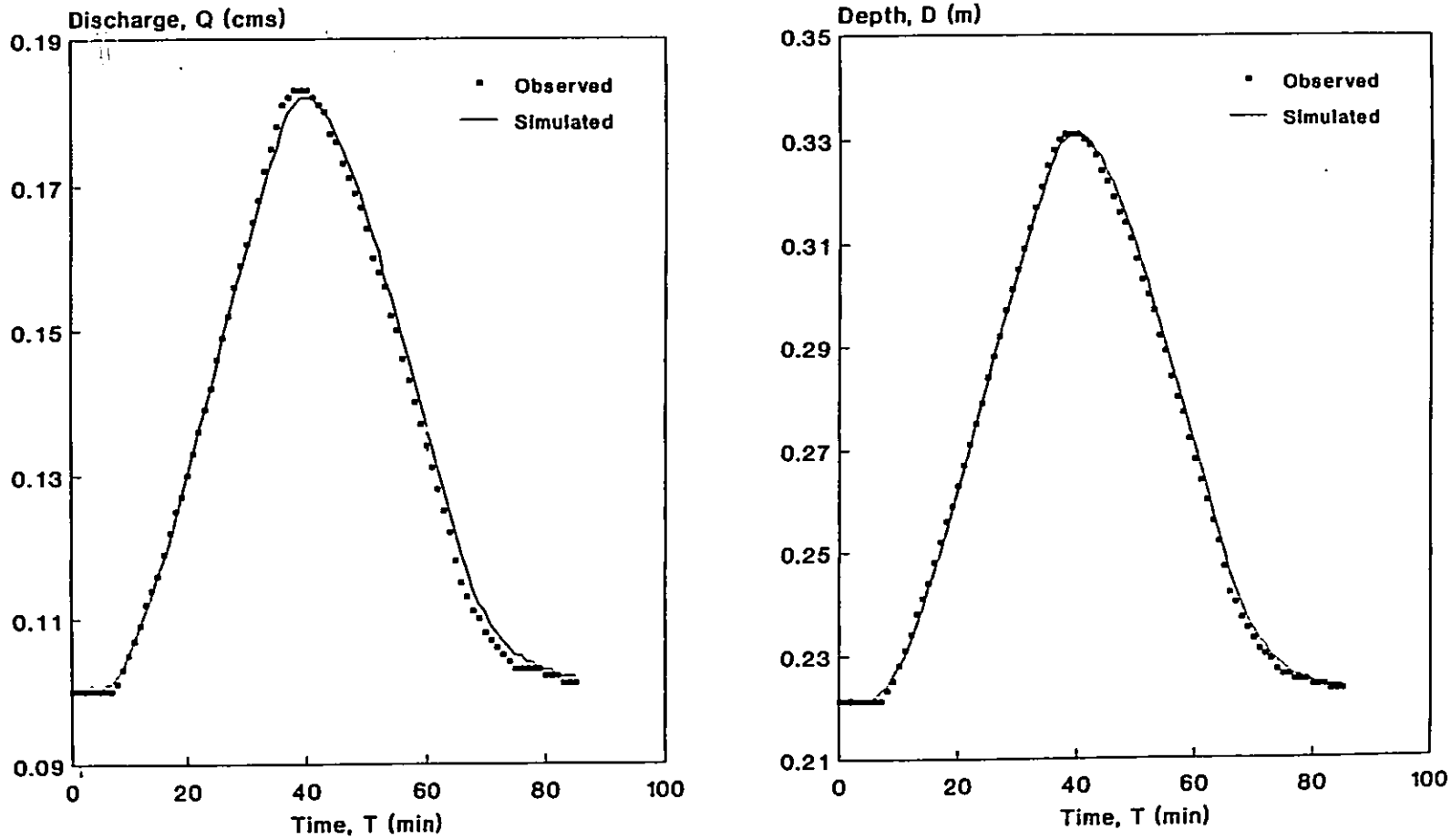

Figure 7.5 Simulated vs. Observed Discharge and Depth Hydrographs Using a Detailed Representation of Inflow Hydrograph in ONE-D, (Treske's Data, Case 3)

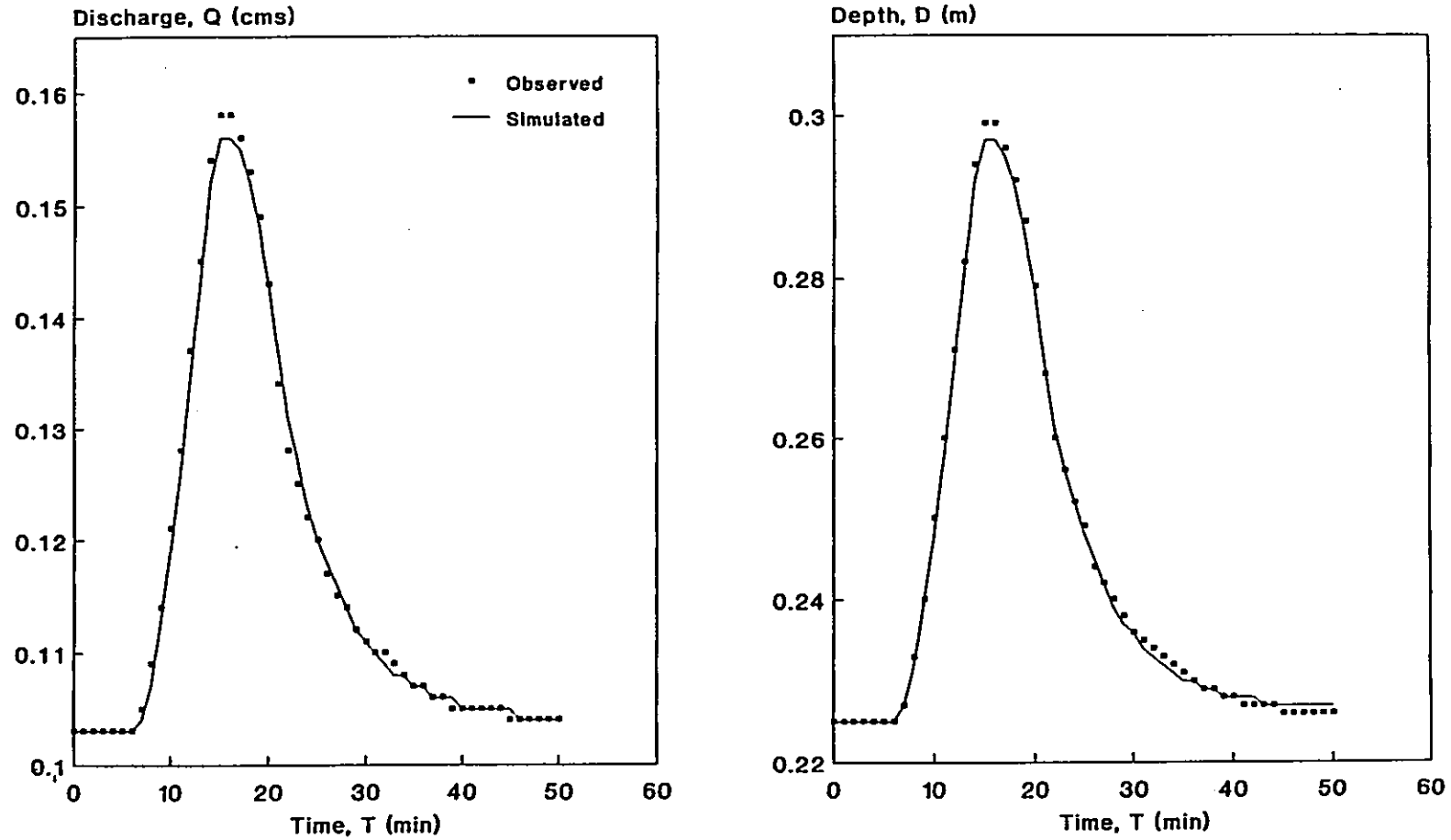

Figure 7.6 Simulated vs. Observed Discharge and Depth Hydrographs using ONE-D, (Treske's data, case 1).

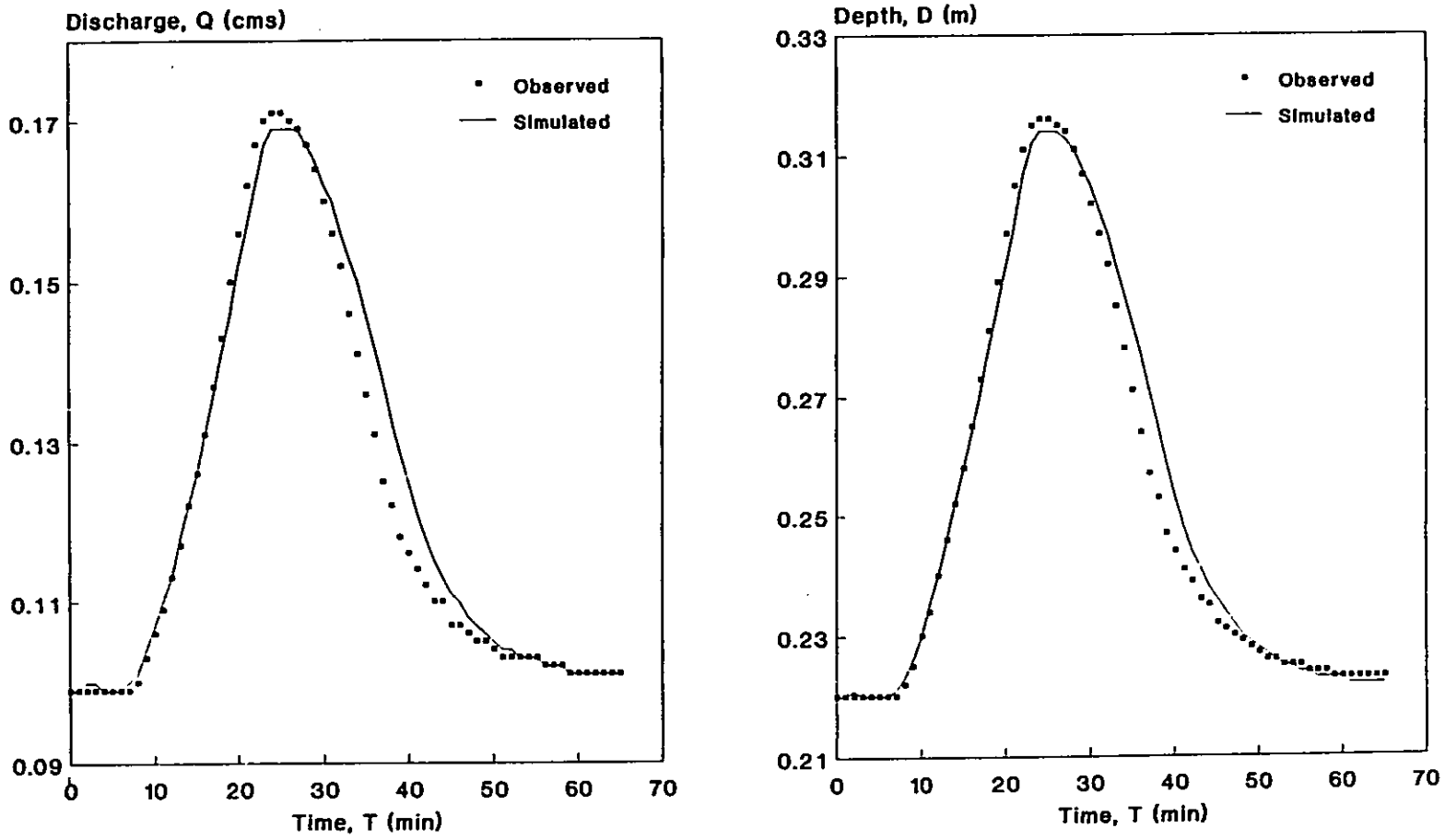

Figure 7.7 Simulated vs. Observed Discharge and Depth Hydrographs using ONE-D, (Treske's data, case 2).

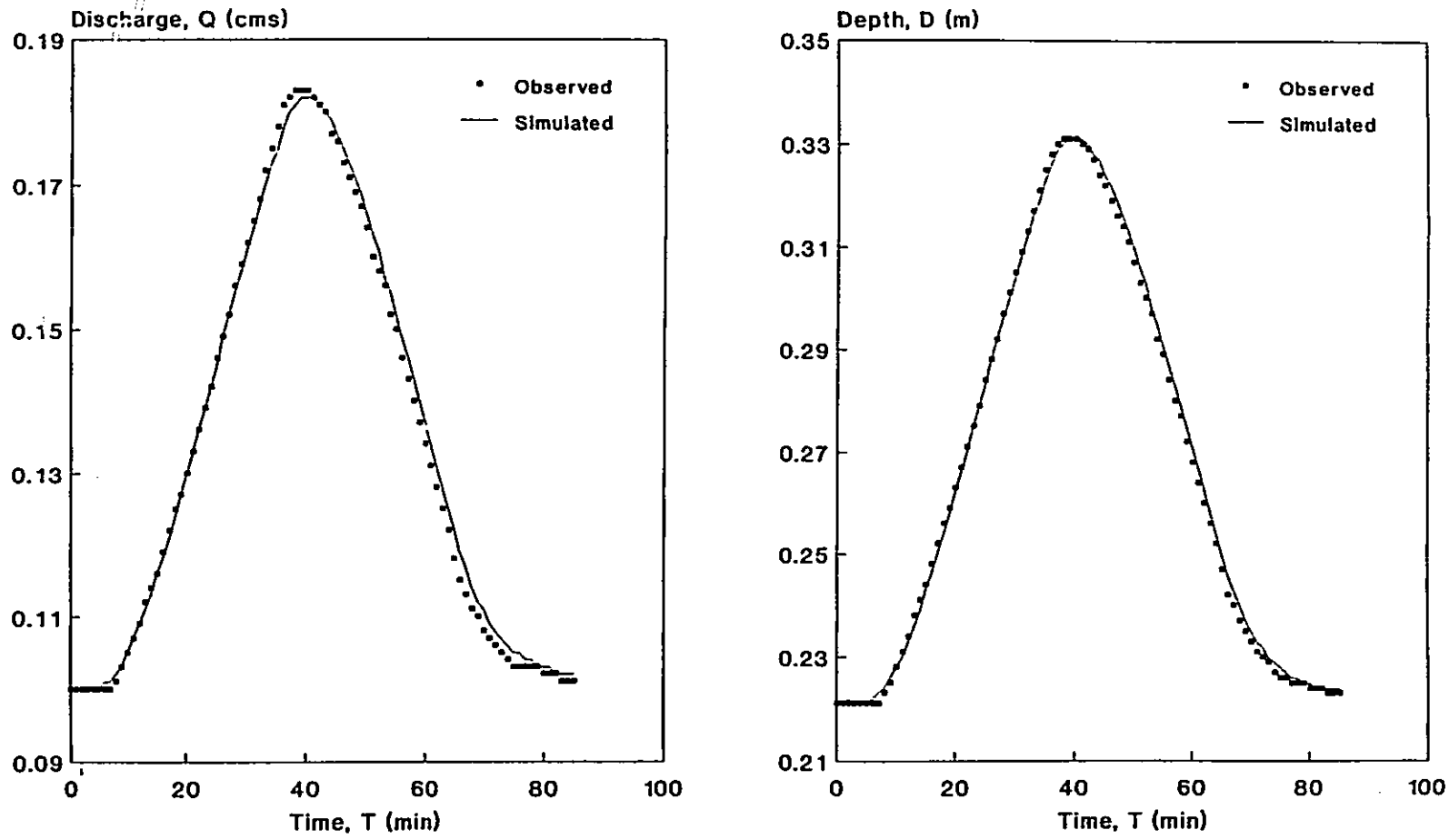

Figure 7.8 Simulated vs. Observed Discharge and Depth Hydrographs using ONE-D, (Treske's data, case 3).

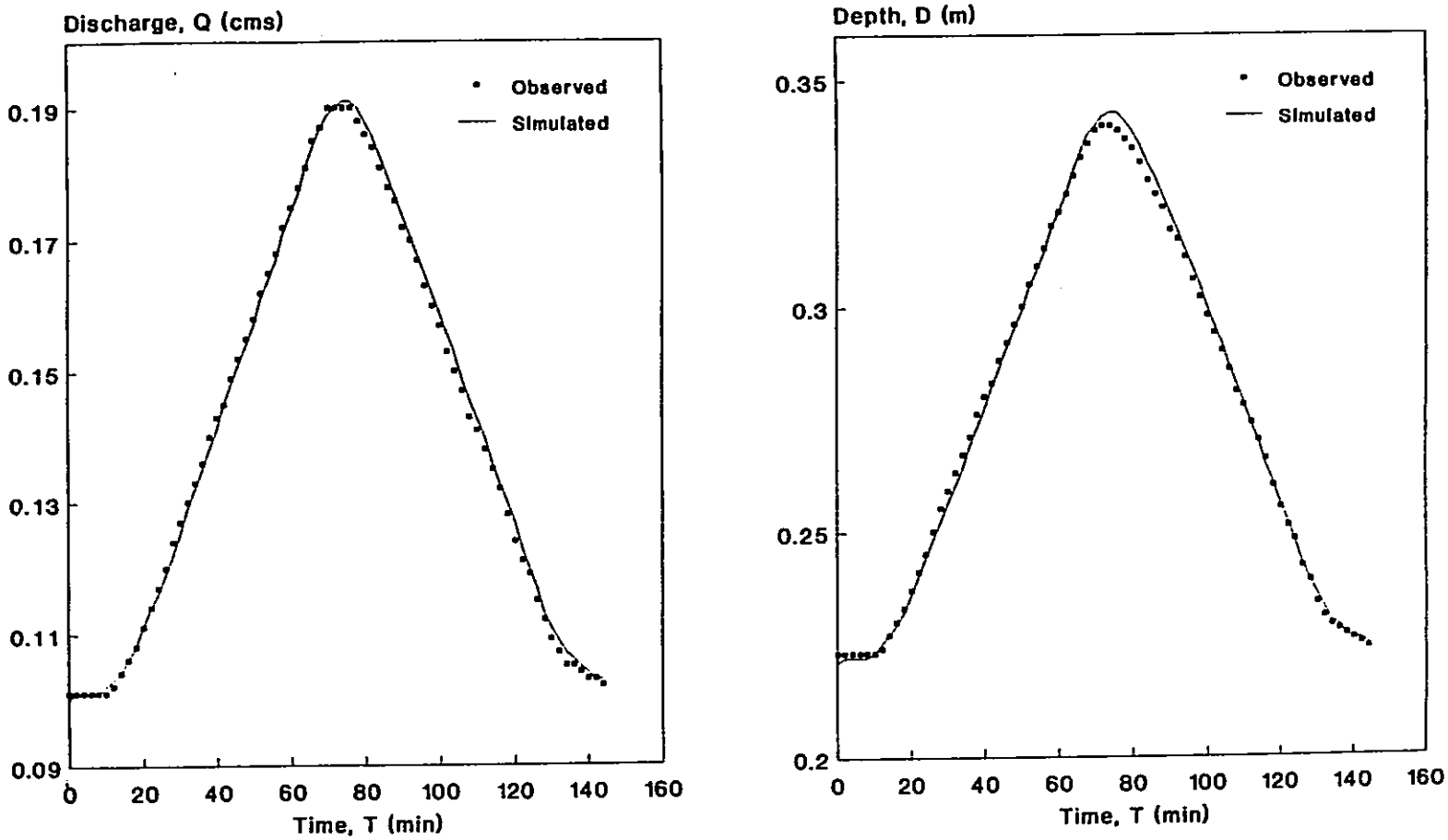

Figure 7.9 Simulated vs. Observed Discharge and Depth Hydrographs using ONE-D, (Treske's data, case 4).

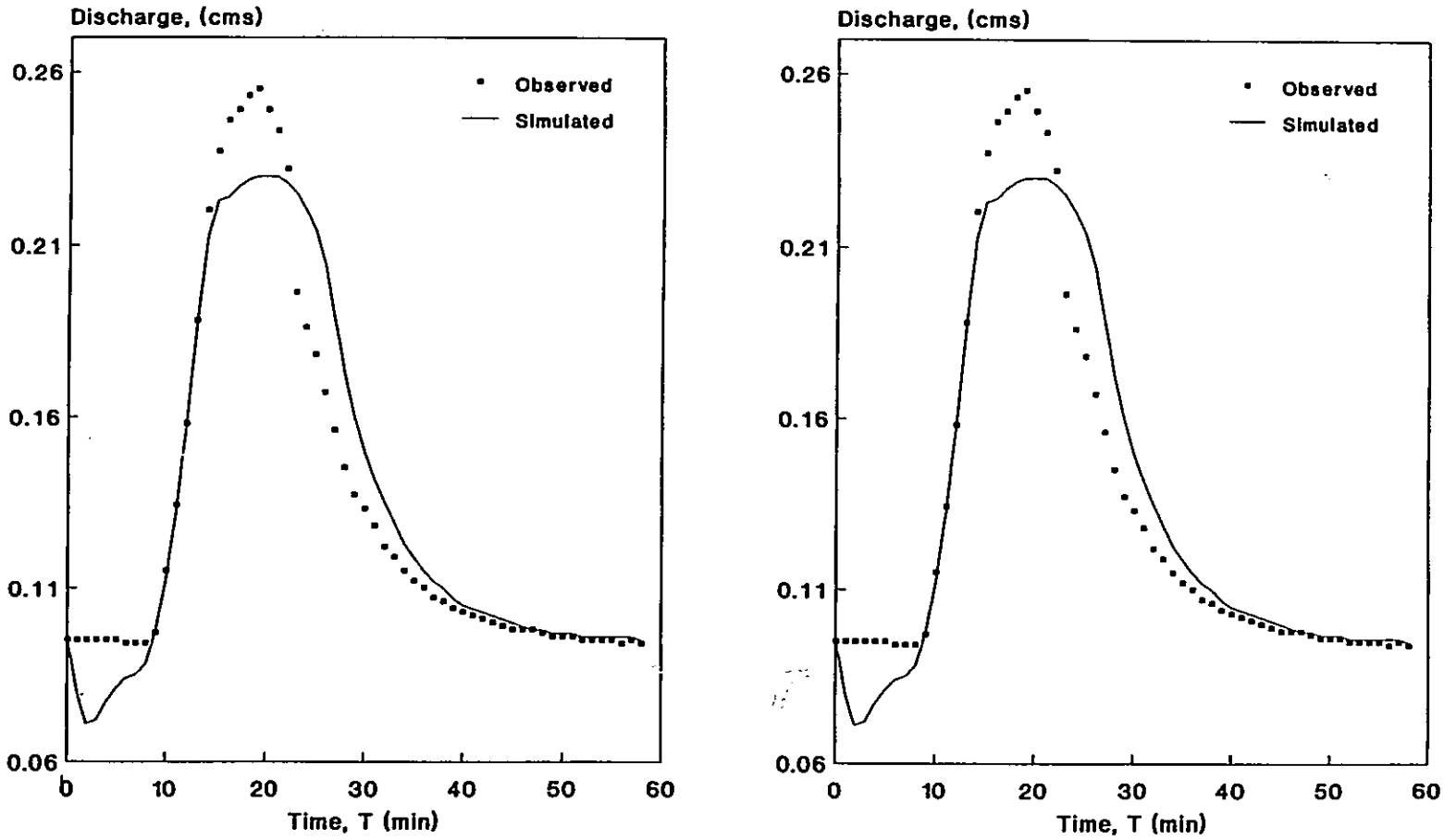

Figure 7.10 Simulated vs. Observed Discharge and Depth Hydrographs with Diagonal Interface Planes Applied to ONE-D, (Treske's data, case 5).

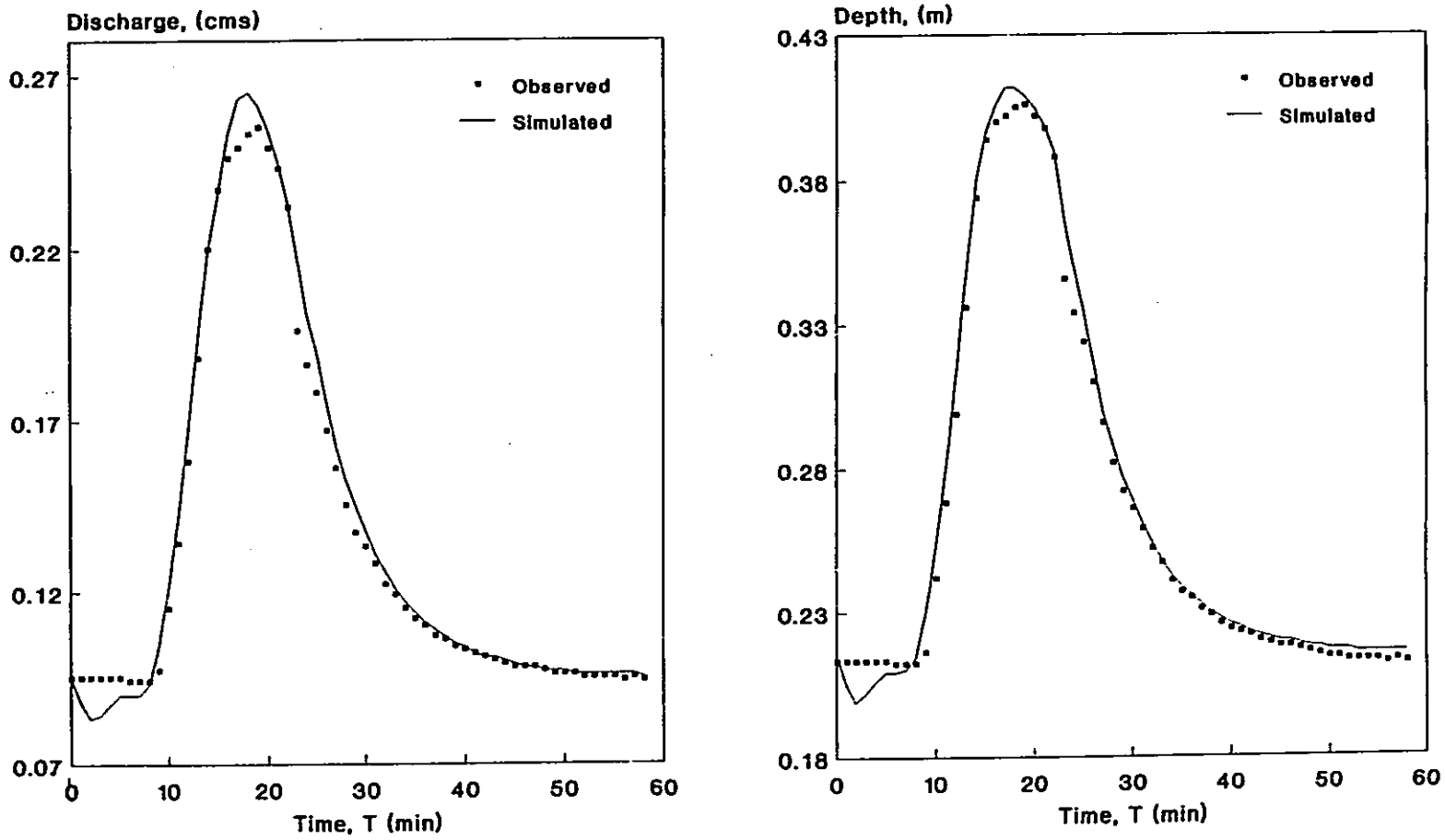

Figure 7.11 Simulated vs. Observed Discharge and Depth Hydrographs with Vertical Interface Planes Applied to ONE-D, (Treske's data, case 5).

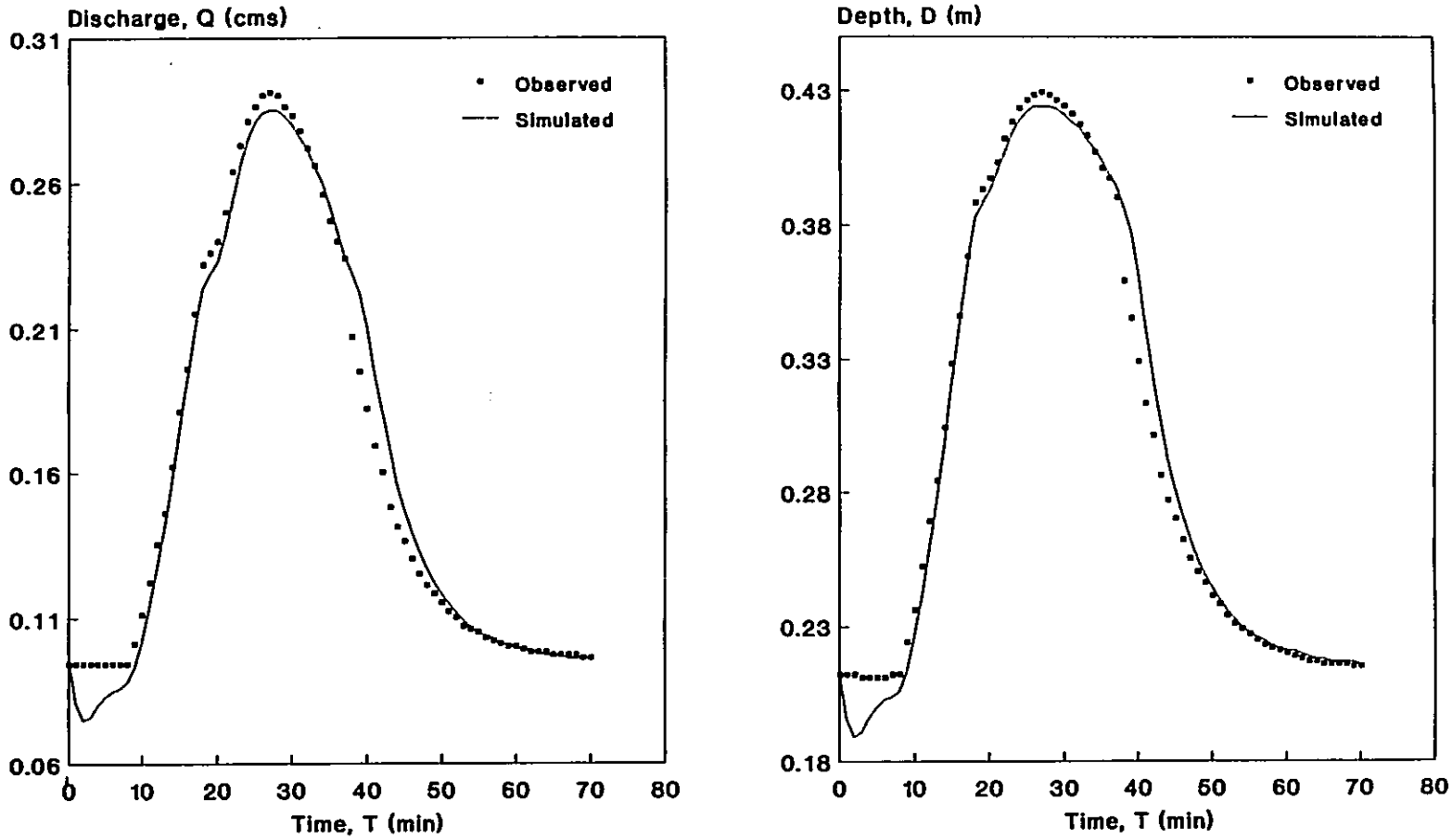

Figure 7.12 Simulated vs. Observed Discharge and Depth Hydrographs with Vertical Interface Planes Applied to ONE-D, (Treske's data, case 6).

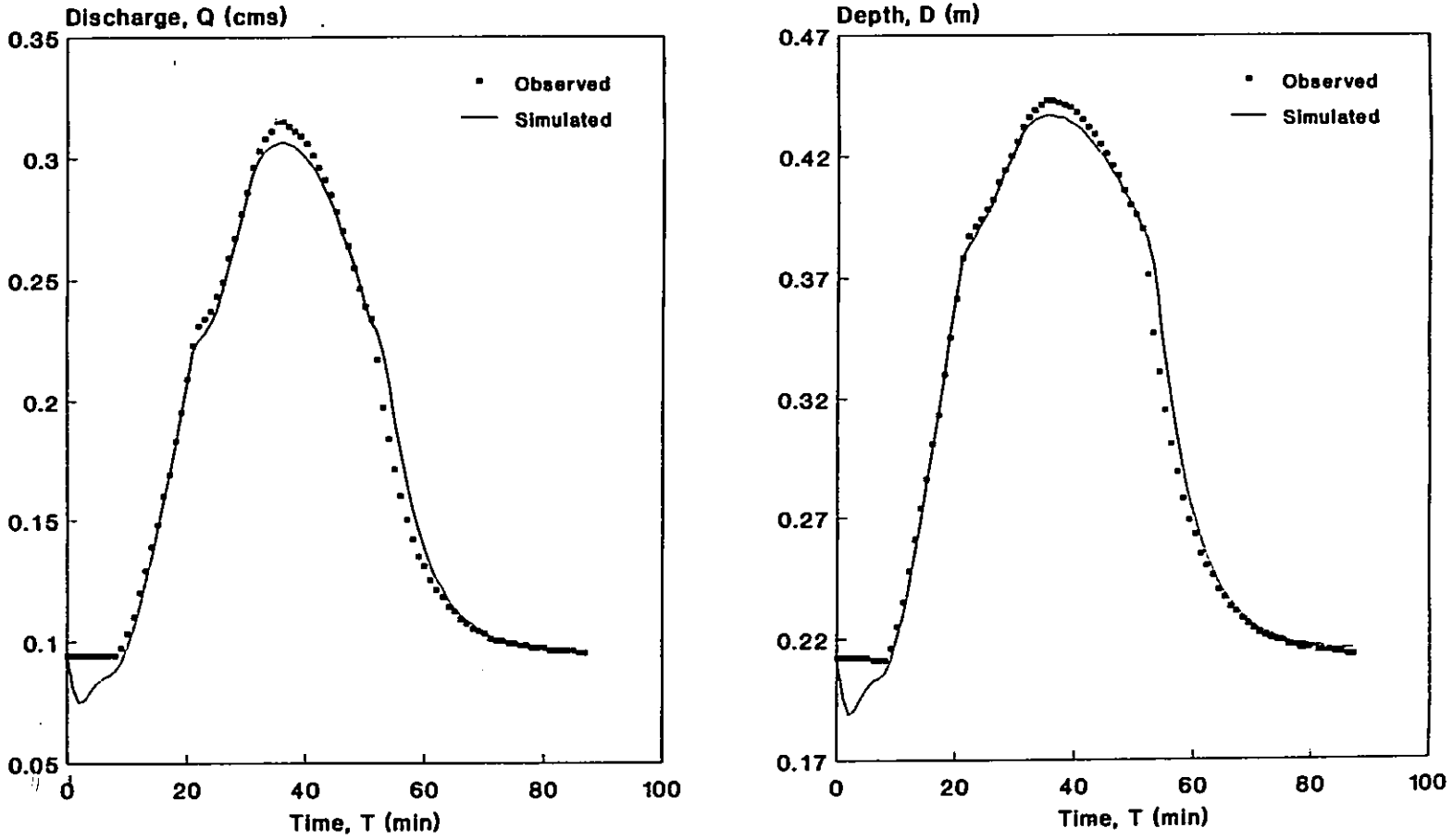

Figure 7.13 Simulated vs. Observed Discharge and Depth Hydrographs with Vertical Interface Planes Applied to ONE-D, (Treske's data, case 7).

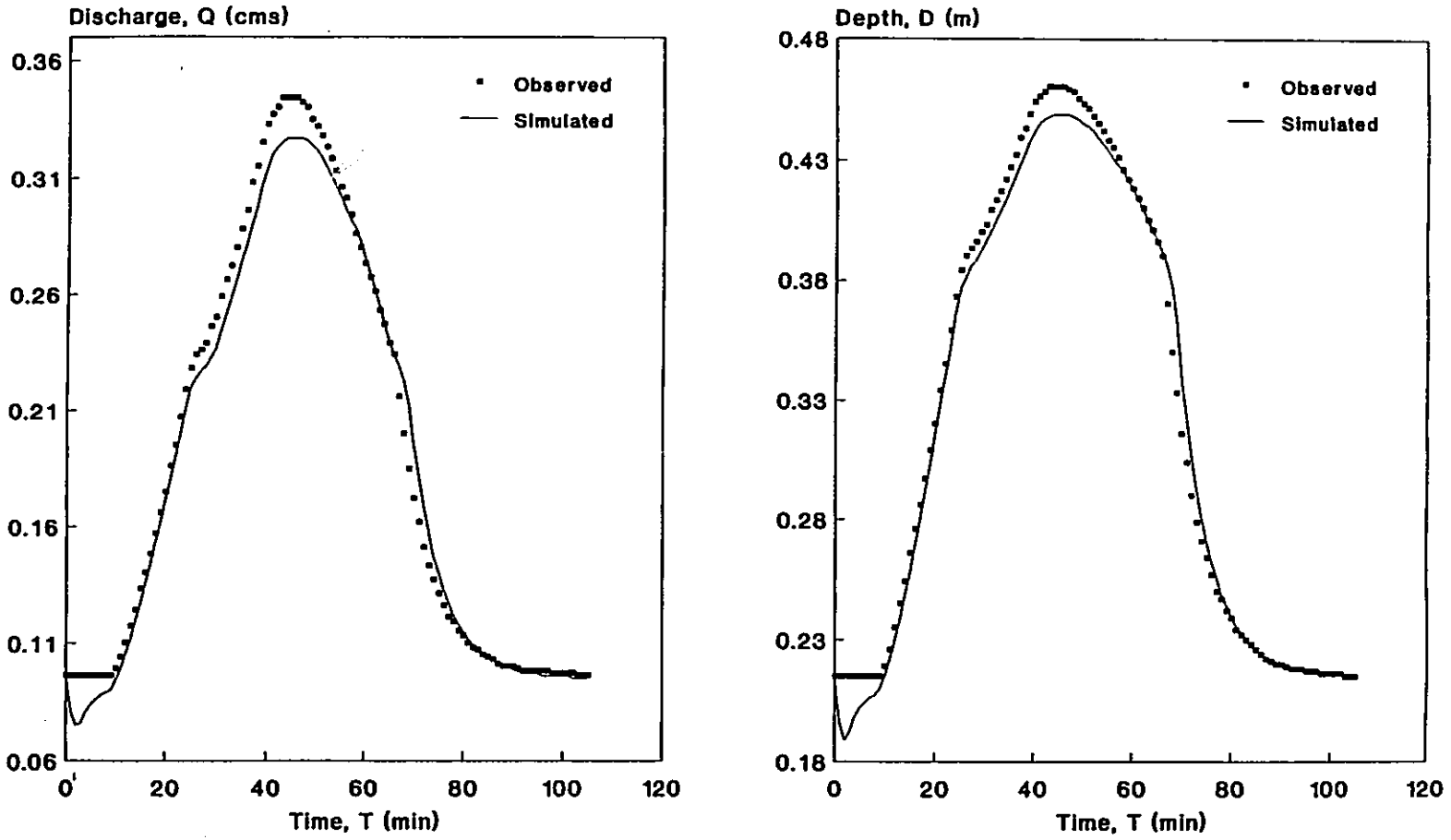

Figure 7.14 Simulated vs. Observed Discharge and Depth Hydrographs with Vertical Interface Planes Applied to ONE-D, (Treske's data, case 8).

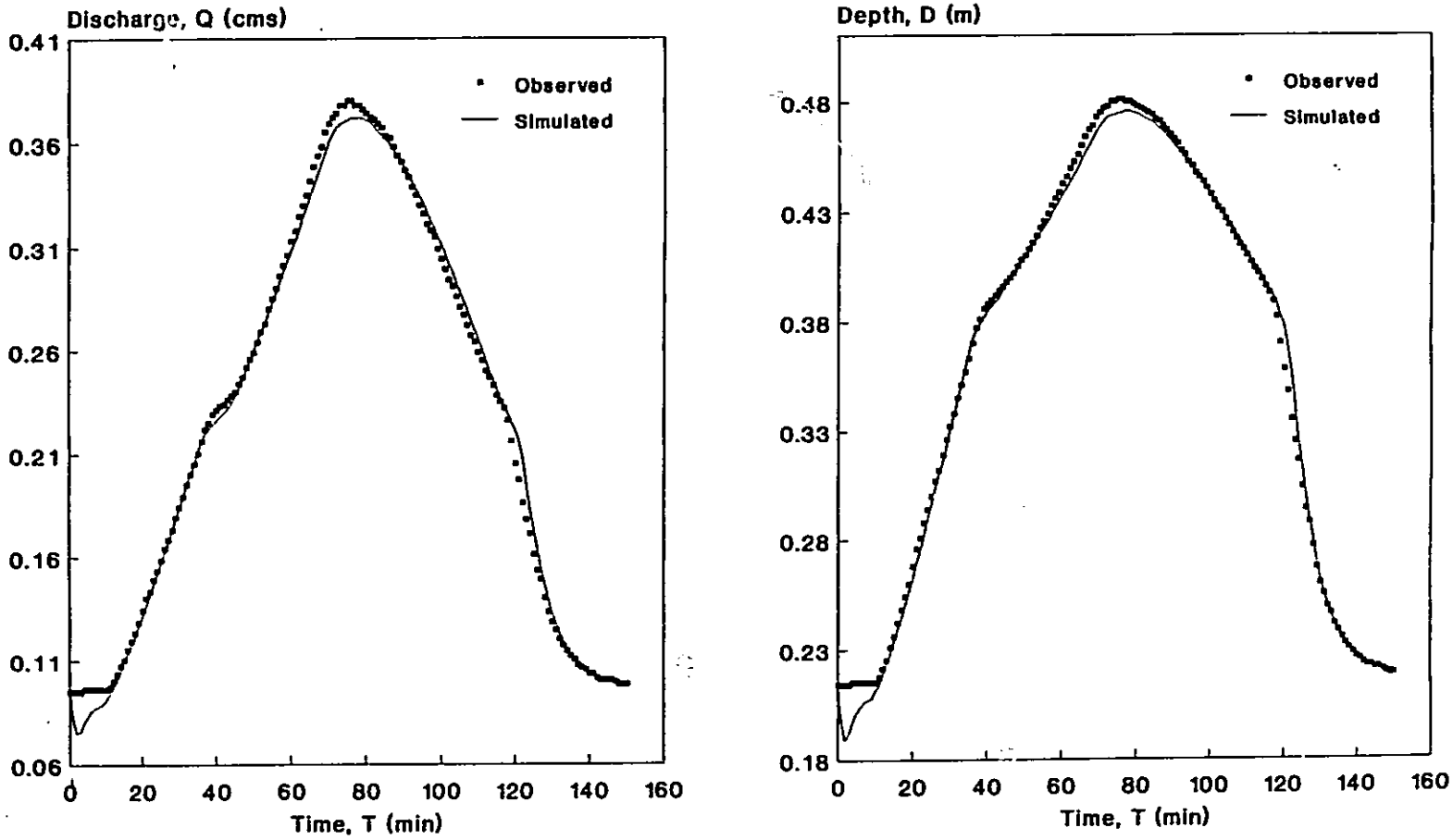

Figure 7.15 Simulated vs. Observed Discharge and Depth Hydrographs with Vertical Interface Planes Applied to ONE-D, (Treske's data, case 9).

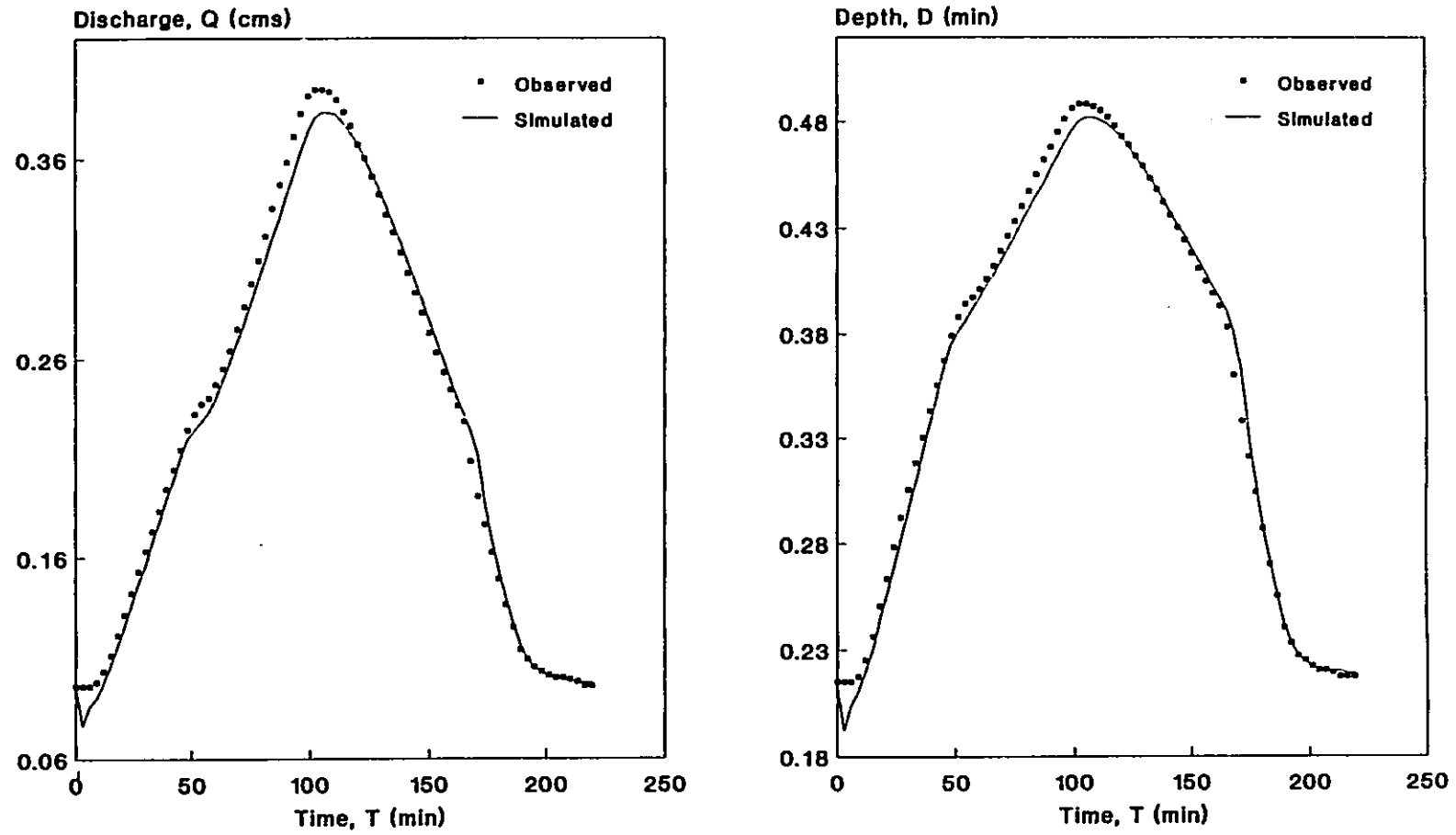

Figure 7.16 Simulated vs. Observed Discharge and Depth Hydrographs with Vertical Interface Planes Applied to ONE-D, (Treske's data, case 10).

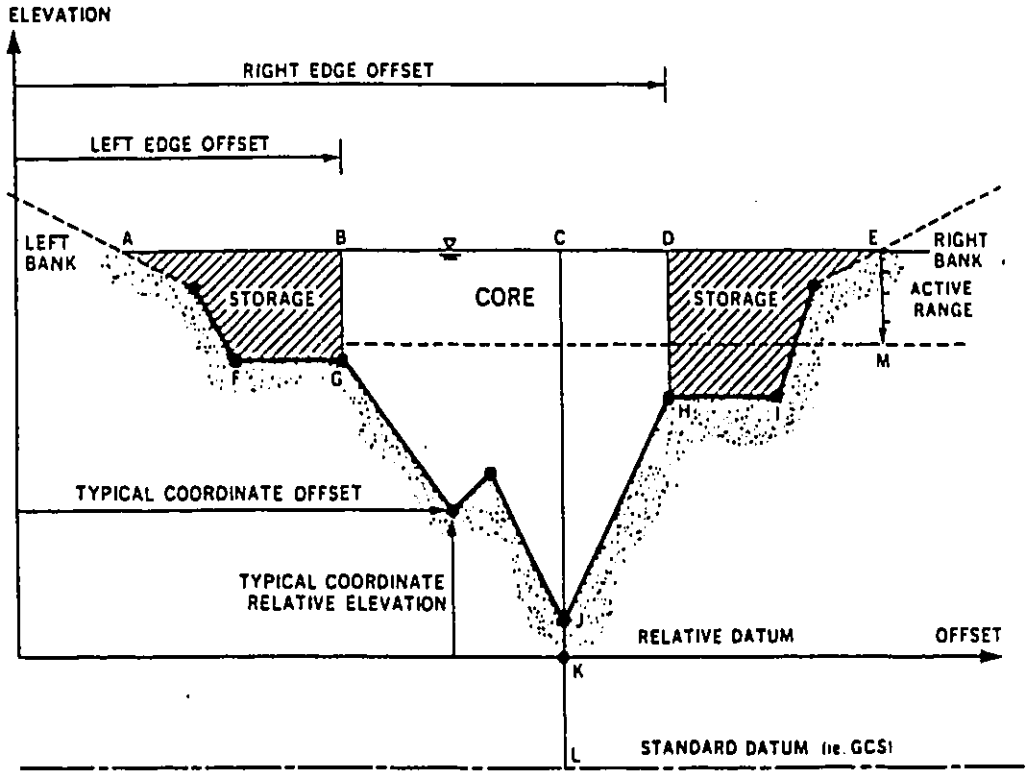

A-E. Total top width
B-D. Core top width (conveyance)
G-J-H Wetted perimeter
A-B-C-D-E-I-H-J-G-F-A. Total area
B-C-D-H-J-G-B. Core area (conveyance)
C-J: Depth
J-K: Relative bottom depth
J-K-L: Standard bottom depth
K-L Datum adjustment
E-M. Active Range (ex. 5 table values)

Figure 7.17 Definition Sketch of Cross-section Parameters Input to the COORD Programs.

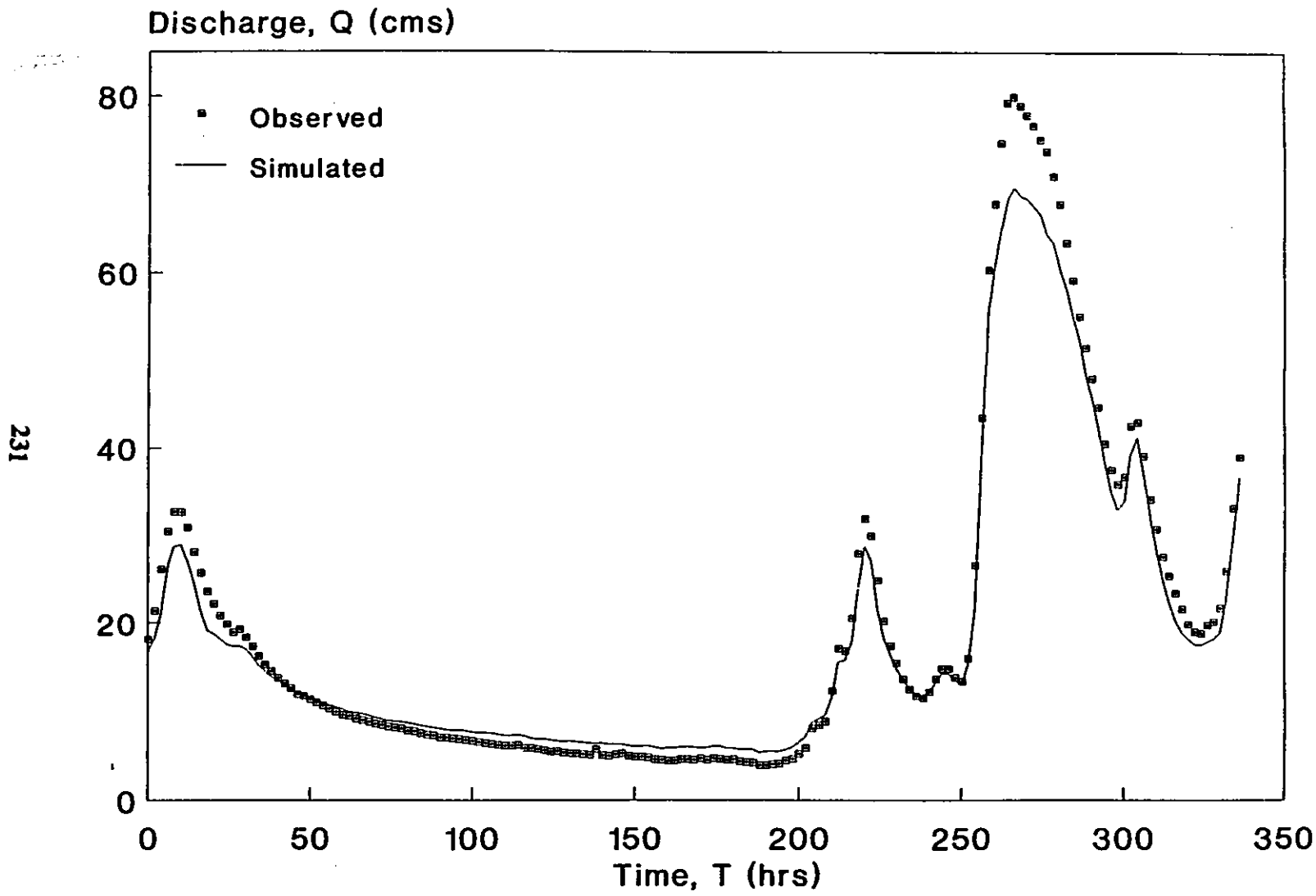

Figure 7.18 Simulated vs. Observed Discharge Hydrograph with ONE-D Applied to Myers' Data Set.

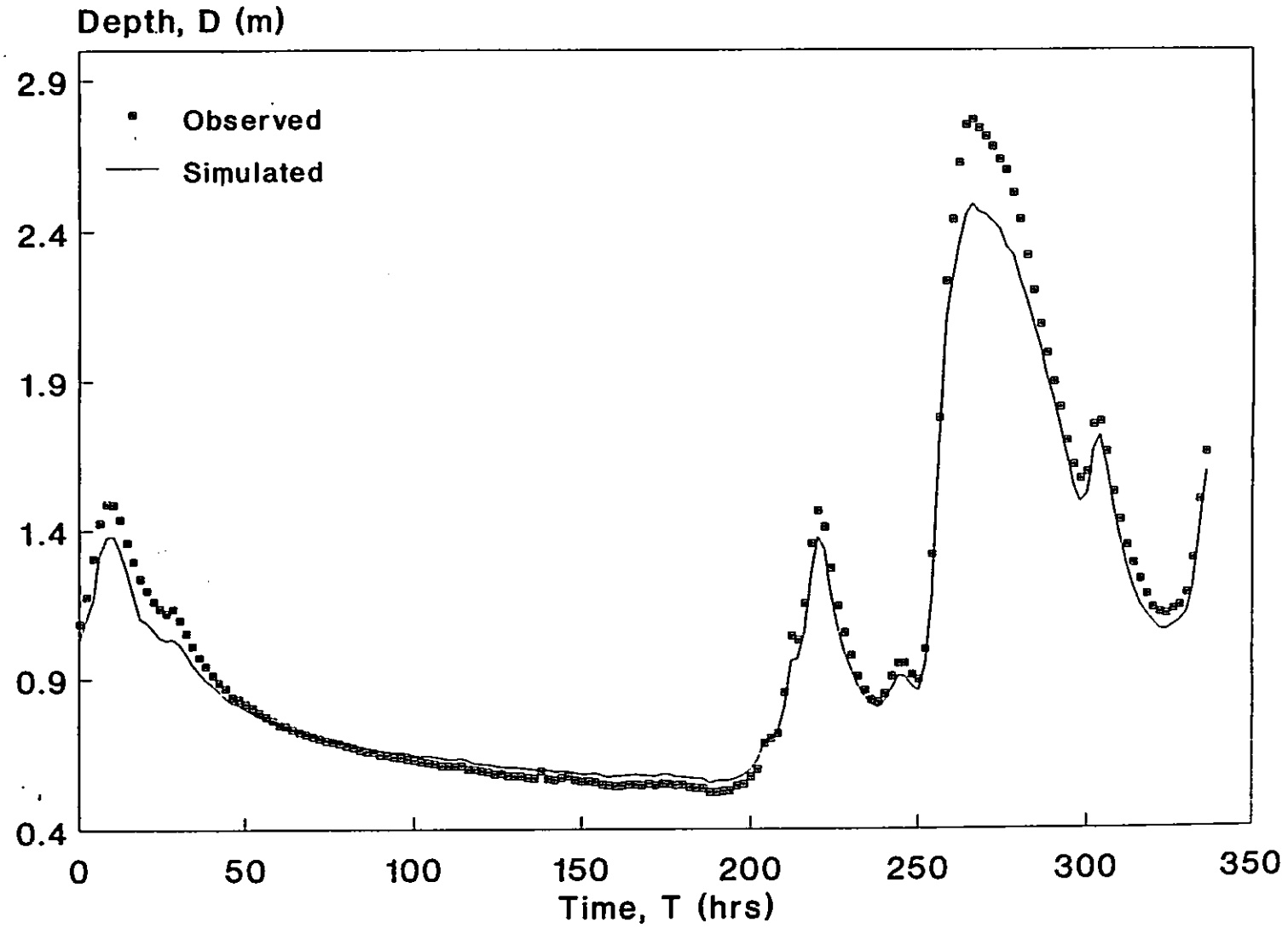

Figure 7.19 Simulated vs. Observed Depth Hydrograph with ONE-D Applied to Myers' Data Set.

CHAPTER 8

RESULTS AND DISCUSSION

8.1 INTRODUCTION

Dynamic flood routing models have the reputation of being difficult to apply. It is critical that proper initial and boundary conditions are established, or models will not execute. In addition, modifications to existing data are usually introduced. A critical task in the application of hydrodynamic models is the determination of the roughness parameter in the friction slope term of the momentum equation. Manning's n is adjusted to reproduce historical observations of stage and discharge. However, in the absence of necessary data (observed stages and discharges), n can be approximated. The adjustment process is referred to as "calibration". Calibration may be either a trial-error process or an automatic iteration procedure.

In general, data has to be manipulated to overcome computational problems experienced when applying dynamic flow routing models. In some instances, no matter how much the data is manipulated, a model may still produce unsuccessful runs. Kouwen (1986) states: "No amount of manipulation of the data could overcome computational problems experienced with both models (MOBED and DWOPER) applied to the Nith (River), but minor changes to the bed profiles did allow both models to be run for the Grand River".

This shows that in certain cases hydrodynamic models can fail to provide solutions for the St. Venant equations no matter what modifications are applied to the related data sets. In some cases, if difficulties are encountered because of the steepness of the river or any other reason, the application of simplified methods should be considered.

8.2 DWOPER SIMULATIONS

DWOPER was applied to simulate unsteady flow in a laboratory channel (Treske, 1980) and a natural channel (Myers, 1991). In both cases, minor modifications were introduced to the data sets to obtain satisfactory simulations of the downstream stage and discharge hydrographs.

Three different approaches to define "off-channel" storage areas were considered in the DWOPER input data file. The first, which viewed the composite flow field as a single hydraulic unit without storage, produced significant differences between simulated and observed depth and discharge hydrographs. The second and third options separated the shallow and deep zones of the compound flow fields using different types of (imaginary) interface planes. The second option, which considered vertical interface planes, gave generally good results for the laboratory data but was less successful when applied to the field data. The third option used diagonal interface planes to define flood plain storage areas. The inclination of the diagonal plane to the horizontal (θ) was adjusted to reflect changing hydraulic conditions. The form of the simulated hydrographs using this particular approach was found to be sensitive to variations in θ. An equation was developed relating

the variation of the angle θ with the ratio of the depth of flow over the flood plain to the total depth of flow.

Due to the fact that DWOPER was developed to simulate large river systems, where flow depths are typically much smaller than the channel widths, Treske's roughness coefficients had to be modified to allow or compensate for the under-estimation of the wetted perimeter (in the case of large rivers, the top width of flow can normally be assumed to be approximately equal to the wetted perimeter). The following equation applies to Treske's simple rectangular channel (corresponding to flood events 1 to 4):

$$n_{eq} = n \left(1 + \frac{2Y}{W} \right)^{\frac{2}{3}} \qquad (8\text{-}1)$$

On the other hand, the following equation applies to flow in Treske's compound channel (i.e. flood events 5 to 10):

$$n_{eq} = n \left(\frac{P}{W} \right)^{\frac{2}{3}} \qquad (8\text{-}2)$$

Inspection of the simulated discharge and depth hydrographs indicates that DWOPER underestimates Treske's observed peak depths and discharges, (figures 8.1 to 8.10). However, DWOPER simulations did not indicate any time delay or phase shift between the corresponding hydrographs. The observed and simulated depth and discharge hydrographs have identical times to peak.

Wormleaton (1982) noted that the most commonly used method of calculating discharge in rectangular compound channels adopts imaginary vertical interface planes to separate shallow and deep zones of the flow field. In the present study, the relative merits of using vertical and diagonal interface planes, as well as the no off-channel storage areas option, were examined. As evidenced in tables 8.1 to 8.6, the vertical interface planes option gave superior results, especially for depths just above the bank-full stage (i.e. small flood plain depths). Nevertheless, diagonal interface planes gave good results. As tables 8.1

to 8.6 indicate, the goodness-of-fit criteria were quite close to those of vertical interface planes with minor differences usually in the second and third significant figures. Therefore, vertical as well as diagonal interface planes produced generally good results in the DWOPER applications.

An inspection of the values in table 8.7 shows that the time step variation has minimal effect on the stability of the four-point implicit scheme used in DWOPER. This table confirms that the selection of the time step size depends on accuracy rather than stability in an implicit technique. A 1-minute time step was used in the DWOPER simulation of Treske's data. This time step resulted in a 1.315 % relative error between simulated and observed peak flow for flood event No. 10, with a total of 222 iterations. This relative error did not change when the time step was reduced to 30 % (18 seconds), with a corresponding 740 iterations. The error was found to increase to 1.939 % when the time step was tripled (180 seconds), which resulted in 74 iterations. Therefore, as table 8.7 indicates, when applying the implicit method for routing flows in a simple rectangular compound channels, changing the time step did not significantly improve the simulated hydrographs. On the other hand, the computer run time was shortened by a increase in the time step.

With regards to Myers' data set, when compared to the "vertical interface planes" and the "no off-channel storage" options, the outward-facing diagonal interface planes gave best-fit hydrographs, (table 8.8). This finding for the case of natural channel was expected and confirmed the conclusions of Wormleaton (1982). Certain modifications to Myers' values for Manning's n had to be made to obtain satisfactory DWOPER simulations. As noted in the discussion of section 5.8.5, Manning's n for the bank-full depth condition had to be changed from Myers' value (0.042) to 0.030.

The problem of stability arises when applying DWOPER to Myers' data set. It has been established elsewhere that the selection of the time step in an implicit formulation is based on accuracy rather than stability, (Fread, 1987). However, this conclusion was not

found to apply when a relatively large time step was used in Myers' data simulations. Investigating figure 8.11 shows that instability occurs around the peak of the hydrograph. Also, there exists a phase shift or time delay, where the observed hydrograph lags behind the simulated by approximately six hours. If simulated and observed hydrographs were, in fact, plotted on the same graph on the basis of assuming the time 6 hours as the origin for the simulated hydrograph (i.e. translate hypothetically the time axis of the simulated hydrograph by 6 hours), the two hydrographs would then have a compatible shape with some instability occurring around the peak values. Accordingly, as noted in section 5.8.3, the time step had to be reduced to overcome these problems.

To sum up, the overall DWOPER simulations were satisfactory as peak values were simulated within less than 5 % difference relative to the observed, and with a good-fit for other parts of the hydrographs.

8.3 EXTRAN SIMULATIONS

EXTRAN uses an explicit scheme to solve the unsteady flow equations. Applying EXTRAN to data sets required modifications of the data before successful runs were obtained. Even with data manipulation, simulated depths and discharges did not compare favourably with the corresponding observed values. A number of manipulations were introduced to the data to improve the ability to converge to a solution. Also, a change was made to incorporate boundary conditions in the reach. In the explicit formulation of EXTRAN, the time step is limited by the Courant criterion. Time steps of the order of several seconds or few minutes on the maximum can be used. Therefore, the corresponding number of iterations is very high compared to modelling the same event using an implicit scheme. Explicit schemes were found to be time consuming, in that a run for Myers' data set would take up to 45 minutes as compared to a couple of minutes using DWOPER.

For the case of Treske's data set, different time steps were selected to detect the effect of time step variation on the simulated results. The maximum allowable time step

was 7 seconds, based on the Courant criterion for a distance step of 15 m. The time step was varied between 1 and 7 seconds to determine the effect on the downstream simulated results. Table 8.9 shows that changing the time step within acceptable limits (Courant criteria) did not introduce noticeable improvements. In addition, the distance step was changed to detect its effect on the simulated hydrographs. Varying the distance step did introduce considerable improvements, (figure 8.12 and table 8.10).

A close inspection of the results shows that there is a phase shift in the hydrographs. This means that peak flows and stages were early (not on time) except for case 9. In other cases, peaks were occurring one time increment (one minute) before their observed peaking time, (figures 8.1 to 8.10). This can be thought to be due to the time step size, distance step size, and/or Manning's roughness coefficient. However, the time step was small enough to satisfy the Courant condition. In addition, the distance step was large enough to cover one wave length. Therefore, the main problem in the early peaking hydrograph lies in Manning's n. As expected, EXTRAN was very sensitive to values of Manning's n. EXTRAN had to be calibrated to adjust n. For in-bank flows, n was increased to 0.020 whereas Treske's value was 0.012 for his "smooth" channel. Although considerable, this increase is still acceptable compared to the data manipulations introduced by Kouwen (1986), who used resistance values approximately two to three times what they should have been in order to avoid a "failed" run.

With regard to Myers' data set, the same data manipulations were introduced. The time step had to be extremely small (in the order of several seconds) to satisfy the stability condition. The simulated results were not particularly good, especially at the peak where depth was under-estimated by 10.21 % and the discharge by 12.97 %. No phase lag or time shift was noted between observed and simulated results using EXTRAN.

Comparing DWOPER and EXTRAN simulations, one can conclude that DWOPER gave generally superior results for the "laboratory" and "field" cases under consideration, (figures 8.1 to 8.10 and tables 8.11 to 8.20).

8.4 ONE-D SIMULATIONS

ONE-D is a one-dimensional hydrodynamic model that uses the Galerkan techniques of weighted residuals to solve the complete form of the St. Venant equations in an implicit finite difference form. Compared to EXTRAN simulations a small number of data manipulations were necessary in this instance. For Treske's data set, as a result of calibration, Manning's roughness coefficient was slightly modified to achieve better simulations. Two different options to separate the main channel and flood plain flow fields were used. The first, which applied diagonal interface plains, did not produce a good agreement between simulated and observed hydrographs. The second, which applied vertical interface planes, resulted in a good match between the corresponding simulated and observed hydrographs. It is worth noting that the vertical interface planes were recommended for use in the ONE-D manual. Furthermore, it was recommended to augment the top width slightly (and arbitrarily) near the bank-full depth of the channel. The reason for this is to increase the wetted perimeter and minimize the effects of any abrupt change at the bank-full depth.

Time steps were selected based on accuracy rather than stability. However, a check was made to make sure that the time step was less than the time of travel of the wave through a distance step. In applying ONE-D to data sets, the accuracy of the "initial conditions" was studied. It was concluded that the initial conditions play an important role in the convergence of the numerical technique. Moreover, their impact is more pronounced at the starting time of the simulation. Investigating the depth hydrographs (figures 8.1 to 8.10) shows that depth decreases and then starts to increase for the first few time steps. This means that storage is occurring in the channel. This can be remedied by using "better-evaluated" initial conditions. Another approach involves starting the simulation based on a steady-state run of the model. The solution then catches up and converges faster.

Another effort was made to check the effect of accuracy of representation of the inflow hydrograph on the simulated hydrograph and the type of the interpolation function

used to interpolate between coordinates on the inflow hydrograph. It was found that linear interpolation is good as long as the hydrograph is represented by an ample number of coordinates. However, the third-degree parabolic function proved to suit more cases. The third-degree function assumes the same slope before and after a coordinate, whereas linear interpolation changes slope (point of inflection).

Applying ONE-D to Myers' data set requires almost the same data manipulations. The model was run for a steady-state condition and then for a transient case. The time step size was a problem for the case of Myers' data set. Velocities were relatively high in the river channel and consequently the travel time through a distance step was relatively short. Increasing the size of the distance step would result in accuracy problems and would violate the minimum allowable number of distance steps. Selecting a time step of 60 seconds would be the allowable time for the wave to travel to the next distance increment and satisfying the Courant criteria. However, a maximum allowable time step, up to 15 times that based on Courant criteria, can be used. In this instance, a time step of 5 minutes was selected. This small time step resulted in a high number of iterations and consequently is time consuming.

8.5 STATISTICAL CRITERIA

In general, no single statistical goodness-of-fit criterion is sufficient to adequately assess the measure of fit between simulated and observed hydrographs. Different goodness-of-fit criteria are weighted in favour of different hydrograph components (volumes, peak flows, maximum depths ...etc). Thus, no single criterion is universally the best and the criteria ultimately selected should depend on the objective of the modelling exercise. The criteria selected to assess the goodness-of-fit of the simulated hydrographs are presented in chapter 4. In this study the following criteria were adopted:

- Graphical techniques,

- Sum of squares (SS),
- Nash and Sutcliffe (N & S),
- Root mean square error (RMSE),
- Standard error of estimate (SEE),
- Reduced error of estimate (REE),
- Proportional error of estimate (PEE), and
- Total absolute relative error (TARE).

Except for N & S, which should approach 1.0 for better simulations, the main goal is to minimize all of the above objective functions.

8.6 DEFINING THE FLOOD PLAIN ZONES

In the context of applying the DWOPER model eq. 5-14 was developed to define the hydraulic boundaries of the flood plains, using outward-facing diagonal interface planes. It was found that the inclination of these planes varies mainly with flood plain depth, although roughness distributions and other geometrical factors seem to have some influence on it. In practice, however, the mean angles of inclination at various stages may be used as an approximation for flow computations. Yen and Overton (1973) reached a similar conclusion through the application of inward diagonal interface planes. Wormleaton (1982) concluded that, for diagonal interface planes, a smaller apparent shear stress occurs across these interface planes which renders them more suitable than vertical planes for discharge computations. Nevertheless, vertical interface planes are found to be quite suitable in the case of rectangular compound channels.

Equation 5-14 was used by Yilmaz (1992) to compute uniform flows in laboratory compound channels made of plexiglass. He compared different methods for computing discharges in compound channels including ones employing vertical, horizontal, and diagonal interface planes (eq. 5-14), the Dracos and Hardegger (1987) method, in addition to other methods. It was concluded that assuming measured discharges are sufficiently accurate, then the calculated ones using eq. 5-14 were the most accurate. Equation 5-14 is therefore recommended for use in steady and unsteady flow computations in channels with flood plains.

8.7 CONCLUSIONS

A number of modifications were made to the laboratory and field data sets to improve the efficiency and the ability to converge to a solution. However, the required modifications differ from one model to another, based on the assumptions adopted in developing the different models. Recent literature on the subject seems to indicate that finite difference techniques to solve the complete form of the St. Venant equations are becoming the norm in solving flood routing problems.

In general terms, DWOPER, EXTRAN, and ONE-D are three hydrodynamic unsteady flow routing models that share the same concept of solving the complete form of the St. Venant equations using finite difference techniques. However, they differ in the method of solution. While DWOPER uses the four-point implicit finite difference scheme, EXTRAN uses the explicit, enhanced explicit, or iterative techniques, and ONE-D uses the Galerkan techniques of weighted residuals to solve the linearized forms of the equations.

Examination of the simulated results (figures 8.1 to 8.10) and statistical goodness of fit techniques (tables 8.11 to 8.20) indicates that ONE-D was superior to DWOPER and EXTRAN when applied to model (in-bank) flows in the single rectangular channel of Treske (1980). However, beyond the in-bank flow depth DWOPER gave the best results, whether applying vertical or outward-facing diagonal interface planes. EXTRAN shows

considerable over-estimation of channel discharge capacity at low flood plain depths. DWOPER and ONE-D, on the other hand, show minor under-estimation of peak stages and discharges. Furthermore, an inspection of table 8.21 shows that DWOPER was superior in simulating flows in the natural non-prismatic channel, (Myers, 1991). In addition, EXTRAN simulations for Myers' data set was better than those obtained using ONE-D.

Inspection of figures 8.1 to 8.10 indicate that simulated peak stages and discharges, except for some cases of EXTRAN simulations, were occurring at the same peaking time as those observed. In EXTRAN, peaks occurred one time step before the actual peaking time . This may be due to an over-estimation of Manning's roughness coefficient. Yen and Overton (1973) indicated that Manning's n for flow computations reflects not only the influence of boundary roughness but also the effects of channel geometry.

Finally, inspecting the simulated results and the statistical goodness-of-fit criteria one can conclude that DWOPER was superior to both EXTRAN and ONE-D and that ONE-D was generally better than EXTRAN.

Table 8.1 Statistical Criteria Employed to Evaluate the Goodness-of-Fit of Simulated Hydrographs Using Diagonal Interfaces, No-Storage, and Vertical Interfaces in DWOPER, (Treske's Data, Case 5).

Criterion	Observed	Diagonal	No Storage	Vertical
Q_p (m^3/s)	0.255	0.255	0.255	0.252
T_p (min)	19.00	19.00	19.00	19.00
Graphical	N/A	Best	Good	Better
SS	N/A	0.0020	0.0399	0.0021
N & S	N/A	0.9883	0.7667	0.9877
RMSE	N/A	0.0058	0.0260	0.0060
SEE	N/A	0.0059	0.0265	0.0061
REE	N/A	0.1081	0.4830	0.1108
PEE	N/A	0.0404	0.1806	0.0414
TARE	N/A	1.5018	7.3042	1.6281

Criterion	Observed	Diagonal	No Storage	Vertical
D_p (m)	0.406	0.405	0.405	0.405
T_p (min)	19.00	19.00	19.00	19.00
Graphical	N/A	Best	Good	Better
SS	N/A	0.0029	0.0638	0.0031
N & S	N/A	0.9889	0.7556	0.9881
RMSE	N/A	0.0070	0.0329	0.0072
SEE	N/A	0.0071	0.0335	0.0074
REE	N/A	0.1054	0.4944	0.1090
PEE	N/A	0.0258	0.1211	0.0267
TARE	N/A	0.9603	4.6682	1.0705

Table 8.2 Statistical Criteria Employed to Evaluate the Goodness-of-Fit of Simulated Hydrographs Using Diagonal Interfaces, No-Storage, and Vertical Interfaces in DWOPER, (Treske's Data, Case 6).

Criterion	Observed	Diagonal	No Storage	Vertical
Q_p (m^3/s)	0.291	0.275	0.289	0.289
T_p (min)	27.00	27.00	27.00	27.00
Graphical	N/A	Better	Good	Best
SS	N/A	0.0036	0.0037	0.0009
N & S	N/A	0.9901	0.9898	0.9975
RMSE	N/A	0.0071	0.0072	0.0036
SEE	N/A	0.0072	0.0073	0.0036
REE	N/A	0.0996	0.1010	0.0498
PEE	N/A	0.0403	0.0408	0.0201
TARE	N/A	1.7355	1.4592	0.9699

Criterion	Observed	Diagonal	No Storage	Vertical
D_p (m)	0.429	0.418	0.427	0.427
T_p (min)	27.00	27.00	27.00	27.00
Graphical	N/A	Better	Good	Best
SS	N/A	0.0032	0.0340	0.0011
N & S	N/A	0.9934	0.9303	0.9977
RMSE	N/A	0.0067	0.0219	0.0039
SEE	N/A	0.0068	0.0222	0.0040
REE	N/A	0.0810	0.2640	0.0475
PEE	N/A	0.0219	0.0715	0.0129
TARE	N/A	0.9491	0.8040	0.5749

Table 8.3 Statistical Criteria Employed to Evaluate the Goodness-of-Fit of Simulated Hydrographs Using Diagonal Interfaces, No-Storage, and Vertical Interfaces in DWOPER, (Treske's Data, Case 7).

Criterion	Observed	Diagonal	No Storage	Vertical
Q_p (m^3/s)	0.315	0.300	0.306	0.309
T_p (min)	35.00	35.00	35.00	35.00
Graphical	N/A	Best	Good	Better
SS	N/A	0.0030	0.0353	0.0165
N & S	N/A	0.9948	0.9388	0.9714
RMSE	N/A	0.0058	0.0200	0.0137
SEE	N/A	0.0059	0.0203	0.0139
REE	N/A	0.0721	0.2475	0.1691
PEE	N/A	0.0302	0.1038	0.0709
TARE	N/A	1.7414	6.1131	1.3346

Criterion	Observed	Diagonal	No Storage	Vertical
D_p (m)	0.443	0.433	0.439	0.439
T_p (min)	35.00	35.00	35.00	35.00
Graphical	N/A	Best	Good	Better
SS	N/A	0.0022	0.0842	0.0008
N & S	N/A	0.9969	0.8817	0.9989
RMSE	N/A	0.0050	0.0309	0.0030
SEE	N/A	0.0051	0.0313	0.0030
REE	N/A	0.0556	0.3439	0.0335
PEE	N/A	0.0156	0.0964	0.0094
TARE	N/A	0.9984	0.7669	0.7044

Table 8.4 Statistical Criteria Employed to Evaluate the Goodness-of-Fit of Simulated Hydrographs Using Diagonal Interfaces, No-Storage, and Vertical Interfaces in DWOPER, (Treske's Data, Case 8).

Criterion	Observed	Diagonal	No Storage	Vertical
Q_p (m^3/s)	0.344	0.323	0.340	0.328
T_p (min)	43-47	45.00	45-46	45.00
Graphical	N/A	better	Good	Best
SS	N/A	0.0075	0.0454	0.0038
N & S	N/A	0.9915	0.9483	0.9957
RMSE	N/A	0.0101	0.0248	0.0072
SEE	N/A	0.0102	0.0251	0.0073
REE	N/A	0.0924	0.2274	0.0658
PEE	N/A	0.0399	0.0983	0.0284
TARE	N/A	1.9914	6.7071	1.7775

Criterion	Observed	Diagonal	No Storage	Vertical
D_p (m)	0.460	0.445	0.457	0.451
T_p (min)	43-47	45.00	45-46	45.00
Graphical	N/A	Better	Good	Best
SS	N/A	0.0037	0.0391	0.0017
N & S	N/A	0.9962	0.9597	0.9982
RMSE	N/A	0.0071	0.0230	0.0048
SEE	N/A	0.0072	0.0233	0.0049
REE	N/A	0.0617	0.2007	0.0418
PEE	N/A	0.0176	0.0573	0.0120
TARE	N/A	1.0980	3.8586	0.8677

Table 8.5 Statistical Criteria Employed to Evaluate the Goodness-of-Fit of Simulated Hydrographs Using Diagonal Interfaces, No-Storage, and Vertical Interfaces in DWOPER, (Treske's Data, Case 9).

Criterion	Observed	Diagonal	No Storage	Vertical
Q_p (m^3/s)	0.380	0.368	0.371	0.371
T_p (min)	75-76	75.00	75.00	75.00
Graphical	N/A	Better	Good	Best
SS	N/A	0.0062	0.0319	0.0019
N & S	N/A	0.9957	0.9777	0.9987
RMSE	N/A	0.0076	0.0173	0.0042
SEE	N/A	0.0077	0.0175	0.0043
REE	N/A	0.0658	0.1493	0.0364
PEE	N/A	0.0260	0.0590	0.0144
TARE	N/A	2.8947	7.0818	1.7501

Criterion	Observed	Diagonal	No Storage	Vertical
D_p (m)	0.481	0.472	0.485	0.475
T_p (min)	75-76	75.00	75.00	75.00
Graphical	N/A	Better	Good	Best
SS	N/A	0.0039	0.0329	0.0013
N & S	N/A	0.9971	0.9759	0.9990
RMSE	N/A	0.0061	0.0176	0.0035
SEE	N/A	0.0061	0.0178	0.0035
REE	N/A	0.0535	0.1553	0.0309
PEE	N/A	0.0137	0.0398	0.0079
TARE	N/A	1.6462	3.9735	1.0223

Table 8.6 Statistical Criteria Employed to Evaluate the Goodness-of-Fit of Simulated Hydrographs Using Diagonal Interfaces, No-Storage, and Vertical Interfaces in DWOPER, (Treske's Data, Case 10).

Criterion	Observed	Diagonal	No Storage	Vertical
Q_p (m^3/s)	0.394	0.3794	0.3908	0.3794
T_p (min)	105-108	105-108	102-108	105-108
Graphical	N/A	Better	Good	Best
SS	N/A	0.0056	0.0178	0.0031
N & S	N/A	0.9926	0.9765	0.9959
RMSE	N/A	0.0087	0.0155	0.0065
SEE	N/A	0.0088	0.0157	0.0066
REE	N/A	0.0860	0.1533	0.0640
PEE	N/A	0.0346	0.0618	0.0258
TARE	N/A	1.7220	3.4935	1.4289

Criterion	Observed	Diagonal	No Storage	Vertical
D_p (m)	0.488	0.4785	0.4877	0.4816
T_p (min)	105-108	105-108	102-108	105-108
Graphical	N/A	Better	Good	Best
SS	N/A	0.0027	0.0173	0.0018
N & S	N/A	0.9961	0.9750	0.9974
RMSE	N/A	0.0060	0.0153	0.0049
SEE	N/A	0.0061	0.0155	0.0050
REE	N/A	0.0625	0.1582	0.0510
PEE	N/A	0.0162	0.0411	0.0132
TARE	N/A	0.9184	2.0545	0.7862

Table 8.7 Effect of Time Step Variation on the Simulated Depths Using DWOPER, (Treske's Data, Case 10).

Time (min)	Observed Depth (m)	Simulated Depth (m)	Simulated Depth (m)	Simulated Depth (m)
		t=18 sec	t=60 sec	t=180 sec
0	0.215	0.213	0.216	0.216
9	0.217	0.216	0.216	0.219
18	0.250	0.244	0.244	0.247
27	0.292	0.283	0.280	0.283
36	0.330	0.323	0.323	0.323
45	0.367	0.363	0.363	0.363
54	0.394	0.393	0.393	0.393
63	0.406	0.405	0.405	0.405
72	0.426	0.424	0.421	0.424
81	0.447	0.439	0.439	0.439
90	0.468	0.457	0.457	0.460
99	0.486	0.475	0.475	0.475
108	0.487	0.482	0.482	0.482
117	0.478	0.475	0.475	0.475
126	0.464	0.463	0.466	0.463
135	0.448	0.448	0.451	0.448
144	0.430	0.433	0.433	0.433
153	0.411	0.415	0.415	0.415
162	0.393	0.396	0.399	0.396
171	0.338	0.344	0.351	0.347
180	0.287	0.287	0.290	0.290
189	0.240	0.241	0.247	0.244
198	0.225	0.226	0.226	0.226
207	0.220	0.219	0.219	0.219
216	0.217	0.219	0.219	0.219
219	0.217	0.219	0.219	0.219

Table 8.8 Statistical Criteria Employed to Evaluate the Goodness-of-Fit of Simulated Hydrographs Using Diagonal Interfaces, No-Storage, and Vertical Interfaces in the DWOPER application to Myers' Data.

Criterion	Observed	Diagonal	No Storage	Vertical
Q_p (m^3/s)	78.845	77.273	100.292	84.122
T_p (hrs)	268.00	268.00	268.00	268.00
Graphical	N/A	Best	Good	Better
SS	N/A	664.205	4353.1	908.706
N & S	N/A	1.0000	1.0000	1.0000
RMSE	N/A	1.9825	5.0752	2.3188
SEE	N/A	1.9943	5.1055	2.3327
REE	N/A	0.0013	0.0034	0.0016
PEE	N/A	0.0719	0.1841	0.0841
TARE	N/A	15.711	19.386	15.161

Criterion	Observed	Diagonal	No Storage	Vertical
D_p (m)	2.737	2.694	3.319	2.880
T_p (hrs)	268.00	268.00	268.00	268.00
Graphical	N/A	Best	Good	Better
SS	N/A	0.5460	3.2850	0.7200
N & S	N/A	0.9904	0.9425	0.9874
RMSE	N/A	0.0568	0.1394	0.0653
SEE	N/A	0.0572	0.1403	0.0657
REE	N/A	0.0977	0.2397	0.1122
PEE	N/A	0.0474	0.1162	0.0544
TARE	N/A	7.2908	9.9387	7.1949

Table 8.9 Effect of Time Step Variation on the Simulated Discharge Hydrograph Using EXTRAN, (Treske's Data, Case 10).

Time (min)	Observed Discharge	Simulated Discharge	Simulated Discharge	Simulated Discharge
	(cms)	dt=1 sec	dt=5 sec	dt=10 sec
0	0.096	0.100	0.100	0.100
9	0.098	0.100	0.100	0.100
18	0.121	0.120	0.120	0.120
27	0.153	0.150	0.150	0.150
36	0.183	0.190	0.190	0.190
45	0.214	0.220	0.220	0.220
54	0.237	0.240	0.240	0.240
63	0.255	0.270	0.270	0.270
72	0.286	0.300	0.300	0.300
81	0.321	0.330	0.330	0.330
90	0.358	0.360	0.360	0.360
99	0.391	0.390	0.390	0.390
108	0.393	0.390	0.390	0.390
117	0.376	0.370	0.370	0.370
126	0.351	0.340	0.340	0.340
135	0.323	0.310	0.310	0.310
144	0.293	0.280	0.280	0.280
153	0.263	0.260	0.260	0.260
162	0.236	0.220	0.220	0.220
171	0.190	0.170	0.170	0.170
180	0.149	0.140	0.140	0.140
189	0.114	0.110	0.110	0.110
198	0.103	0.100	0.100	0.100
207	0.100	0.100	0.100	0.100
216	0.096	0.100	0.100	0.100
219	0.096	0.100	0.100	0.100
Total % Relative	Absolute Error	230.564	230.564	230.564

Table 8.10 Effect of Distance Step Variation on the Simulated Discharge Hydrograph Using EXTRAN, (Treske's Data, Case 10).

Time (min)	Observed Discharge	Simulated Discharge	Simulated Discharge	Simulated Discharge
	(cms)	dx=70 m	dx=105 m	dx=210 m
0	0.096	0.120	0.100	0.100
9	0.098	0.110	0.100	0.100
18	0.121	0.120	0.120	0.130
27	0.153	0.140	0.150	0.160
36	0.183	0.180	0.190	0.190
45	0.214	0.210	0.220	0.230
54	0.237	0.230	0.240	0.260
63	0.255	0.250	0.270	0.290
72	0.286	0.270	0.300	0.320
81	0.321	0.300	0.330	0.350
90	0.358	0.330	0.360	0.380
99	0.391	0.370	0.390	0.410
108	0.393	0.380	0.390	0.390
117	0.376	0.370	0.370	0.360
126	0.351	0.350	0.340	0.320
135	0.323	0.330	0.310	0.290
144	0.293	0.310	0.280	0.260
153	0.263	0.280	0.260	0.220
162	0.236	0.250	0.220	0.200
171	0.190	0.220	0.170	0.160
180	0.149	0.160	0.140	0.130
189	0.114	0.120	0.110	0.100
198	0.103	0.110	0.100	0.100
207	0.100	0.100	0.100	0.100
216	0.096	0.100	0.100	0.100
219	0.096	0.100	0.100	0.100
Total % Relative	Absolute Error	149.438	84.482	203.882

Table 8.11 Statistical Criteria Employed to Evaluate the Goodness-of-Fit of Simulated Hydrographs Using DWOPER, EXTRAN, and ONE-D, (Treske's Data, Case 1).

Criterion	Observed	DWOPER	EXTRAN	ONE-D
Q_p (m^3/s)	0.158	0.156	0.170	0.156
T_p (min)	15.00	15.00	15.00	15.00
Graphical	N/A	Better	Good	Best
SS	N/A	0.0003	0.0029	0.0001
N & S	N/A	0.9800	0.8067	0.9933
RMSE	N/A	0.0024	0.0075	0.0014
SEE	N/A	0.0025	0.0077	0.0014
REE	N/A	0.1414	0.4397	0.0816
PEE	N/A	0.0205	0.0638	0.0118
TARE	N/A	0.7540	2.6295	0.2871

Criterion	Observed	DWOPER	EXTRAN	ONE-D
D_p (m)	0.299	0.296	0.312	0.297
T_p (min)	15.00	15.00	15.00	15.00
Graphical	N/A	Better	Good	Best
SS	N/A	0.0005	0.0048	0.0001
N & S	N/A	0.9821	0.8286	0.9964
RMSE	N/A	0.0031	0.0097	0.0014
SEE	N/A	0.0032	0.0099	0.0014
REE	N/A	0.1336	0.4140	0.0598
PEE	N/A	0.0128	0.0396	0.0057
TARE	N/A	0.4580	1.6064	0.1493

Table 8.12 Statistical Criteria Employed to Evaluate the Goodness-of-Fit of Simulated Hydrographs Using DWOPER, EXTRAN, and ONE-D, (Treske's Data, Case 2).

Criterion	Observed	DWOPER	EXTRAN	ONE-D
Q_p (m^3/s)	0.171	0.170	0.180	0.169
T_p (min)	24.00	24.00	24.00	24.00
Graphical	N/A	Best	Good	Better
SS	N/A	0.0001	0.0016	0.0011
N & S	N/A	0.9975	0.9600	0.9725
RMSE	N/A	0.0012	0.0049	0.0041
SEE	N/A	0.0013	0.0050	0.0041
REE	N/A	0.0500	0.2000	0.1658
PEE	N/A	0.0099	0.0397	0.0329
TARE	N/A	0.3940	2.0166	1.2929

Criterion	Observed	DWOPER	EXTRAN	ONE-D
D_p (m)	0.316	0.315	0.325	0.311
T_p (min)	24.00	24.00	24.00	24.00
Graphical	N/A	Best	Good	Better
SS	N/A	0.0003	0.0031	0.0013
N & S	N/A	0.9959	0.9575	0.9822
RMSE	N/A	0.0021	0.0069	0.0044
SEE	N/A	0.0022	0.0070	0.0045
REE	N/A	0.0641	0.2061	0.1335
PEE	N/A	0.0084	0.0271	0.0175
TARE	N/A	0.4481	1.3079	0.6900

Table 8.13 Statistical Criteria Employed to Evaluate the Goodness-of-Fit of Simulated Hydrographs Using DWOPER, EXTRAN, and ONE-D, (Treske's Data, Case 3).

Criterion	Observed	DWOPER	EXTRAN	ONE-D
Q_p (m^3/s)	0.183	0.182	0.190	0.182
T_p (min)	39.00	39.00	39.00	39.00
Graphical	N/A	Best	Good	Better
SS	N/A	0.0002	0.0028	0.0003
N & S	N/A	0.9973	0.9616	0.9959
RMSE	N/A	0.0015	0.0057	0.0019
SEE	N/A	0.0015	0.0058	0.0019
REE	N/A	0.0523	0.1958	0.0641
PEE	N/A	0.0112	0.0418	0.0137
TARE	N/A	0.6911	3.0997	0.9153

Criterion	Observed	DWOPER	EXTRAN	ONE-D
D_p (m)	0.331	0.332	0.337	0.331
T_p (min)	39.00	39.00	39.00	39.00
Graphical	N/A	Best	Good	Better
SS	N/A	0.0002	0.0047	0.0003
N & S	N/A	0.9985	0.9638	0.9977
RMSE	N/A	0.0015	0.0074	0.0019
SEE	N/A	0.0015	0.0075	0.0019
REE	N/A	0.0392	0.1901	0.0480
PEE	N/A	0.0057	0.0275	0.0069
TARE	N/A	0.3422	1.9701	0.4803

Table 8.14 Statistical Criteria Employed to Evaluate the Goodness-of-Fit of Simulated Hydrographs Using DWOPER, EXTRAN, and ONE-D, (Treske's Data, Case 4).

Criterion	Observed	DWOPER	EXTRAN	ONE-D
Q_p (m^3/s)	0.190	0.192	0.190	0.191
T_p (min)	37.00	37.00	37.00	37.00
Graphical	N/A	Best	Good	Better
SS	N/A	0.0001	0.0010	0.0002
N & S	N/A	0.9985	0.9851	0.9970
RMSE	N/A	0.0012	0.0037	0.0017
SEE	N/A	0.0012	0.0038	0.0017
REE	N/A	0.0385	0.1219	0.0545
PEE	N/A	0.0081	0.0257	0.0115
TARE	N/A	0.4440	1.5933	0.6366

Criterion	Observed	DWOPER	EXTRAN	ONE-D
D_p (m)	0.340	0.345	0.337	0.343
T_p (min)	37.00	37.00	37.00	37.00
Graphical	N/A	Best	Good	Better
SS	N/A	0.0003	0.0019	0.0003
N & S	N/A	0.9974	0.9837	0.9974
RMSE	N/A	0.0020	0.0051	0.0020
SEE	N/A	0.0021	0.0052	0.0020
REE	N/A	0.0507	0.1275	0.0507
PEE	N/A	0.0073	0.0183	0.0073
TARE	N/A	0.4001	1.0831	0.4142

Table 8.15 Statistical Criteria Employed to Evaluate the Goodness-of-Fit of Simulated Hydrographs Using DWOPER, EXTRAN, and ONE-D, (Treske's Data, Case 5).

Criterion	Observed	DWOPER	EXTRAN	ONE-D
Q_p (m^3/s)	0.255	0.252	0.270	0.246
T_p (min)	19.00	19.00	18.00	19.00
Graphical	N/A	Best	Good	Better
SS	N/A	0.0021	0.0132	0.0068
N & S	N/A	0.9877	0.9228	0.9602
RMSE	N/A	0.0060	0.0150	0.0107
SEE	N/A	0.0061	0.0152	0.0109
REE	N/A	0.1108	0.2778	0.1994
PEE	N/A	0.0414	0.1039	0.0746
TARE	N/A	1.6281	3.7522	3.0390

Criterion	Observed	DWOPER	EXTRAN	ONE-D
D_p (m)	0.406	0.405	0.415	0.401
T_p (min)	19.00	19.00	18.00	19.00
Graphical	N/A	Best	Good	Better
SS	N/A	0.0031	0.0206	0.0080
N & S	N/A	0.9881	0.9211	0.9693
RMSE	N/A	0.0072	0.0187	0.0116
SEE	N/A	0.0074	0.0190	0.0118
REE	N/A	0.1090	0.2809	0.1751
PEE	N/A	0.0267	0.0688	0.0429
TARE	N/A	1.0705	2.5511	1.7922

Table 8.16 Statistical Criteria Employed to Evaluate the Goodness-of-Fit of Simulated Hydrographs Using DWOPER, EXTRAN, and ONE-D, (Treske's Data, Case 6).

Criterion	Observed	DWOPER	EXTRAN	ONE-D
Q_p (m^3/s)	0.291	0.289	0.310	0.285
T_p (min)	27.00	27.00	26.00	27.00
Graphical	N/A	Best	Good	Better
SS	N/A	0.0009	0.0171	0.0066
N & S	N/A	0.9975	0.9529	0.9818
RMSE	N/A	0.0036	0.0155	0.0096
SEE	N/A	0.0036	0.0157	0.0098
REE	N/A	0.0498	0.2170	0.1348
PEE	N/A	0.0201	0.0878	0.0546
TARE	N/A	0.9699	4.7376	3.271

Criterion	Observed	DWOPER	EXTRAN	ONE-D
D_p (m)	0.429	0.427	0.439	0.424
T_p (min)	27.00	27.00	26.00	27.00
Graphical	N/A	Best	Good	Better
SS	N/A	0.0011	0.0192	0.0076
N & S	N/A	0.9977	0.9607	0.9844
RMSE	N/A	0.0039	0.0164	0.0103
SEE	N/A	0.0040	0.0167	0.0105
REE	N/A	0.0475	0.1984	0.1248
PEE	N/A	0.0129	0.0537	0.0338
TARE	N/A	0.5749	2.8777	1.7473

Table 8.17 Statistical Criteria Employed to Evaluate the Goodness-of-Fit of Simulated Hydrographs Using DWOPER, EXTRAN, and ONE-D, (Treske's Data, Case 7).

Criterion	Observed	DWOPER	EXTRAN	ONE-D
Q_p (m^3/s)	0.315	0.309	0.330	0.307
T_p (min)	35.00	35.00	34.00	36.00
Graphical	N/A	Best	Good	Better
SS	N/A	0.0165	0.0261	0.0206
N & S	N/A	0.9714	0.9548	0.9643
RMSE	N/A	0.0137	0.0172	0.0153
SEE	N/A	0.0139	0.0174	0.0155
REE	N/A	0.1691	0.2127	0.1889
PEE	N/A	0.0709	0.0892	0.0793
TARE	N/A	1.3346	6.2588	3.0382

Criterion	Observed	DWOPER	EXTRAN	ONE-D
D_p (m)	0.443	0.439	0.451	0.437
T_p (min)	35.00	35.00	34.00	35.00
Graphical	N/A	Best	Good	Better
SS	N/A	0.0008	0.0244	0.0890
N & S	N/A	0.9989	0.9657	0.8750
RMSE	N/A	0.0030	0.0167	0.0318
SEE	N/A	0.0030	0.0168	0.0322
REE	N/A	0.0335	0.1851	0.3536
PEE	N/A	0.0094	0.0519	0.0992
TARE	N/A	0.7044	3.7208	1.6845

Table 8.18 Statistical Criteria Employed to Evaluate the Goodness-of-Fit of Simulated Hydrographs Using DWOPER, EXTRAN, and ONE-D, (Treske's Data, Case 8).

Criterion	Observed	DWOPER	EXTRAN	ONE-D
Q_p (m^3/s)	0.344	0.328	0.360	0.327
T_p (min)	43-47	45.00	41.00	45.00
Graphical	N/A	Best	Better	Good
SS	N/A	0.0038	0.0220	0.0220
N & S	N/A	0.9957	0.9749	0.9749
RMSE	N/A	0.0072	0.0172	0.0172
SEE	N/A	0.0073	0.0175	0.0175
REE	N/A	0.0658	0.1583	0.1583
PEE	N/A	0.0284	0.0684	0.0684
TARE	N/A	1.7775	10.049	4.5306

Criterion	Observed	DWOPER	EXTRAN	ONE-D
D_p (m)	0.460	0.451	0.469	0.449
T_p (min)	43-47	45.00	41.00	45.00
Graphical	N/A	Best	Better	Good
SS	N/A	0.0017	0.0260	0.0920
N & S	N/A	0.9982	0.9732	0.9053
RMSE	N/A	0.0048	0.0187	0.0353
SEE	N/A	0.0049	0.0190	0.0357
REE	N/A	0.0418	0.1636	0.3078
PEE	N/A	0.0120	0.0467	0.0879
TARE	N/A	0.8677	4.1685	2.2345

Table 8.19 Statistical Criteria Employed to Evaluate the Goodness-of-Fit of Simulated Hydrographs Using DWOPER, EXTRAN, and ONE-D, (Treske's Data, Case 9).

Criterion	Observed	DWOPER	EXTRAN	ONE-D
Q_p (m^3/s)	0.380	0.371	0.360	0.372
T_p (min)	75-76	75.00	75.00	75.00
Graphical	N/A	Best	Good	Better
SS	N/A	0.0019	0.0887	0.0063
N & S	N/A	0.9987	0.9380	0.9956
RMSE	N/A	0.0042	0.0289	0.0077
SEE	N/A	0.0043	0.0292	0.0078
REE	N/A	0.0364	0.2490	0.0664
PEE	N/A	0.0144	0.0984	0.0262
TARE	N/A	1.7501	13.794	3.8680

Criterion	Observed	DWOPER	EXTRAN	ONE-D
D_p (m)	0.481	0.475	0.469	0.475
T_p (min)	75-76	75.00	75.00	75.00
Graphical	N/A	Best	Good	Better
SS	N/A	0.0013	0.0723	0.0058
N & S	N/A	0.9990	0.9470	0.9958
RMSE	N/A	0.0035	0.0261	0.0074
SEE	N/A	0.0035	0.0264	0.0075
REE	N/A	0.0309	0.2301	0.0652
PEE	N/A	0.0079	0.0591	0.0167
TARE	N/A	1.0223	7.1693	1.9703

Table 8.20 Statistical Criteria Employed to Evaluate the Goodness-of-Fit of Simulated Hydrographs Using DWOPER, EXTRAN, and ONE-D, (Treske's Data, Case 10).

Criterion	Observed	DWOPER	EXTRAN	ONE-D
Q_p (m^3/s)	0.394	0.3794	0.400	0.383
T_p (min)	105-108	105-108	102-105	105-108
Graphical	N/A	Best	Good	Better
SS	N/A	0.0056	0.0070	0.0056
N & S	N/A	0.9926	0.9908	0.9926
RMSE	N/A	0.0087	0.0097	0.0087
SEE	N/A	0.0088	0.0099	0.0088
REE	N/A	0.0860	0.0962	0.0860
PEE	N/A	0.0346	0.0387	0.0346
TARE	N/A	1.7220	2.7046	2.4149

Criterion	Observed	DWOPER	EXTRAN	ONE-D
D_p (m)	0.488	0.4816	0.4930	0.4820
T_p (min)	105-108	105-108	102-105	105-108
Graphical	N/A	Best	Good	Better
SS	N/A	0.0027	0.0070	0.0042
N & S	N/A	0.9961	0.9899	0.9939
RMSE	N/A	0.0060	0.0097	0.0075
SEE	N/A	0.0061	0.0099	0.0076
REE	N/A	0.0625	0.1006	0.0780
PEE	N/A	0.0162	0.0261	0.0202
TARE	N/A	0.9184	1.6294	1.2531

Table 8.21 Statistical Criteria Employed to Evaluate the Goodness-of-Fit of Simulated Hydrographs with DWOPER, EXTRAN, and ONE-D Applied to Myers' Data.

Criterion	Observed	DWOPER	EXTRAN	ONE-D
Q_p (m^3/s)	78.845	77.273	68.690	68.693
T_p (hrs)	268.00	268.00	268.00	268.00
Graphical	N/A	Best	Better	Good
SS	N/A	664.205	1477.6	1497.5
N & S	N/A	1.0000	1.0000	1.0000
RMSE	N/A	1.9825	2.9569	2.9767
SEE	N/A	1.9943	2.9745	2.9945
REE	N/A	0.0013	0.0020	0.0020
PEE	N/A	0.0719	0.1073	0.1080
TARE	N/A	15.711	24.389	24.458

Criterion	Observed	DWOPER	EXTRAN	ONE-D
D_p (m)	2.737	2.694	2.461	2.603
T_p (hrs)	268.00	268.00	268.00	268.00
Graphical	N/A	Best	Better	Good
SS	N/A	0.5460	1.1990	1.6590
N & S	N/A	0.9904	0.9790	0.9710
RMSE	N/A	0.0568	0.0842	0.0991
SEE	N/A	0.0572	0.0847	0.0997
REE	N/A	0.0977	0.1448	0.1704
PEE	N/A	0.0474	0.0702	0.0826
TARE	N/A	7.2908	10.605	18.846

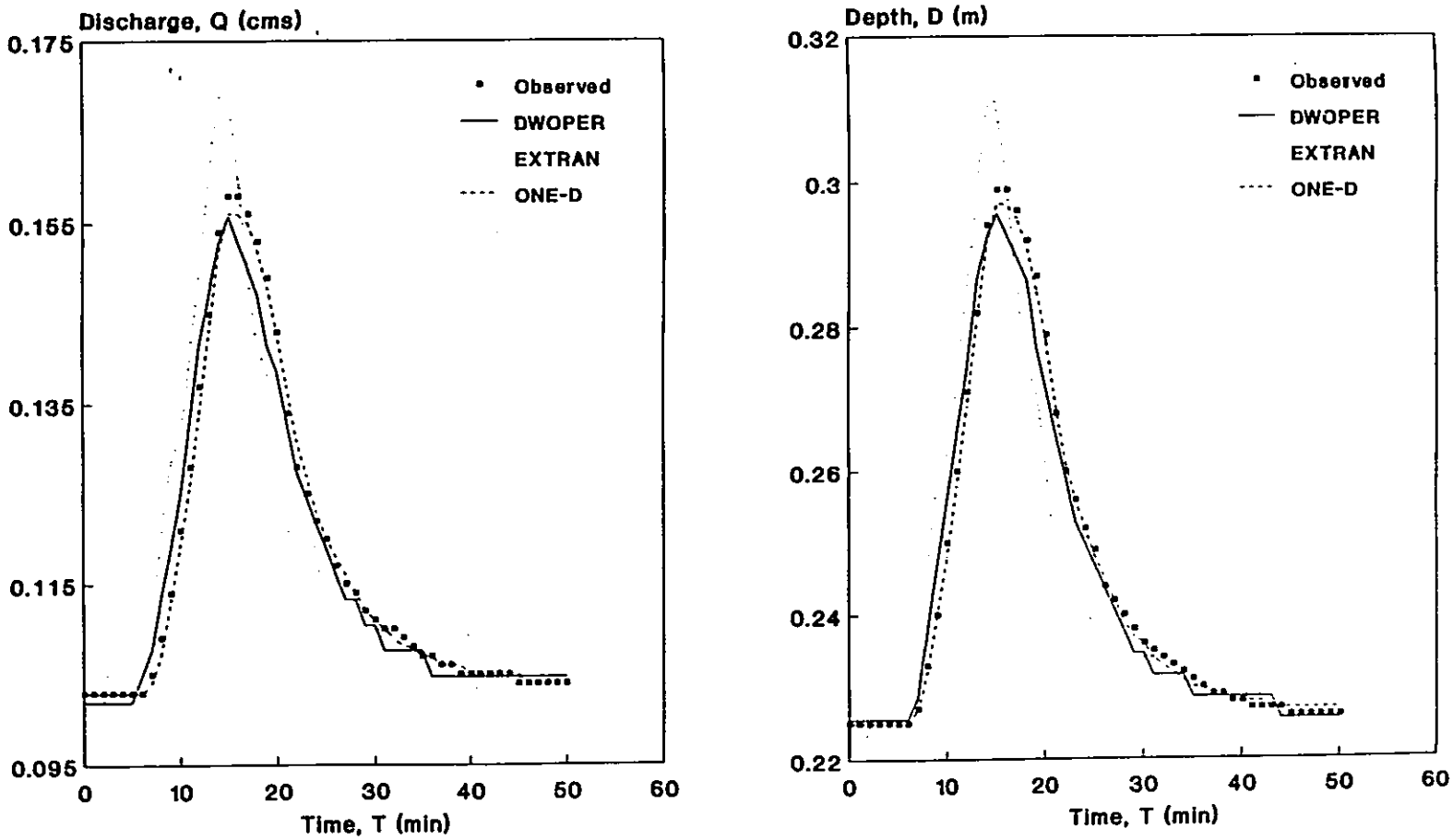

Figure 8.1 Simulated vs. Observed Discharge and Depth Hydrographs Using DWOPER, EXTRAN, and ONE-D, (Treske's Data, Case 1).

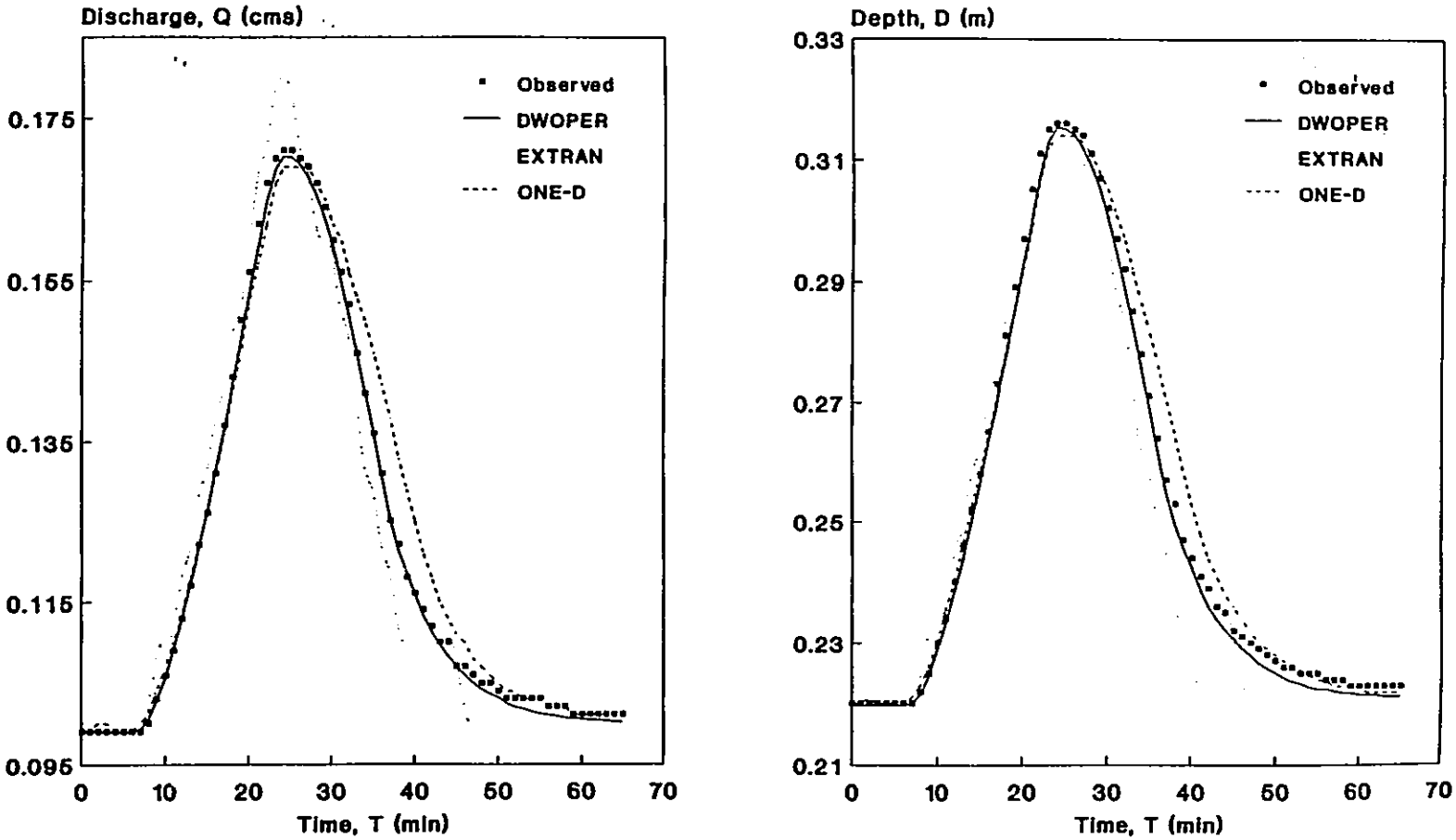

Figure 8.2 Simulated vs. Observed Discharge and Depth Hydrographs Using DWOPER, EXTRAN, and ONE-D, (Treske's Data, Case 2).

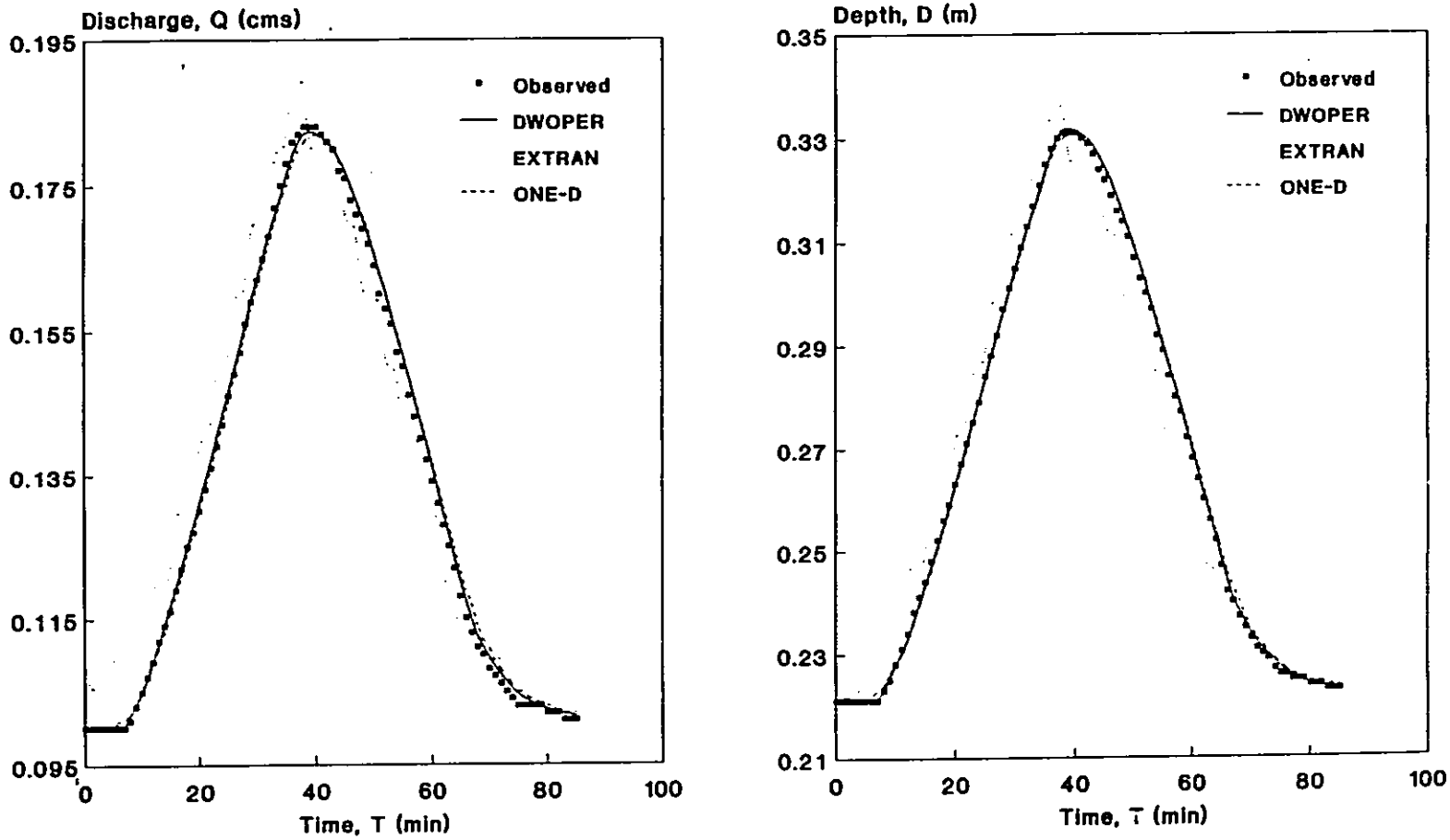

Figure 8.3 Simulated vs. Observed Discharge and Depth Hydrographs Using DWOPER, EXTRAN, and ONE-D, (Treske's Data, Case 3).

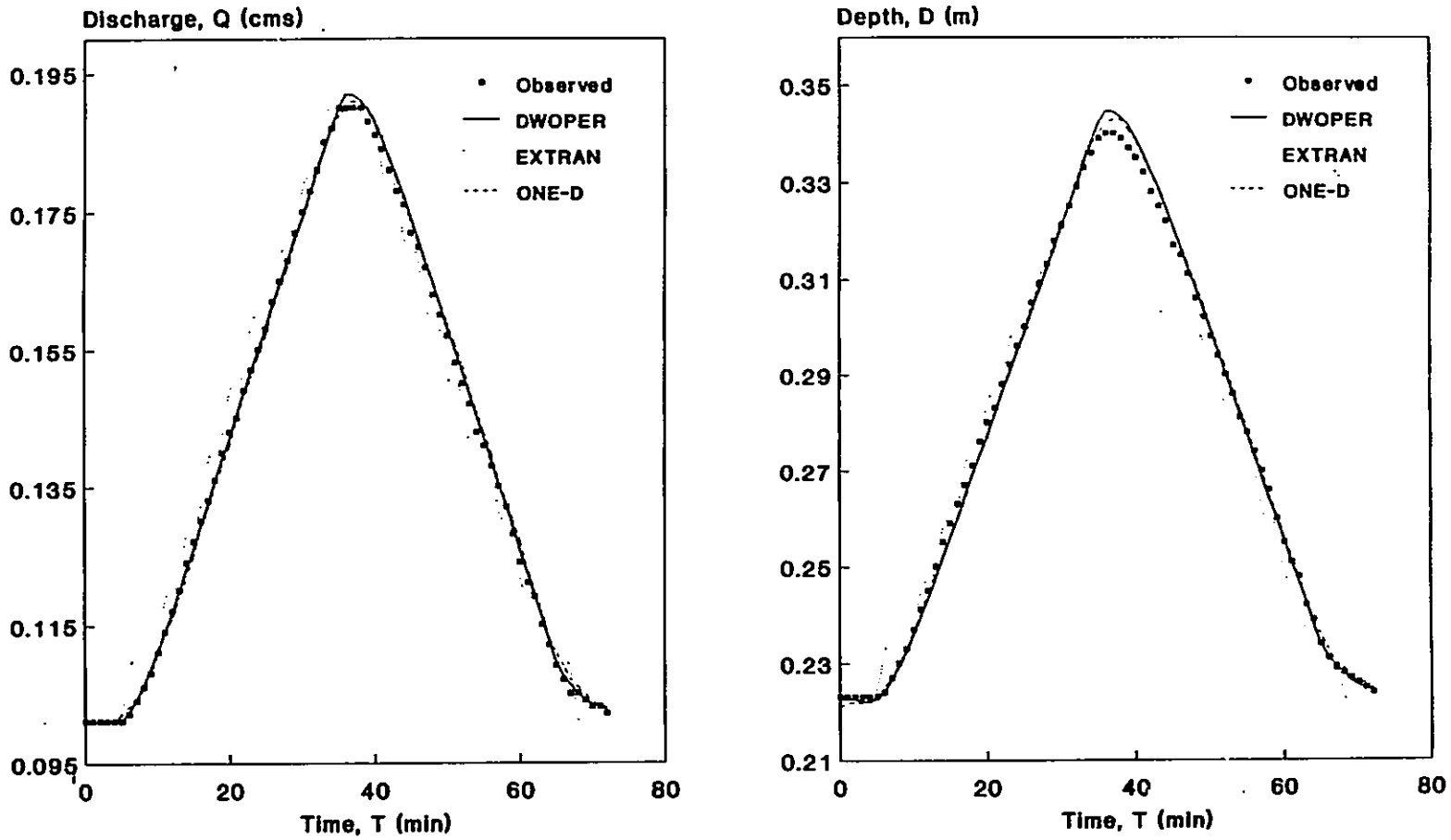

Figure 8.4 Simulated vs. Observed Discharge and Depth Hydrographs Using DWOPER, EXTRAN, and ONE-D, (Treske's Data, Case 4).

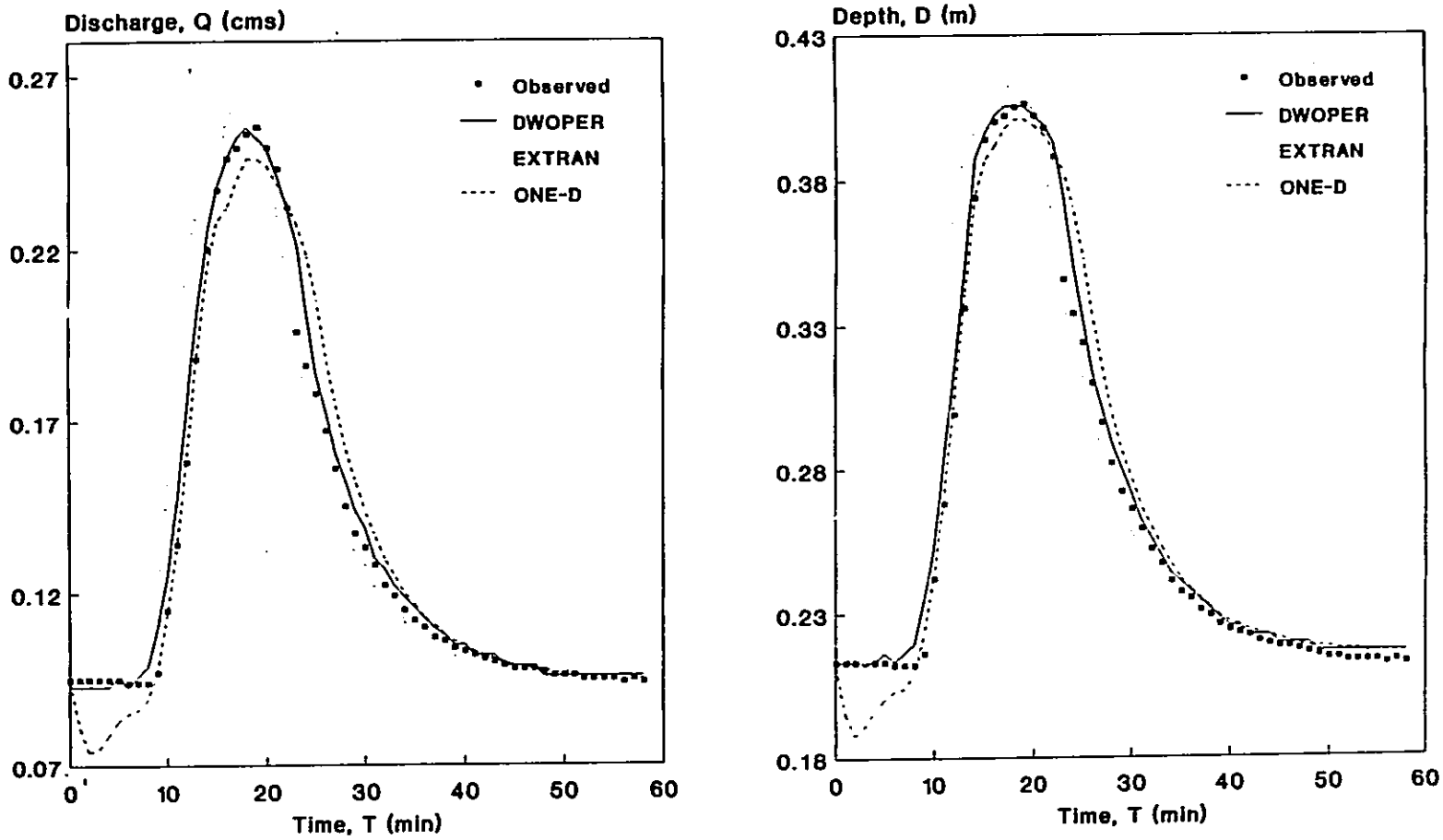

Figure 8.5 Simulated vs. Observed Discharge and Depth Hydrographs Using DWOPER, EXTRAN, and ONE-D, (Treske's Data, Case 5).

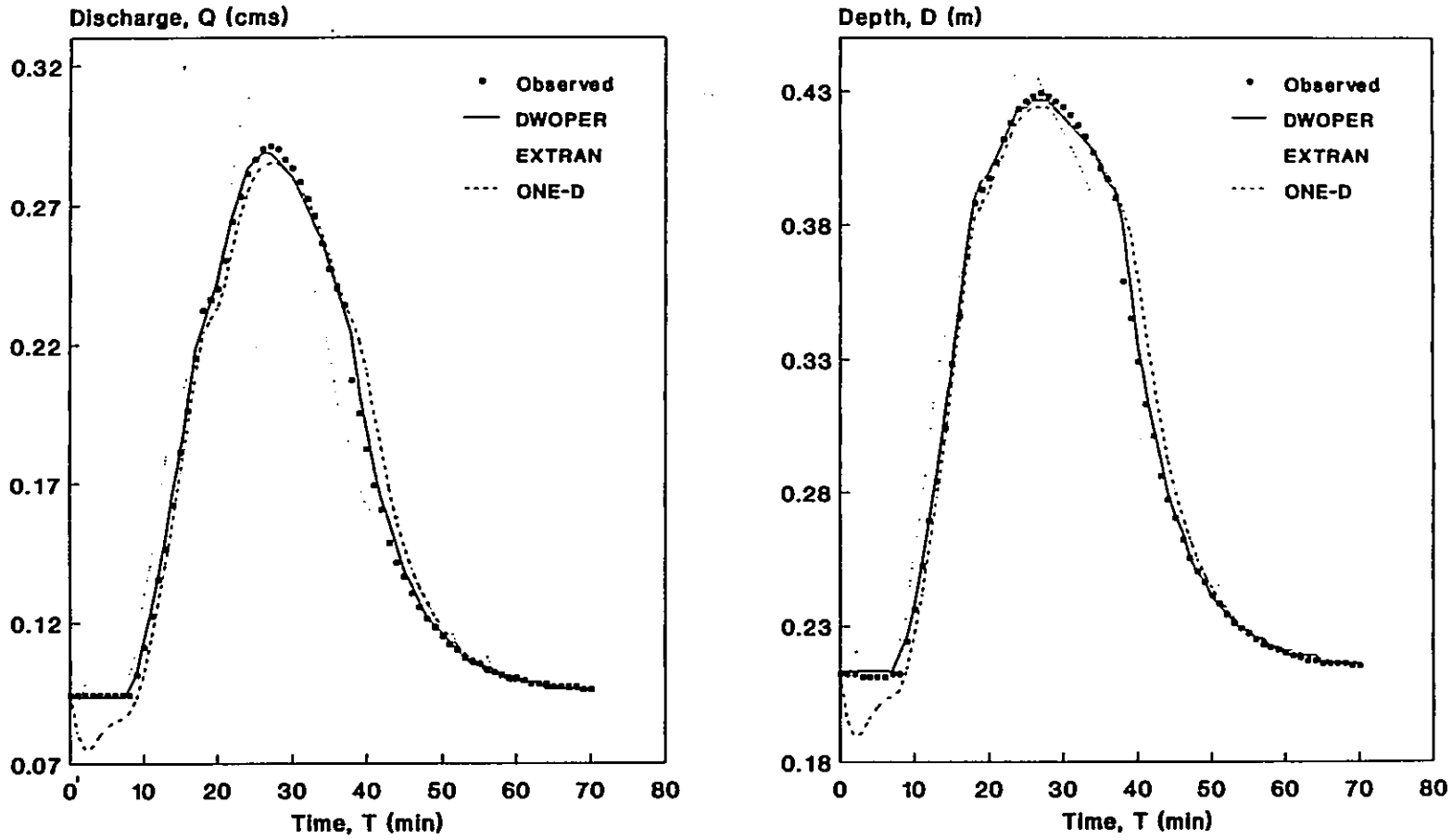

Figure 8.6 Simulated vs. Observed Discharge and Depth Hydrographs Using DWOPER, EXTRAN, and ONE-D, (Treske's Data, Case 6).

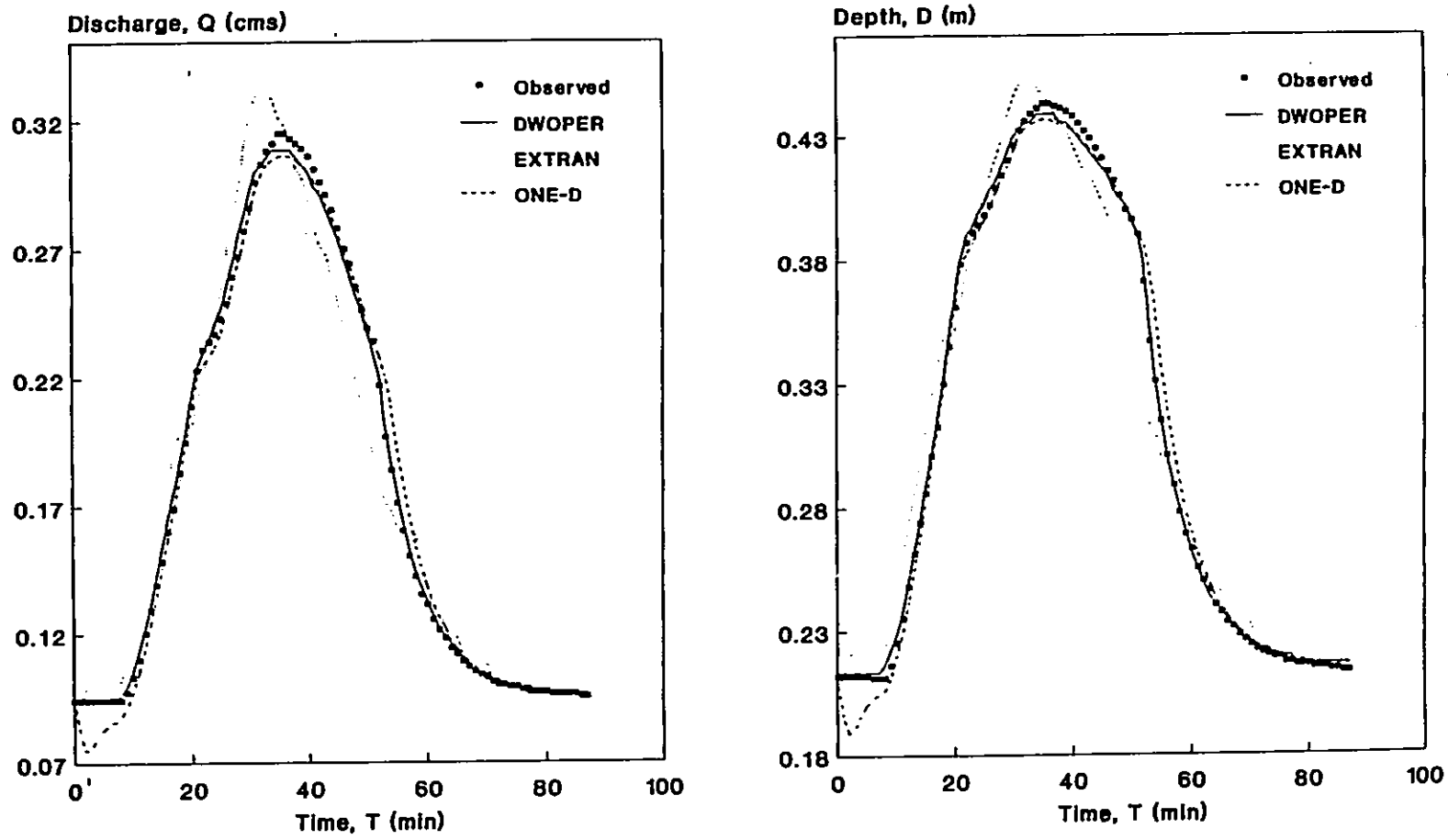

Figure 8.7 Simulated vs. Observed Discharge and Depth Hydrographs Using DWOPER, EXTRAN, and ONE-D, (Treske's Data, Case 7).

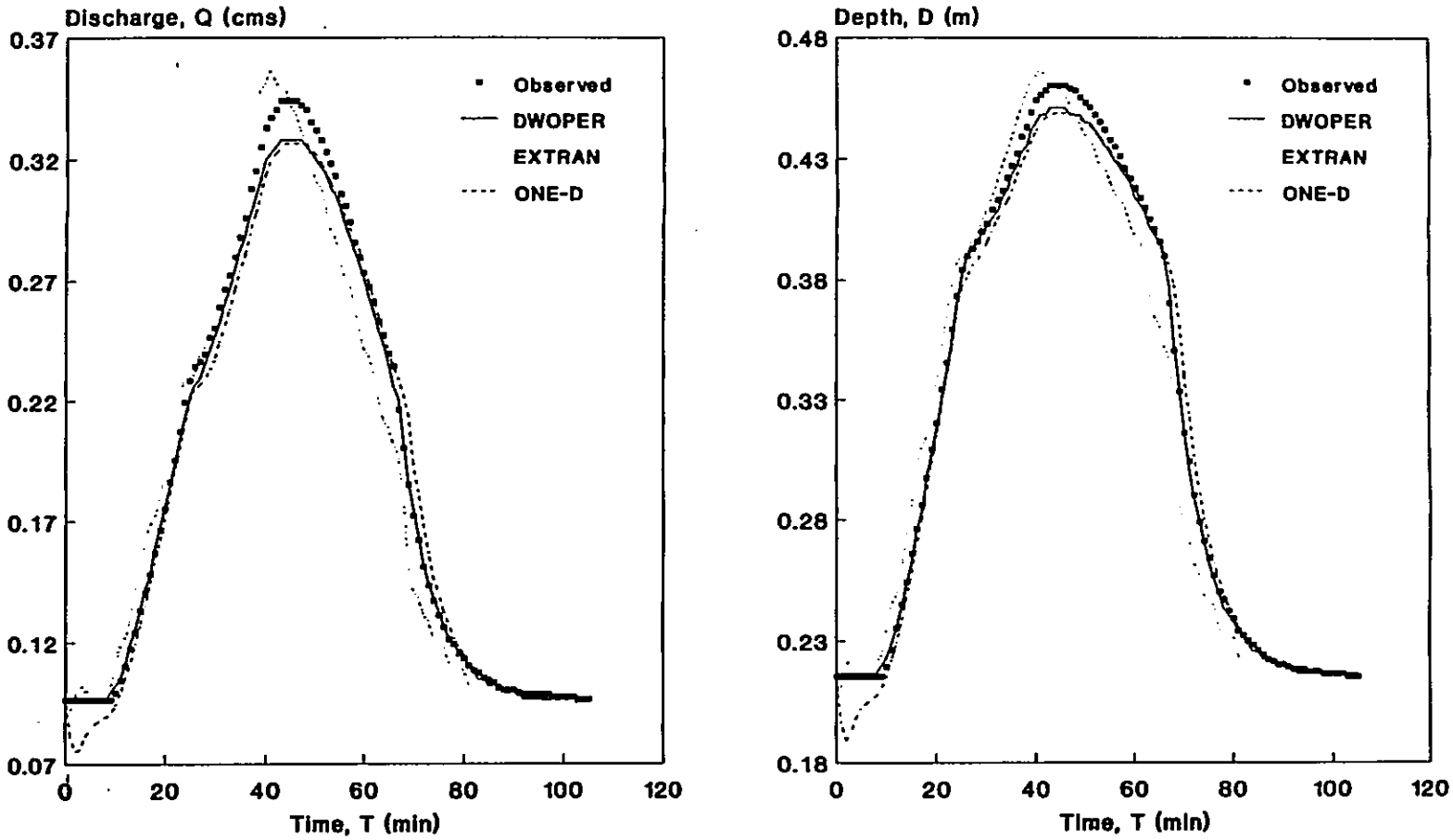

Figure 8.8 Simulated vs. Observed Discharge and Depth Hydrographs Using DWOPER, EXTRAN, and ONE-D, (Treske's Data, Case 8).

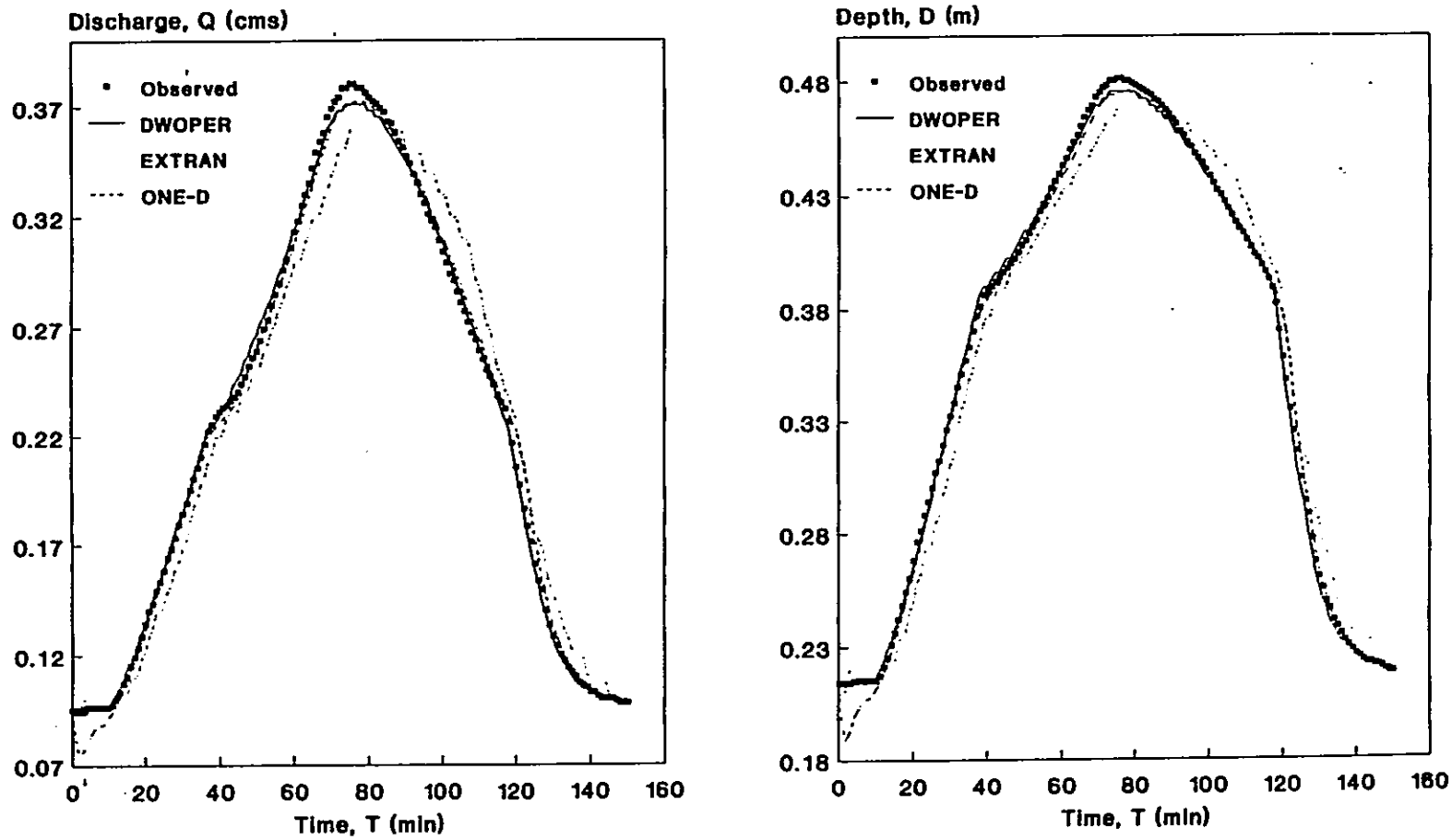

Figure 8.9 Simulated vs. Observed Discharge and Depth Hydrographs Using DWOPER, EXTRAN, and ONE-D, (Treske's Data, Case 9).

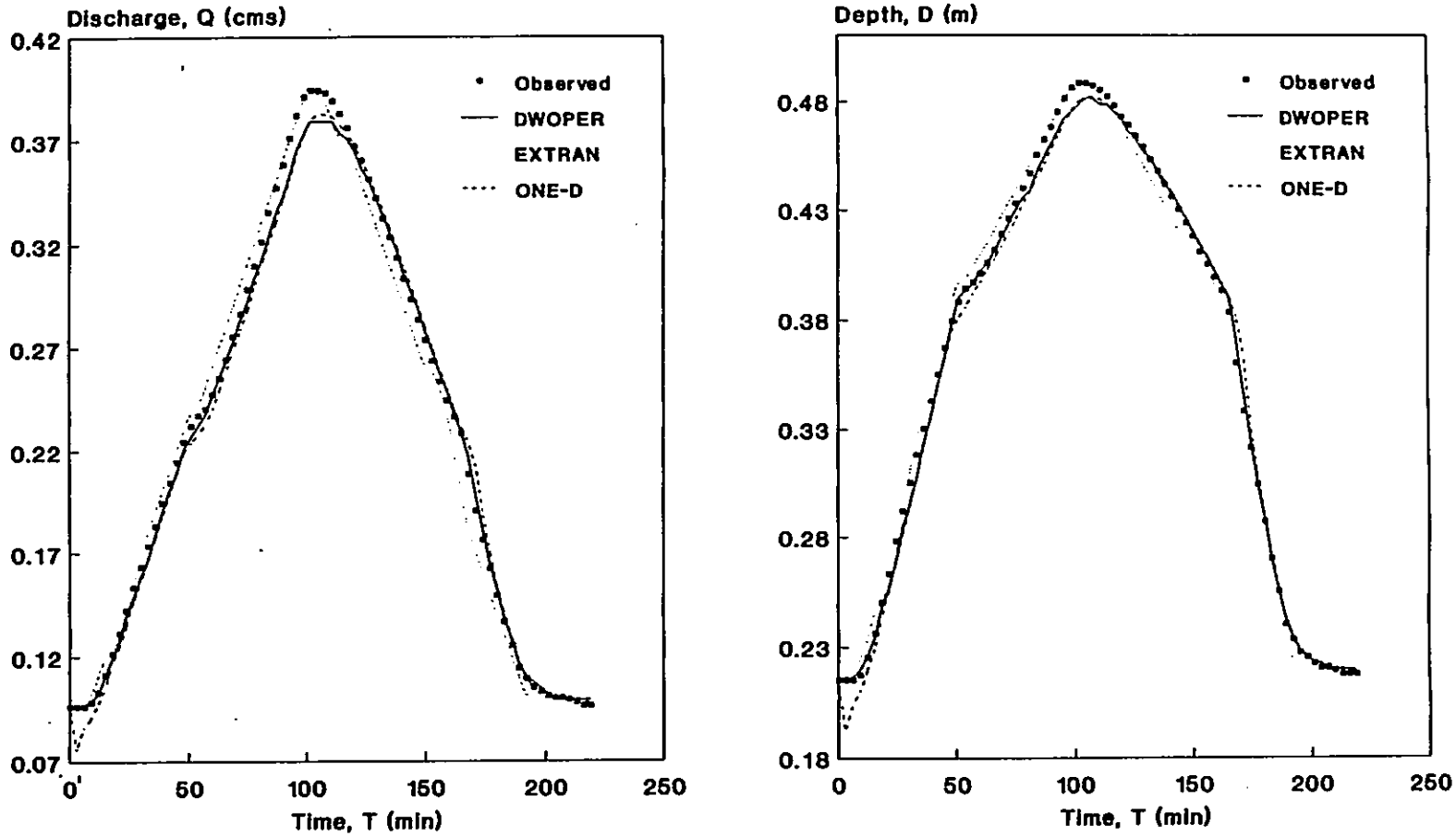

Figure 8.10 Simulated vs. Observed Discharge and Depth Hydrographs Using DWOPER, EXTRAN, and ONE-D, (Treske's Data, Case 10).

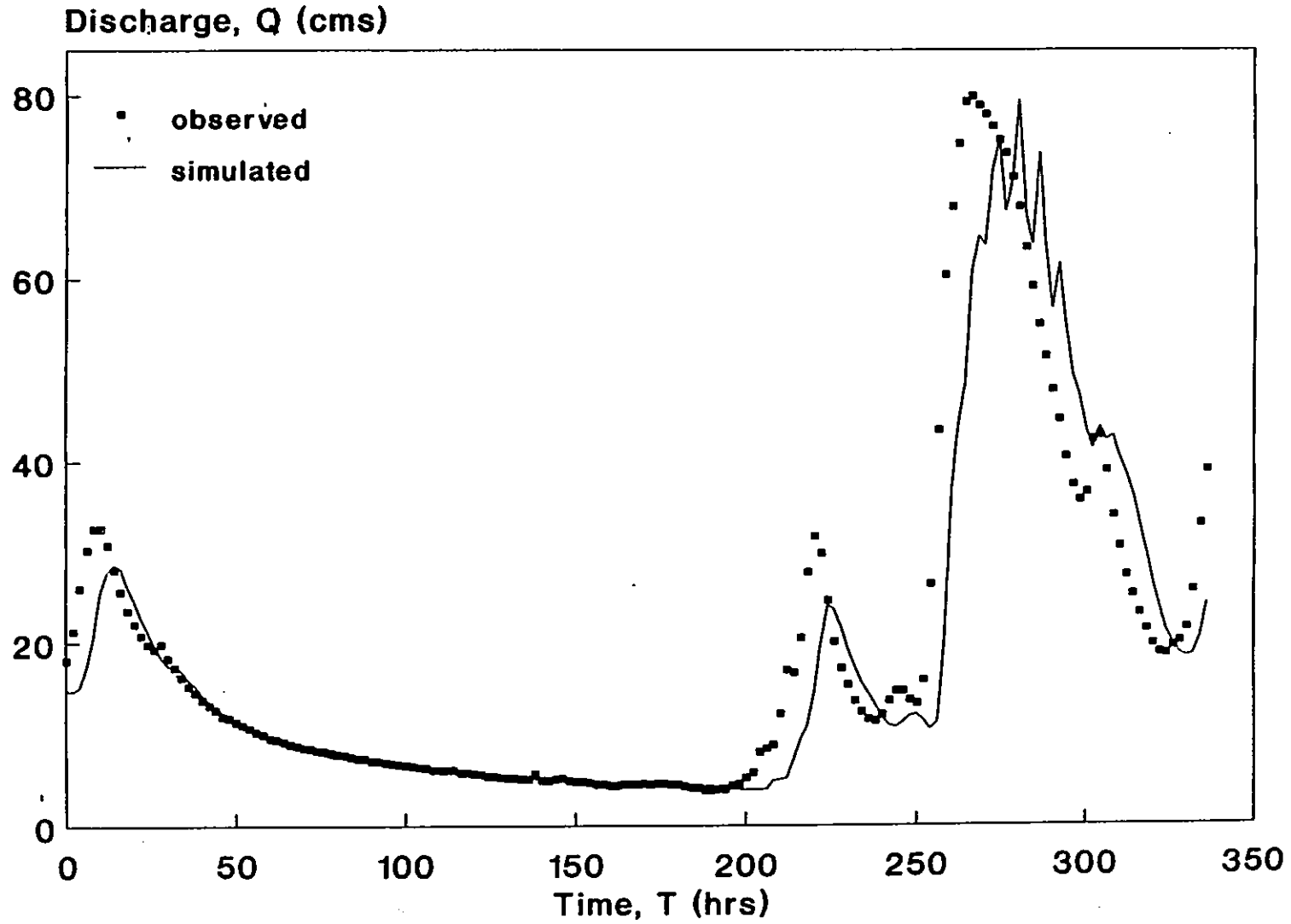

Figure 8.11 Effect of a Large Time Step (30 minutes) on the Stability and Accuracy of the Simulated Discharge Hydrograph for Myers' Data using DWOPER.

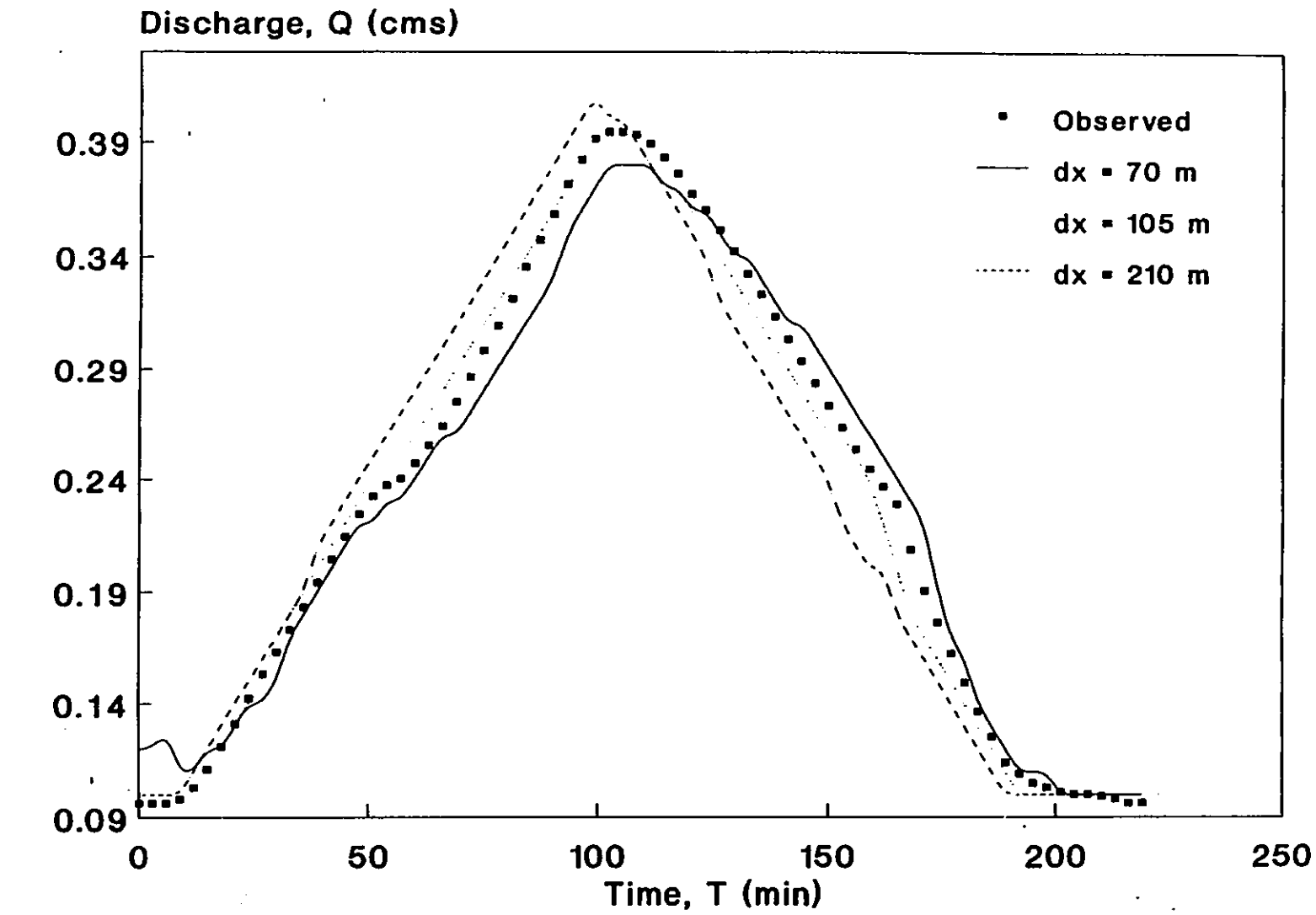

Figure 8.12 Effect of Distance Step Variation on the Simulated Discharge Hydrograph Using EXTRAN, (Treske's Data, Case 10).

CHAPTER 9

CONCLUSIONS AND RECOMMENDATIONS

9.1 CONCLUSIONS

In this study, a comparative evaluation of three dynamic flow routing models (DWOPER, EXTRAN, and ONE-D) was performed. The three models were applied successfully to model simple- and compound-channel flows in a straight experimental compound prismatic channel and in a compound river channel. Based on these applications, the following were the main conclusions:

1- For the present research, different statistical goodness-of-fit techniques were investigated to evaluate the performance of the three hydrodynamic models under consideration. The graphical assessment technique was employed occasionally. Simulated results were plotted on the same graph against observed data, and a visual check was performed. This method gives a good appreciation of the impact

of parameter variation on model performance. However, it may be misleading in some occasions when a visual check is made for the rising and recession parts of the hydrograph. A visual check may appear to have an excellent fit, but the actual relative error at that point could be substantial (up to 30 % in some instances).

2- Statistical goodness-of-fit techniques were used in this research to evaluate model performance . Several methods were used including: sum of squares criteria, Nash and Sutcliffe (N & S) method, RMSE, SEE, REE, PEE, and TARE.

3- Matching peak stage or discharge should not be the only criterion in deciding whether the simulated results are acceptable or not. This is due to the fact that while an excellent fit may occur around the peak value, a poor fit may be achieved on the rising and recession parts of the corresponding hydrograph.

4- A new "goodness-of-fit" method was introduced which determined the relative percent error at every point of the simulated hydrograph. Absolute values of the corresponding relative percent errors (at every point) were summed to give the total absolute percent relative error or the total absolute relative error (TARE). In general, hydrographs with the least total absolute relative errors would give the best-fit.

5- DWOPER was applied successfully to model flow in a straight experimental prismatic channel and in a compound non-prismatic river channel. The following were the main conclusions:

5.1- In the case of Treske's data, changing the weighting factor did not significantly improve the simulated hydrographs.

5.2- DWOPER assumes the top width as the wetted perimeter. This assumption is generally not valid for modelling laboratory (Treske's) data. Accordingly,

a relationship to compensate for the under-estimation of the wetted perimeter had to be introduced.

5.3- In the case of both data sets, assuming an irregular channel cross-section with no storage did not produce satisfactory simulations. This was thought to be can be due to the fact that depths over the flood plains were small and thus flood plain roughness would have a major impact on flood plain conveyance. In addition, the wetted perimeter changes dramatically at the bank-full depth.

5.4- Introducing (imaginary) vertical and outward-facing diagonal interface planes, to separate the main channel and flood plain zones of compound channels, gave generally good results.

5.5- Compared to diagonal interface planes, vertical interface planes produced smaller overall error in the simulated hydrographs for Treske's laboratory data but were less successful when applied to Myers' field data.

5.6- The inclination of the diagonal interface planes to the horizontal was adjusted to reflect changing hydraulic conditions. Equation 5-14 was developed to define the flood plain hydraulic boundaries. This equation relates the variation of Θ with the ratio of the flood plain depth to the total flow depth.

6- EXTRAN was applied to model flow in a prismatic rectangular laboratory channel (Treske, 1981), and a field non-prismatic natural channel (Myers, 1991). Being an explicit model, EXTRAN has a restriction on the size of the computational time step due to reasons of numerical stability. The stability criterion indicates that the computational time step is substantially reduced as the hydraulic depth (A/B) increases. Therefore, small time steps, in the order of a few minutes or seconds, are

used. In addition, careful choice of the time step and the distance step should be made to ensure a successful run.

7- In general, EXTRAN produced good simulations. However, some discrepancies appeared at various points on the simulated hydrographs.

8- A number of modifications were made to the laboratory and field data sets to improve efficiency and the model's ability to converge to a solution. However, the required modifications differ from one model to another, based on the assumptions adopted in developing the different models.

9- Examination of the simulated results of the three models and the statistical goodness-of-fit techniques indicates that ONE-D was superior to DWOPER and EXTRAN when applied to model (in-bank) flows in the single rectangular channel of Treske (1980). However, beyond the in-bank flow depth DWOPER's performance was superior, whether applying vertical or outward-facing diagonal interface planes.

10- EXTRAN shows considerable over-estimation of channel discharge capacity at low flood plain depths. DWOPER and ONE-D, on the other hand, show minor under-estimation of peak stages and discharges. Furthermore, an inspection of the results shows that DWOPER was superior in simulating flows in the natural non-prismatic channel, (Myers, 1991). In addition, EXTRAN simulations for Myers' data set were better than those obtained using ONE-D.

11- Inspection of the model simulations indicates that simulated peak stages and discharges, except for some cases of EXTRAN simulations, were occurring at the same peaking time as those observed. In the case of EXTRAN, peaks occurred one time step before the actual peaking time . This may be due to an over-estimation of Manning's roughness coefficient. Yen and Overton (1973) indicated that

Manning's n for flow computations reflects not only the influence of boundary roughness but also the effects of channel geometry.

12- Finally, inspecting the model simulations and the statistical goodness-of-fit criteria one can conclude that DWOPER was superior to the both EXTRAN and ONE-D models and ONE-D was generally superior to EXTRAN.

9.2 RECOMMENDATIONS FOR FUTURE RESEARCH

1- In this study, only the "no storage option", and vertical and diagonal interface planes (separating shallow and deep regions of the flow field) were considered. It would be appropriate, therefore, to examine other possible storage alternatives, such as horizontal interface plains, or a "parabolic-type function".

2- The models examined in this study do not account for lateral momentum transfer (LMT). Thus, it would be important to study this phenomenon by developing a model that accounts for LMT.

3- Available models quantify LMT based on steady-state flow conditions. It is necessary to investigate this mechanism experimentally under unsteady flow conditions.

4- DWOPER assumes the channel top width to be equal to the wetted perimeter. It is recommended to modify the formulation of the model to use the actual wetted perimeter in calculations.

5- The equation defining the flood plain hydraulic boundaries (eq. 5-14) considers the inclination of the diagonal interface plains (θ) is a function of the ratio of the depth of flood plain flow to the total flow depth. An investigation should be made to study the effects of other parameters on θ, such as Manning's roughness coefficient

and the channel geometry.

6- In addition to Treske's and Myers' data, the validity of eq. 5-14 was checked by applying it to Yilmaz's experimental steady-state data. It is recommended to check its application and validity based on other data sets.

7- DWOPER, EXTRAN, and ONE-D are only applicable to channels with rigid boundaries. Future research efforts should modify these models to make them applicable to channels with mobile beds, (note that the modified model: ONE-D-SED has already been developed).

8- These models were applied to simple and compound straight channels. Future research efforts should apply them to meandering channels with flood plains.

9- In this study, three flood routing models were applied to model subcritical flow conditions. It would be appropriate to study their performance under supercritical flow conditions.

REFERENCES

[1] Abbott, M.B., "An Introduction To The Method Of Characteristics," American Elseviers, New York, 1966.

[2] Abbott, M.B., "Discussion of Review of Models of Tidal Waters by J.B. Hinwood and I.G. Wallis," Journal of the Hydraulics Division, ASCE, Vol. 102, No. HY8, pp. 1145-1148, 1976.

[3] Abbott, M.B., and Ionescu, F., "On the Numerical Computation of Nearly Horizontal Flows," Journal of the Hydraulic Research, Vol. 5, No. 2, pp. 97-117, 1967.

[4] Aitken, A.P., "Assessing Systematic Errors in Rainfall-Runoff Models," Journal of Hydrology, 20:121-36, 1973.

[5] Amein, M., "Streamflow Routing On Computer By Characteristics Water Resources Research, Vol. 2, No. 1, First Quarter 1966, pp. 123-130.

[6] Amein, M., and Chu, H.L., "Implicit Numerical Modelling Of Unsteady Flows," Journal of the Hydraulics Division, ASCE, Vol. 101, No. HY6, 1975, pp. 717-1451.

[7] Amein, M., and Fang, C., "Implicit Flood Routing In Natural Channels," Journal Of The Hydraulic Division, ASCE, No. HY12, December, 1970, pp. 2481-2500.

[8] Amorocho, J., and Strelkoff, T.S., "Hydraulic Transients In The California Aqueduct," Report No. 2, Water Science And Engineering Paper No. 1008, Department of Water Science And Engineering, University Of California At Davis, June, 1965.

[9] Baltzer, R.A., and Lai, C., "Computer Simulation Of Unsteady Flows In Water-Ways," Journal Of The Hydraulic Division, ASCE, Vol. 94, No. HY4, 1968, pp. 1083-1117.

[10] Boussinesq, J., "Theory Of The Liquid Intumescene, Called A Solitary Wave Or A Wave Of Translation, Propagated In A Channel Of Rectangular Cross-Section," Comptes Rendus, Vol. 72, Academy Science, Paris, 1871, pp. 755-759.

[11] Brakensiek, D.L., "An Implicit Flood Routing Method," Hydraulics Division

Specialty Conference, ASCE, Tucson, Arizona, 1965.

[12] Bravo, S.C.A., Harely, B.M., and Perkins, F.E., "A Linear Distributed Model of Catchment Runoff," Hydrodynamics Laboratory Report 123 , Department of Civil Engineering, Massachusetts Institute of Technology, Cambridge, Massachusetts, 1970.

[13] Chaudhry, Y.M., and Contactor, D.N., "Application of Implicit Method to Surges in Channels," Water Resources Research, Vol. 9, No. 6, pp. 1605-1612, 1973.

[14] Chen, Y.H., and Simon, D.B., "Mathematical Modelling of Alluvial Channels," Symp. on Modelling Techniques, ASCE, New York, N.Y., pp. 466-483, 1975.

[15] Chow, V.T., "Open-Channel Hydraulics," McGraw-Hill Book Co., New York, pp. 601-604, 1959.

[16] Clarke, R.T., "A Review of Some Mathematical Models Used in Hydrology, with Observations on Their Calibration and Use," Journal of Hydrology, 19:1-19, 1973.

[17] Cooley, R.L., and Moin, S.A., "Finite Element Solution of Saint-Venant Equations," Journal of the Hydraulics Division, ASCE, Vol. 102, No. HY6, pp. 759-775, 1976.

[18] CSCE Task Committee on Evaluation of River Models, "Comparative Evaluation of River Models," Proceedings of the CSCE annual Conference, Hamilton, 1990.

[19] Cunge, J.A., "Etude d'un Schema de Differences Finies Applique a l'Integration Numerique d'un Certain Type d'Equation Hyperbolique d'Ecoulement," Thesis, Grenoble University, France, 1966.

[20] Cunge, J.A., "On the Subject of a Flood Propagation Computation Method (Muskingum Method)," Journal of Hydraulic Research, Vol. 7, No. 2, pp. 205-230, 1969.

[21] Cunge, J.A., Rapidly Varying Flow in Power and Pumping Canals, in: K. Mahmood and V. Yevjevich (Editors), Unsteady Flow in Open Channels, Vol. II, Chapter 14, pp. 539-586, Water Resources Publications, Fort Collins, Colorado, 1975.

[22] Cunge, J.A, and Wegner, M., "Integration Numerique des Equations D'Ecoulement De Barre de Saint-Venant Par Un Schema Implicite De Differences Finies," La Houille Blanche, Grenoble, France, No. 1, pp. 33-39, 1964.

[23] Chatila, J.G., and Townsend, R.D., "The Off-Channel Storage Consideration in Modelling Compound Channel Flows," Proceedings of the CSCE Bi-annual Conference, Quebec City, Vol. II, May, 1992.

[24] Dawdy, D.R., and O'Donnell, T., "Mathematical Model of Catchment Behaviour," Journal of the Hydraulics Division, Proceedings of ASCE, Vol. 91, No. HY4, pp. 123-137, 1965.

[25] De Long , L.L., "Mass Conservation: 1-D Open Channel Flow Equations," Journal of the Hydraulic Engineering, Vol. 115, No. 2, pp.263-269, Feb., 1989.

[26] De Saint Venant, A.J.C. Barre', "Théorie du mouvement non-permanent des Eaux avec Application aux crues des Rivieres et a l'introduction des Mareées dans leur lit," (Theory of Unsteady Water Flow, with Apllication to River Floods and to Propagation of Tides in River Channels), Comptes Rendus, Vol. 73, Academy Science, Paris, 1871, pp. 148-154, 237-240.

[27] Diskin, M.H., and Simon, E., "A Procedure for the Selection of Objective Functions for Hydrologic Simulation Models," Journal of Hydrology, 34(1/2):129-49, 1977.

[28] Dooge, J.C.I., "Linear Theory Of Hydraulic Systems," Technical Bulletin No. 1468, USDA Agriculture Research Service, 1973.

[29] Dracos, T., and Hardegger, P., "Steady Uniform Flow in Prismatic Channels with Flood Plains," Journal of Hydraulic Research, Vol. 25, No. 2, pp. 169-185, 1987.

[30] Dronkers, J.J., and Schönfeld, J.C., "Tidal Computations in Shallow Water," ASCE Proc., Vol. 81, separate No. 714, pp. 50, June, 1955.

[31] Dronkers, J.J., "Tidal Computations In Rivers And Coastal Waters," Interscience Publishers, Inc., New York, 1964.

[32] Dronkers, J.J., "Tidal Computations for Rivers, Coastal Areas, and Seas," Journal of the Hydraulics Division, ASCE, Vol. 95, No. HY1, pp. 29-77, 1969.

[33] EXTRAN, EXTRAN Input Data Manual, EPA, 1973.

[34] Fletcher, A.G., and Hamilton, W.S., "Flood Routing In Irregular Channel," Journal of The Engineering Mechanics Division, ASCE, Vol. 93, No. EM3, June, 1967, pp. 45-62.

[35] Fletcher, R. and Powell, M.J.D., "A Rapidly Convergent Descent Method for

Minimization," Computer Journal,6(2):163-86, 1963.

[36] Fread, D.L., "Effect of Time Step Size in Implicit Routing," Water Resources Bulletin, American Water Resources Association, Vol.9, No. 2, Mar., 1973, pp. 338-351.

[37] Fread,D.L., "Numerical Properties Of Implicit Four-Point Finite Difference Equations Of Unsteady Flow," NOAA Technical Memorandum NWS HYDRO 18, NOAA, March 1974, pp. 88.

[38] Fread, D.L., "Discussion Of Comparison Of Four Numerical Methods For Flood Routing," R.K. Price, Journal Of The Hydraulic Division, ASCE, Vol. 101, No. HY3, 1975, pp. 565-567.

[39] Fread, D.L. "Flood Routing: A Synopsis of Past, Present, Future Capability," Proceedings of the International Symposium on Rainfall-Runoff Modelling, Mississippi State, Miss., May 18-22, 1981.

[40] Fread, D.L., DWOPER Manual, 1978, Revised Version, April, 1987.

[41] Friedrichs and Lewy 1928.

[42] Garrison, J.M., Granju, J.P., and Price, J.T., "Unsteady Flow Simulation in Rivers and Reservoirs," Journal of the Hydraulics Division, ASCE, Vol. 95, No. HY5, pp.1559-1576, 1969.

[43] Gburek, W.J., and Overton, D.E., "Subcritical Kinematic Flow in a Stable Stream," Journal of the Hydraulics Division, ASCE, Vol. 99, No. HY9, pp. 1433-1447, 1973.

[44] Gunaratnam, D.J., and Perkins, F.E., "Numerical Solution of Unsteady Flows in Open Channels," Hydrodynamic Laboratory Report 127, Department of Civil Engineering, Massachusetts Institute of Technology, Cambridge, Massachusetts, 1970.

[45] Harder, J.A., and Armacost, L.V., "Wave Propagation in Rivers," Hydraulic Engineering Laboratory, Report No. 1, Series 8, University of California, Berkeley, 1966.

[46] Harley, B.M., "Linear Routing in Uniform Channels," Thesis, University College, Cork, Ireland, 1967.

[47] Harley, B.M., Perkins, F.E., and Eagleson, P.S., "A Modular Distributed Model of

Catchment Dynamics," Hydrodynamics Laboratory Report 133, Department of Civil Engineering, Massachusetts Institute of Technology, Cambridge, Massachusetts, 1970.

[48] Harleman, D.R.F., and Lee, C.H., "The Computation of Tides and Currents in Estuaries and Canals," U.S. Army Corps of Engineers Report, Oct., 1967.

[49] Harleman, D., ONE-D input data manual, MIT, 1974.

[50] Harris, G.S., "Real Time Routing Of Flood Hydrographs In Storm Sewers," Journal Of The Hydraulics Division, ASCE, Vol. 96, No. HY6, 1970, pp. 1247-1260.

[51] Henderson, F.M., "Open Channel Flow," Macmillan Company, New York, 1966.

[52] Henderson, F.M., and Wooding, R.A., "Overland Flow and Groundwater Flow from Steady Rainfall of Finite Duration," Journal of Geophysical Research, Vol. 69, No. 8, April, 1964.

[53] Hinwood, J.B., and Wallis, I.G., "Classification of Models of Tidal Waters," Journal of the Hydraulics Division, ASCE, Vol. 101, No. HY10, pp. 1315-1331, 1975a.

[54] Hinwood, J.B., and Wallis, I.G., "Review of Models of Tidal Waters," Journal of the Hydraulics Division, ASCE, Vol. 101, No. HY11, pp. 1405-1421, 1975b.

[55] Ibbitt, R.P., and O'Donnell, T., "Fitting Methods for Conceptual Catchment Models," Journal of the Hydraulics Division, Proceedings of ASCE, Vol. 100, No. HY7, pp. 005-1109, 1971.

[56] Isaacson, E., Stoker, J.J., and Troesch, A., "Numerical Solution of Flood Prediction and River Regulation Problems," Report II, Courant Institute Of Mathematical Science, No. IMM 205, 1954.

[57] Issacson, E., Stoker, J.J., and Troesch, A., "Numerical Solution Of Flood Prediction And River Regulation Problems," Report III, Courant Institute Of Mathematical Science, No. IMM-NYU 235, October, 1956.

[58] Isaacson, E., Stoker, J.J., and Troesch, A., "Numerical Solution Problems in Rivers," Journal of the Hydraulics Division, ASCE, Vol. 84, No. HY5, pp. 1-18, 1958.

[59] Johnson, B.H., "Unsteady Flow Computations on the Ohio-Cumberland-Tennessee-Mississippi River System," Technical Report H-74-8, Hydraulics Laboratory, Waterways Experiment Station, U.S. Army Corps of Engineers, 1974.

[60] Johnston, P.R., and Pilgrim, D.H., "Parameter Optimization for Watershed Models," Water Resources Res., Vol. 12 No. 3, June, 1976.

[61] Keefer, T.N., and McQuivey, R.S., "Multiple Linearization Flow Routing Model," Journal of the Hydraulics Division, ASCE, Vol. 100, No. HY7, pp. 1031-1046, 1974.

[62] Keulegan, G.H., and Patterson, G.W., "Effect of Turbulence and Channel Slope in Translation Waves," Journal of Research, National Bureau of Standards, Vol. 30, Research Paper pr1544, June, 1943.

[63] Kleitz, M., "Note sur la theorie du mouvement non permanent des liquides et sur application a la propagation des crues des rivieres (Note on the theory of unsteady flow of liquids and on application to flood propagation in rivers)," Annales des ponts et chaussees, ser. 5, vol. 16, 2e semestre, pp. 133-196, 1877.

[64] Kouwen, N., "Flood Routing Sensitivity Study," Final Report, Project No. 111-11-02, Waterloo Research Institute, University of Waterloo, Waterloo, Ontario, 1984.

[65] Kouwen, N., "Dynamic Wave Flood Routing Sensitivity Study," Project No. 111-11-02, Waterloo Research Institute, University of Waterloo, 1986.

[66] Lai, C., "Flows Of Homogeneous Density In Tidal Reaches. Solution By The Method Of Characteristics," Open-File Report, United States Department Of The Interior, Geological Survey, Washington, D.C., 1965.

[67] Lai, C., "Flows Of Homogeneous Density In Tidal Reaches. Solution By The Implicit Method," Open-File Report, United States Department Of The Interior, Geological Survey, Washington, D.C., August, 1965.

[68] Lai, C., "Numerical Modelling of Unsteady Open-Channel Flow," in Advances in Hydroscience, Vol. 14, B.C.Yen, ed., Academic Press, Orlando, Fl, pp. 161-333, 1986.

[69] Laplace, P.S., 1776, "Researches On Some Points Of The World System," Memoir, Vol. 9, Academy Science, Paris.

[70] Li, H.L., "Numerical Computation for Two-Dimensional Riverbed Deformation in Estuaries," Third International Symposium on River Sedimentation, University of Mississippi, 31 March- 4 April, pp. 344-353, 1986.

[71] Li, R.M., Simons, D.B., and Stevens, M.A., "Nonlinear Kinematic Wave

Approximation for Water Routing," Water Resources Research, Vol. 11, No. 2, pp. 245-252, 1975.

[72] Li, R.M., Simons, D.B., Shiao, L.S., and Chen, Y.H., "Kinematic Wave Approximation for Flood Routing," in: Rivers '76, Symposium on Inland Waterways for Navigation, Flood Control, and Water Diversion, Vol. I, ASCE, pp. 377-398, 1976.

[73] Liggett, J.A., "Mathematical Flow Determination in Open Channels," ASCE-Proc., Journal of Engineering Mechanics Division, Vol. 94, No. EM4, pp. 947-963, Aug., 1968.

[74] Liggett, J.A., and Woolhiser, D.A., "Difference Solutions Of The Shallow-Water Equations," Journal Of The Engineering Mechanics Division, ASCE, Vol. 93, No. EM2, Proc. Paper 5189, April, 1967.

[75] Lighthill, M.J., and Whitman, G.D., "On Kinematic Floods, I, Flood Movements in Long Rivers," Proceedings, Royal Society, A229, pp. 281-316, London, 1955.

[76] Linsley, R.K., Kohler, M.A., and Paulhus, J.L.H., "Applied Hydrology," McGraw Hill Book Co., New York, pp. 502-530, 1949.

[77] Linsley, R.K., Kohler, M.A., and Paulhus, J.L.H., "Hydrology for Engineers," McGraw Hill Book Co., New York, pp. 116-244, 1958.

[78] Maddaus, W.O., "A Distributed Linear Representation Of Surface Runoff," Hydrodynamics Laboratory Report 115, Massachusetts Institute Of Technology, Cambridge, Massachusetts, 1969.

[79] Manely, R.E., "Improving the Accuracy of Flow Measurements of Open Channel Sites," Water Services, Vol. 81, No. 98, Dec., 1977.

[80] Manley, R.E., "Bration of Hydrological Model Using Optimization Technique," Journal of the Hydraulic Division, ASCE, Vol. 104, No. HY2, Feb., 1978.

[81] Massau, J., "Appendice au Memoire sur l'integration graphique (Appendix to Memoir on Graphical Integration), Annales de l'Association des Ingenieurs sortis des Ecoles Speciales de Gand, Vol. 12, pp. 185-444, Ghent, Belgium, 1889.

[82] McCarthy, G.T., "The Unit Hydrograph and Flood Routing," Paper Presented at Conference of the North Atlantic Division of U.S. Corps of Engineers, New London, Connecticut, 1938.

[83] Meyers, J.S., and Schultz, E.A., "Panama Canal: The Sea-Level Project," in a Symposium: Tidal Currents, Transactions, ASCE, Vol. 114, pp.668-671, 1949.

[84] Miller, W.A., and Cunge, J.A., "Simplified Equations of Unsteady Flow," in: K. Mahmood and V. Yevjevich (Editors), Unsteady Flow in Open Channels, Vol. I, Chapter 5, Water Resources Publications, Fort Collins, Colorado, pp. 183-257, 1975.

[85] Miller, W.A., and Yevjevich, V., "Unsteady Flow In Open Channels," Bibliography, Vol. III, Water Resources Publications, Fort Collins, Colorado, 1975.

[86] Morasse, B., "Generation of the 1968 Hydrometric Data of the Lower Fraser River; Using the ONE-D Hydrodynamic Model, "Internal Report, WPM-IWD-Environment Canada, 1985.

[87] Myers, W.R.C., Personal Communication, University of Ulster at Jordanstown, N. Ireland, 1991.

[88] Nash, J.E., and Sutcliffe, J.V., "River Flow Forecasting Through Conceptual Models," Part I, A Discussion of Principles, Journal of Hydrology, 10(3):282-290, 1970.

[89] Nelder, J.A., and Mead, R., "Simplex Method for Function Minimization," Computer Journal, Vol. 7, No. 4, pp.308-313, Jan., 1965.

[90] Newton, I. , 1687, Propositions, Royal Society, London, pp. 44-46.

[91] Nishnabotna River, "Methodology for Crop and Pasture Inundation Damage Appraisal: Training Manual for Hydrologists on Watershed Protection and Flood Prevention Work Plan Parties," Preliminary Draft, U.S. Soil Conservation Service, Milwaukee, Wis., 1954.

[92] Patry, G.G., and Marino, M.A., "Non-Linear Runoff Modeling: Parameter Identification," ASCE Journal of Hydraulic Engineering, 109(6):865-80, 1983.

[93] Peregine, D.H., "Long Waves on a Beach," Journal of Fluid Mechanics, Vol. 27, Part 4, pp. 815-827, 1967.

[94] Poisson, S.D., 1816, "Memoir On The Theory Of Waves," Memoir, Vol. 1, Academy Science, Paris, pp. 71-186.

[95] Ponce, V.M., Indlekofer, H., and Simons, D.B., "Convergence of Four-Point Implicit Water Wave Models," Journal of the Hydraulics Division, Proc. ASCE,

Vol. 104, No. HY7, pp.947-958, June, 1978.

[96] Preissmann, A., "Propagation des Intumescenes dans les Canaux et Rivieres," Congres de l'Association Francaise de Calcul, Grenoble, France, pp. 433-442, 1961.

[97] Price, R., "Comparison of Four Numerical Methods for Flood Routing," Journal of the Hydraulics Division, Vol. 108, No. HY7, July, 1974, pp.879-899.

[98] Price, R.K., "Flood Studies Report," Vol. III, Flood Routing Studies, Natural Environment Research Council, London, U.K., 1975.

[99] Quick, M.C., and Pipes, A., "Nonlinear Channel Routing by Computer," Journal of the Hydraulics Division, ASCE, Vol. 101, No. HY6, pp. 651-664, 1975.

[100] Quinn, F.H., and Wylie, E.B., "Transient Analysis of the Detroit River by the Implicit Method," Water Resources Research, Vol. 8, No. 6 pp. 1461-1469, Dec. 1972

[101] Richtmyer, R.D., and Morton, K.W., "Difference Methods for Initial Value Problems," Interscience Publishers, New York, second Edition, 1957.

[102] Richtmyer, R.D., "A Survey of Difference Methods for Non-Steady Fluid Dynamics," NCAR Technical Notes 63-2, National Centre for Atmospheric Research, Boulder, Colorado, 1962.

[103] Rockwood, D.M., "Columbia Basin Streamflow Routing by Computer," Journal of Waterways and Harbors Division," Proceedings of ASCE, Vol. 94, No. WW5, pp. 1874-1915, 1958.

[104] Sauer, V.B., "Unit-Response Method of Open-Channel Flow Routing," Journal of the Hydraulics Division, Proceedings of ASCE, Vol. 99, No. HY1, pp. 1979-1993, 1973.

[105] Schönfeld, J.C., "Propagation of Tides and Similar Waves," Staatsdrukkerijen-Vitgevenijbedijf, 's-Gravenhage, Netherlands, 1951.

[106] Seddon, "River Hydraulics," ACSE, 1900.

[107] Singh, V.P., and McCann, R.C., "Mathematical Modelling of Catchment Response," Proceedings of the International Conference on Water Resources Development, Taipei, Taiwan, Vol. 2, pp. 587-597, 1980.

[108] Sivaloganathan, K., "Flood Routing by the Characteristic Methods," Journal of the Hydraulics Division, Proc. ASCE, Vol. 104, No. HY7, July, 1978, pp. 1075-1091.

[109] Stoker, J.J., "Numerical Solution of Flood Prediction and River Regulation Problems, I: Derivation of Basic Theory and Formulation of Numerical Methods of Attack," New York University, Institute of Mathematical Sciences, Report No. IMM-200, 1953.

[110] Stoker, J.J., "Water Waves," Interscience, 1957.

[111] Streeter, V.L., and Wylie, E.B., "Hydraulic Transients," McGraw-Hill Book Co., Inc., New York, N.Y., 1967.

[112] Strelkoff, T., "Numerical Solution Of The Saint-Venant Equations," Journal Of The Hydraulics Division, ASCE, Vol. 96, No. HY1, January, 1970, pp. 223-252.

[113] Strelkoff, T., and Amorocho, J., "Gradually Varied Unsteady Flow In A Controlled Canal System," Proceedings , International Association For Hydraulic Research, Eleventh International Congress, Leningrad, No. 3.16,8 pp. Also, Vol. VI, Transactions of the Congress (I.A.H.R.XI Congress), Discussion, 1965, pp. 317-320.

[114] Sydor, M., Brown, G., Chang, H., Boutot, W., and Morasse, B., "Getting the Best of Both Worlds-Application of Systems Analysis; from Micro to Super Computers," Conference at the University of Manitoba, Winnipeg, May, 2-5, 1989.

[115] Tatum, F.E., "A Simplified Method of Routing Flood Flows Through Natural Valley Storage," Unpublished Memorandum, U.S. Engineer's Office, Rock Island, Ill., May 29, 1940.

[116] Thatcher,M.L., and Harleman, D.R.F., "Mathematical Model for the Prediction of Unsteady Salinity Intrusion in Estauries," Dept. Civil eng., Ralph M. Parsons Lab., Water Resources Hydrodyn., Report No. 144, pp.232, Feb., 1972.

[117] Tingsanchali, T., and Ackermann, N.L., "Effects of Overbank Flow in Flood Computations," Journal Of The Hydraulics Division, ASCE, Vol. 102, No. HY7, July, 1976, pp. 1013-1025.

[118] Treske, A., "Experimentelle Uberprufung numerischer Berechrungsverfahven von Hachwasserwellen," Report of Hydraulics Research Station, TU Munchen, 44:1-133, 1980.

[119] U.S. Army Corps Of Engineers 1935.

[120] Vasil'ev, O.F., Temnoeva, T.A., and Shugrin, S.M., "Cheslinnii 5etod Rascheta Neustanovivshikhsia Techenni v Otkritikh Ruslakh" ("Numerical Method Of Calculating Unsteady Flows In Open Channels,"), Izvestiia Akademii Nauk S.S.S.R., Mekhanika, No. 2, 1965, pp.17-25; (in Russian).

[121] Vicens, G.J., Rodriguez-Itrube, I., and Schaake, J.C., "Bayesian Framework for the Use of Regional Information in Hydrology," Journal of Water Resources Res., Vol. 11, No. 3, pp.405-414, June, 1975.

[122] Viessmann, W., Knapp, J.W., Lewis, G.L., and Harbaugh, T.E., "Introduction to Hydrology," second edition, New York, Harper and Row, 1977.

[123] Wallis, J.R., and Todini, E., "Comment Upon the Residual Mass Curve Coefficient," Journal of Hydrology, Vol. 24, pp. 210-205, Feb., 1975.

[124] Wood, E.F., Rodriguez-Itrube, I., and Schaake, J.C., "Methodology of Bayesian Inference and Decision Making Applied to Extreme Hydrologic Events," MIT Dept. Civil Eng., Ralph M. Parsons Lab., Water Resources Hyd., Report No. 178, pp.297, Jan., 1974.

[125] Wood, E.F., Harely, B.M., and Perkins, F.R., "Operational Characteristics of a Numerical Solution for the Simulation of Open Channel Flow," Report No. 150, M.I.T., R72-30, June, 1972.

[126] Wooding, R.A., "A Hydraulic Model for the Catchment-Stream Problem," Journal of Hydrology 3, pp.254-267, 1965.

[127] Wormleaton, Allen, J., and Hadjipanos, P., "Discharge Assessment In Compound Channel Flow," Journal Of The Hydraulics Division, ASCE, Vol. 108, No. HY9, Sept., 1982, pp. 975-994.

[128] Wright, R.R., and Carstens, H.R., "Linear Momentum Flux To Overbank Sections," Journal Of The Hydraulic Division, ASCE, Vol. 96, No. HY9, Sept., 1970, pp. 1781-1793.

[129] Wylie, B., "Unsteady Free-Surface Flow Computations," Journal of the Hydraulics Division, ASCE, Vol.96, No. HY3, Proc. Paper 7683, Nov., 1970, pp.2241-2251.

[130] Yen, B.C., "Hydraulics for Sewers," Advances of Hydroscience, Founding Editor V.T. Chow, Academic Press, pp. 1-122, 1986.

[131] Yen, C.L., and Overton, D.E., "Shape Effects On Resistance In FloodPlain

Channels," Journal Of The Hydraulic Division, ASCE, Vol. 99, No.HY1, Jan., 1973, pp. 219-238.

[132] Yilmaz, S., 1992, Undergraduate project, University of Ottawa, Ontario.

[133] Zheleznyakov, G.V., "Relative Deficit of Mean Velocity of Instable River Flow; Kinematic Effect in River Beds with Floodplains," Proceedings of the Eleventh International Conference of the International Association for Hydraulic Research, Leningrad, U.S.S.R. 1965.

[134] Zheleznyakov, G.V., "Interaction of Channel and Floodplain Streams," Proceedings, Fourteenth International Conference of the International Association for Hydraulic Research, Paris, France, 1971.

APPENDIX A

EXTRAN data input manual summarizes the sequence of discharge and head computations as follows:

1-Compute half-step discharge at $t+\Delta t/2$ in all links based on preceding full-step values of head at connecting junctions.

2-Compute half-step flow transfers by weirs, orifices, and pumps at time $t+\Delta t/2$ based on preceding full-step values of head at transfer junction.

3-Compute half-step head at all nodes at time $t+\Delta t/2$ based on average of preceding full-step and current half-step discharges in all connecting conduits, plus flow transfers at the current half-step.

4-Compute full-step flow discharge in all links at time $t+\Delta t$ based on half-step heads at all connecting nodes.

5-Compute full-step flow transfers between nodes at time $t+\Delta t$ based on current half-step and current full-step discharges, plus flow transfers at the current full-step.

6-Compute full-step head at time $t+\Delta t$ for all nodes based on average of preceding full-step and current full-step discharges, plus transfers at the current full-step.

EXTRAN input data manual summarizes the following procedure for time step computations:

-At the start of the simulation a time step of DELT/4.0 is used, or 4 small time steps.

-Subsequently, the small time step is based on the current smallest conduit C and the last time factor T_f. The starting T_f is 3.0. This means that a small time step of 3 times the minimum C is selected.

-When convergence fails T_f is reduced by 1.0. The minimum allowable T_f is 0.0.

-When the model converges within 2 iterations Tf is increased by 1. The maximum T_f is 3.0.

- In summary, the model works between 0.5 * minC and 3.0 * minC. The number of small time steps is always a whole number.

Also, EXTRAN input data manual states the sequence of flow computations in links and head calculations at nodes summarized as:

- Determine the next time step size. Find the new step based on the preceding time step's conduit velocity and depth using eq. 4-50. Find the number of time steps within this time steps based on the calculated T_f* minC and DELT input on data group B1.

- Compute the first iteration discharge at $t+\Delta t$ in all links based on preceding time step values of head at connecting junctions.

- Compute first iteration flow transfers by weirs, orifices, and pumps at time $t+\Delta t$ based on preceding time step values of head at transfer junctions.

- Compute first iteration head at all nodes at time $t+\Delta t$ based on the average of initial time step flow and first iteration flow in any connecting conduits, plus flow transfers at the current time step.

- Repeat steps 2 thru 4 with new estimates for conduit flows and junction heads until all conduits and junctions converge. If iterations exceed ITMAX (max. allowable numbers of iterations) decrease the time step by 1/2. If convergence happen within 2 iterations increase the Courant number by 1.0.